We are obliged to place utmost emphasis on the development and improvement of the activities of the Mineral Research and Exploration Department and to increase as well the planned exploration of the uncovered mineral reserves currently profitability envisaged.

We have commissioned the Mineral Research and Exploration Institute with the realization of geological investigations on the unknown mineral wealth of the country within the framework of a three - year programme. They will achieve. We do expect successful results.

We do possess an ample potential of mineral wealth deserving due consideration within the framework of exploitation and development activities.

In our opinion, which is presently based on the investigations and available data, Turkey possesses a rich assortment of raw materials justifying the establishment of a mining industry and a substantial amount of underground resources required by the home market and foreign trade as well.

The amount of detailed data and information collected on the mineral wealth of the country shows remarkable increases compared with the past year.

Kemal Atatürk

MIDDLE CAMBRIAN TRILOBITE SUCCESSION IN THE ÇALTEPE FORMATION AT BAĞBAŞI (HADIM-KONYA) CENTRAL TAURUS, TURKEY

William T. DEAN

University College, Cardiff

and

Necdet ÖZGÜL

Mineral Research and Exploration Institute of Turkey, Ankara

ABSTRACT.— In the Bağbaşı area, about 12 km north of Hadım, the Red Nodular Limestone Member of the Çaltepe Formation which crops out in a tectonic window contains valuable biostratigraphic data for the higher levels of the formation. Trilobites from the measured sections of «Bağbaşı I» and «Bağbaşı II» in the Red Nodular Limestone indicate an early Middle Cambrian age and include: *Agraulos, Asturiaspis, Conocoryphe (Conocoryphe), Corynexochus, Ctenocephalus (Harttella), Paradoxides* (s.1), *Pardailhania* and *Peronofsis*. The trilobites are similar to specimens found in the corresponding strata near Seydişehir and display marked affinities with Middle Cambrian faunas in Spain and the Montagne Noire, Southwestern France. The Red Nodular Limestone Member is younger than the strata known variously as the «Formation D» and «Tiyek Formation in the Amanos Mountains of Southern Turkey and older than the Sosink Formation in Southeastern Turkey; the later two are also Cambrian in age.

INTRODUCTION

In the deep valley of the River Göksu, 100 km south of Konya, large outcrops of Lower Paleozoic rocks appear in a magnificent tectonic window (Fig. 1), under several superposed nappes of Eocene age (Özgül, 1971; Özgül and Gedik, 1973; Özgül, 1976). The Lower Paleozoic formations comprise extensive shales (Seydişehir Formation) of Upper Cambrian-Ordovician age overlying conspicuous nodular limestone and dolomitic limestone of Cambrian age known as Çaltepe Formation.

In July 1973 a few Middle Cambrian trilobites were collected by the authors from the Red Nodular Limestone Member of the Çaltepe Formation at Bağbaşı (formerly known as Egiste in Blumenthal, 1947) 12 km north-nortwest of Hadim. A more prolonged joint visit in June 1977 produced a larger collection from the two measured sections shown in Figure 2.

At Bağbaşı, in contrast with the type section at the Çaltepe (Seydişehir), the upper part of the Çaltepe Formation proved to be fairly fossiliferous and thus provides valuable biostratigraphic data for the higher levels of the formation. Tentative correlations are proposed with middle Cambrian successions in southeastern Turkey and southwestern Europe.

ÇALTEPE FORMATION

Originally considered as Devonian by Blumenthal (1947) the Lower and Middle Cambrian age of the Çaltepe Formation was established-, by means of trilobite faunas (Dean and Monod, 1971) and conodont faunas (Özgül and Gedik, 1973) at Seydişehir and Hadım regions.

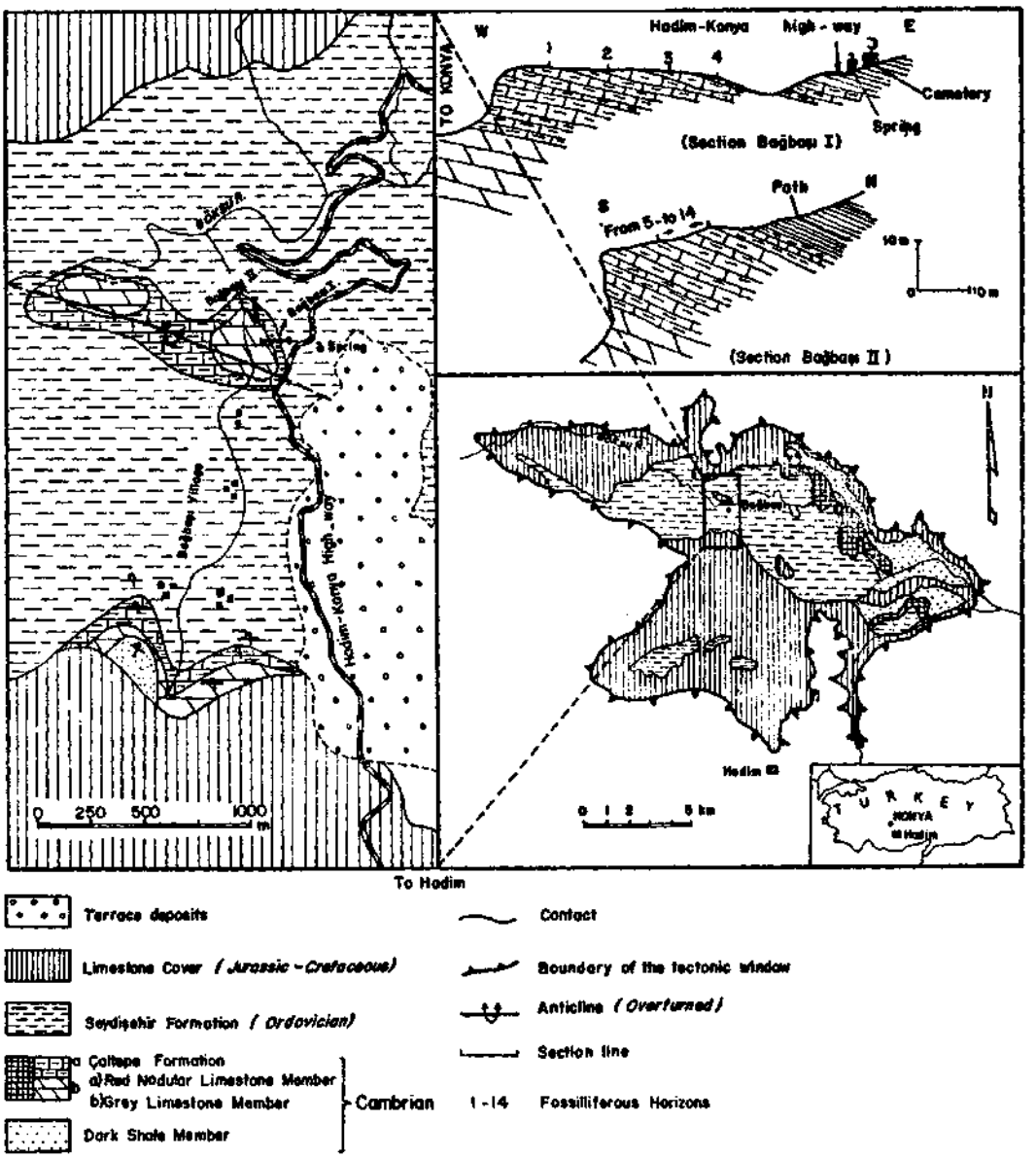

Fig. 1 - Geologic maps of the Bağbaşı region and schematic cross sections of the «Bağbaşı I» and «Bağbaşı II».

The section at the southeastern end of Çaltepe (sometimes written Idrisgal), situated between Beyşehir and Seydişehir, was designated as stratotype for the Formation (Dean and Monod, 1970, p. 416). The succession was divided into four members, the lowest then being known alternatively as the Çaltepe Dolomite and the upper three grouped as the Çaltepe Limestone. They were listed later (Dean, 1976, p. 356) as follows:

Red Nodular Limestone Member	40 m	Middle Cambrian
Light-grey Limestone Member	10 m	
Black Limestone Member	30 m	Lower Cambrian
Dolomite Member	50 m	
(base not seen)		

The faunas are now being studied and preliminary results indicate that the Dolomite Member (unfossiliferous), Black Limestone Member and lowest fifth of the Light-grey Limestone Member are of Lower Cambrian age; the upper fourfifths of the Light-grey Limestone Member, and the Red Nodular Limestone Member are Middle Cambrian in age.

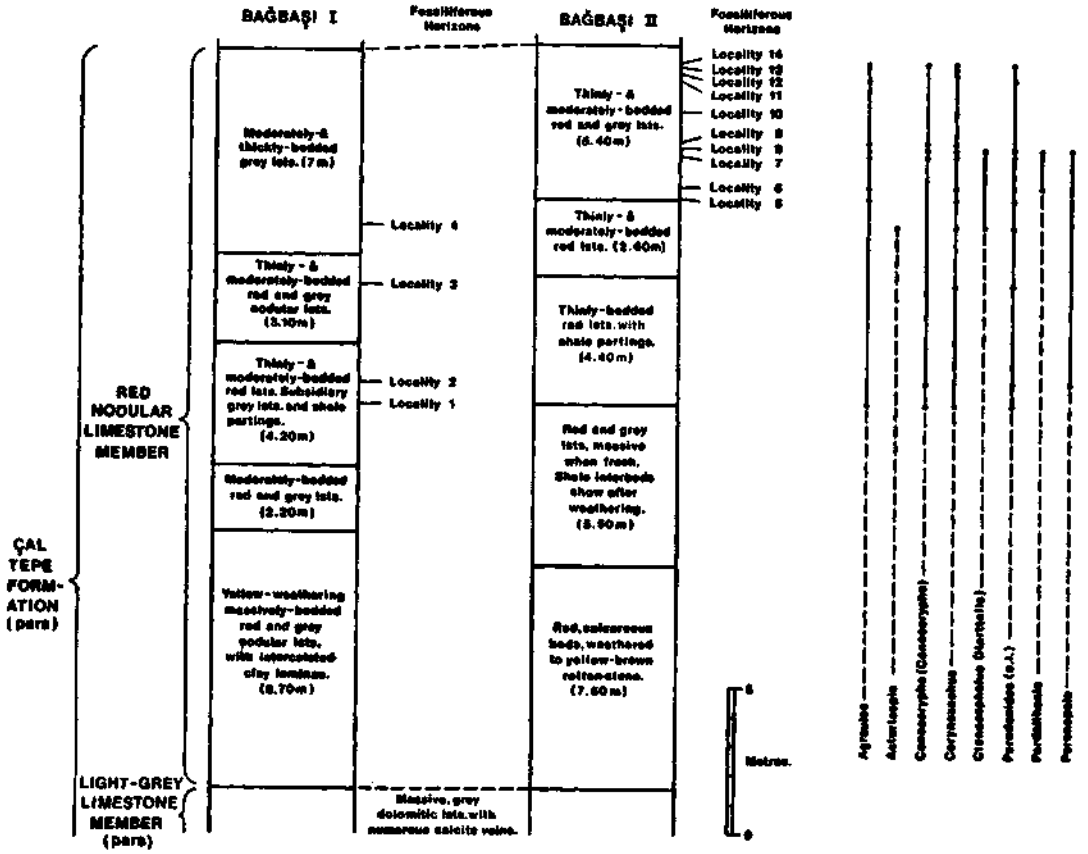

Fig. 2 - The trilobites of the Red Nodular Limestone Member at the measured sections «Bağbaşı I» and «Bağbaşı II».

The geographic extension of the Çaltepe outcrops southeastwards along the Taurus Mountains into the Hadım region, 75 km from Seydişehir, was first demonstrated by Necdet Özgül who published a geological map of the area *(in* Özgül and Gedik, 1973) and indicated more than 150 m of unfossiliferous, dark shales underlying limestones of the Çaltepe Formation in the Göksu valley.

The village of Bağbaşı is situated beside the mountain road which runs north from Hadım towards Konya. In this area the rocks of the Çaltepe Formation are folded into an anticline with axis WNW-ESE, The large stream at Bağbaşı flows north-northwest through a steepsided gorge to meet the valley of the River Göksu, and it is in the eastern side of this gorge that the two measured sections are located (Fig. 1). In each instance the section begins immediately above the top of massive limestone of the Light-grey Limestone Member; the latter are exposed at the base of cliffs formed by qonspicous, red strata of the Red Nodular Limestone Member, here about 25 m thick.

Bağbaşı **section I** (Fig. 1 and 2)

A short distance north of Bağbaşı village, a prominent spring is situated beside the Konya road and west of the local cemetery. West of the road, and opposite the spring, the side of the gorge descends towards a cliff some 12 m high and it is here that the measured section is sited. The basal portion is marked by a small, retrogressive notch immediately above the conformable junction with the Light-grey Limestone Member. Most of the cliff is made up of some 11 m of massive, red or pink and grey, nodular limestones, with subsidiary beds appearing more thinly-bedded upon weathering. At some points fossil debris was visible in cross section, but no recognisable specimens could be extracted. The upper portion of the section also comprises red and grey, nodular limestones but the strata are less massively bedded, partings of red clay and shale are more, in evidence, and recognisable fossils were obtained from four levels. Fossils were found most commonly in grey limestones which had undergone some recrystallisation, and in general were much less abundant in the red limestones, some of which included calcilutites. The lowest identifiable material, including particularly *Corynexochus,* was collected 13 m above the base of the Member. The fauna, found through a thickness of about 5.40 m, is relatively poor in genera and species (Fig. 2); almost all are trilobites, with rare inarticulate brachiopods. No complete exoskeletons were found and the remains consist mostly of cranidia. Those of small forms such as *Corynexochus* commonly occur unbroken, but large ones such as *Paradoxides* are usually in fragments.

Bağbaşı section II (Fig. 1 and 2)

Although situated only 500 m north of Section I, the strata of the Second section proved more fossiliferous, with ten levels yielding trilobites and occasional brachiopods. In this instance the fossils occurred slightly higher in the succession, being found only in the topmost 5.40 m of a sequence 25.4 m thick. At this point in the gorge the lowest 20 m of the Member, mostly red limestones (with shale intercalations) are deeply weathered to produce a yellow-brown rottenstone. As at Section I recognisable fossils were found mostly in grey limestone bands.

CORRELATION AND AGE OF THE RED NODULAR LIMESTONE MEMBER

As interpreted by the writers, the Red Nodular Limestone Member at Bağbaşı is slightly more than 25 m thick and its upper limit is drawn where there is a change to thinly-bedded limestones with interbedded, brown-weathering, grey shales. These «passage beds», 4 metres thick, are followed by a thick sequence (still under investigation) of shales with only minor developments of thinly-bedded limestones in which a few Middle Cambrian fossils were found.

In the (Çaltepe type area Dean and Monod (1970) showed the limestones of the Çaltepe Formation overlain by a conspicuous unit of yellow shales, 50 metres thick. This Yellow Shale Member was grouped with the succeeding Seydişehir Formation (of Ordovician age) on lithological grounds; since then, fragments of *Paradoxides* (s.l.) have been found in impersistent limestone beds within the yellow shales and the latter may eventually merit separate formational status. The relationship of the Yellow Shale Member and the Seydişehir Formation at the Çaltepe is not clearly seen and according to Olivier Monod (personal communication) could be unconformable; certainly no Upper Cambrian, or even latest Middle Cambrian, strata are yet known from that area.

At Bağbaşı the strata overlying the Red Nodular Limestone Member, though apparently analogous to the Yellow Shale Member at the (Çaltepe, not only are different lithologically, but probably extend much higher in the succession, judging from Gedik's assessment *(in Ö*zgül and Gedik, 1973) of Upper Cambrian and Tremadoc conodonts from strata assigned to the Seydişehir Formation in the Göksu Valley north of Bağbaşı.

Trilobite genera found so far in the two Bağbaşı sections are as follows: *Agraulos, Asturiaspis, Conocoryphe (Conocoryphe) Corynsxochus, Ctenocephahts (Harttella), Paradoxides* (s.l.), *Pardailhania* and *Peronopsis.* Although detailed studies are not yet complete it is apparent that the fauna, found also in the Red Nodular Limestone Member at the Çaltepe, shows strongest affinities with those of the Iberian Peninsula and Southwestern France. In recent years the Spanish faunas have become better known from the work of Sdzuy who (1971) divided the Middle Cambrian into a succession of «Pisos» or «Niveles» (= horizons), which may eventually be superseded by more formal zones. The subdivisions listed in ascending stratigraphic order by Sdzuy are as follows:

(I) Nivel provisionaly assigned to the Middle Cambrian on account of its containing *Paradoxides (Acadoparadoxides) mureroensis* Sdzuy; (II) Nivel de *Conocoryphe ovata* Sdzuy; (III) Nivel de *Acadoknus;* (IV) Piso de *Badulesia;* (V) Piso de *Pardailhania;* (VI) Piso de *Solenopleuropsis;* and (VII) Piso sin Solenopleuropsidae.

The vertical ranges of genera in the Red Nodular Limestone Member with reference to the Spanish faunas may be summarised as follows: *Agraulos,* most of (V) and lower (VI); *Asturiaspis,* upper half of (II) to lower half of (v); *Conocoryphe (Conocoryphe},* (II), (IV), (VI) and lower (VII); *Corynexochus,* upper two-thirds of (11) to lowest quarter of (V); *Ctenocephalus (Harttella),* most of (IV), through (V) to lowest (VI); *Paradoxides* (s.l.) ranges throughout; *Pardailhania,* highest (IV) and all of (V); *Peronopsis,* uppermost (IV), through (V) and (VI) to lower (VII). On the basis of these comparisons, the fauna of the Red Nodular Limestone Member at Bağbaşı agrees best with that of the Piso de *Pardailhania,* and probably with the middle or lowest third of that subdivision as the Turkish specimens are identified as *P.* cf. *hispida* (Thoral),

In Southwestern France the classic sections in the Montagne Noire, known from the researches of Marcel Thoral and earlier workers, have been revised by Courtessole (1973), who divided the Middle Cambrian succession, which is developed for the most part in a shale facies and therefore liable to exhibit some differences from the faunal assemblages in the limestones of the Turkish sequences, into 10 «Niveaux Paleontologique», denoted as $A_{1)}$ A_2 and B to I. The vertical ranges in France of the genera found at Bağbaşı using Courtessole's terminology, is as follows: *Agraulos,* A_1, A_2, ? B; *Asfuriaspis,* not recorded from the Montagne Noire; *Conocoryphe (Conocoryphe),* B, C, F and H; *Corynexochus,* A_1 and A_2; *Ctenocephalus (Harttella),* A_1, A_2, B and ? C; *Paradoxides* (s.l.), A_1 to I; *Pardailhania,* A_1 and A_2; *Peronopsis,* C to I. Using these criteria, the fauna of the Red Nodular Limestone Member at Bağbaşı may be correlated with Niveau A or thereabouts.

Thus evidence to date suggests an early Middle Cambrian age for the Red Nodular Limestone Member at Bağbaşı; the same is perhaps true also for the same Member at the Çaltepe, though recent re-investigation of the latter section indicates a greater thickness of limestones there, the faunas of which have been collected but not yet determined. The record of *Solenopleuropsis (in* Dean and Monod, 1970, p. 418) from the Red Nodular Limestone Member at a locality southeast of the Çaltepe is now regarded as a misidentification of a fragmentary *Pardailhania.* By analogy with the Spanish and Southern French faunas, the strata in the Amanos Mountains of south Central Turkey, known variously as Formation D (Dean and Krummenacher, 1961) and Tiyek Formation «C_3» (Ketin, 1966), are slightly older than the Red Nodular Limestone Member; they contain the trilobite *Badulesia* and represent a shale facies not yet known elsewhere in the Taurus region. The Çaltepe and Bağbaşı are however, older than those from the Sosink Formation in the Derik-Mardin area of Southeastern Turkey (see Dean, 1976, for review; Monod, 1977). The latter trilobites, now being described by W.T.Do include *Solenopleuropsis* and are of late Middle Cambrian age.

REFERENCES

Blumenthal, M.M., 1947, Geologie der Taurustketten im Hinterland von Seydişehir und Beyşehir: MTA Publ., Set. D, 2, 242, Ankara.

Courtessole, R., 1973, Le Cambrien moyen de la Montagne Noire: 248, Toulouse.

Dean, W.T., 1976, Cambrian and Ordovician correlation and trilqbite distribution in Turkey: Fossils and Strata, 5, 353-373.

———and Krummenacher, R., 1961, Cambrian trilobites from the Amanos Mountains, Turkey: Palaeontology, 4, 71-81.

———and Monod, O., 1970, The Lower Paleozoic stratigraphy and faunas of the Taurus Mountains near Beyşehir, Turkey, I. Stratigraphy: Bull. Brit. Mus. (Nat. Hist.) Geol., 19, 411-426.

Ketin, t., 1966, Cambrian outcrops in southeastern Turkey and their comparison with the Cambrian of East Iran: Bull. Mineral Research and Explo. Inst. Turkey, 66, 77-89.

Monod, O., 1977, Recherches geologiques dans le Taurus occidental au sud de Beyşehir (Turquie): These Universite Paris-Sud Orsay.

Özgül, N., 1971, The importance of block movements in structural evolution of the northern part of Central Taurus: Bull. Geol. Soc. Turkey, 14, 85-101.

———, 1976, Some geological aspects of the Taurus Orogenic belt (Turkey): Bull. Geol. Soc. Turkey, 19, 65-78.

———and Gedik, I., 1973, Orta Toroslar'da alt Paleozoyik yaşta Çaltepe Kireçtaşı ve Seydişehir Formasyonu'nun stratigrafisi ve konodont faunası hakkında yeni bilgiler: Bull. Geol. Soc. Turkey, 16, 39-52.

Sdzuy, K., 1971, La Subdivision Biostratigrafica y la Correlacion del Cambrico Medio de Espana: Publ. I, Congr. Hisp. Luso Amer. Geol. Econ., 2, Seccion I, 769-782.

FORMATION OF THE GRABENS IN SOUTHWESTERN ANATOLIA

Jean François DUMONT, Şükrü UYSAL, Şakir ŞİMŞEK and İ. Hakkı KARAMANDERESİ

Mineral Research and Exploration Institute of Turkey, Ankara

and

Jean LETOUZEY

Institut Franfais du Petrole Rueil Malmaison

ABSTRACT. — Tectonic compression and tensional directions at the Miocene-Quaternary interval are tried to be determined on the basis of results obtained from the evaluation of faults in Southwestern Anatolian Miocene-Quaternary sediments. Faults evaluation, one of the newest structural evaluation methods; gives more or less the same results with seismotectonic data. Studies carried out on Menderes and Burdur grabens showed a certain mechanism of graben formation in the areas under consideration. And it may thus be suggested that there is a compressive phase followed by a tensional one. Furthermore alternating tension and compression directions are normal to each other.

Through regional studies, the following phases are determined:

1. Late Miocene-Early Pliocene compression phase: compression in NW-SE direction, and compression in NE-SW direction.

2. Pliocene graben formation: Beginning in Pliocene, the graben formation continued with N-S directed tension through late Pliocene.

3. Old Quaternary Compression phase: N-S directed compression in Burdur and WNW-ESE directed compression in Sarayköy (Denizli) areas.

4. Young Quaternary graben formation: NE-SW directed tension in Menderes Graben and NW-SW directed tension in Burdur.

INTRODUCTION

Major inter-continental or intra-continental tectonic phenomena may be divided in two types. The first type is represented by thrust faults, overturned faults and strike-slip faults developed as a result of compressive tectanics. Graben formation resulting from tensional tectonics is covered under the second type.

In previous years, compressive and tensional tectonics were interpreted as processes independently occurring, since information and data on plate tectonics were limited.

The sequence of Alpine tectonic phases were established by Aubouin (1973), who considered the phases characterized by tensional tectonics and following the tectonic phases producing compression, as neotectonics. Aubouin, however, in a later work conducted in 1977, used the term «Mediterrenean period to identify the phases he has previously considered neotectonic.

Studies carried out on the Alps, have shown that the formation of grabens is closely related to compressive tectonics. McKenzie (1972) however, explains the formation of Western Anatolian grabens as relateid to the movement of Anatolia from east to west.

Tapponier (1977) claims that the grabens developed in the internal parts of the continents are formed parallel to the compressive direction.

Dewey and Şengör (1979) state that the E-W compressive direction produced resulting from the convergence of Gondwana and Euro-Asia, has led to a N-S divergence in the West.

FAULT EVALUATION

Study of faults is one of the newest methods employed in the evaluation of structural features. Anderson was the first to conduct mechanical studies on faults in 1942. Complex fault systems were studied by Arthaud in 1969. Through the studies of other workers (e.g. Carey and Brunier, 1974; Angelier and Mechler, 1977; Angelier and Goguel, 1978 and Angelier, 1979) in the following years fault evaluation method has been proved to be a reliable means to solve problems related to structure.

In the neotectonic studies also, fault evaluation may prove to be effective, in case the stratigraphy is well known. Thrust faults and tectonic activities leading to the formation of grabens, may easily be recognized since they cause considerable morphological changes, such as changes in sedimentary features, erosion, etc.

Tectonics, however, causing strike faults are hard to recognize as these may not produce distinct morphological changes.

Various workers carried out stratigraphical (Becker Platen, 1970; Bdring, 1971 and Kastelli 1972), sedimentological (Leflef, 1979, oral communications) and geomorphological (Erin?, 1955) studies on the Young Tertiary sediments of SW Turkey. Although the beginning of the graben formation is well established in these studies, compressional tectonics affecting the area prior to the formation of grabens are not considered. It should however be noted that the Upper Miocene-Lower Pliocene compression phase, is in fact a tectonic phase which can be observed in the area extending from eastern Turkey to western Greece, however locally (Mercier, 1977; Angelier 1977a; Poisson, 1977; Dewey and Şengör, 1979; Dumont *et al,* 1979; Dumont, 1979; Letouzey and Özer, 1978). Faults developed in western Turkey as a result of compressional tectonics, are characterized by lateral movement and do not produce distinct morphological changes. Some workers however, consider that the present subduction of the Aegean Arc is related to this phase (Angelier, 1977a,b; Dewey and Şengör, 1979). Results obtained from stratigraphical, sedimentological and geomorphological studies conducted on the Old Quaternary formations, also supports the same idea. It may therefore be concluded that the previous writers failed to established Old Quaternary compression phase, as it has not caused important morphological changes.

Two methods are employed presently in the evaluation of faults, i.e. graphic method and computer-based method. In the graphic method which is simpler than the latter, fields of minimum, medium and maximum force, producing faulting, are established (Angelier and Mechler, 1977), and to arrive at a reliable conclusion, faults however belonging to the same tectonic phase, differing in strike are used. Through mathematical evaluation of the results thus obtained, the details of the compression and tension directions are understood (Angelier and Goguel, 1978; Angelier, 1979). In the interpretations of earthquake epicenter mechanism in seismotectonic surveys and in the graphic method as well, the data to be evaluated are same: and it may therefore be concluded that there exists a true relationship between the seismotectonic patterns and the results obtained from older faults. The same method is employed in each case, i.e. in the evaluation of faults, basic data used is the movement of older faults, whereas in the seismotectonic evaluations, faults producing earthquakes are used. Results of measurements conducted in the Quaternary sediments of the Büyük Men-

deres Graben and Burdur area, show parallellism with the seismotectonic results of Ritsema (1974). Results of measurements, however, show a slight difference from seismotectonic data obtained by McKenzie in 1976 (Dumont *et al.*, 1980).

FAULT EVALUATION RESULTS

Through results obtained from regional studies, a mechanism related to the formation of grabens in the Menderes and Burdur Grabens is established.

Efes fault

Efes fault located S of Küçük Menderes Valley is on the western extension of the Büyük Menderes Graben, and has been a focus of five rhythmic movements. The first of these movements has occurred in the direction of strike and was followed by a tension nearly perpendicular to the previous compression direction (Fig. 1). The first two movements have taken place prior to late Pliocene graben formation and are capped by Plio-Quaternary slope debris. Southwestern Turkey, however, is characterized by a strong N-S or NE-SW compression, producing a nappe by the end of Miocene (Graciansky, 1972; Poisson, 1976). Direction of compression in the Efes fault, determined by the writers of the present work is conformable with the NE-SW trending Aksu phase; it however, differs from the phase described above. Efes fault, may well be considered to be related to a younger compression phase, e.g. Old Quaternary compression phase, since the age of the slope debris found in the area is not known for certain. It should however be noted that compression direction of the Old Quaternary compression phase, i.e. N-S or NW-SE, is not in conformity with the movement of the Efes fault.

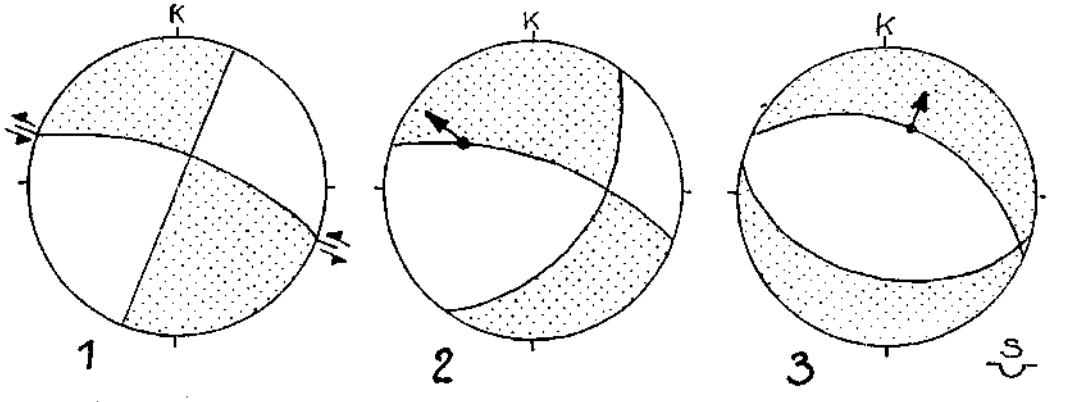

Fig. 1 - The view of the first three movements of the Efes Fault on the lower hemisphere of Smith net. Arrows are showing fault line and movement (1 - Left lateral; 2 - Normal left; 3 - Normal). Dotted areas contain tension, and white areas compression directions. 1 and 2 - indicating movements following each other at the end of Miocene - beginning of Pliocene; 3 - Pliocene movement.

Sarayköy

Pliocene limestones occurring on the western margin of the Denizli plain, were affected by three rhythmic movements. The first of these movements has resulted from N-S tension and may be correlated with the Late Pliocene graben formation. The second movement is represented by a WNW-ESE compression intersecting the normal faults of the first phase. The compression phase

described here is reflected by nearly oblique or lateral fault lines (Fig. 2). In the third phase, faults developed during the second phase as a result of NNE-SSW tension, are intersected by normal faults. Faults developed in this phase are covered by" Early Quaternary travertines in the Pamukkale area. Although detailed stratigrafical data and information are lacking, it may presumed that the tectonic compression predominating in the second phase, has been effective in the Pliocene-Pleistocene interval.

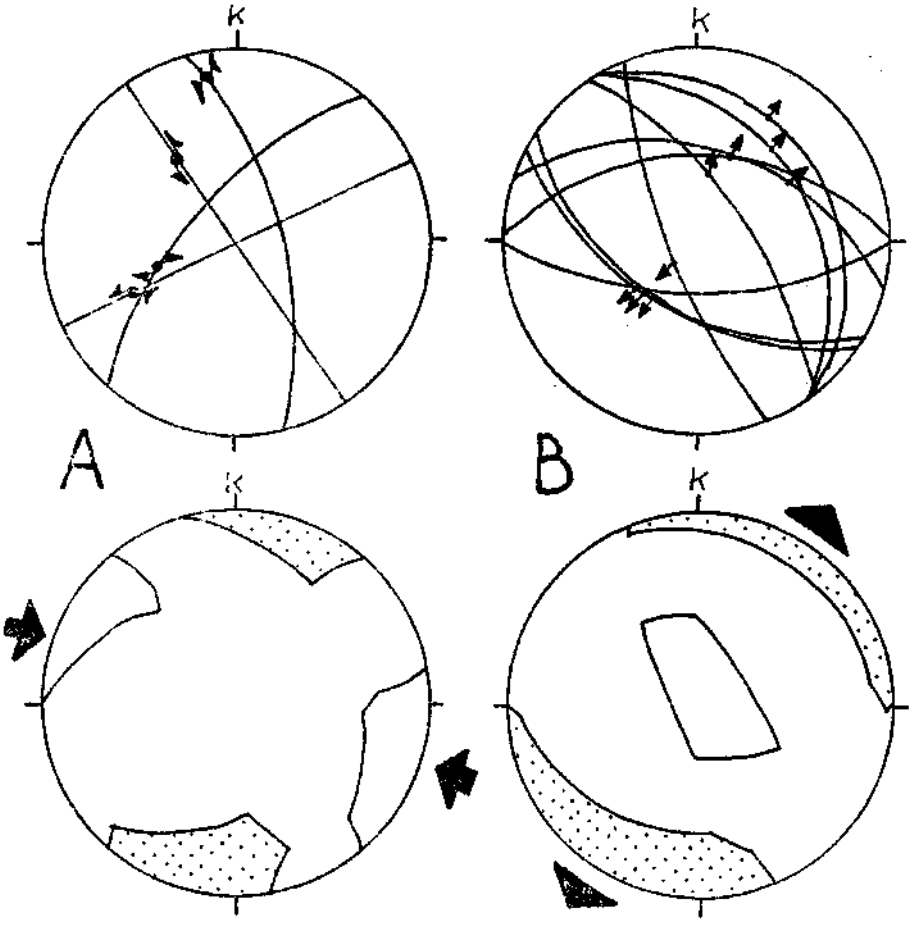

Fig. 2 - Faults formed at Sarayköy Sazak village in Upper Pliocene (upper part) and their solution by right-angle method. Dotted areas contain tension, and white areas compression directions. WNW - ESE compression at A, and NNE-SSW tension at B can be seen (Smith net, lower hemisphere).

Burdur

A lacustrine sequence, ranging in age from Pliocene to Pleistocene occurs on the eastern flanks of the Burdur graben (Bering, 1971). NE-SW trending left-strike faults have been observed in the Pleistocene sediments occurring in the vicinity of Günalan village (Dumont *et al.,* 1979). Results of measurements indicate that these faults have developed due to a N-S compression (Fig. 3). In another locality, the slickenside of the strike fault, developed as a result of the same movement, is intersected by a normal fault. Study of the slickenside described here, suggests the effects of a E-W tension. Evaluation of the fault developed within the Young Quaternary slope

debris unconformably overlying the Pliocene, also suggests the effects of a NW-SE tension. These results are in conformity with the seismotectonic results obtained by Ritsema (1974) and McKenzie (1976). Since it is clear that an entirely different tension must have been in effect in the Young Quaternary-Actual interval, the graben formation phase resulting from E-W tension, following a compression phase, should have taken place by Late Pleistocene or Early Holocene.

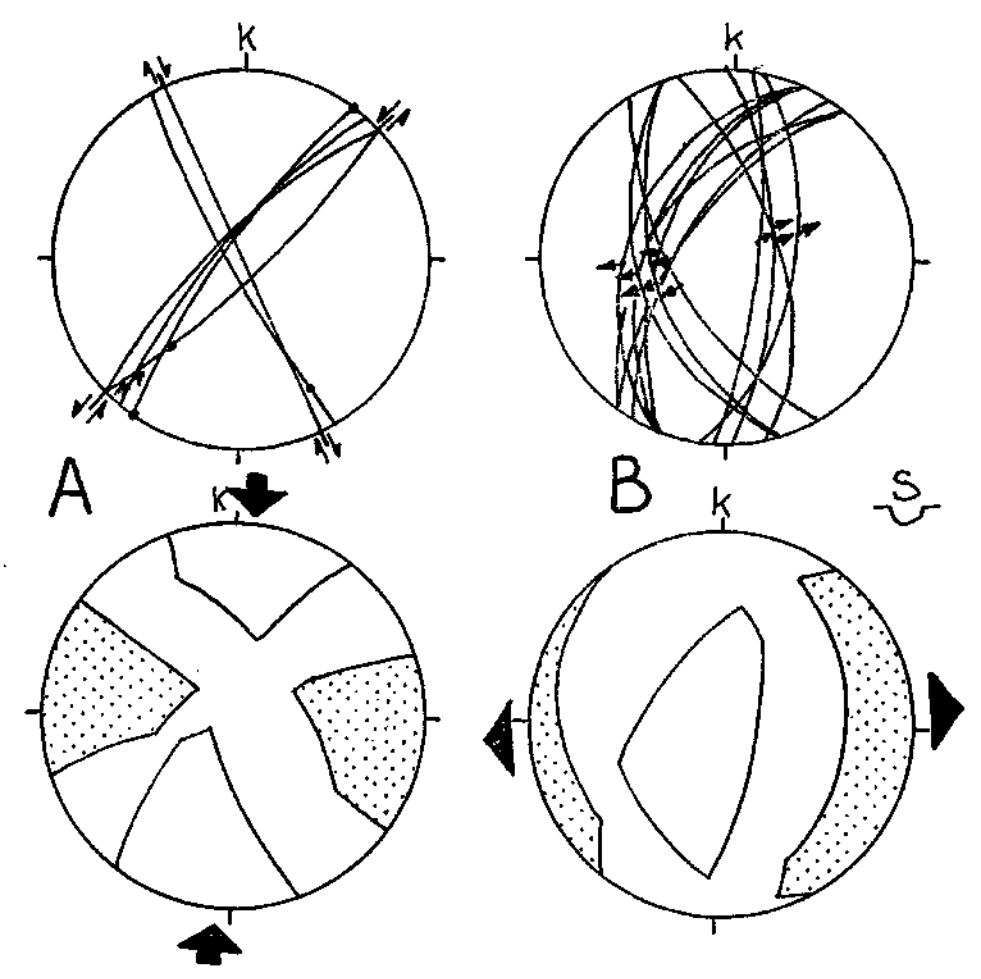

Fig. 3 - Faults formed at Burdur in Pliocene-Pleistocene (upper part) and their solution by right-angle method. Dotted areas contain tension and white areas compression directions. N-S compression at A and E-W tension directions at B can be seen.

ALTERNATING PHASES AND GRABEN FORMATION

Evaluation of results

On the basis of results obtained, it has been presumed that a compression phase must have prevailed prior to graben formation tectonics Previous studies on stratigraphy indicate that two major graben formation periods prevailed in Southwestern Turkey. The first period affecting SW Turkey has occurred during Uppermost Miocene (Becker Platen, 1970; Lüttig and Steffens, 1976) or

Lower Pliocene (Kastelli, 1972) and is followed by the second period, which mainly affected the Denizli and Burdur regions in Old Quaternary. Although other graben formation phases must have also occurred in SW Turkey, these shall not be covered here as it has been assumed that such phases were in fact a continuation of the previous periods or were produced by a totally different tectonic phenomenon, e.g. subduction mechanism (Le Pichon and Angelier, 1979). Furthermore, prior to the graben formation phases, compression tectonics must have prevailed in the region.

Conclusions to be drawn from the compression and tension directions observed in the area are as follows:

1. A compression phase, followed by a graben formation phase (tension) can be distinguished.

2. Directions of compression and tension phases are nearly perpendicular.

3. Compression tectonics are characteristically reflected by strikeslip faults; and since the effects produced by this phase are not strong, morphology of the area don not show substantial changes.

Mechanical explanation

Figure 4A shows maximum, medium and minimum compression directions in the case of compression tectonics. Figure 4B on the other hand, reflects a case where the tension tectonics are dominating. Here the maximum compression is reduced to medium compression, which in turn becomes the greatest compression observed. The effects of the tension phase (Graben formation) continue, even after the effects of the horizontal greatest compression do reach a termination point. It should however be noted that the region continues to undergo a homogenous movement, taking place on a regional scale, regardless the termination of the effects of the compression. Should this be the case, there shall be a conformity with the explanation given by McKenzie (1976) for grabens and the pattern suggested by the writers of the present paper.

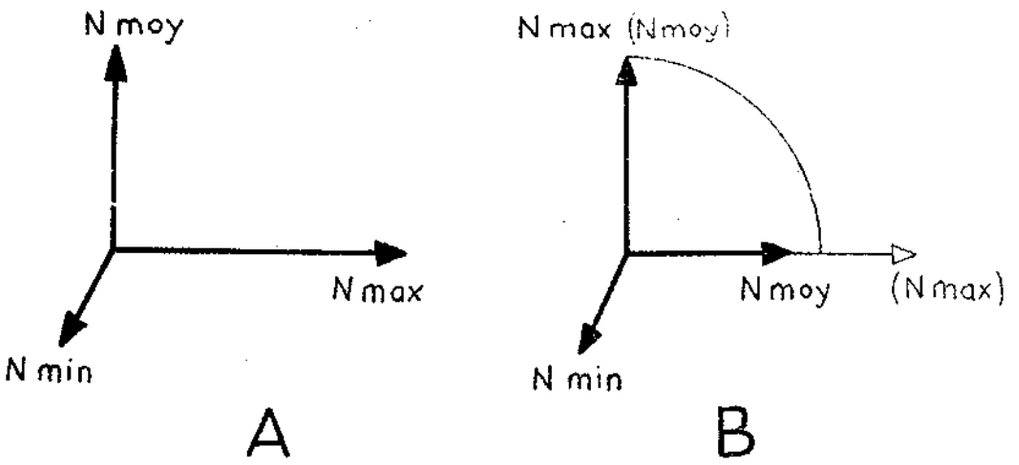

Fig. 4 - A - The figure indicates maximum, medium and minimum compression directions during the state at which compression tectonics is dominant; B - State at which tension tectonics is dominant: Maximum compression is decreased and turned to medium and medium compression of state A is maximum *now*. The effect of horizontal compression is then finished and tension effect (graben formation) is continued with an increasing importance.

DISCUSSION ON GRABENS - WESTERN TURKEY

McKenzie (1972) in a previous work on the plate tectonics, suggests that the grabens located in western Turkey, represent a transition zone between the Anatolian and Aegean plates. The same idea is further supported by Dewey and Şengör (1979). McKenzie in a later work (1976) suggests that complex tectonic features observed in the region are related to an ancient structure, since he does not consider the area located between the Anatolian arid Aegean plates a simple plate boundary. Workers such as Mercier (1977, p. 668), Angelier (1977b, p. 657), Lemeille *et al.,* (1977, p. 674) proved the presence of a number of faults in Anatolia and Greece as well, undergoing repeated movement. According to these workers, movement in some faults continue since Miocene.

Based on the results obtained it may be concluded that the oldest movement in the fault zones developed on the margins of the grabens, has occurred in the direction of strike (in case the basement rocks are observable). The writers further believe that such movements have occurred in Miocene or before (Efes, Muğla, Kovada Grabens). It is also observed that the grabens formed in the present region, follow previously developed fractures and may therefore be found throughout the area.

Taponnier (1977) considers graben formation as an equivalent of tension fractures developed parallel to the direction of compression in the metallurgical tests. Taponnier further claims that the grabens are surface indications of tension fractures developed parallel to the direction of compression in intracontinental regions.

It should however be noted that the region or continent to be affected from such a phenomenon, should be homogenous and unfractured. The writers of the present paper believe that the development of tension fractures in continents previously fractured and broken is impossible since movements will occur along the present fractures. Furthermore according to the pattern suggested, traces of compression, however locally, must have been left during graben formation. In fact no regional compression has been observed in the area. The area is characterized by the presence of a compression phase, followed by tectonics producing grabens.

IMPORTANT TECTONIC PHENOMENA TAKING PLACE IN THE UPPER MIOCENE-QUATERNARY INTERVAL

Late Miocene-Early Pliocene compression phase (Fig. 5A)

During the Late Miocene-Early Pliocene compression phase, the entire Aegean and Anatolian region is affected. Late Miocene-Early Pliocene compression tectonics taking place following the N-S to NW-SE trending Taurus compression phases have led to the development of an entirely new structural pattern (Poisson, 1977; Letouzey and Özer, 1978; Dumont, 1979). Some workers consider that the subduction of Aegean Arc during Plio-Quaternary is closely related to the compression phase referred above (Mercier, .1977; Angelier, 1977*a,b;* Dewey and Şengör 1979). In contrast to the northward movement of the Arabian plate due to left-lateral mdvement of the Levantin Fault and the divergence of the Red Sea, the compressional effects of the African plate were substantially subdued as a result of the left-lateral movement described above.

Eastern Turkey

Results obtained by Letouzey and Özer (1978) from micro-tectonic studies, show that in the Late-Miocene-Early Pliocene interval the compression directions in the Adana, Tarsus and Erzincan areas and Hatay and Mut had been NW-SE and E-W, respectively.

Southwest Turkey

Upper Miocene horizons of the Söke area (Becker Platen, 1970) are affected by a ENE-WSW trending compression phase, which resulted in the development of strikeslip faults. Efes and Muğla (Düğrek) faults are, believed to have been affected from this compression phase. To the N of Antalya ENE-WSW trending compression tectonics, leading to Late Tortonian-Early Pliocene thrusting, had prevailed (Poisson, 1977; Dumont *et al.*, 1979; Dumont, 1979).

Aegean Region

In various parts of the region, compression tectonics represented by Late Miocene-Pliocene overturned faults and strikeslip faults have been observed. A strong tectonic phase leading to the development of major overturned faults and thrusting has prevailed in the following localities-Istankoy (Kos) island (Jarrige *et al.,* 1976), Sakız (Chios) island and Nykoria (Lemeille *et al.*, 1977); Sisam (Samos) island (Angelier, 1976); Eube (Guernet, 1971);Zanti and Sefeloni islands W of Corinth Gulf (Sorel, 1976).

Lower Pliocene sediments occurring in the present region are believed to have been affected from this phase.

GRABEN FORMATION IN PLIOCENE (Fig. 5B)

Results obtained from stratigrafic and paleogeographic studies indicate that the graben formation in Southwest Turkey started in the interval between Late Miocene and Early Pliocene (Becker Platen, 1970; Bering, 1971; Kastelli, 1972). According to Leflef (1979, oral communications), sedimentological studies further support this conclusion. In the Efes and Söke areas, fault lines developed as a result of Late Miocene-Early Pliocene compression tectonics, are intersected by normal faults belonging to the graben formation phase. The formation of grabens in Western Turkey, had continued throughout Pliocene (Becker Platen, 1970; Mercier, 1977; Angelier, 1977); in Burdur and Söke areas however, this phase has not been so strong, the areas in question being rather characterized by paleogeographic changes (Bering, 1971). Mercier (1977) on the other hand notes that compression tectonics are absent in the Pliocene sediments occurring on the Sefaloni and Zanti islands (Western Greece) located on the western extension of the Aegean Arc.

OLD QUATERNARY COMPRESSION PHASE (Fig. 5C)

Old Quaternary compression tectonics, which differ from Upper Miocene-Lower Pliocene compression tectonics, can be observed in the region extending from Central Anatolia to Western Greece. The convergence of Arabian and Euro-Asian plates and African and Euroasian plates has produced considerable compressional effects.

Aegean Region and Greece

The region as a whole may be divided in two areas-Area I : In this area, comprising of the outskirts of the Aegean Arc (Preapulien zone, Rhodes and Crete islands) the compression direction is nearly perpendicular to the Aegean Arc (Angelier, 1977a and *b)* In the internal parts of the Aegean Arc, however, to the N of volcanic arc, the compression directions developed are diverse (Mercier, 1977).

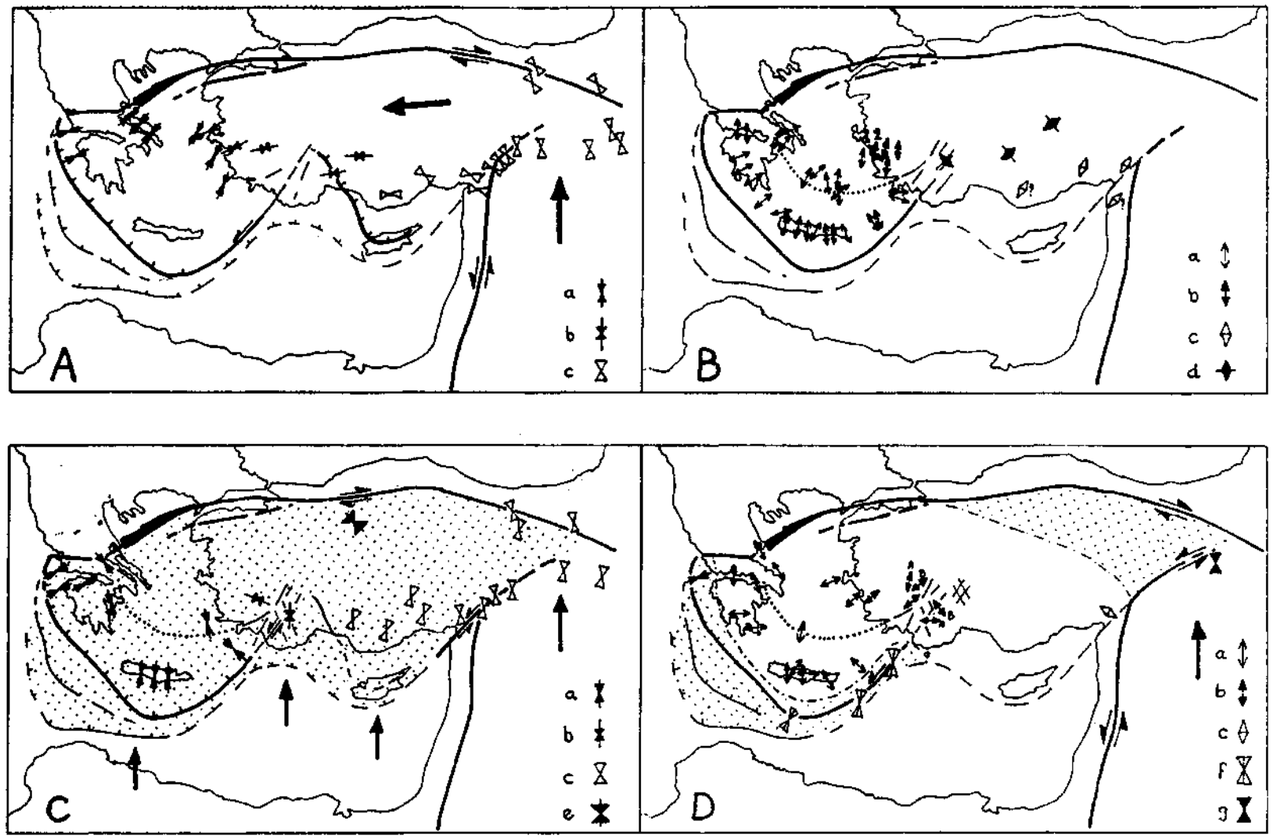

Fig. 5 - Tectonic compression and tension directions seen in Turkey from the end of Miocene until today;

a - Angelier, 1977a,b and Mercier, 1977; b - Dumont, 1979; Dumont *et al.*, 1979; Dumont *et* al., 1980; c - Letouzey and Özer, 1978; d - Tectonic directions according to general geological data; e - Nebert, 1958; f - Ritsema, 1979; McKenzie, 1978; g - Personal communication on Lice earthquake (with Arpat, E., 1976).

A - Compression tectonics phase of the end of Miocene-early Pliocene; large arrows show the movements directions of Arabian and Anatolian plates. B - Tension tectonics of the end of Pliocene; 1 - Tension direction at the beginning, 2 - Tension direction at Efes during the end of Pliocene is shown. Northern Anatolian Fault movements of Levantine and Southern Anatolian Faults and the subduction form couldn't be shown because of the unsufficiency of data. C - Old Quaternary (End of Pleistocene-Early Holocene); Compression tectonics. Whole of Aegean and Anatolian are under the effect of a N-S compression. D - Holocene and Today; Aegean subduction zone which is under a compression effect (Ritsema, 1974) and Eastern Anatolia which is effected by the compression of Arabian plate are the dotted regions. Tension tectonics is dominant at Aegean and Western Anatolia. There may be an alternation of compression and tension tectonics at the western cordon of the Northern Anatolian Fault.

Southwest Turkey

Old Quaternary compression tectonics are observed in the Burdur and Sarayköy areas. In contrast to the N-S striking compression in Burdur, Sarayköy area is characterized by a WNW-ESE compression. These two areas, located on the extension of the Aegean volcanic arc are divided from each other by a line extending from Gökova gulf to Çivril. The line mentioned here, is also referred to by Çağlayan *et al.*, (1980). Burdur area, like the outskirts of the Aegean Arc, is subject to the effects of the African and Euro-Asian plates converging in N-S direction. Compression in the Sarayköy area, shows a change of direction as shown in Figure 6, due to Gökova-Çivril line.

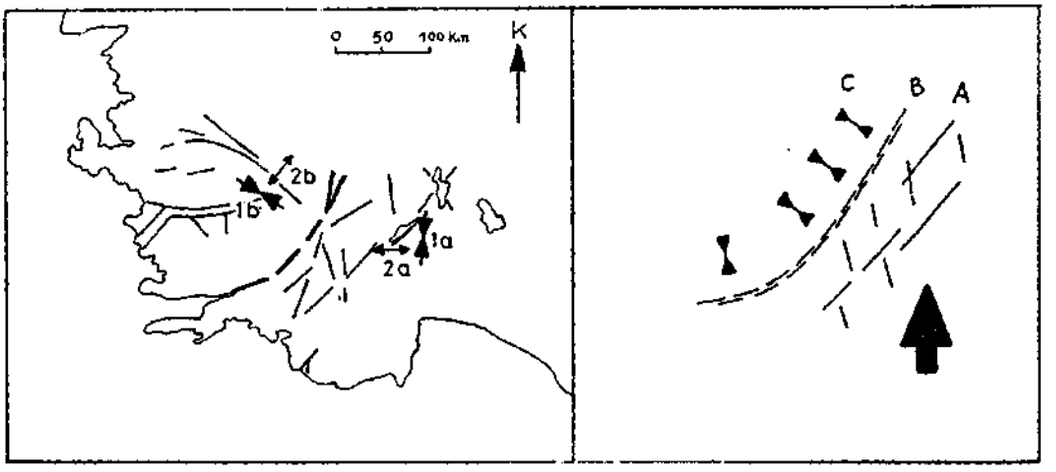

Fig. 6 - Compression tectonics (1) and following tension tectonics (2) at (a) Burdur and (b) Sarayköy-Sazak at left. Schematic drowing at right shows A: Burdur area which is under the influence of compression of African continent, B: Gökova-Acıgöl line which is on the continuation of Aegean volcanic arch and C: Inner Aegean region; compression direction changes because of line B, and it turns to a perpendicular direction to that line.

Central and Eastern Turkey

Compression direction in the Plio-Quaternary sediments occurring N of Alanya, in the İskenderun Gulf and Eastern Turkey is NNE-SSW. Compression tectonics in the surroundings of Ankara has produced thrusting (Nebert, 1958). NW-SE compression direction observed in this area, is conformable with the trend of the North Anatolian Fault.

QUATERNARY GRABEN FORMATION (Fig. 5D)

A new tectonic phase producing grabens has taken place in Young Quaternary. In Burdur area, the major tectonic phenomena, i.e. graben-formation, has occurred in Late Pleistocene or Early Holocene (Bering, ,1970), resulting from E-W trending tensional effects. In Sarayköy area however, NNE-SSW trending tension and graben formation phase have occurred synchronously. Graben formation which started in Young Quaternary is known to continue to actual times (Arpat and Şaroğlu, 1975; Arpat and Bingöl, 1969). Faults affecting Young Quaternary sediments have diverse trends, i.e. NE-SW in Pamukkale and Kuşadası, NW-SE in Burdur (Dumont *et al.,* 1980). Based on the results obtained from seismotectonic studies, the direction of tension in the Menderes

Massive is determined to be NE-SW (Ritsema, 1974; Papazachos and Komnihakis, 1977). McKenzie (1976) however, states that the area discussed, here, is subject to the effects of a NNE-SSW trending tension. The same writers have further established the presence of a NW-SE trending tension in the Burdur area. Results of the seismotectonic studies covering Menderes and Burdur areas, are in conformity with the tension directions determined in Young Quaternary sediments. .

According to Nebert (1958) Old Quaternary compression phase was followed by tectonics producing grabens in Central Anatolia. In the İskenderun area as well the Old Quaternary compression tectonics are followed by a NW-SE tension (Letouzey and Özer, 1978) direction, which is perpendicular to the previous tension direction.

CONCLUSIONS

Evaluation of the results obtained from regional studies show that the entire Aegean region and Anatolia is affected from Miocene-Pliocene compression phase followed by Pliocene graben formation and Old Quaternary compression phase followed by Quaternary graben formation. It is thus evident that grabens are formed within an alternating compression and tension pattern. The region indicated with dots in Figure 5C, shows areas subject to compression. During Old Quaternary, the entire Aegean region and Anatolia has been subject to compressional effects. At present however, only the Aegean Subduction Zone (Fig. 5D) (Ritsema, 1974) and S9me parts of Eastern Turkey, which are directly affected by the movement of the Arabian plate, are continuously subject to the effects of compression. In regions such as Aegean, Western and Central Turkey, tension tectonics prevail, with compression tectonics being taking place only very locally.

Manuscript received July 3, 1980

Translated by: Filiz E. DİKMEN

BIBLIOGRAPHY

Anderson, E.M., 1942, The Dynamics of Faulting: Oliver and Body, Edinburgh, 206.

Angelier, J., 1976, Sur l'alternance Plio-Quaternaire des mouvements extensifs et compressifs en Egee orientale; Tile de Samos (Grece): C.R. Acad. Sc. Paris, 283, 463-466.

———, 1977a, Sur l'evolation tectonique depuis le Miocene superieur d'un arc insulaire mediterranean: l'arc Egeen: Rev. Geog. Phys. Geol. Dyn., XIX, 3, 271-294, Paris.

———, 1977b, Essai sur la neotectonique et les derniers stades tarditectoniques de l'arc egeen, et de l'Egee meridionale: Bull. Soc. Geol. France, XIX, 651-662.

———, 1979, Determination of the mean principal directions of stresses for a given fault population: Tectonophysics, 56, T17-T26.

———and Mechler, P., 1977, Sur une methode graphique de recherche des contraintes principales egalement utilisable en tectonique et en seismologie: la methode des diedies droits: Bull. Soc. Geol. France, (7), XIX, 6, 309-1318.

Angelier, J., and Goguel, 1978, Sur une methode simpfe de determination des axes principaux des contraintes pour une population de failles: C.R. Acad. Sci. Paris, 288, 307-310.

Arthaud, F., 1969, Methode de determination graphique des directions de raccourcissement, d'allongement etintermediare d'une population de failles: Bull. Soc. Geol. France, (7), XI, 729-737.

Aubouin, J., 1973, Des tectoniques superposees et de letir signification par rapport aux modeles geophysiques: l'exemple des Dinarides; pal£otectonique, tectonique, tarditectonique, neotectonique: Bull. Soc. Geol. France, (7), XV, 426-460.

———, 1977, Mediterrande orientale et Mediterranee occidentale: Esquisse d'une comparaiscn du cadre alpin: Bull. Soc. Geol. France, (7), XIX, 421-435.

Arpat, E. and Bingöl, E., 1969, The rift system of the western Turkey throughts on its development: M.T.A. Bull., 73, 9.

———and Şaroğlu, F., 1975, Türkiye'deki bazı önemli genç tektonik olaylar: Türkiye Jeol, Kur. Bült, 18,1, 91-101.

Becker Platen, J.D., 1970, Lithostratigraphische Untersuchungcn im Kanozoikum südwest Anatolien(Turkei): Beih. Geol. Jb. 97, 244, Hannover.

Bering, D., 1971, Lithostratigraphie, Entwicklung and Seegeschichte des neogenen und quartaren intramontanen Becken der pisidischen Seenregion (Südanatolien): Beih. Geol. Jb. 101, Hannover.

Carey, E. and Brunier, B., 1974, Analyse theorique et numerique d'un modele mecanique elementaire applique a 1'etude d'une population de Failles: C.R. Acad. Sc. Paris, 279, 891-894.

Çağlayan, A.M.; Öztürk, E.M.; Öztürk, Z.; Sav, H. and Akat, U., 1980, Menderes masifi güneyine ait bulgular ve yapısal yorum: Jeo. Müh. Derg., 10, 9-17.

Dewey, J.F. and Şengör, A.M.C., 1979, Aegean and surrounding regions complex multiplate and continuum tectonics in a convergent zone: Geol. Soc. Am. Bui., 90, 84-92.

Dumont, J.F., 1979, Les deformations tectoniques superposes posterieures aux nappes Cretacees dans la coupole de Karacahisar au nord-est de Tangle d'lsparta (Taurides Occidentales, Turquie): C.R. Som. Soc. Geol. France, Fasc. 3, 13(5-139.

———; Pisson, A. and Şahinci, A., 1979, Sur 1'existence de coulissements senestres regents a 1'extre'mite' orientale de 1'arc egeen (sud-Ouest de la Turquie): C.R. Ac. Sc. Paris, 289, 261-264.

———; Uysal, Ş.; Şimşek, Ş.; Karamanderesi, İ.H. and Coşkun, S.B., 1980, Türkiye'nin Güneybatısında Üst Miyosen'den günümüze kadar görülen tektonik basınç ve çekimleri: 34. T.J.K. Bilimsel and Teknik Kurultayı, Ankara.

Erinç, S., 1955, Orta Ege Bölgesinin jeomorfolojisi: Maden Tetkik Arama Enst. Rap., 2217, Ankara.

Guernet, Cl., 1971, Etudes geologiques en Eubee et dans le regions voisines (Grece): These Doctoral Sci. Nat,, Universite de Paris, 395.

Graciansky, P.C. de, 1972, Recherches geologiques dans le taurus Lycien occidental: These, Universite de Paris-Sud, Orsay.

Jarrige, J.J.; Angelier, J.; Bousquet B.; Keravdren, B. and Mercier, J., 1976, Les deformations mio-plio-pleistocenes a Kos (arc egeen interne oriental) (resume): 4^{e} Reun. Ann. Sc. Terre, Paris, 232.

Kastelli, M., 1972, Denizli, Sarayköy, Tekkehamam kaplıcası civarının jeolojik etüdü ve jeotermal alan olanakları: Maden Tetkik Arama Enst., Rap., 5744, Ankara.

Lemeille, F.; Gauthier, A.J.; Jarrige, J.J. and Philip, H., 1977, Evolution neotectonique du domaine egeen et de sa bordure externewientale, une mise au point: Bull. Soc. Geol. France, (7), XIX, 673-677.

Le Pichon X. and Angelier, J., 1979, The Hellenic arc and Trench system: a key to the neotectonic Evolution of the Eastern Mediterranean Area: Tectonophysics, 60; 1-42.

Letouzey, J. and Özer, B., 1978, Analyse structurale et etude des photos satellite en Turquie orientale au Nord de la plate-forme Arabique: Rapport Institut Franfais du Petrole, 258551 (unpublished).

Lüttig, G. and Steffens, P., 1976, Explanatory notes for the Paleogeographic Atlas of Turkey from the Oligocene to the Pleistocene: Bund. fur. Geow. und Rahst. 64, Hannover..

Mercier, J.L., 1977, L'arc egeen, une bordure deformee de la plaque eurasiatique; reflexions sur un exemple d'etude neotectonique: Bull. Soc. Geol. France, (7), XIX, 663-672.

McKenzie, D.P., 1972, Active Tectonics of the Mediterranean region: Royal Astronomical Society Geophysical Journal, u. 30, 109-185.

———, 1976, Can plate Tectonics describe continental deformation. In: Structural History of Mediterranean Basins: Ed. Technip.

Nebert, K., 1958, 19 Anadolu'nun en genç Jeolojik Tektonik olayı hakkında bir etüt. Ankara vilayetinin (Kayı-Bucak) civarındaki Wallachien orojenez safhasının ispatı: Maden Tetkik Arama Enst. Rap., 50, 16-29.

Papazachos, B.C. and Comninakis, P.E., 1976, Modes of lithospheric interaction in the Aegean Area. In: Structural History of the Mediterranean Basins: Ed. Technip. 319-331.

Poisson, A., 1976, Essai d'interpretation d'une transversale Korkuteli-Denizli (Taurus Quest Anatolien). Bull. Soc. Geol. France, (7), XVIII, 499-510.

———, 1977, Recherches geologiques dans les Taurides Occidentals: These, Universitfi de Paris-Sud, Orsay.

Ritsema, A.R., 1974, The earthquake mechanisms of the Balkan region: Roy. Nether 1. Meteorl. Inst. De. Bult., Scientif. Rep., 74-4, 36.

Sorel, D., 1976, Tectonique et neotectonique dc la zone preapulienne: Bull. Soc. Geol. France, (7), XVIII, 187-188.

Taponnier, P., 1977, Evolution tectonique du Systeme alpin en Mediterranee: Bull. Soc. Geol. France, (7), XIX 437-460.

DETERMINATION OF ZIRCONIUM IN BROOK SEDIMENTS BY XRF SPECTROSCOPHY

Saim ÖZKAR, Tanıl AKYÜZ, Ercan ALPARSLAN and Macide TÜRKALP

Mineral Research and Exploration Institute of Turkey, Ankara

ABSTRACT.— For the determination of zirconium by X-Ray fluorescence spectroscopy in the enriched samples taken from the Sart gold research area, a new method in which rubidium is first used as an internal standard has **been** suggested. The concentrations provided by this new method in the determination of zirconium in the brook sediments and the results obtained by wet chemical analysis show (exhibit) a good conformity.

INTRODUCTION

Zirconium research works were not given the necessary importance in Turkey. Zirconium was occasionally included in some heavy mineral research studies. Recently, it has also taken place among the heavy mineral considered during the gold studies carried out in Sart area. According to this project, the determinations of zirconium and some other elements have been requested in the 47 enriched brook sediment samples taken from various parts of the area. By making use of semi-quantitative results obtained by the optical emission spectrography, the elements of these samples that are in adequate amounts for final determinations have been specified. The determinations of chromium, titanium, lanthanum and thorium elements have been made by ordinary (usual) methods.

There has not been a (particular) fixed method in the XRF spectroscopy suitable for obtaining rapid results concerning the zirconium determination in the samples that are of unusual structures and contents and also seen for the first time. By considering the facts that the interest in zirconium will increase and consequently a large amount of samples will be confronted in future, the suggestion (proposal) of a new method of analysis that will provide rapid and reliable results for zirconium determination studies by XRF spectroscopy has been appreciated.

DETERMINATION OF ZIRCONIUM IN BROOK SEDIMENTS

In the determination of zirconium by X-Ray fluorescence spectroscopy, the relation between the intensity of ZrK pig and the zirconium concentration of the sample is used (Albany, 1952). If the matrices of the samples and standards measured are not completely different, this relationship is directly proportional. But, since the analysis pig will be affected in a different way from the matrix does in the samples that have different structures and contents, the relationship may lose its proportionality which leads to (causes) wrong results of analysis. Due to the structure of the matrix, deviation from the direct proportionality may be observed as positive or negative. One of the best ways used to minimize the faults caused by the effect of matrix is the internal standard method (Adler, 1955). Although elements such as molybdenum (Brooks, 1970) and niobium (Hakkila, 1964) are used as internal standards for zirconium determination, since the brook sediments contain these elements in various proportions, it is impossible for them to be used as internal standards in the zir-

conium determination of the brook sediments. By the literature studies in which the criteria concerning the selection of the internal standard (Alparslan,1976) have been considered, it has been clear that rubidium can be used as internal standard element in the analysis of this type of broot sediment samples that have a different structure. It is obviously impossible for rubidium to be originally present in the brook sediments for all its compounds are soluble in water. Rubidmm provides the other necessary conditions to be used as internal standard element in the determination of zirconium. As a matter of fact, by preliminary test, it has been concluded that rubidium may be used as an appropriate internal standard element in the zirconium determination of samples taken from brook sediments of different structures.

The samples and the standards have been prepared by melting methods (Hooper, 1969). Two seperate mixtures of 1.2 % and 6.0 % RbCl concentrations have been obtained by dissolving the chlorure salt of rubidium in water, which is chosen as the internal element for zirconium, and by letting it absorb the melting substance, i.e. lithium tetraborate ($Li_2B_4O_7$). 100 mg of the sample or the appropriate standard prepared was added to the 1000 mg part taken from one of these mixtures and they have been melted in 1100°C for 20 minutes. The beads formed by cooling were increased to 1500 mg by the addition of binder cellulose and they have been ground less than 200 mesh and molded as tablets by pressing. As standards were being prepared, a mixture sythesized by making use of semi-quantitative results obtained by the optical emission specktra of the samples was used. In certain amounts fine-powdered ZrO_2 (spex) was added to this mixture which has a similar matrix to that of the samples, and a series of standards, concentrations known, have been obtained.

The measurements of the standards and the tablet shaped samples were made by the SPC-S vacuum spectrometer of the General Electric Company. The working conditions are given in Table 1.

Table 1 - The measurement conditions in which rubidium is used as internal standard element for zirconium determination in the brook sediment samples

Crystal	: Fibril
Anticathode	: W
Tube tension	: 50 KV
Tube flux intensity	: 40 mA
Crack width	: 1.27 mm
Duration of measurement	: 20 seconds
Pressure	: Vacuum
Tension of counter	: 1240 V
Space between windows	: 2-6 V
Angles (2θ)	: ZrK_α = 31°.55
	RbK_α = 37°.40
	RbK_β = 33°.20

As internal standard pigs that may be added to ZrK_a (20 = 31°.55) which has been selected as analysis pig, RbK_a(20 = 37°.40) in 1.2 % RbCl concentrated samples and standards and RbK_b (20 = 33°.20) pig in 6.0 % RbCl concentrated samples and standards have been measured. By the evaluation of the measurement results, the pig intensity ratios of $IZrK_a$ / $IRbK_a$ and $IZrK_a$ / $IRbK_b$ have been formed. By making seperate graphs of these proportions against the zirconium concentrations of the standards, two working curves have been obtained.

The spectra of 6.0 % RbCl concentrated standard when RbK_b pig is measured as internal standard are shown in Figure 1. Although the ZrK_a and RbK_b pigs are to each other within the seperative limits of the spectrometer, they do not affect one another in the concentration interval designated in Figure 1. By preparing graphs of $IZrK_a$ / $IRbK_b$ intensity ratios taken from this spectrum and the zirconium concentrations of the standards, a working curve, correlation coefficient 0.999, has been obtained (Fig. 2). But, as the zirconium concentration increases, ZrK_a pig gets larger in equal proportion and affects the RbK_b pig. As a result of this, RbK_b pig seems to be larger than it is and the $IZrK_a$ / $IRbK_b$ intensity ratio decreases. And this results in a negative deviation in the highly concentrated part of the working curve. The working curve, seen as a straight line up to 1.5 % ZrO_2 concentration, bends towards the horizontal axis in the concentrations above the boundary (limit). The RbK_a pig which is considered to give better results for the concentrations above this limit takes place in the spectrum some distance from the ZrK_b pig that enables it not to be affected by all the concentrations. The spectra of 1.2 % RbCl concentrated standards in which RbK_a pig is taken as internal standard are shown in Figure 3. The working curve obtained by the preparation of the graph of $IzrK_a$ /$IRbK_a$ pig intensity ratio taken from this spectrum against the ZrO concentrations of more than 1.5 % is a straight line and the correlation coefficient is 0.996 (Fig. 4). As it is seen, in the part bearing high zirconium concentrates in which negative deviations are observed in the pig intensity ratio $IZrK_a$ / $lRbK_a$, the working curve has been formed as a straight line without any deviations, the intensity ratio $IZrK_a$ / $IRbK_b$ has been used.

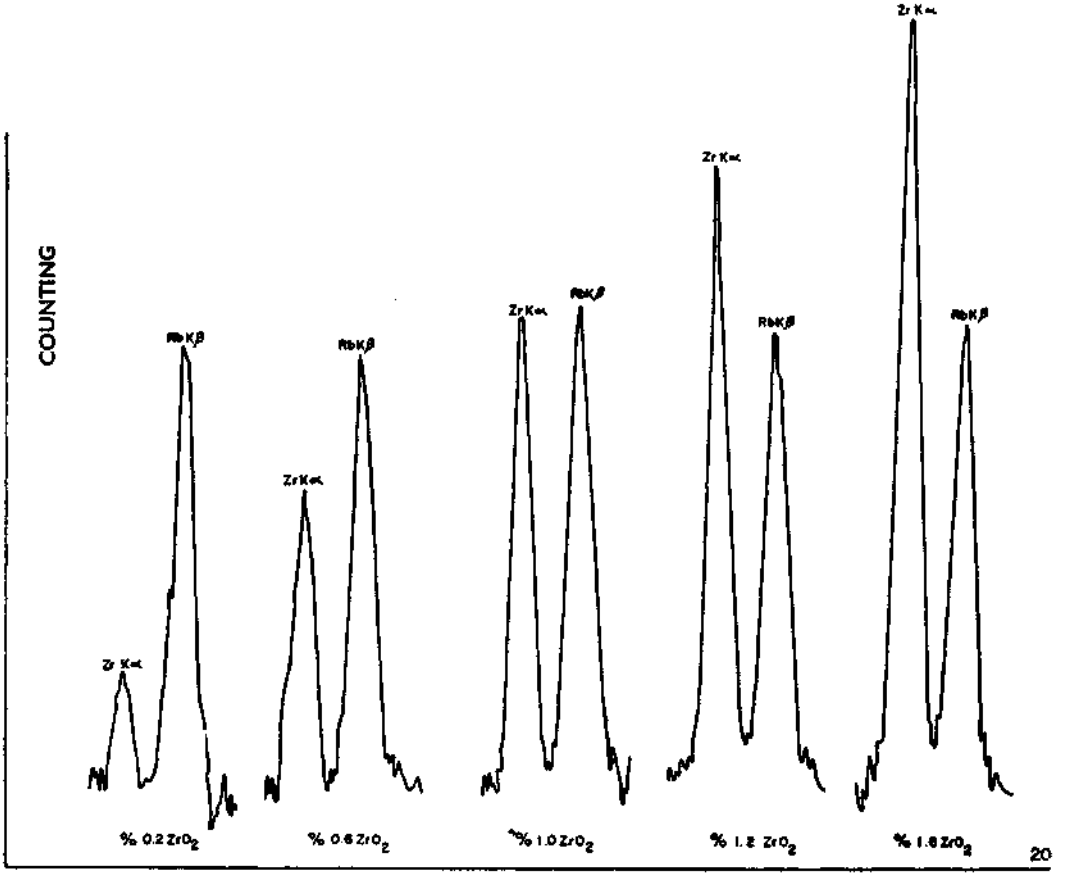

Fig. - 1

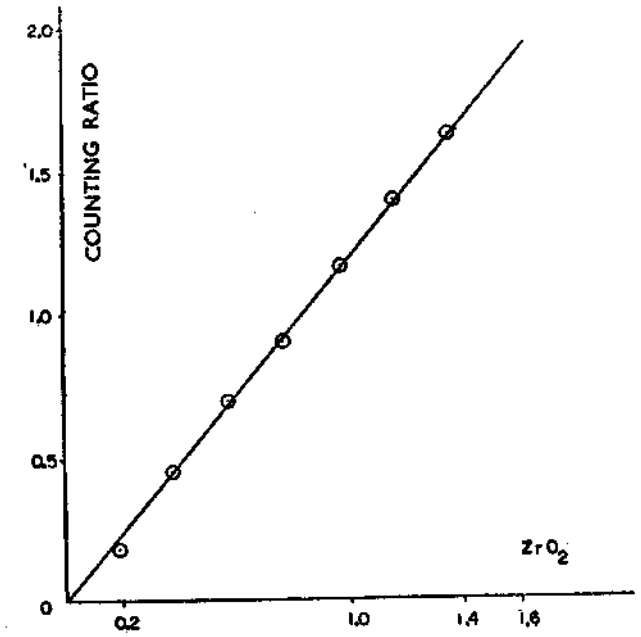
COUNTING RATIO
2.0
1.5
1.0
0.5
0
0.2
1.0
1.4
1.6
ZrO2

Fig. 2 -

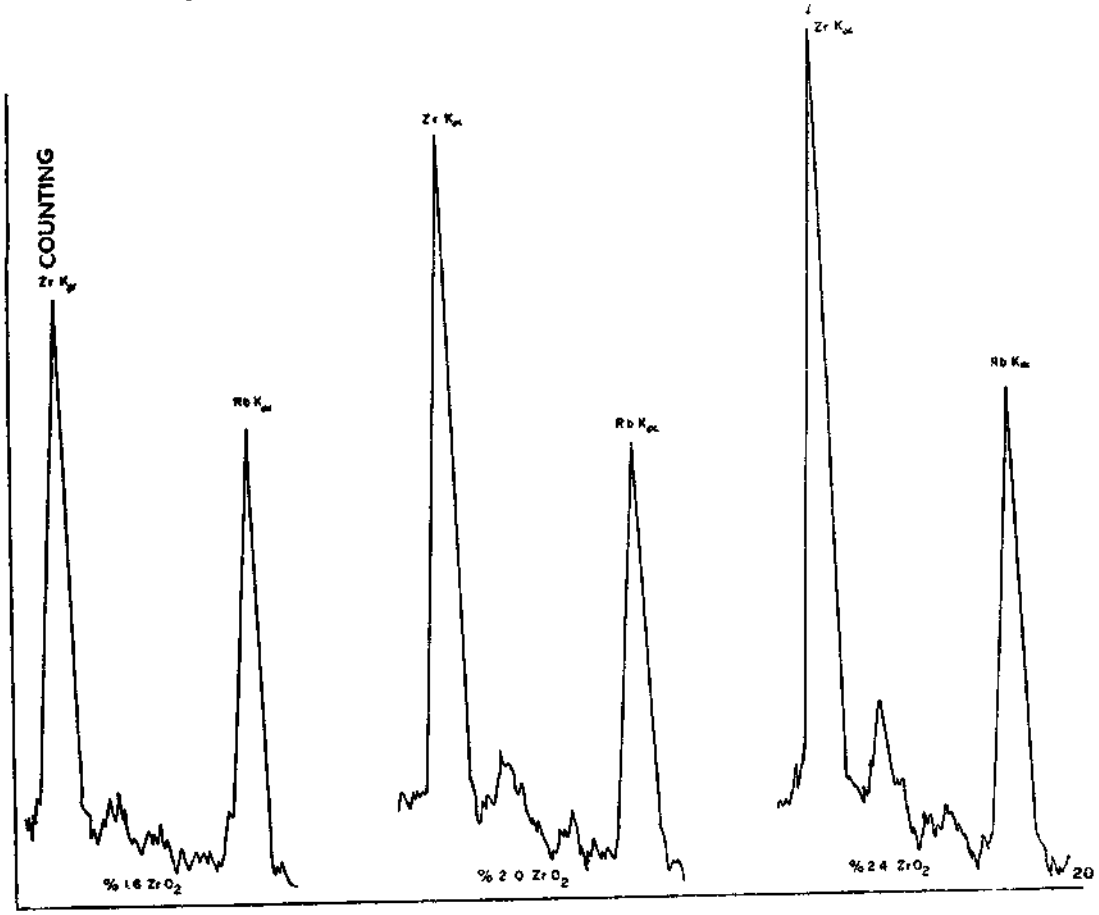
COUNTING
Zr Kα
Rb Kα
% 1.6 ZrO2
% 2.0 ZrO2
% 2.4 ZrO2
20

Fig. 3 -

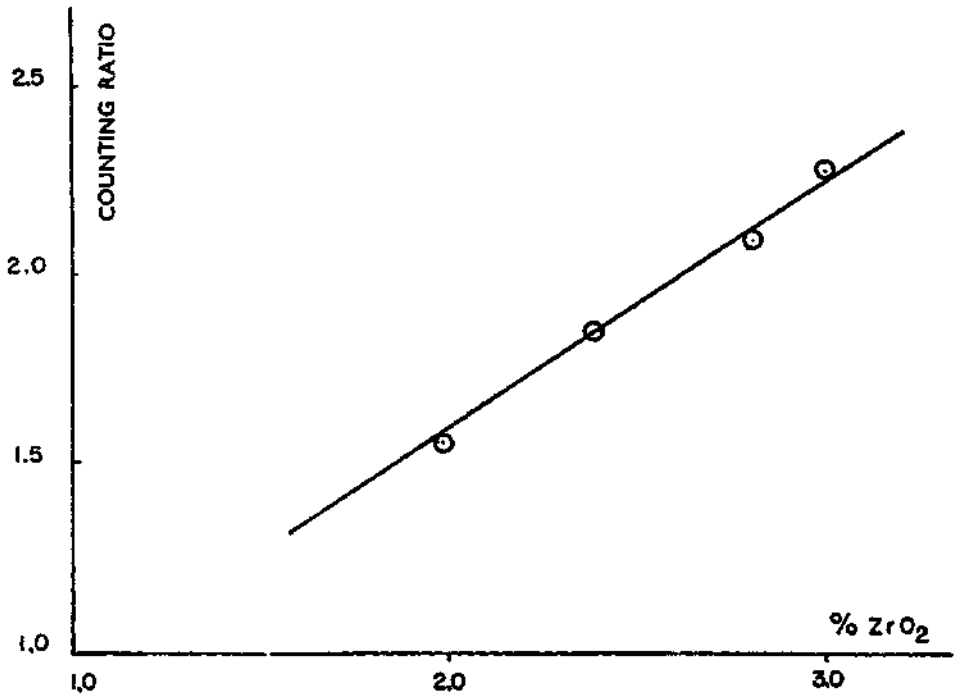

Fig. 4 -

RESULTS

The zirconium concentrates of the samples have been determined by making use of one of the working curves according to their zirconium contents and pig intensity ratios obtained by measurements. Results obtained by this method display a great difference from the values obtained by measurements in which no internal standards have been used. The values provided by wet chemical analysis of 5 brook sediment samples containing different amounts of zirconium, show a better conformity with the zirconium concentrates obtained by the new method in which rubidium has been as the internal standard. Table 2. shows merely the analysis results of 5 brook sediment samples of which chemical analyses are completed.

Table 2 - The zirconium concentrates of 5 brook sediment samples provided by XRF, chemical analyses done (as ZrO_2 %)

Sample no.	*Without internal standard*	*With internal standard*	*Chemical analysis*
1	2.66	3.06	3.00
2	0.95	1.20	1.28
3	1.88	2.18	2.16
4	0.78	0.90	1.00
5	0.27	0.39	0.45

In this method, the corruptive elements that may influence the zirconium analysis results may be U, Pb, Bi, Pt, Au, Te, Y, Hf. But, according to the results obtained by the semi-quantitative results of the optical emission spectrograph of the brook sediment samples analized, none of these elements is of enough amount to affect the analysis pigs. A new analysis method which provides rapid and reliable results easily applicable to samples of different structures and contents such as brook sediments and in which rubidium is for the first time used as internal standard for low and high zirconium concentrates, has been suggested in the present article.

ACKNOWLEDGEMENTS

The authors would like to thank Mr. Fahrettin Çokgürses, Chemical Engineer (M.Sc.), who has carried out the wet chemical analyses and also to Mr: Şahin Taş, Physical Engineer (M.Sc.), who has carried out the semi-quantitative emission spectrograph analyses.

Manuscript received May 4, 1978

Translated by: Esin ERDEM

REFERENCES

Adler, I. and Axelrod, J.M., 1955, The preparation of fused samples in x-ray fluorescence analysis. Spectrochim Acta., 7,91.

Albany, N.Y., 1952, The determination of zirconium by XRF. J. Opt. Soc. Am., 42,673.

Alparslan, E.; Akyüz, T. and Saltoğlu, T., 1976, X ışınları floresans spektrometresinde iç standart kullanılarak yapılan, Ba, Sr, Fe nikel analizleri. Spektroskopi Derg., 2, 67-72.

Brooks, G.K., 1970, Concentration of zirconium and hafnium in some igneous and metamorphic rocks and minerals. Geochim. Cosmochim. Acta, 34, 411-416.

Hakkila, E.A.; Hurley, R.G. and Waterbury, G.R., 1964, x-ray fluorescence spectrometric determination of zirconium and molybdenum in the presence of uranium. Anal. Chem., 36, 2094.

Hopper, P.R. and Atkins, L., 1969, The preparation of fused samples in x-ray fluorescence analysis. Mineralogical Mag., 37, 409-413.

BAKIR-ÇİNKO-KURŞUN KARIŞIK KONSANTRELERİNİN SÜLFATLAŞTIRICI KAVURMA VE ÇÖZELTME YÖNTEMİYLE ÜRETİM OLANAKLARI ÜZERİNE BİR ARAŞTIRMA

Yavuz AYTEKİN

Ege Üniversitesi Maden Mühendisliği Bölümü, İzmir

ÖZ. — Doğu Karadeniz Bölgesindeki kurşun-çinko-bakır ve diğer faydalı metallerden en az birkaçını içeren kompleks cevherler üzerinde yapılan cevher hazırlama laboratuvar çalışmaları, bu cevherlerden yüksek bîr verim ve yeterli bir konsantre tenörü ile ancak karışık konsantre üretimlerinin mümkün olduğunu ortaya koymuştur. Bu nedenle de doğrudan karışık konsantrelerden metal üretimi için çalışmalar önem kazanmıştır.

Yapılan sülfatlayıcı kavurma ve bunun peşinden çözeltme deneyleriyle konsantrenin mekanik ön hazırlanması ve uygun şartlarda kavrulması sonunda içerisinde bakır ve çinkoyu yüksek bir verimle ve selektif olarak çözeltiye almanın mümkün olduğu görülmüştür. 400°C civarındaki bir sülfatlayıcı kavurmadan sonra bakırın % 97 si, 650°C civarındaki bir kavurmadan sonra ise çinkonun % 95 i selektif olarak çözeltiye alınabilmektedir. Elde edilen çözeltiler ayrı ayrı bakır ve çinko elektroliz işlemlerine uygundur. Sistemin bu büyük üstünlüğünün yanı sıra, kavurma dolayısiyle çıkan kükürt gazlarını zararsız hale getirme zorunluğu, sakıncalı tarafıdır.

Elde edilen deneysel sonuçlara göre bir prensip akım şeması verilmiştir.

GİRİŞ

Türkiye için büyük önemi olduğu bilinen Doğu Karadeniz Bölgesindeki kompleks bakır-çinko-kurşun cevherlerinin işletilebilmesi için gerekli ön çalışmalar son birkaç yıldır sürdürülmektedir (Addemir, 1977; Akdağ, 1979; Akın ve Erden, 1977; Aytekin, 1973a ve *b,* 1976, 1977 ve 1978). Doğu Karadeniz Bölgesindeki, ekonomik oldukları Maden Tetkik ve Arama Enstitüsünün raporlarına göre ortaya çıkmış olan veya henüz üzerinde çalışmalar yapılan yahut ileride yapılacak olan yataklardaki kompleks cevherleşmelerin, cevher hazırlama tekniği yönünden (mineral içerikleri, minerallerin tane irilik dağılımları ve giriftlikleri bakımından) büyük benzerlikler gösterdiği de ortaya konmuştur (Aytekin, 1973a; Unan, 1971). Laboratuvar çapında yapılan çalışmalar, bu cevherlerin özel şartlar altında flotasyon yoluyle zenginleştirilmelerinin belli bir aşamaya kadar mümkün olduğunu göstermiştir (Aytekin, 1976). Bu cevherlerden yüksek bir metal verimiyle (bakır için % 92, çinko ve kurşun için % 96) karışık konsantre üretmek mümkün olmaktadır. Ancak seçkin flotasyon denemeleri doyurucu sonuçlar vermemiştir. Seçkin metal verimi bakır için % 81, çinko ve kurşun için % 67 civarında kalmıştır. Diğer taraftan elde edilen karışık konsantrelerin mevcut pirometalurjik yöntemlerle işlenemeyeceği anlaşılmıştır (Aytekin, 1976; Berg ve Pape, 1978; Çakır, 1976; Gack, 1978; Lindner, 1966; Pawlek, 1977).

Dolayısıyle bu cevherlerin zenginleştirme işlemlerinin tamamlanabilmesi için yaş kimyasal hazırlama yöntemlerinin denenmesi zorunluğu ortaya çıkmıştır. Bu amaçla yapılan deneyler ve bunların sonuçlarından, burada yalnızca bir kısmı, sülfatlaştırıcı kavurma ve onu takiben çözeltme (liçing) yöntemiyle yapılan deneyler ve elde edilen sonuçlar özetlenecektir.

MALZEME VE YÖNTEM

Numune

Ön deneylerde kullanılan konsantrenin kimyasal bileşimi ve bu konsantreden yapılan elek analizleriyle bu elek aralıklarının kimyasal analizlerinin sonuçlan Tablo 1 de özetlenmiştir. Aynı karışık konsantrenin söz konusu elek aralıkları mineral bileşimi ve dağılımı Tablo 2 de gösterilmiştir.

Bu karışık konsantrenin komple analizi şöyledir: % 12.27 Cu, % 12.68 Zn, % 23.78 Pb, % 15.35 Fe, % 35.73 S, % 0.42 Si, % 0.0034 Co, % 0.085 Ca, 211 gr/t Ag, 47.6 gr/t Au. Kavurma işleminden sonra her bir çözeltme deneyi için saf suda ve sülfürik asitte çözünen ve artıkta kalan bakır ve çinko analiz değerlerinden elde edilen aritmetik ortalamalara göre konsantre % 12.63 Cu, % 11.25 Zn içermektedir. Bu değerler hata sınırı içinde kabul edilebilmektedir.

Yapılan çok sayıdaki ön deneylerin bir kısmında ve optimal şartların saptanması maksadıyla yapılan deneylerde bu konsantre kullanılmıştır.

Araştırma düzeneği

Kavurma işlemleri, 1000 mm uzunluğunda ve 270 mm çapındaki W.C. Heraus GmbH-Hanau Firmasına ait laboratuvar kavurma fırınının ortasına yerleştirilmiş olan 30 mm iç çapındaki ateşe dayanıklı boru içerisinde yapılmıştır (Şek. 1). Bu borunun içerisine ve orta yerine numuneler,

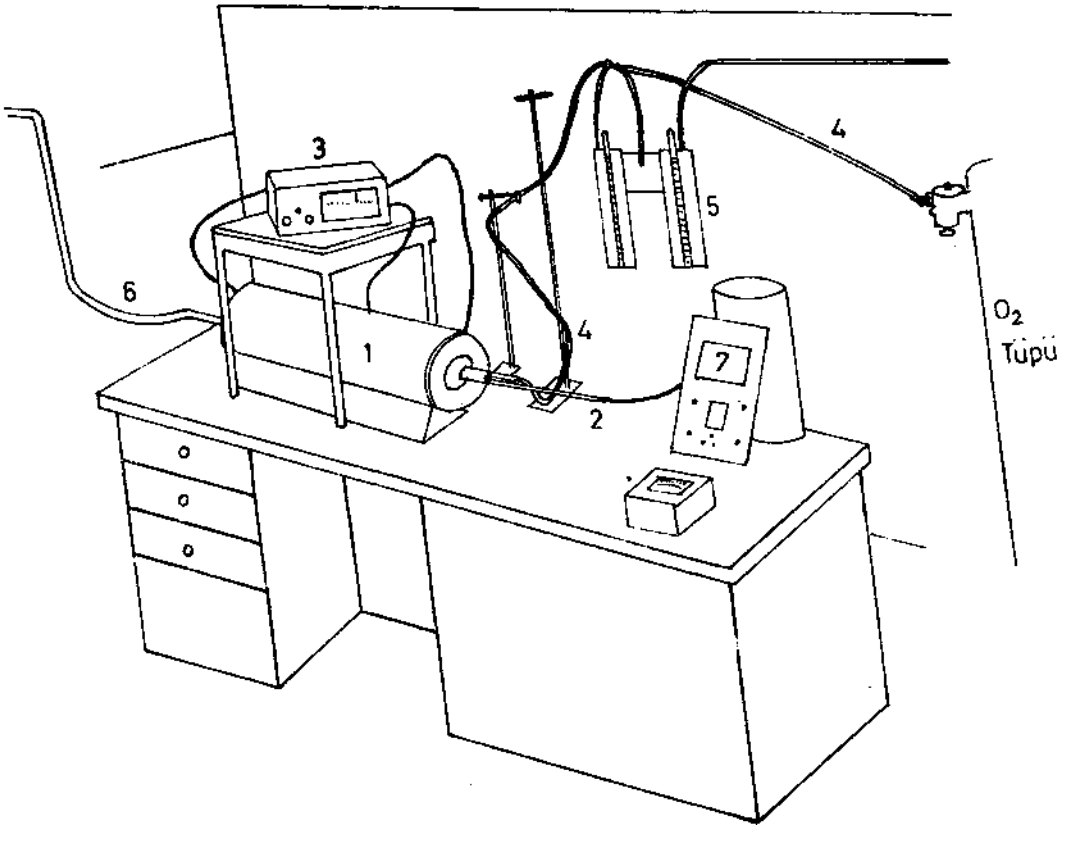

Şek. 1 - Kavurma deneyi düzeneği.
1 - Kavurma fırını; 2 - Termokupl (boru içi sıcaklığı); 3 - Isı ayarlayıcı; 4 - Hava girişi; 5 - Rotometre (hava ölçücü); 6 - Gaz çıkışı; 7 - Termokupl (sıcaklık ayarlayıcı).

Tablo 1 - Karışık konsantrenin elek ve kimyasal analizi

Ag (gr/t)	*Ca*	*Elek aralığı* (mm)	*Elek analizi* %	Σ % ↓	Σ % ↑	*Kimyasal analizler (%)* *Cu*	*Zn*	*Pb*	*Fe*	*S*	*Si*	*Co*	*Au* (gr/t)
175	0.083	0.45-0.25	15.9	15.9	100.0	15.99	7.55	17.53	19.13	39.51	0.042	0.002	51.5
159	0.051	0.25-0.20	6.1	22.0	84.1	16.39	8.63	16.49	19.52	38.79	0.004	0.002	52.6
139	0.058	0.20-0.10	30.9	52.9	78.0	14.82	11.74	18.54	18.75	36.02	0.004	0.003	50.4
226	0.078	0.10-0.08	10.0	62.9	47.1	11.32	15.60	22.64	14.39	32.59	1.669	0.003	43.5
121	0.087	0.08-0.056	14.2	77.1	37.1	10.53	15.71	23.61	12.75	36.20	0.514	0.004	40.5
317	0.113	0.056-0.025	12.8	89.9	22.9	10.34	15.08	27.00	11.60	35.69	0.430	0.001	60.8
386	0.170	0.025-0.000	10.1	100.0	10.1	8.33	11.51	40.64	9.67	29.80	0.439	0.004	37.2
211	0.085	Konsantre	100.0			12.27	12.68	23.78	15.35	35.73	0.421	0.003	47.6

ya küçük porselen kayıkçıklar içinde itilerek veya daha sonra yapılan özel bir numune borusu içinde yerleştirilmiştir. Porselen numune kayıkçığına her seferinde 10 gr numune doldurulmuştur. Porselen kayıkçıklarda kavurmada, kavurma için gerekli havanın numunenin her tarafından homojen

Tablo 2 - Karışık konsantrenin mineral bileşimi ve dağılımı

Elek aralığı (mm)	*Elek analizi*	*Mineral bileşimleri (%)*					
	Σ%↑	*$CuFeS_2$*	*FeS_2*	*PbS*	*ZnS*	*Si*	*ΣMin.*
0.45 - 0.25	100.0	46.2	10.9	20.2	11.5	0.09	88.97
0.25 - 0.20	84.0	47.2	11.0	19.0	12.9	0.01	90.20
0.20 - 0.10	78.0	42.8	12.3	21.4	17.5	0.01	94.01
0.10 - 0.08	47.1	32.7	9.5	26.2	23.2	3.57	95.22
0.08 - 0.056	37.1	30.4	7.5	27.3	23.4	1.10	89.70
0.056 - 0.025	22.9	29.9	13.1	31.2	22.5	0.92	97.52
0.025 - 0.00	10.1	24.1	5.0	46.9	17.2	0.94	94.13
Konsantre	**100.0**	**35.4**	**9.8**	**27.5**	**18.9**	**0.90**	**92.50**

geçişine imkan olmadığından, kavrulan numunede tabakalaşma şeklinde farklı kavrulmalar olduğu, renk farkından saptanmıştır. Kayıkçıklar içindeki kavurmanın numunenin her tarafında homojen bir şekilde olmadığı hususu aynı şekilde başka çalışmalarda da saptanmış olduğundan (Addemir, 1977), sonradan numune, kavurma borusuna özel kaplar içinde verilmiştir. Bu kaplar iki tarafı elekle kapatılmış ve her biri aynı boyutta, 50 gr numune alabilen silindirik borular şeklinde yapılmıştır. Kavurma borusu içine bir ucu çengelli metal bir çubukla itilen böyle bir kabın şematik görünüşü Şekil 2 de verilmiştir. Fırın içi sıcaklığı özellikle kavurma işleminin yapıldığı merkezde, bir termokupl yardımiyle ∓ 1°C hatayla ölçülebilmiş ve bir sıcaklık ayarlayıcısı (kontakt termometre) yardımiyle ∓ 5°C hata ile belirli bir sıcaklıkta sabit tutularak ayarlanabilmiştir.

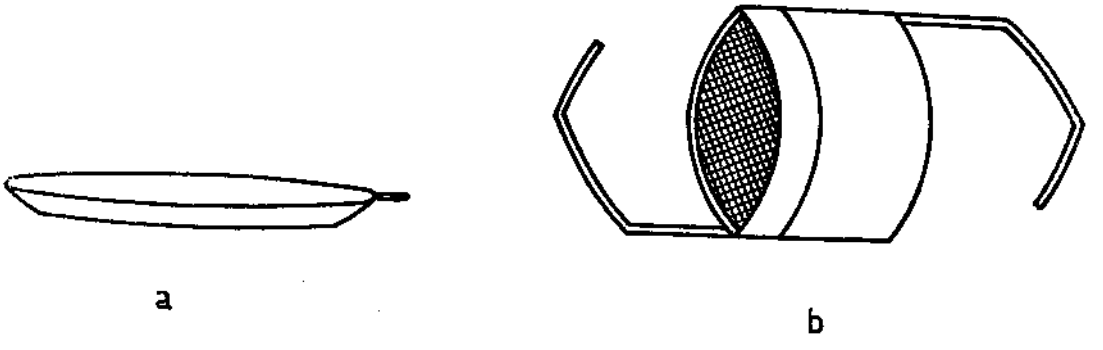

Şek. 2 - Numune kavurma kaplan.
a - Porselen kayıkçık; b - İki tarafı hava geçişme elverişli özel kavurma kabı.

Küçük bir hava pompasından veya bir tüpten alınan hava bir rotometreden geçirilerek belirli ve ayarlı bir miktarda kavurma borusu içine verilmiştir.

Tablo 3 - Giresun-Harşit-Köprübaşı konsantresinin elek analizi ve her bir elek aralığının kimyasal analizleri

No.	*Elek aralığı (mm)*	*Elek analizi* ≥ % ↓	*Elek analizi* ≥ % ↑	*Kimyasal analizler (%)* Pb	Zn	Cu	Fe	Sb	Cd	S	Si	*Ag (gr/t)*	*Au (gr/t)*
H 1	0.40-0.20	10.92	100.00	30.99	22.07	3.61	5.03	2.20	0.159	33.41	2.02	1054	23.2
H 2	0.20-0.125	19.06	89.08	32.70	22.13	3.74	5.82	1.95	0.162	32.71	1.17	632	21.8
H 3	0.125-0.075	19.81	70.02	33.95	21.47	4.52	5.92	2.20	0.158	32.51	1.02	1119	23.1
H 4	0.075-0.050	16.06	50.01	35.57	21.53	4.36	4.28	2.98	0.153	30.79	1.17	708	20.7
H 5	0.050-0.028	16.38	34.15	38.14	19.97	4.79	3.92	3.03	0.165	29.88	1.31	726	14.3
H 6	0.028-0.000	17.77	17.77	40.97	18.50	4.49	3.01	3.22	0.158	29.01	1.51	243	12.7
H O	**Konsantre**	**100.00**	—	**35.20**	**20.87**	**3.99**	**4.35**	**2.71**	**0.164**	**32.79**	**1.47**	**687**	**19.4**

Karışık konsantrenin ince öğütme işlemi laboratuvar tipi bir çubuklu değirmende ve her seferinde aynı şartlar altında yapılmıştır. Öğütmeler sonunda elde edilen elek analizleri şöyledir (Tablo 4):

Tablo 4 - Öğütmeler sonunda elde edilen elek analizleri

Elek aralığı (mikron)	*Elek analizi B*		*Elek analizi C*		*Elek analizi D*	
	%	Σ%	%	Σ%	%	Σ%
150 - 100	0.6	100.0	0.6	100.0	0.1	100.0
100 - 75	6.4	99.4	8.7	99.4	7.9	99.9
75 - 60	17.5	93.0	26.9	90.7	30.5	92.0
60 - 45	17.0	75.5	29.8	63.8	34.8	61.5
45 - 00	58.5	58.5	34.0	34.0	26.7	26.7

Bu numunenin çok ince öğütme işlemi Siebtechnik Vibratom tipi dört kaplı titreşimli değirmende yapılmıştır. Titreşimli değirmen öğütme şartlan şöyledir (Rolf ve Gock, 1976):

Öğütme kabı hacmi : 5.5 lt
Titreşim sayısı : 1450 1/dak
Titreşim miktarı : 5.5 mm
Bilye dolgusu : 22 mm bilye 8.7 kg
16 mm bilye 9.3 kg
toplam bilye 18.0 kg
Numune miktarı : 300 gr

Öğütülmüş ve kavrulmuş numunelerin yapıları Raster elektron mikroskopu ve Philips PW 1130/90 X-ray difraktometre aygıtında incelenmiştir.

Yapılan seri deneylerde saptanması istenen şartlardan optimal değeri bulunmak istenen değiştirilerek, diğerleri ön deneylerden elde edilen sonuçlara göre sabit tutulmuş ve böylece optimal kavurma şartları saptanmıştır.

Kavrulan numuneler önce damıtık suda, sonra 0.1 veya 1 molar sülfürik asit içerisinde çözündürülmüşlerdir. Bu amaçla her seferinde en az 2.5 gr kavrulmuş numune alınmıştır.

Kavrulmuş numunelerin çözeltme deneyleri ve kimyasal analizler için izlenen yöntem

Kavrulmuş nümunelerdeki bakır ve çinkonun suda ve sülfürik asitte hangi oranlarda çözündüklerini ve çökeltide kalan miktarları saptamak için her numuneye aşağıdaki çözeltme ve kimyasal analiz yöntemi tatbik edilmiştir:

Her seferinde kavrulmuş malzemeden, malzemeyi karakterize eden 2.5 gr numune alınmıştır. Bu numune önce saf su ile karıştırılarak çözeltmeye tabi tutulmuştur. Filtre üstü 1 mol H_2SO_4 içerisinde tekrar çözeltilmiş ve süzülmüştür. Bu ikinci çözelti % 3 lük 10 ml H_2O_2 ve gerekli olandan yaklaşık 40 ml fazla NH_4OH ile muamele edilmiştir. Bu çözeltilerin her ikisi de saf su ile ayrı ayrı 250 ml ye tamamlandıktan sonra bakır ve çinko analizleri yapılmıştır. Bu maksatla önce çözeltilerde fotometrik yolla (mavi renkleşme yardımiyle) bakır tayini yapılmıştır. Sonra bu çözeltiden 100 ml daha alınarak 0.1 mol EDTA (etilen diamin tetra asetik asit) ile titrasyon yoluyle bakır+çinko tayini yapılmıştır. 100 ml lik çözelti 1 gr numuneye karşılıktır. Bakır+çinko miktarından, daha önce yapılan tayinle elde edilen bakır miktarı çıkarılarak çinko miktarı saptanmıştır.

Artığın bakır ve çinko analizi için yukarıdaki çökelti, kral suyunda ($HC1+HN0_3$) muamele ediimiş,* sonra su ilâve edilerek, yukarıda özetlenen analiz yöntemi tekrarlanmış, çökeltide kalan bakır ve çinko miktarları saptanmıştır.

Çözeltme işlemlerinin ve kimyasal analizlerin doğruluğu, çözeltiye alman, çökeltide kalan metal miktarlarının toplamının kullanılan kavrulmuş numunedeki metal miktarına eşit olup olmadığının görülmesiyle kontrol edilmiştir.

ÖN DENEYLER

Ön deneylerin büyük bir kısmı porselen kayıkçıklar içinde yapılmıştır. Kavrulan numuneler gözle ve ışık mikroskopu ile incelenmiştir. Düşük (250°-350°C) sıcaklıklarda kavrulan numuneler boşaltıldığında, kendiliğinden ufalanmaktadırlar. Kavurma süresi arttıkça renk koyudan açık renge doğru değişmektedir. 420°C sıcaklıktan itibaren numune, kayıkçığın şeklini alarak poröz yapıda bir katılaşma meydana gelmektedir. Numunenin her tarafında renk homojenliği vardır. 500°C de katılaşmış numunelerde renk farklılığı yoktur, ancak poröz yapı yalnızca kayıkçığın üst kısmında belirgindir. Kavurma süresi arttıkça kayıkçığın dip tarafında kalan kısımların daha koyu renkte olduğu ayırt edilebilmektedir. Daha ince taneli numunelerle çalışıldığında renk farkı daha da belirginleşmektedir. 510°C sıcaklıkta farklı hava miktarlarıyle yapılan kavurma deneylerinde, gözle veya mikroskop altında incelenmelerinde, numunelerin birbirine benzer renk farklılıkları gösterdikleri görülmüştür. Üstte nispeten açık renkli poröz bir yapı, ortada biraz daha koyuca, en altta daha koyu renk farkını seçmek mümkündür.

590°C sıcaklıktan itibaren yapılan kavurmalarda renk farkı belirgindir. Üstte ve altta kahverengi olan numune, ikisi arasında koyu bir renk almıştır ve daha kompakttır. 650°C den itibaren buna ilâveten kayıkçıkların dip tarafında ergimiş kurşun birikimi izlenmektedir.

Yapılan 42 adet ön deneye ait saf suda ve 1 mol H_2SO_4 içerisinde çözünen Zn ve Cu miktarlarıyle artıkta kalan Zn ve Cu miktarlarına ait analiz sonuçları Tablo *4a* ve 4/b de görülmektedir. Bu tablonun son iki sütununda saf suda ve asitte çözünen miktarların toplamları ve bu çözünen miktarların, çözeltiye alınabilen metal verimi olarak yüzde cinsinden değerleri verilmiştir, 1 mol ve 0.1 mol H_2SO_4 içerisinde yapılan çözeltmelerin birbirlerinden önemli farklılık göstermediği anlaşılmıştır.

Bu değerlerin grafikler haline getirilmesiyle konsantrenin kavrulması için gerekli optimal şartların eğilimleri ortaya çıkmıştır. Bunlardan faydalanarak daha az sayıda deneyle optimal şartların ortaya konması mümkün olmuştur. Bu deneylerden aynı zamanda hava miktarının artışıyle suda ve asitte çözünen miktarın belli bir değerden itibaren artmadığı, fakat suda çözünme oranının arttığı saptanmıştır.

Tablolarda verilen numune simgeleri şu şekilde özetlenmiştir: Örneğin 500 R3 L 30 K 10 simgesinde, 500 kavurma işleminin 500°C sıcaklık altında, R3 kavurma işleminin üç saat süreyle yapıldığını, L30 verilen hava miktarının 30 cm^3/sn olduğunu, K1O numuneye % 10 oranında kömür karıştırıldığını, I 15 numunenin kavrulmadan önce titreşimli değirmende 15 dakika, I 240, 240 dakika süreyle ince öğütmeye tabi tutulduğunu göstermektedir.

* Çözme işlemi tamamlandıktan sonra H2SO4 ilâve edilerek SO_3 buharları görülünceye kadar buharlaştırılmıştır.

Tablo 4a - Ön deneyler çeşitli şartlar altında kavrulan konsantrelerde, saf suda ve H_2SO_4 çözünen bakır miktarı ve çözeltiye alabilme randımanları

Numune simgesi	Toplam Cu (%)	Saf suda Cu (%)	Saf suda R (%)	H_2SO_4-su Cu (%)	H_2SO_4-su R (%)	Artıkta Cu (%)	Artıkta R (%)	H_2SO_4 te Cu (%)	H_2SO_4 te R (%)
350 R1/4 L30	14.3	0.8	5.6	1.4	9.9	12.1	84.6	2.2	15.4
350 R1/2 L30	14.2	1.5	10.5	2.1	14.8	10.6	74.6	3.6	25.4
350 R1 L30	14.0	2.1	15.0	2.8	20.0	9.1	65.0	4.9	35.0
350 R1 1/2 L30	14.0	2.7	19.3	2.9	20.7	8.4	60.0	5.6	40.0
350 R2 1/2 L30	14.4	3.2	22.2	3.1	21.5	8.1	56.2	6.3	43.7
350 R4 L30	14.3	4.0	27.9	3.1	21.6	7.2	50.3	7.1	49.7
350 R6 L30	14.3	3.9	27.3	2.0	14.0	8.4	58.7	5.9	41.3
350 R19 L30	14.2	4.6	32.4	2.8	19.7	6.8	47.9	7.4	52.1
420 R2 1/2 L30	14.4	3.9	27.1	2.8	19.4	7.7	53.5	6.7	46.5
420 R4 L30	14.1	4.6	32.6	2.9	20.5	6.6	46.8	7.5	53.2
420 R6 L30	14.1	4.6	32.6	1.3	9.2	8.2	58.2	5.9	41.8
420 R8 L30	13.9	6.9	49.6	2.0	14.4	5.0	36.0	8.9	64.0
500 R2 L20	13.4	2.7	20.1	1.6	11.9	9.1	67.9	4.3	32.1
500 R2 1/2 L20	14.0	3.7	26.4	2.4	17.1	7.9	56.4	6.1	43.6
500 R4 L20	13.5	5.5	40.7	2.2	16.3	5.8	43.0	7.7	57.0
500 R6 L20	13.9	5.6	40.3	1.5	10.8	6.8	48.9	7.1	51.1
500 R3 L30	13.2	5.9	44.7	1.6	12.1	5.7	43.2	7.5	56.8
500 R3 L30K10	13.7	5.0	36.5	2.1	15.3	6.6	48.2	7.1	51.8
500 R3 L30K20	12.7	3.8	29.9	2.9	22.8	6.0	47.3	6.7	52.7
500 R3 L30K30	11.8	3.2	27.1	3.3	28.0	5.3	44.9	6.5	55.1
500 R3 L30K50	9.9	2.9	29.3	3.3	33.3	3.7	37.4	6.2	62.6
500 R2 L20 I240	12.6	5.6	44.4	5.1	40.5	1.9	15.1	10.7	84.9
500 R4 L20 I240	12.6	6.0	47.6	4.7	37.3	1.9	15.1	10.7	84.9
500 R6 L20 I240	12.2	7.1	58.2	3.8	31.1	1.3	10.7	10.9	89.3
500 R6 L20 I240 B	12.6	7.3	57.9	3.1	24.6	2.2	17.5	10.4	82.5
500 R6 L20 I15	12.3	7.4	60.2	3.3	26.8	1.6	13.0	10.7	87.0
500 R3 L30 I240	12.6	6.5	51.6	4.2	33.3	1.9	15.1	10.7	84.9
500 R3 L30 I240 B	12.2	8.1	56.4	2.6	21.3	1.5	12.3	10.7	87.7
	11.1	8.0	—	2.0	—	1.8	—	10.0	84.7
510 R2 L30 (0.1 M)	13.1	3.3	25.2	0.9	6.9	8.9	67.9	4.2	32.1
510 R2 L50	13.3	3.4	25.6	1.7	12.8	8.2	61.7	5.1	38.3
510 R2 L100	13.0	3.1	23.8	1.6	12.3	8.3	63.8	4.7	36.1
510 R2 L200	14.1	3.1	22.0	2.4	17.0	8.6	61.0	5.5	39.0
510 R2 L200 B	13.4	3.3	24.6	0.8	06.0	9.3	69.4	4.1	30.6
590 R6 L30 (0.1 M)	12.3	1.8	14.6	1.7	13.8	8.8	71.5	3.5	28.4
590 R6 L30 B	12.3	1.8	14.6	3.6	29.2	6.9	56.1	5.4	43.9
590 R6 L30 C	12.6	1.6	12.7	3.5	27.8	7.5	59.5	5.1	40.5
590 R8 1/2 L30	12.0	2.4	20.0	2.1	17.5	7.5	62.5	4.5	37.5
630 R11 L20 (0.1 M)	10.5	1.1	10.5	4.3	40.9	5.1	48.6	5.4	51.4
630 R11 L20	12.0	1.7	14.2	4.5	37.5	5.8	48.3	6.2	51.6
650 R2 1/2 L20	15.6	0.7	4.5	4.2	26.9	10.7	68.6	4.9	31.4
650 R6 L20 (0.1 M)	13.3	1.0	7.5	2.2	16.5	10.1	75.9	3.2	24.1
650 R6 L20	14.9	0.8	5.4	3.4	22.8	10.7	71.8	4.2	28.2

Tablo 4*b* - Ön deneyler çeşitli şartlar altında kavrulan numunelerden saf suda ve H_2SO_4 te çözünen çinko miktarları ve çözeltiye alabilme randımanları

Numune simgesi	Toplam Zn (%)	Saf suda Zn (%)	Saf suda R (%)	H_2SO_4-su Zn (%)	H_2SO_4-su R (%)	Artıkta Zn (%)	Artıkta R (%)	H_2SO_4 te Zn (%)	H_2SO_4 te R (%)
350 R 1/4 L30	11.9	0.4	3.4	0.1	0.8	11.4	95.8	0.5	4.2
350 R 1/2 L30	11.7	0.5	4.2	0.1	0.8	11.1	94.9	0.6	5.1
350 R1 L30	12.3	0.6	4.8	0.1	0.8	11.6	94.3	0.7	5.7
350 R1 1/2 L30	12.0	0.7	5.8	0.1	0.8	11.2	93.3	0.8	6.7
350 R2 2 1/2 L30	11.7	0.7	6.0	0.1	0.8	10.9	93.2	0.8	6.8
350 R4 L30	11.7	0.7	6.0	0.1	0.8	10.9	93.2	0.8	6.8
350 R6 L30	11.4	0.6	5.3	0.0	0.0	10.8	94.7	0.6	5.3
350 R19 L30	14.8	4.1	27.7	0.0	0.0	10.7	72.3	4.1	27.7
420 R2 1/2 L30	11.7	1.4	12.0	0.1	0.8	10.2	87.2	1.5	12.8
420 R4 L30	10.9	0.0	0.0	0.1	0.9	10.8	99.1	0.1	0.9
420 R6 L30	11.3	1.0	8.8	0.1	0.9	10.2	90.3	1.1	9.7
420 R8 L30	9.4	0.0	0.0	0.2	2.1	9.2	97.9	0.2	2.1
500 R2 L20	12.2	1.6	13.1	0.1	0.8	10.5	86.1	1.6	13.1
500 R2 1/2 L20	14.0	3.7	26.4	2.4	17.1	7.9	56.4	6.1	43.6
500 R4 L20	11.6	2.3	19.8	0.3	2.6	9.0	77.6	2.6	22.4
500 R6 L20	10.6	1.7	16.0	0.2	1.9	8.7	82.1	1.9	17.9
500 R3 L30	11.2	1.5	13.4	0.1	0.9	9.6	85.7	1.6	14.3
500 R3 L30 K10	11.3	1.5	13.3	0.1	0.9	9.7	85.8	1.6	14.2
500 R3 L30 K20	11.3	2.5	22.1	0.3	2.6	8.5	75.2	2.8	24.8
500 R3 L30 K33	12.5	5.2	41.6	0.3	2.4	7.0	56.0	5.5	44.0
500 R3 L50 K50	8.6	2.6	30.2	0.3	3.5	5.7	66.2	2.9	33.7
500 R2 L20 I240	9.2	5.6	60.9	1.6	17.4	2.0	21.7	7.2	78.3
500 R4 L20 I240	10.4	6.6	63.5	1.7	16.3	2.1	20.2	8.3	79.8
500 R6 L20 I240	9.9	6.7	67.7	1.3	13.1	1.9	19.1	8.0	80.9
500 R6 L20 I240	10.0	6.5	65.0	0.5	5.0	3.0	30.0	7.0	70.0
500 R6 L20 I15	10.3	7.3	70.9	1.2	11.6	1.8	17.5	8.5	82.5
500 R3 L30 I240	10.4	6.4	61.5	2.3	22.1	1.7	16.3	8.7	83.6
500 R3 L30 I240	9.7	6.7	—	1.4	—	1.6	—	8.1	83.5
	10.6	6.5	—	1.0	—	2.1	—	7.5	78.1
510 R2 L30 (0.1 M)	11.1	1.3	11.7	0.0	0.0	2.8	88.3	1.3	11.7
510 R2 L50	11.8	1.6	13.6	0.1	0.8	10.1	85.6	1.7	14.4
510 R2 L100	11.8	1.3	11.0	0.1	0.8	10.4	88.1	1.4	11.9
510 R2 L200	12.1	1.4	11.6	0.2	1.7	10.5	86.8	1.6	13.2
510 R2 L200 B	11.7	1.4	11.9	0.7	6.1	9.6	82.0	2.1	18.0
590 R6 L30 (0.1 M)	9.5	4.3	45.2	0.3	3.2	4.9	51.6	4.5	48.4
590 R6 L30	9.5	4.3	45.2	0.3	3.2	4.9	51.6	4.6	48.4
590 R6 L30	11.1	3.8	34.2	0.8	7.2	6.5	58.6	4.6	41.4
590 R8 1/2 L30	11.3	5.5	48.7	0.5	4.4	5.3	46.9	6.0	53.1
650 R11 L20 (0.1 M)	9.5	6.7	70.5	0.5	5.2	2.3	24.2	7.2	75.8
630 R11 L20 (1 M)	11.8	6.0	50.8	1.4	11.9	4.4	37.2	7.4	62.7
650 R 2 1/2 L20	12.1	2.9	24.0	1.0	8.2	8.2	67.8	3.9	32.2
650 R6 L20 (0.1 M)	11.4	3.8	33.3	0.4	3.5	7.2	63.1	4.2	36.8
650 R6 L20 (1 M)	12.8	3.4	26.5	0.9	7.0	8.5	66.4	4.3	33.6

DENEYLER

Optimal şartları saptamak maksadıyle ön deneylerden elde edilen verilere göre yapılan kavurma deneylerini üç ayrı grupta toplamak mümkündür. Birinci grupta optimal kavurma sıcaklığını saptamak amacıyle yapılan deneyler yer almaktadır. 250°-650°C sıcaklıklar ve bunlar arasındaki değişik sıcaklıklarda yapılan kavurma deneyleri yardımiyle bakır ve çinkonun en iyi çözünebildikleri kavurma sıcaklıkları saptanabilmiştir.

İkinci grup deneyler, sabit sıcaklık ve kavurma sürelerinde, aynı incelikteki konsantre ile değişik hava beslemeleri altında yapılan deneylerdir. Bir küçük hava pompasıyle kavurma borusu içine bir rotometrede ölçülerek gönderilen hava miktarları değişik deneylerde 20-130 cm^3/dak arasındaki değerlerde sabit tutulmuş, böylece hava miktarının kavurmaya etkisi incelenmiştir.

Üçüncü grup deneyler, aynı incelikteki konsantre, sabit sıcaklıklar ve hava miktarları altında 15 dakika ile 1 saat kavurma süreleri arasında yapılan deneylerdir. Bu deneylerin sonuçlarından, kavurma süresinin diğer şartlara göre en uygun olan miktarlarını görmek mümkün olmuştur.

Kavrulan konsantrenin farklı tane iriliklerinde, farklı kavurma sonuçları vermesi gerektiğinden, öğütülmemiş konsantre ile çubuklu değirmende öğütülmüş konsantre ve titreşimli değirmende öğütülmüş konsantreyle yapılmış ön deneyler, yeterli ve belirgin sonuçlar verdiğinden, konsantre titreşimli değirmende 15 dakikalık bir ince öğütmeye tabi tutulmuş ve deneylerin çoğunda tane iriliği bu düzeyde bırakılmıştır.

Söz konusu deneylerin verdikleri sonuçlar bakır için Tablo 5a, çinko için Tablo 5*b* de görülmektedir.

DENEY SONUÇLARI

Kavurma ve çözeltme deney sonuçları Şekil 3,4 ve 5 te özetlenmiştir.

Kavurma süresinin kavurmaya etkisi Şekil 3 te görülmektedir. Kavurma süresi arttıkça çözeltiye geçen çinko ve bakır metal oranları da artmaktadır. Bu artış düşük sıcaklıklarda ve yüksek sıcaklıklarda birbirinden farklıdır. Çözeltiye geçmedeki verim artışı, özelikle kavurmanın başlangıcında yüksektir. Bu yükseliş belirli bir süreden sonra ya azalmakta veya ortadan kalkmaktadır. Yüksek sıcaklıklarda belirli bir süreden sonra bir verim artışı artık söz konusu değilken, düşük sıcaklıklarda gittikçe azalan bir artış söz konusudur. Nitekim 350°C sıcaklıkta yapılan kavurmada 19 saatta dahi bir verim artışı varken, 650°C sıcaklıktaki kavurmada, bakır için 1.5, çinko için 1 saat sonra artık bir verim artışı yoktur.

Diğer taraftan kavurma süresi arttıkça saf suda çözünen metal miktarıyle asitte çözünen metal-miktarı arasındaki farkın da, suda çözünen metal miktarı lehine, özellikle düşük sıcaklıklarda, birlikte artmakta olduğu görülmektedir (Şek. 3).

Verimin yüksek veya düşük olması, kavurma süresinden başka diğer faktörlere de büyük ölçüde bağlı kalmaktadır. Nitekim 350°C sıcaklıkta yapılan kavurmada, bakırın çinkoya oranla daha yüksek verimle çözeltiye geçmesine karşın, 500°C sıcaklıkta aradaki bu fark azalmıştır. Hatta 650°C sıcaklıkta durum tersine dönmüş, çinko verimi bakır verimine göre bariz bir şekilde artmıştır. Şekil 4 te kavurma havası miktarıyle çözünebilen metal verimi arasındaki bağıntı görülmektedir. 500°C sıcaklıkta iki saat süreyle kavrulmuş ince öğütülmemiş konsantre ile 570°C sıcaklıkta iki saat süreyle kavrulmuş ince öğütülmüş konsantrenin çözünme verimlerindeki hava miktarının değişimine uygun olarak görülen durumlar benzerlik göstermektedir. Verilen hava miktarının

Tablo 5*a* - Çeşitli şartlar altında kavrulan konsantrelerde, saf suda ve mol H_2SO_4 te çözünen bakır miktarları ve çözeltiye alınabilme randımanları

Numune simgesi	*Toplam*	*Saf suda*		H_2SO_4 - *su*		*Artıkta*		H_2SO_4 *te*	
	Cu (%)	*Cu (%)*	*R (%)*	*Cu (%)*	*R (%)*	*Cu (%)*	*R (%)*	*Cu (%)*	*R (%)*
250 R2 L40 I15	13.2	6.3	47.7	4.9	37.1	2.0	15.2	11.2	84.8
350 R2 L40 I15	13.2	8.5	64.4	4.1	31.0	0.6	4.5	12.6	95.5
450 R2 L40 I15	13.3	10.3	77.4	2.6	19.5	0.4	3.0	12.9	97.0
550 R2 L40 I15	13.3	8.7	65.4	2.9	21.8	1.7	12.8	11.6	87.2
590 R2 L40 I15	13.2	5.6	42.4	5.1	38.6	2.5	18.9	10.7	81.1
650 R2 L40 I15	13.2	2.7	20.4	5.6	42.4	3.9	29.5	8.3	62.9
570 R2 I15 L20	13.1	8.4	64.1	2.1	16.0	2.6	19.9	10.5	80.1
570 R2 I15 L30	13.4	9.9	73.8	2.5	18.6	1.0	7.5	12.4	92.5
570 R2 I15 L40	13.2	9.5	72.0	2.4	18.1	1.3	9.8	11.9	90.2
570 R2 I15 L50	13.3	9.9	74.4	2.2	16.5	1.2	9.0	12.1	91.0
570 R2 I15 L100	13.4	10.4	77.6	1.8	13.4	1.2	9.0	12.2	91.0
570 R2 I15 L130	13.1	10.1	77.1	1.5	11.4	1.5	11.4	11.6	88.6
650 R1/4 L40 I15	13.1	3.9	29.8	1.6	12.2	7.6	58.0	5.5	42.0
650 R1/2 L40 I15	13.4	5.1	38.0	1.7	12.7	6.6	49.2	6.8	50.8
650 R1 L40 I15	13.2	5.9	44.7	1.7	12.9	5.6	42.4	7.6	57.6
650 R11/2 L40 I15	13.3	7.1	53.4	0.8	6.0	4.4	33.1	8.9	66.9
650 R21/2 L40 I15	13.2	7.4	56.1	1.6	12.1	4.2	31.8	9.0	68.2
650 R4 L40 I15	13.4	7.3	54.5	1.8	13.4	4.3	32.1	9.1	67.9
650 R8 L40 I15	13.1	6.5	49.6	1.9	14.5	4.7	35.9	8.4	64.1
Kavrulmamış I15	11.1	0.0	0.0	0.1	0.9	11.0	99.1	—	—

Tablo 5*b* - Çeşitli şartlar altında kavrulan konsantrelerde, saf suda ve mol H_2SO_4 te çözünen çinko miktarları ve çözeltiye alınabilme randımanları

Numune simgesi	Toplam Zn (%)	Saf suda Zn (%)	Saf suda R (%)	H_2SO_4-su Zn (%)	H_2SO_4-su R (%)	Artıkta Zn (%)	Artıkta R (%)	H_2SO_4 te Zn (%)	H_2SO_4 te R (%)
250 R2 L40 I15	11.0	1.1	10.0	0.2	1.8	9.7	88.2	1.3	11.8
350 R2 L40 I15	10.9	0.7	6.4	0.1	0.9	10.1	92.6	0.8	7.4
450 R2 L40 I15	11.1	1.0	9.0	0.2	1.8	8.9	80.2	1.2	10.8
550 R2 L40 I15	10.9	5.4	49.5	1.3	11.9	4.2	38.5	6.7	61.5
590 R2 L40 I15	10.9	9.0	82.3	1.0	9.2	0.9	8.2	10.0	91.7
650 R2 L40 I15	11.0	9.6	87.3	0.7	6.4	0.7	6.4	10.3	93.6
570 R2 I15 L20	11.2	8.7	77.7	1.7	15.2	1.5	13.4	9.7	86.6
570 R2 I15 L30	10.9	8.4	77.1	0.8	7.3	1.7	15.6	9.2	84.4
570 R2 I15 L40	10.9	8.4	77.1	1.3	11.9	1.2	11.0	9.7	89.0
570 R2 I15 L50	11.0	7.9	71.8	1.6	14.5	1.5	13.6	9.5	86.4
570 R2 I15 L100	11.0	8.1	73.6	1.6	14.5	1.4	12.7	9.6	87.2
570 R2 I15 L130	10.9	7.8	71.5	1.4	12.8	1.7	15.6	9.2	84.4
650 R1/4 L40 I15	10.8	5.7	52.8	1.5	13.8	5.1	47.2	7.2	66.7
650 R1/2 L40 I15	10.9	6.9	63.3	2.1	19.3	2.2	20.2	8.7	79.8
650 R1 L40 I15	11.1	8.4	75.7	2.1	18.9	0.6	5.4	10.5	94.6
650 R11/2 L40 I15	11.0	8.2	74.5	2.0	18.2	0.8	7.2	10.2	92.8
650 R21/2	11.0	8.6	78.2	1.8	16.4	0.6	5.4	10.4	94.6
650 R4	11.1	9.4	84.7	1.1	9.9	0.6	5.4	10.5	94.6
650 R8	10.9	9.7	89.0	0.7	6.4	0.5	4.6	10.4	95.4

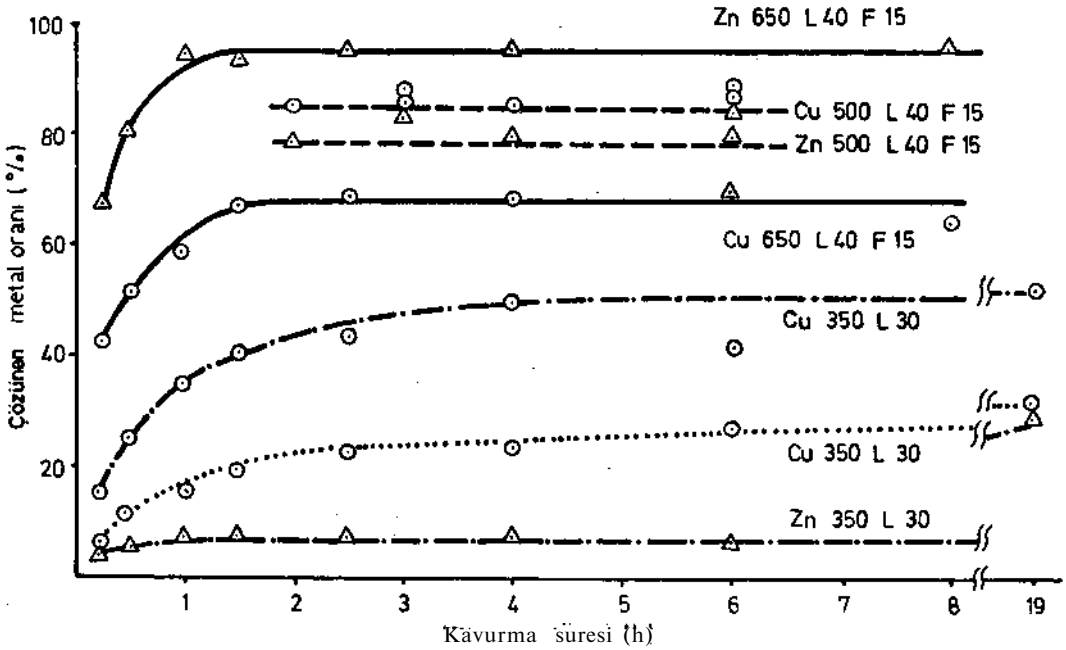

Şek. 3 - Çözünen metal miktarının kavurma süresine bağlı olarak değişimi.
Zn 650° - 650°C kavurmadaki çinko çözünmesi; L40 - Hava miktarı 40 cm3/sn; F15 - 15 dakika titreşimli öğütülmüş numune.

artırılmasıyla belirli bir değerden sonra verimde bir farklılık görülmemektedir. Çinko için bu durum en düşük hava miktarı olarak çalışılmış bulunan 20 cm^3/sn den itibaren görülmektedir. Bakır veriminde ise 30-40 cm^3/sn hava miktarına kadar yavaş bir artış görülmekte, bu değerden sonra bir verim artışı izlenmemektedir.

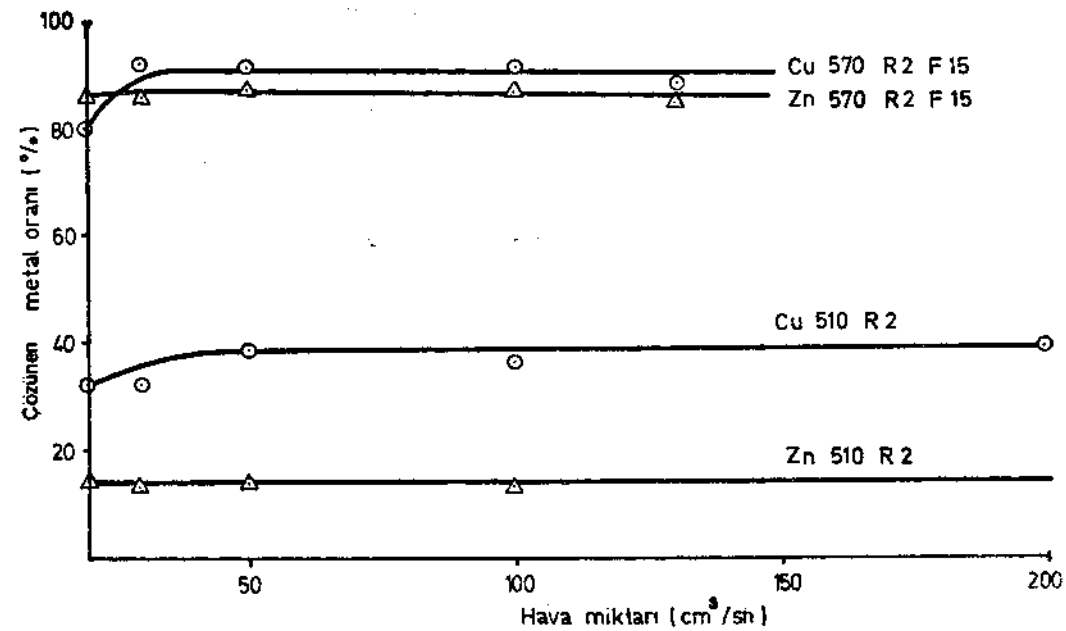

Şek. 4 - Çözünen metal miktarının öğütme miktarı ve kavurma süresine bağlı olarak değişimi.
Cu 510° - 510°C kavurmadaki bakır çözünmesi; **R2**-Kavurma süresi 2 saat; F 15 - 15 dakika titreşimli değirmende öğütülmüş numune.

Şekil 5 te, kavurma sıcaklığı ile çözeltiye alınabilen metal verimleri arasındaki bağıntı gösterilmiştir. Bu eğrilerin ifade ettiği sonuçlar birçok bakımdan özellikle ilginçtir.

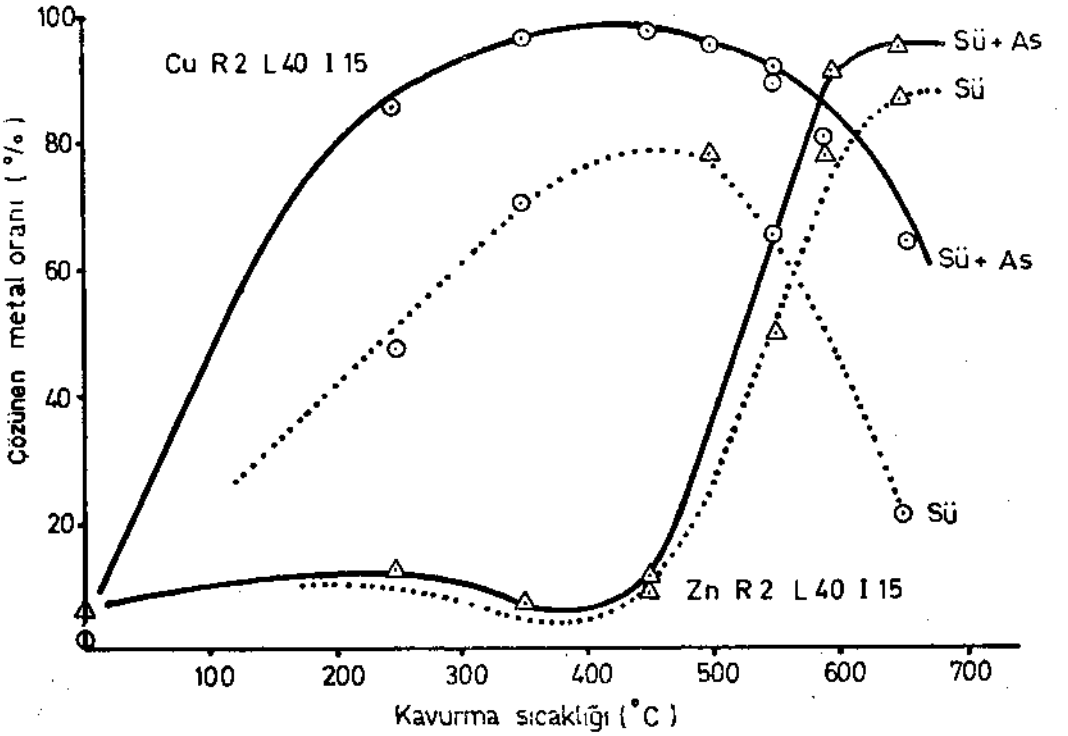

Şek. 5 - Çözünen metal oranının kavurma sıcaklığına bağlı olarak değişimi.
Cu - Bakır çözünme eğrisi; R2 - Kavurma süresi 2 saat; L40 - Hava miktarı 40 cm3/sn; 115 - 15 dakika titreşimli değirmende öğütülmüş numune.

Oldukça uygun şartlar altında yapılmış olan bu deneyler, karışık konsantredeki bakır ve çinko metallerinin % 95 in üzerinde verimlerle çözeltiye alınmalarının mümkün olduğunu göstermektedir.

Kavurma işleminden sonra çinko ve bakırın büyük kısmı saf suda çözünmektedir. örneğin 350°C sıcaklıkta kavurmada, çözeltiye geçen bakırın yaklaşık % 67 si, çinkonun % 85 i saf suda, geriye kalanı seyreltik sülfürik asitte çözünmektedir. Bu oranlar 400°C de bakır için % 75, çinko için % 70, 500° de bakır için % 75, çinko için % 70, 650°C de bakır için % 30, çinko için % 90 civarındadır.

Bakır verim eğrisi 350°-500°C arasında bir maksimuma eriştikten sonra alçalmaktadır. Oysaki çinko verim eğrisi bu kavurma sıcaklıklarında minimum değere haizdir. Çinko verim eğrisi 650°C civarında maksimuma erişmektedir. Verim eğrilerinin bu şekilde değişik sıcaklıklarda maksimum vermesi ve bakırın maksimum verdiği değerlerde çinkonun minimum vermesi, çözeltiden metal üretimi bakımından çok ilginçtir. Çünkü bakır ve çinkonun çözeltiye alınmalarından sonra redüksiyon elektrolizi yoluyle metalik olarak elde edilmeleri gerekmektedir. Elektrolizin mümkün olabilmesi için elektrolit içerisinde aynı zamanda bakır ve çinkonun birlikte bulunması arzu edilmemektedir. Bunun için her iki metalin yeteri kadar seçici olarak ayrı ayrı çözeltiye alınmaları gerekmektedir. Dolayısıyle kavurma ve çözeltme işleminin çinko ve bakır karışık konsantrelerinde

bu olanağı sağladığını görmek büyük önem göstermektedir. Bu durumda 400°C civarında yapılacak bir kavurmayla % 97 ye varan bir metal verimi ile bakır, 650°C civarındaki bir kavurmayla % 95 e varan bir metal verimi ile çinkoyu çözeltiye almak mümkün olacaktır. Herhangi bir solvent ekstraksiyon işlemine tabi tutmadan bakır çözeltisi içinde % 5-8 oranında çinko ve çinko çözeltisinde çok daha az oranda bakır, metalik olarak bulunabilecektir.

Kavurma sıcaklığının yanı sıra, tane iriliğinin de sülfatlaştırıcı kavurma ve bunu takiben seyreltik sülfürik asit içerisinde çözeltme işleminde etkin faktörler arasında dominant karakteri haiz olduğu görülmektedir. Nitekim aynı şartlar altında, fakat farklı tane iriliklerinde yapılmış olan deneylerin ince öğütmenin lehine bariz farklı sonuçlar verdiği görülmektedir (Şek.4).

SONUÇLARIN İRDELENMESİ

Elde edilen deney sonuçlarına göre Karadeniz Bölgesindeki kompleks bakır-çinko-kurşun cevherlerinden flotasyon yoluyle elde edilecek karışık konsantreden kavurma - çözeltme - elektroliz yöntemleriyle elektrolitik bakır ve çinko ile kurşun üretmek mümkündür. Uygulanacak bu yöntemlerin hepsi sanayi çapında denenmiş, uygulanmasında beklenmeyen problemlerle karşılaşılmayacak olan yöntemlerdir. Bu yöntemin diğer yöntemlere göre şu üstünlüklerini sıralamak gerekir:

1. Bu cevherlerin karışık konsantrelerinden doyurucu seçilmiş konsantreler elde etmek mümkün değildir. Şayet mümkün olsaydı bile, pahalı olan pirometalurjik yöntem yerine, gerek yatırım masrafları gerek işletme masrafları bakımından daha ucuz olan böyle bir hidrometalurjik yöntemin tatbik edilmesi elbetteki daha uygundur.

2. Bu yöntemin pirometalurjik zenginleştirme yöntemine oranla elverişli olan diğer-tarafı ise, metal.vefimlerinin çok daha yüksek oluşudur. Çünkü pirometalurjik yöntemde karışık konsantreden, seçilmiş konsantreye, seçilmiş konsantreden metale ve metalden elektrolitik bakır veya çinkoya geçişte ayrı ayrı dikkate alınması gereken verim kayıpları olacaktır. Oysaki bu yöntemde işlem basamağı sayısı azalmıştır. Esasen çözeltiye almadaki verini çok yüksektir.

3. Kavurma yapmadan çözeltiye alma yöntemine göre (yüksek basınç ve sıcaklıkta veya normal basınç ve sıcaklıkta), bu yöntemin önemli üstünlüğünün biri, seçilmiş çözeltiye alabilme imkânı olduğunun saptanmasıdır. Nitekim 400°C dolayında kavurmadan sonra bakırın % 97 sinin ve 650°C civarında kavurmada .çinkonun % 95 inin çözeltiye alınmasının mümkün olacağı görülmektedir.

4. Diğer çözeltme ve elektroliz etme olanaklarına göre bu yöntemin önemli diğer üstünlüğü çözeltiye demirin geçmemesidir. Diğer çözeltme yöntemlerinde demir de çözeltiye alınacağından, -demirin çözeltiden çok ince tane haline getirdikten sonra (jarosit oluşumu ile veya diğer yöntemlerle) çözeltiden ayrılmasındaki güçlükler bilinmektedir.

Bu yöntemin çok önemli olan sakıncalı yanı, kavurma sırasında çıkan zararlı gazların çevreye verdikleri zarardır. Her ne kadar bu gazlardan sülfürik asit üretimine gidilerek bu sakınca azaltılmakta ve Türkiye'de bir sülfürik asit fazlasından değil, eksikliğinden bahsetmek mümkünse de, bu şekilde zararlı gazların tamamen giderilebildiğini iddia etmek güçtür.

Her ne kadar kavurma yöntemleri halen dünyanın her tarafında kullanılmakta, ise de, bütün araştırmalar kavurma işlemini sırf bu sebepten devreden çıkarmaya yöneliktir.

Dolayısıyle bu önemli sakınca bir tarafa itildiğinde, optimal koşulları saptanmış olan bu kavurma - çözeltme - elektroliz yöntemi, Doğu Karadeniz Bölgesindeki kompleks bakır-çinko-kurşun cevherlerinden yüksek bir verimle elde edilebilen karışık konsantreden elektrolitik bakır ve çinko ile kurşun metallerinin üretimi için öncelikle kullanılabilecek bir yöntemdir.

PRENSİP AKIM ŞEMASI

Doğu Karadeniz Bölgesi kompleks Cu-Zn-Pb yataklarının cevher hazırlama yönünden incelenmesi konulu yayında bu cevherler için bir prensip akım şeması verilmişti (Unan, 1971). Bu şemanın seçici flotasyonla ilgili kısmı, bu çalışma sonuçlarına göre değiştirilerek yeni bir akım şeması verilmiştir (Şek. 6). Böylece bir taraftan ekonomik açıdan düşük metal verimi dolayısiyle elverişli olmayan seçici flotasyon yerine, ince öğütme-kavurma-çözeltme elektroliz yöntemi getirilmiştir. Diğer taraftan bu şema ile bakır ve çinko için seçkin konsantrelerden öteye rafine metal üretimine kadar olan işlemler kapsama alınmıştır.

ÖNERİLER

Varılan sonuçlara göre önerilen prensip akım şeması basit bir pilot tesiste denenmelidir.. Verilen prensip akım şemasında görülen işlemlerin hepsi bugün uygulamada sanayi ölçüsünde kullanılmakta olan işlemlerdir. Ancak böyle bir akım şeması bu cevherler için laboratuvar deney sonuçlarına göre çıkmıştır. Bu akım şemasının pilot çapta denenmesinde bir zorlukla veya prensipte değişik bir sonuçla karşılaşılacağı sanılmamâktadır.

Ancak yöntemdeki kavurma işlemi sırasında çıkacak zararlı gazların giderilmesi veya bunlardan faydalanılması gerekmektedir. Bu ise ilâve bir külfet getirmektedir. Halen dünyanın birçok yerinde kavurma yapmadan çözeltiye alma yolları araştırılmaktadır. Birkaç yıl içerisinde böyle bir yolla çözeltiye alma işleminin sanayide kullanılır duruma gelmesi mümkün olabilir. Bu takdirde burada önerilen prensip akım şemasını yeniden gözden geçirmek gerekebilir. Esasen bu çalışma, kavurma yapmadan bakır ve çinkoyu ayrı ayrı çözeltiye alabilme amacına yönelik çalışmaların bu anlamda başlangıcımıoluşturmaktadır.

KATKI BELİRTME

Bu araştırma, Berlin Teknik Üniversitesi Yöntem Tekniği (Verfahrenstechnik) Enstitüsü cevher hazırlama, saflaştırma, biriketleme ve koklaştırma bölümünde, Alexander von Humboldt-Stiftung tarafından verilen araştırma bursundan faydalanılarak yapılmış çalışmaların bir bölümünü teşkil etmektedir. Almanya'daki çalışmaları için bu maddî olanağı veren Alexander von Humboldt vakfına ve enstitüsünde çalışma olanaklarını cömertçe sunan Sayın) Prof. Dr.-rer, nat. W. Simonis ve Prof. Dr.-Ing. W. Plate'ye yazar içten teşekkürlerini sunar.

X - ray ve elektronmikroskobi incelemelerinde enstitü olanaklarını sunan Maden Yatakları Kürsüsü Şefi Sayın Prof. Dr.-Ing. A. Wilke'ye ve bu konularda bana yardımcı olan Sayın Dr. -ing. habil. H. Akın'a, yazar özellikle teşekkür eder.

Yazar, çalışmaları sırasında arkadaşlık ve meslektaşlık yardımlarım esirgemeyen Metalürji Enstitüsünden Sayın Prof. Dr.-Ing. R. Kammel ve Prof. Dr.-Ing. Gerlach ve özellikle günlerce birlikte laboratuvarda çalışma ve tartışma yakınlığını gösteren bu enstitünün kurucusu emeritüs Prof. Dr. -Ing.Pawlek'e teşekkürlerini sunar.

PRENSİP AKIM SEMASI

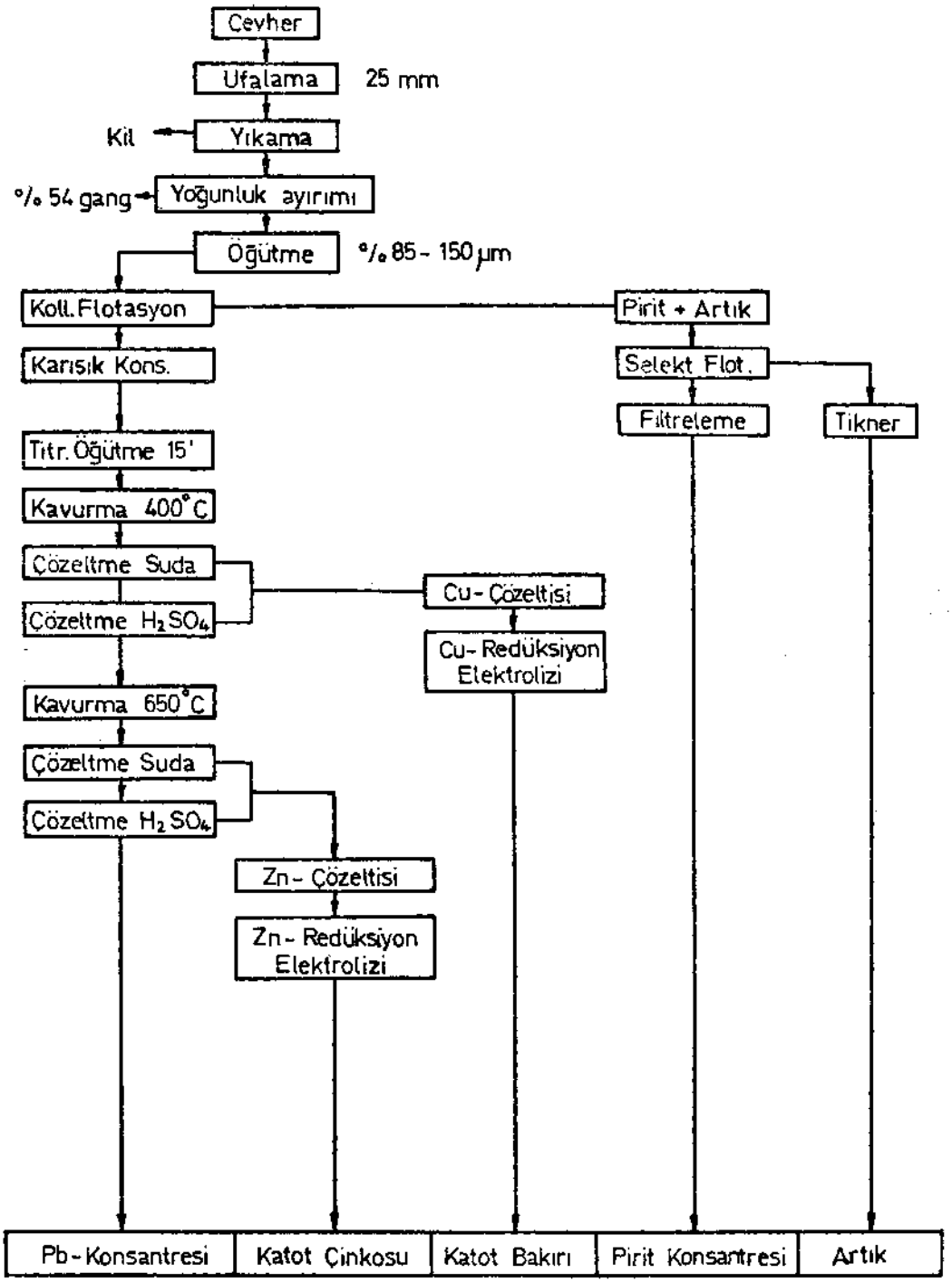

Şek. 6 - Prensip akım şeması.

Yazar, karakteristik konsantre numunelerinin sağlanmasında yardımcı olan Demir-Export'dan (Ankara) Sayın U. Keser, N. Yaz ve Aslan Avcı ile İzmir'den H. Yavaş'a teşekkür eder.

Yayma verildiği tarih, l ekim 1979

DEĞÎNÎLEN BELGELER

Addemir, O., 1977, Kompleks sülfürlü cevherlerin Sülfatlayıcı kavurma yoluyle doğrudan metalurjik değerlendirilmesi ve Lahanos cevheri üzerine incelenmesi: Doktora tezi, İ.T.Ü. Metalürji Fak., İstanbul.

Akdağ, M., 1979, Karışık bakır-kurşun-çinko konsantrelerinin oksijenli ortamda sülfürik asit-ferrik sülfat çözücülerinde çözeltme olanaklarının araştırılması: Doktora tezi, Ege Üniv. Mak. Fak. Maden Müh. Bölümü, izmir.

Akın, H. ve Erden, M.T., 1977, Harşit-Köprübaşı polimetalik maden yatağındaki cevher dağılımı: Mâden Tetkik ve Arama Ens. Derg., 89, 1-9.

Aytekin, Y., 1973a, Karadeniz Bölgesi bakır yataklarını değerlendirme imkânları: TBTAK IV. Bilim Kongresi, Ankara.

———, 1973b, Karadeniz Bölgesi bakır ve bakıra bağlı kurşun-çinko potansiyeli ve bu potansiyelin verdiği imkânlar: Madencilik, MMO Derg. 12, sayı 2, Ankara.

———, 1976, Doğu Karadeniz Bölgesindeki bakır-kurşun-çinko kompleks yataklarının cevher hazırlama yönünden incelenmesi: TBTAK -MAG- 284, 303, ser. 32, Ankara.

———ve Akal, F., 1978, Kompleks bakır-kurşun-çinko konsantrelerinin sülfatlayıcı kavurma ve liç yoluyle değerlendirilmesi üzerine araştırma: Diploma projesi, E.Ü. Maden Mühendisliği Bölümü, izmir.

———ve Akdağ, M., 1977, Çok ince öğütülmüş bulk konsantrelerinden sülfürik asit liçi ve bunun Doğu Karadeniz kompleks cevherlerine uygulama olanakları: Türkiye 2. Metalürji Bilimsel ve Teknik Kongresine tebliğ, şubat.

Berg, A. ve Pape, F., 1978, Neuere Erfahrungen bei der Wirbelschichtröstung von Zinkkonzentraten: Erzmetall Bd. 31, H,5.

Çakır, A.F., 1976, Harşit-Köprübaşı kompleks Cu-Pb-Zn-Sb-Ag-Cd cevher konsantresinin ferrik klorür çözeltisinde liçi: Doçentlik tezi,İ.T.Ü., istanbul.

Gock, E., 1978, Beeinflussung des Löseverhaltens von Kupferkies durch Festkörperreaktionen bei der Schwingmahlung: Erzmetall Bd. 31, 282-287.

Lindner, K.H., 1966, Über den Einfluss der Feinstmahlung auf die Eigenschaften des Mahlgutes, Diss. 83, TU Berlin.

Pawlek, F.E., 1977, Einfluss von Korngrösse mineralogischer Beschaffenheit auf die Laugbarkeit von Kupferkonzentration, TU Berlin.

Rolf, L., ve Gock, E., 1976, Untersuchungen zur Optimierung der Schwingmahlung chemie-anlagen + verfahren, 27-31.

Tkacova, K.; Hochmanova, I. ve Mihalik, V., 1975, Veranderung der Oberflâcheneigenschaften feinkörniger Minerale wâhrend des Zerkleinerungprocesses (ÇSSR, Kosice) Freiberger Forschungshefte A 531, 167-174.

Unan, C., 1971, Espiye-Kızılkayalar bakirli pirit yataklarının mineralojik etüdü: TBTAK Proje MAG-201.

MINERALOGY OF THE MADENBELENITEPE (SOĞUKPINAR-BURSA) TIN MINERALIZATION

Ahmet ÇAĞATAY, Yılmaz ALTUN and Bülent ARMAN

Mineral Research and Exploration Institute of Turkey

ABSTRACT. — Tin mineralization occurs in the greisenized granite porphyry in Madenbelenitepe area. Stannite is the major tin mineral. Cassiterite is found in trace amounts. Associated minerals are arsenopyrite, pyrite, sphalarite, fahlerz (tennantite-tetrahedrite), galena, chalcopyrite, bournonite, boulangerite, rutile and pyrrhotite. Gangue minerals are represented by quartz, muscovite, sericite and minor amounts of apatite.

To the East of Madenbelenitepe mineralization, scheelite, wolframite and molibdenite occurs in granite, greisenized granite and granite porphyry. Pyrite, arsenopyrite, cosalite, scheelite, wolframite (partly altered to scheelite), molibdenite, specularite, sphalarite, tennantite, chalcopyrite and tourmaline occurs in hydrothermal quartz veins intersecting granites and metamorphic schists.

Madenbelenitepe tin mineralization shows many features similar to those observed in the upper zones of other tin mineralizations found throughout the world, and the mineralization described here, is seemingly a «hydrothermal quartz greissem type formed at high temperatures.

INTRODUCTION

The use of tin minerals in Asia Minor dates back to times immemorial, and although some believe that at least for the past 4,000 years tin has been used by the inhabitants of this part of the globe, opinions regarding the origin of the tin minerals used are contradictory (Kaptan, 1976). The writers of the present work believe that the study of tin mineralization occurring in Madenbelenitepe area shall contribute to the understanding of whether tin minerals used by the inhabitants of Asia Minor were extracted from local sources or brought to the region from sources outside.

Madenbelenitepe tin mineralization, outcropping on the southern flanks of Handeresi valley, occurs in Soğukpınar village, Keles, Bursa Province (Fig. 1). The area was first sampled by A. Çağatay in September 1979, during a trip made within the framework of Project (Exploration Project for Polymetils, Wolfram in particular, in Northwest Anatolia), and with other personnel associated with this Project. During this trip, several other deposits and mineralized areas were visited and samples were collected for preliminary investigations. The area was visited again in April 1980, as abundant stannite and other minerals as well, were determined during polished section studies of the samples collected from the area. During the second trip made to the area by the writers of the present work and the project personnel, the mineralized area and its surroundings were studied and samples were collected for further studies.

Field observations, microscopic studies and the results obtained from the analyses indicate that Madenbelenitepe tin mineralization has some potential value. The purpose of the present work, which describes tin minerals and other associated minerals occurring in the area, is to show that the area under investigation is a favorable environment in terms of tin mineralization.

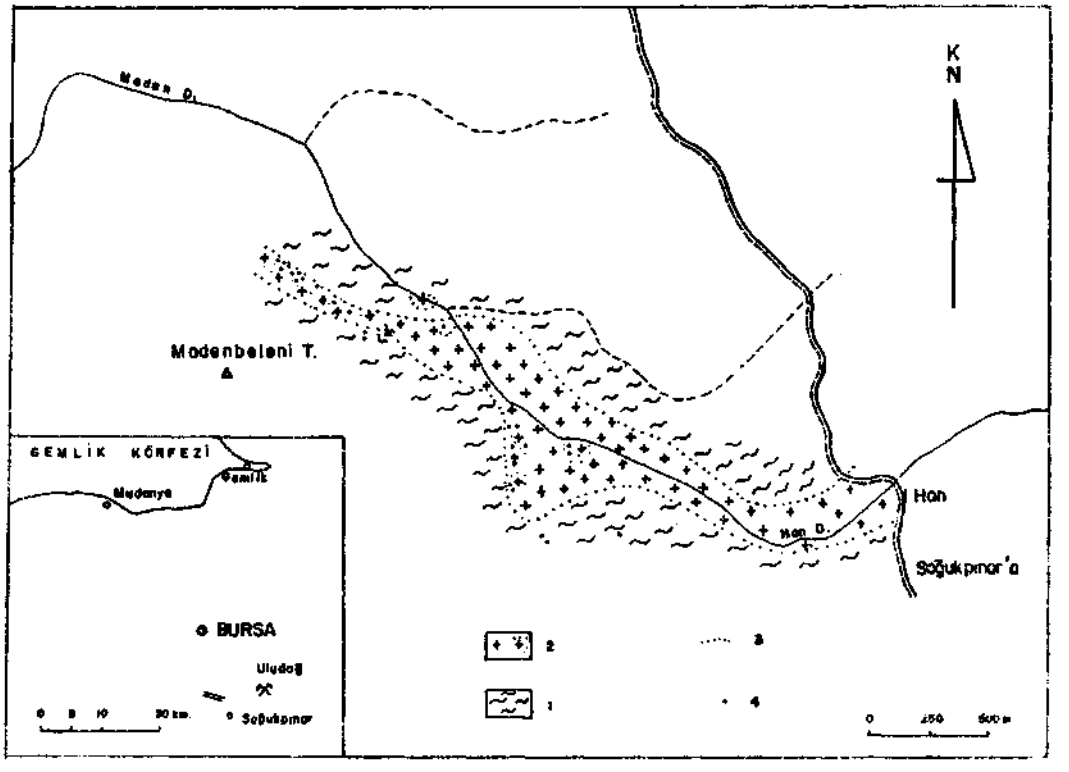

Fig. 1 - Location and Geological Map of the Area.
1 - Metamorphic rocks; 2 - Granite, granite porphyry (local greisenization); 3 - Contact; 4 - Sample locations.

FIELD OBSERVATIONS

Madenbelenitepe tin mineralization occurs in the Handeresi Valley, extending E-W to the south of Uludağ granite and within the granite porphyry outcropping S of the valley and along the granite porphyry contact. Granite porphyry outcropping in a narrow belt between the metamorphic schists (mica-quartz schist, epidote-actinolite-quartz-chlorite schist and calc schist) and marbles on the southern flanks of Handeresi valley (Fig. 1 and 2), locally grade into two-mica granite in the east and lower parts. Madenbelenitepe mineralization may be traced in a narrow zone, as much as 500 meters long, in the greisenized portions of the granite porphyry. The same is also true for the outcrops and ancient adits and trenches. Adits and other passages, partly favoring entrance, are known to have been opened in the near past for zinc and lead production. In the lower horizons, however, several workings have been observed, which may have been ancient adits and trenches.

Granite porphyry, on the whole partly altered, has been subject to strong hydrothermal alteration (i.e. greisenization) effects, in mineralized areas. To the W of the mineralized area, greisenization is characteristically in the form of an internal greisenization» (Scherba, 1970; Smirnov, 1976). Mineralization in this part of the area, is essentially in the form of stockworks and fills in the fissures and fractures developed, within the greisenized granite porphyry. According to Tischendorf (1969, 1970 and 1973) and Stemprok (1971), this type of mineralization is closely related to grano-

toids. Hydrothermal quartz, arsenopyrite, pyrite, sphalarit eand galenite may be seen in the veins, even with the naked eye. To the east of the mineralized area however, the grain size of these minerals is typically smaller and epidotization, chloritization, hematitization and silicification is very common along the contact between the granite porphyry and metamorphic schists.

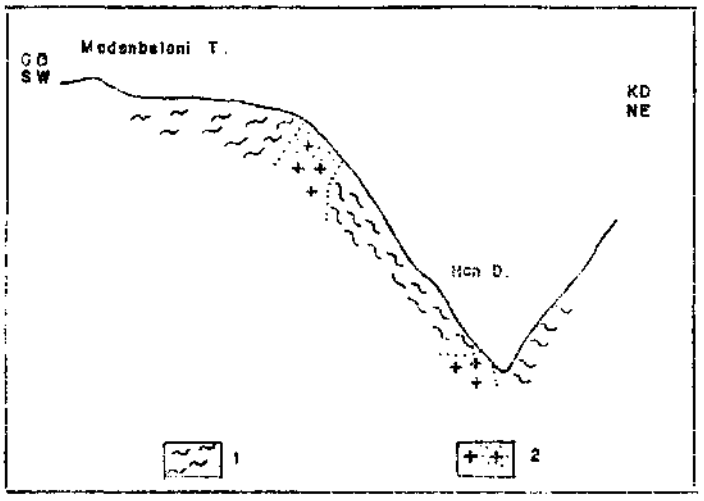

Fig. 2 - Diagramatic Geological Section.
1 - Metamorphic rocks; 2 - Granite, granite porphyry (local greisenization).

Further to the east of Madenbelenitepe tin mineralization, granite porphyry, granite and abundant hydrothermal quartz veins, of varying thickness and intersecting the former two, can be observed. Quartz veins, as much as 1-2 m locally, form elevations on the land surface due to their hardness and occur widely dispersed throughout the area as a result of their breaking and disaggregation. Ore minerals are common in the authoctonous and allochtonous quartz veins and fragments, these will be treated in detail in the chapter on the Microscopic Study of Hydrothermal Quartz Veins.

Recrystallized limestones occurring along the granite porphyry contact to the W and S of the mineralized area, have been altered into hornfels as a result of silicification, and form elevations on the land surface and may occur in the form of boulders.

MICROSCOPIC STUDIES

Granite, greisenized granite, granite porphyry, and greisenized granite porphyry closely related to mineralization and ore and hydrothermal quartz veins occurring in the area were studied in detail.

Granite-greisenized granite

The rock characterized by crystalline, sub-idiomorphic texture comprises of quartz, oligoclase, microcline, orthoclase, biotite and muscovite and accessory minerals such as scheelite, rutile, apatite, topaz and pyrite (Plate I, fig. 1).

Quartz is hypidiomorphic and shows interlocking texture. Feldspar, mostly idiomorphic and sub-idiomorphic, consists of oligoclase and minor microcline and orthoclase. Perthitization, sericitization and argillization can be observed in places. Mica is represented by brown colored biotite and muscovite. Biotite, however locally, has been altered to muscovite along the cleavage planes. Minute rutile needles and apatite crystals are common. Accessory minerals are represented by scheelite, coarse rutile crystals, apatite and sparse topaz (Plate I, fig. 1).

Granite is greisenized in places (Plate I, fig. 2) and contains quartz and muscovite. Quartz is hypidiomorphic and shows interlocking texture, while muscovite occurs as aggregates. Greisenized granite also contains minor amounts of orthoclase, microcline, sparse biotite and apatite, rutile, pyrite and molibdenite as accessory minerals.

Granite porphyry and greisenized granite porphyry

Granite porphyry samples collected outside the mineralized area, are typically porphyritic and contain quartz, feldspar and muscovite phenocrysts (Plate I, fig. 3).

Quartz crystals, idiomorphic, sub-idiomorphic and hypidiomorphic, have been locally effected by magmatic corrosion. Feldspar is composed of oligoclase and minor orthoclase and sericitization is widespread. Muscovite, an alteration product of biotite, contains rutile needles and crystals along the cleavages planes (Plate I, fig. 4).

Matrix is composed of microcrystalline quartz, feldspar and sericite. Accessory minerals are rutile, apatite and pyrite.

Effects of hydrothermal alteration, commonly observed in the granite porphyry, are stronger near the ore zone, where the rock consists of quartz, muscovite and sericite, occurring as gangue minerals associated with the ore.

Ore minerals

Samples collected from Madenbelenitepe area contain stannite group minerals, i.e. stannite, isostannite, hexastannite, minor cassiterite and other metallic minerals such as arsenopyrite, pyrite, sphalarite, galenite, fahlerz (tennantite-tetrahedrite), bournonite, chalcopyrite, boulangerite, rutile and pyrrhotite. In the following chapters, tin minerals shall be described in detail, whereas others shall be treated only briefly.

Tin minerals

Stannite group covers a wide range of similar minerals. Studies carried out on this group of minerals by various writers (Levy, 1956,1957,1966; Moh, 1960,1961,1969,1971; Ramdohr, 1975) indicate that the minerals belonging to this group, are hard to distinguish on the basis of their microscopic features only. In the present work, such tin minerals as stannite, isostannite and hexastannite were determined in the samples collected from the area under investigation and these will be classified and treated as stannite.

Stannite. — Stannite, formed after arsenopyrite and pyrite, replaces the latter (Plate I, fig.5; Plate II, fig. 2), and occurs as hypidiomorphic crystals in the interstices between arsenopyrite and pyrite. Stannite crystals may be as much as 1-1.5 mm, and may show linear arrangement along the smooth edges, due to anisotropism (Plate I, fig. 5).

As the crystal structure of stannite has many similarities to that of sphalarite, intergrowing is a very common feature. Stannite may form exsolutions (Plate I, fig. 6) and inclusions (Plate I, fig. 7), in sphalarite along certain crystallographic directions; sphalarite in turn may form exsolutions arranged along certain crystallographic directions and inclusions as well, enveloping stannite exsolutions. Stannite developing simultaneously with sphalarite, replaces and is replaced by the latter.

Fahlerz and galenite, younger than stannite, intersect the latter. The same is also true for chalcopyrite, although rarely. Sub-rounded stannite inclusions are very common in the fahlerz and galenite veinlets. Very minute chalcopyrite exsolutions (hardly distinguishable at 500 x magnification) may sometimes be observed in stannite.

Very thin and parallel twinning laminae are not uncommon in stannite, which shows distinct reflection pleochroism and anisotrophy under polarized light (Plate I, fig. 5). Stannite, formed at relatively high temperatures, has been altered to isostannite and hexastannite, owing to decreases in temperature; and as a result isostannite and hexastannite may occur as intergrowths. Isostannite and hexastannite intergrowths are very common in and around sphalarite and they may sometimes occur interlocked with ordinary stannite. Stannite, formed as the alteration product of isostannite and hexastannite, however, occurs in lesser amounts compared to ordinary stannite.

Cassiterite. — Cassiterite has been identified in a limited number of samples taken from the area, as idiomorphic crystals, as much as 10-20 microns in size, and in trace amounts. Cassiterite occurs in the fahlerz veinlets intersecting stannite, and has been formed as a result of element exchange between these minerals (Plate II, fig. 1). During the element exchange, copper present in the composition of stannite has been used by fahlerz, remaining tin forming Cassiterite. Ramdohr (1975) reports that such Cassiterite formations are common in areas where chalcopyrite intersects the stannite.

Other ore minerals

Arsenopyrite. — Arsenopyrite, occurring very widespread and as idiomorphic crystals (Plate II, fig. 2), is the oldest ore mineral following pyrite I, present in trace amounts, and rutile. The coarsest arsenopyrite crystal contained in the samples collected from the area under investigation, has been measured to be 0.8 x 0.4 mm. Rutile and pyrite I inclusions are common in arsenopyrite, which occasionally shows cataclastic texture and occurs either as inclusions in other ore minerals or being entirely replaced by the latter.

Pyrite. — Pyrite shows two distinst modes of formation. Pyrite I, occurring in trace amounts and as idiomorphic crystals, is the oldest mineral after rutile. Pyrite II, however, younger than rutile, pyrite I and -arsenopyrite, is older than other ore minerals. Pyrite II crystals, generally idiomorphic or sub-idiomorphic, may be as much as 2 mm, and show cataclastic texture in places (Plate II, fig. 3). Pyrite II, encloses rutile, arsenopyrite and however rarely, pyrrhotite inclusions. Other minerals replacing Pyrite II, occur as grains and veinlets in the latter (Plate II,.fig. 3).

Sphalarite. — Occurring as hypidiomorphic crystals in the interstices between idiomorphic quartz, arsenopyrite and pyrite crystals, encloses stannite and to a lesser degree, chalcopyrite exsolutions (Plate II, fig. 4). Stannite and chalcopyrite exsolutions enclosed along certain crystallographic directions in sphalarite, are indicative of a zonal growth. Chalcopyrite exsolutions, generally envelope coarser crystals compared to stannite exsolutions, and may be interlocked with the latter. It may thus be concluded that sphalaritfc is contemporary with stannite and chalcopyrite, younger than rutile,. arsenopyrite and pyrites and older than other minerals. Fissures and minute

fractures developed in sphalarite, showing cataclastic texture, are filled by fahlerz, galenite (Plate II, fig. l),chalcopyrite and carbonate minerals. Sphalarite can also form exsolutions in these minerals.

Fahlerz (tennantite-tetrahedrite). — Like sphalarite, hypidiomorphic fahlerfc crystals occur between idiomorphic quartz, arsenopyrite and pyrite crystals. Fahlerz, younger than sphalarite and stannite, replaces arsenopyrite, sphalarite and stannite along the fissures (Plate II, fig. l). Such reaction minerals as bournonite and boulangerite are common along the contact, where fahlerz has been replaced by galenite; such relationship may sometimes lead to the formation of a myrmekitic texture also (Plate II, fig. 5), and arsenopyrite, pyrite, quartz, sphalarite and stannite inclusions and galenite intrusions are therefore, not uncommon in fahlerz. Chalcopyrite contained in minor amounts is presumed to have been formed contemporary with the fahlerz.

Galenite. — Since galenite is the youngest mineral following chalcopyrite, which replaces the former, replaces all other minerals and encloses them as inclusions. Minute grains of boulangerite and bournonite, formed partly as a result of replacement of fahlerz by galenite, are very common and abundant in galenite. Galenite has been altered to sericite along the cleavage planes and grain margins. Native silver grains, as much as 3-5 microns, have been identified in the samples collected from the stockwork ores occurring to the W of Madenbelenitepe mineralization.

Chalcopyrite. — Chalcopyrite occurring in minor amounts, may be divided into three age groups - the oldest chalcopyrite is represented by those (Plate III, fig. 4) enclosed in sphalarite and stannite as minute inclusions and exsolutions. These are believed to have been formed simultaneous with the sphalarite and stannite, whereas chalcopyrite occurring as minute grains in fahlerz are contemporary with fahlerz. Chalcopyrite veinlets intersecting galenite and other minerals in Madenbelenitepe mineralization, on the other hand, is the youngest mineral.

Bournonite. — Bournonite, has been formed at the contact between fahlerz and galenite, at least partly replaced by the former, as a reaction product. Bournonite, occurring as intergrowths with galenite and fahlerz, forms myrmekitic texture with galenite (Plate II, fig. 5). In some bournonite crystals, parallel twinning laminae may be observed (Plate II, fig. 6).

Boulangerite. — Occurs as sub-rounded, worm-like grains in galenite, rod-like grains in the gangue and as a reaction product along the galenite-fahlerz contact.

Rutile. — Rutile is the oldest ore mineral, and occurs in minor amounts and different forms. Minute rutile needles and rods occur along the cleavage planes developed in muscovite and as inclusions enclosed in the pyrite and arsenopyrite crystals. Rutile needles may be as much as 60x12 microns. Idiomorphic to sub-idiomorphic rutile crystals, showing cataclastic texture and rarely as much as 100-200 microns, were also observed. Parallel twinning laminae, generally developed in one and rarely in two directions are not uncommon.

Pyrrhotite. — Occurs in small amounts and as minute and sub-rounded inclusions in pyrite.

Hydrothermal quartz veins

Samples collected from the hydrothermal quartz veins contain hypidiomorphic quartz, minor sericite, tourmaline, scheelite and opaque minerals. Opaque minerals are represented by cosalite, wolframite, which is altered to scheelite along the margins, molybdenite, pyrite, sphalarite, arsenopyrite, fahlerz, chalcopyrite, specularite and covelline.

ANALYSES

Microprobe analysis

Results obtained from microprobe analyses of the stannite crystals identified in the samples collected, confirm microscopic observations. Studies carried out on stannite (Plate II, fig. 7), have shown that major constituents are Cu, Fe, Zn, Sn and S; Ag, present in trace amounts is accessory mineral. Quantitative microprobe analyses on stannite however, could not be made, due to the unavailability of necessary standard solutions. Results obtained from qualitative microprobe analyses, i.e. Cu K a, Fe K a, and Sn K a, made on a stannite crystals are given in Plate II, figures 8,9 and 10.

Semi-quantitative optical spectrographic analyses

Semi-quantitative optical spectrographic analyses were made on four seperate samples, containing stannite (Table 1).

Table 1 - Results of semi-quantitative optical spectrographic analysis

Samples		*I*	*II*	*III*	*IV*	*Dedection limits*
Elements (%)	Sn	0.2	0.1	0.04	0.2	
	Fe	> 4, ≃ 10	> 4, ≃ 7	> 4, ≃ 7	> 4, ≃ 10	
	Cu	0.3	0.3	0.1	0.4	
	Zn	> 1, ≃ 2	> 1	> 1	> 1	
	Pb	> 1, ≃ 3	0.4	0.4	0.2	
	As	> 1	> 1	> 1	> 1	
	Sb	G	G	G	G	0.02
	Bi	G	G	G	G	0.02
	Ti	0.03	0.04	0.02	0.04	
	Cd	0.02	0.04	0.1	0.03	
	Ag	0.015	0.02	0.01	0.015	
	Au	G	G	G	G	0.002
	Li	G	—	—	G	0.1

CONCLUSIONS

Results obtained from the mineralogicai-petrographical studies of the samples collected fron Soğukpınar Madenbelenitepe mineralization may be briefly described as follows:

1. Greisenization (i.e. hydrothermal alteration) is typical in the granites and granite porphyry outcropping extensively throughout the area. As Deer et al. reports (1962), biotite has been altered to muscovite and as a result of this alteration process, Ti present in the crystal structure of biotite has been released and very minute rutile needles and rods have been formed along the cleavage planes developed in muscovite. Fe released during the alteration process has been used in the crystal structure of pyrite and arsenopyrite.

2. Based on the results obtained from the mineralogical-petrographical study of the samples collected from Madenbelenitepe mineralization, the sequence of formation of the minerals contained is as follows:

Muscovite (alteration product of biotite), sericite (alteration product of feldspar), rutile needles
Quartz (hydrothermal origin), sericite, pyrite I
Arsenopyrite, sericite, quartz
Pyrite II, quartz
Sphalarite, stannite, chalcopyrite
Fahlerz, chalcopyrite, carbonate
Galenite, bournonite, boulangerite
Chalcopyrite

3. Madenbelenitepe mineralization extends over an, area of 500-600 meters. Tin minerals, are relatively more abundant in the stockwork type of ore occurring in the western part of the mineralized area; they occur in lesser amounts in the eastern part of the area under investigation. Fahlerz and bournonite, in particular, increase from west to east.

4. Stockwork ores occurring in the greisenized granite porphyry located to the West of Madenbelenitepe mineralization, have been formed by high-temperature hydrothermal solutions. Based on the textural and structural features observed it may be concluded that mineralization occurring in the west, represents relatively higher-temperature conditions compared to the mineralization observed in the east.

5. Skarn minerals such as epidote, chlorite, quartz, garnet, diopsite, magnetite and hematite occur in small amounts along the contact between the granit porphyry and recrystallized limestones, calc-schists and other metamorphic schists.

6. Granite and greisenized granite occurring on the eastern extension of Madenbelenitepe mineralization contain topaze, apatite, molibdenite, scheelite and wolframite; hydrothermal quartz veins, on the other hand, contain tourmaline, molibdenite, scheelite, wolframite (partly altered to scheelite) and cosalite. These minerals occur in association with tin mineralization (Stemprok, 1965; Schrocke, 1968; Baumann et al., 1974 and Yajima, 1979).

7. The abundance of hydrothermal quartz veins, hornfels and quartz-bearing greissen in the area under investigation, is an indication of the presence of SiO_2 -rich granite. This is also true for tin mineralizations found in other countries (Tischendorf, 1969).

8. The occurrence of stannite and stannite group minerals in the outer zones of tin deposits found in other countries (Ramdohr, 1975) and of cassiterite as well in deeper zones (Mulligan, 1975; Aubert, 1969; Burnol, 1974; Fov, 1969; Hosking, 1970; Mitchell, 1974 and Bromley, 1975), may also be true for Madenbelenitepe mineralization.

9. According to a classification made by Mulligan (1975) Madenbelenitepe tin mineralization belongs to «hydrothermal quartz-greissenD type.

ACKNOWLEDGEMENTS

The writers wish to express their gratitude to N. Pehlivan, N. Yüce, A. Kara and M. Yıldırım, associated with the KAWAP project for the accomplishment of the field work. Special acknowledgement is due N. Öztuğ and S. Alparslan for making micrbprobe analyses of stannite; and M. Güler, T. Akyüz and Ş. Taş for semi-quantitative optic spectrographic analyses of samples. The writers are also indebted to Dr. Orhan Özkoçak and Dr. M.Yıldız for giving valuable-assistance for the completion of this work.

Manuscript received Junt JO, 1980

Translated by: Filiz E. DİKMEN

REFERENCES

Aubert, G., 1969, Les coupoles granitiques de Montebras et Echassieres (Massif Central, Français) et la genese de leurs mineralisations enetain, lithium, tungstene et teryflium: Memoires du B.RG.M. (Bureau de Recherches Geologiques et Minieres), 46 (2 vol.), Paris. ;

Baumann. L; Stemprok, M.; Tischendorf, G. and Zoubek, V., 1974, Metallogeny of tin and tungsten in the Krusne* Hory-Erzgebirge: Internat. Geological Correlation Programme, Excursion Guide, Prag.

Bromley, A.V., 1975, Tin mineralization of Western Europe: is it related to crustal subduction? Institution of Mining and Metallurgy, Transactions/ Section B (Applied earth science), London, B 28 - B 30.

Burnol, L., 1974, Acid granites and associated metallization in the North-Western part of the French Central Masse: International Geological Correlation Programme, Metallization associated with acid magmatism, Symposium Karlovy Vary, 59-76.

Deer, W.A.; Howie, R.A. and Zussman, J., 1962, Rock-forming minerals: 3, Longman, London, 90.

Fox, D.J., 1969, Tin mining in Spain and Portugal.-a paper of information.- Fox, W. editor, A second technical conference on tin, Volume one, Bangkok, 223-265.

Hosking, K.F.G., 1970, The nature of the primary tin ores of the southwest of England: Fox, W editor, A second technical conference on tin, Volume three, International tin council, London, 1157-1244.

Levy, CL., 1956, La stannite jaune du gisement de Vaulry, Haute Vienne: Bull. Soc. franc. Min. 79, Paris, 383-391.

———, 1966, Contribution a la mineralogie des sulfures de cuivre du type Cuax S4: Mem. Bur. Rech. G£ol. et Minieres. Der A.4652, 5499, 158.

———and Prouvest, J., 1957, Rapport entre la chalcopyrite, la stannite et la rlnierite: Bull. Soc. fr. Mineral. 8, 59-66.

Mitchel, A.H.G., 1974, Southwest England granites: magmatism and tin mineralization in a post collision tectonic setting: Institution of Mining and Metallurgy,Transactions / Section B (Applied earth science) London, August, B95 - B97.

Moh, G.H., 1960, Experimentelle Untersuchungen an Zinnkiesen und analogen Germaniumverbindungen: N. Jahrb. Min. Abh., 94, Festband Ramdohr, 1125-1146.

———, 1961, Neue Untersuchungen der Mineralgruppen Zinnkies-Fahlerz: Fortsch. d. Mineralogie, 39, 352.

———, 1969, The tin-sulfur system and related 'minerals: N. Jahrb. Miner., Ill, 227-263.

———and Ottemann, J., 1962, Neue Untersuchungen an Zinnkiesen und Zinnkiesverwandten: N. Jahrb. 99, 1-28.

Mulligan, R., 1975, Geology of Canadian tin occurrences: Geological survey of Canada. Economic geology report, 28, Ottawa, 1-129.

Ramdohr, P., 1975, Die Erzmineralien und ihre Verwachsungen: 4., beartbeitete und enveiterde Auflage: Akademie Verlag Berlin, 587-603.

Schrocke, H., 1968, Zur Bildung von, Zinn-Wolfram-Lagerstatten. Eioe Bemerkung: Mineralium Deposita, 3, Berlittfleidelberg, New,York, 182-184.

Sbcherba, G.N., 1970, Greisens (Part 1,2); Internal. Geology Review, Washington, D.C. 114-150 and 239-255.

Smirnov, V.I., 1976, Geology of mineral deposits: Mir publishers, Moscow, 205-210.

Stemprok, M., 1965, On the relation of tin-tungsten-molybdenum ore deposition to granites: Krystalinikum 3, Prag, 163-181.

———, 1971, Intra-Mineralization granitic dykes in the Krusne Hery metallogenic province: Krystalinikum, 8, Prag, 141-148.

Tischendorf, G., 1969, Über die kausalen Beziehungen zwischen Granitoiden und endogenen Zinnlagerstatten: Zeitschrift f. angewandte Geologie, 15, Berlin 1969, 333-342.

———, 1970, Zur geochemischen Spezialisierung der Granite des westerzgebirgischen Teilplutons: Geologie, 19, Berlin 1970, 25-40.

———,1973, The metallogenic basis of tin exploration in the Erzgebirge: Transactions, Institution of Mining and Metallurgy, 82, B 9-B 24.

Yajima, J. *nd Ohta, E., 1979, Two-stage maneralizatioo and formation process of the Toyoha Deposits, Hokkaido: Japan, Mining Geology, 29 (5)., 291-306.

PLATES

PLATE - I

Fig. 1 - Magnification X 50.
Topaz in granite (between biotite crystals); biotite (with cleavage, gray to dark gray colored) containes rutile (black). Quartz and feldspar (light gray) and pyrite (black) in the matrix.

Fig. 2 - Magnification X 50.
Muscovite (with cleavage and as light-colored accumulations) and quartz (light-colored and without cleavage) in granite as a product of greisenization.

Fig. 3 - Magnification x 50, nicol +.
Sericite flakes (upper and lower right corners), quartz phenocrysts (light gray and white), muscovite (in the middle; with cleavage and light to dark gray), rutile crystals (black, in muscovite), small quartz crystals and sericite flakes in the matrix, developed in granite porphyry as a result of greisenization.

Fig. 4 - Magnification x 100.
Rutile needles and crystals (black) developed along the cleavage planes of muscovite which is the alteration product of biotite in granite porphyry, apatite (with high relief, upper left corner).

Fig. 5 - Magnification x 400, in oil, nicol +.
Pyrite (light gray), stannite (gray to dark gray, anisotropic, in pyrite). Arsenopyrite (idiomorphic, in stannite). Gangue and gaps (black).

Fig. 6 - Magnification x 600, in oil.
Stannite exsolutions (light gray) developed along crystallographic directions in sphalarite (gray). Gangue and gaps (black).

Fig. 7 - Magnification x 600, in oil, nicol +.
Stannite (light gray) inclusions and exsolutions in sphalarite (gray). Arsenopyrite (white and idiomorphic).

Fig. 8 - Magnification x 600, in oil.
Iso-stannite (gray) and hexastannite (light gray) formed from high temperature stannite, sphalarite and gangue (dark colored).


1

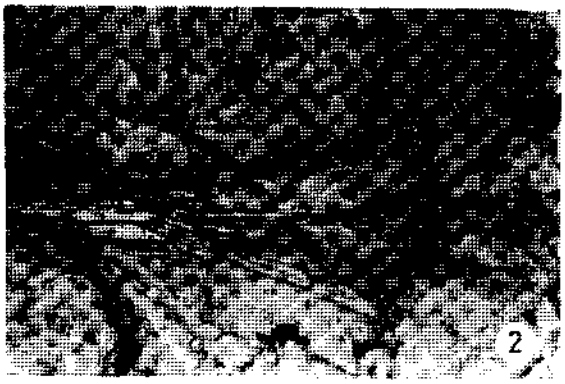
2

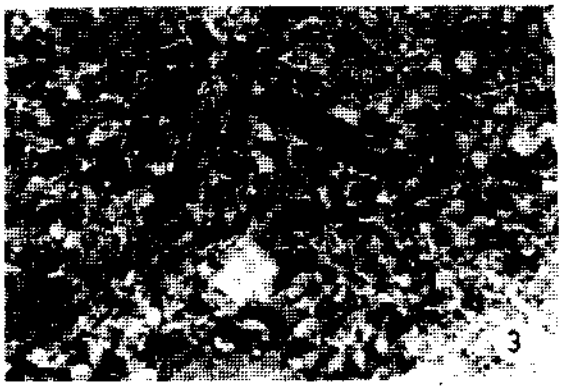
3

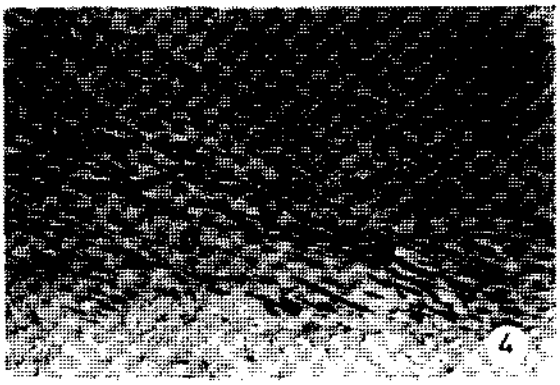
4

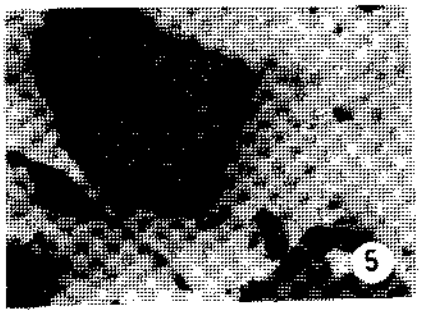
5

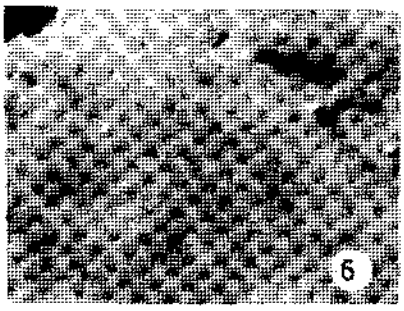
6


7

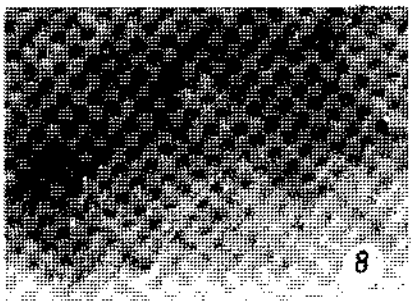
8

PLATE - II

Fig. 1 - Magnification x 600.
Cassiterite (dark gray) formed along the fahlerz (lighter gray) veinlets intersecting stannite (light gray) in sphalarite. Arsenopyrite (white and idiomorphic), galenite (white) veinlets intersecting sphalarite with fahlerz. Quartz and gaps (black).

Fig. 2 - Magnification x 200.
Stannite (gray) between arsenopyrite (idiomorphic and white). Quartz (black).

Fig. 3 - Magnification x 400, in oil.
Fahlerz (gray) fills fissures between cataclastic pyrite (light gray), Gangue (black).

Fig. 4 - Magnification x 400, in oil.
Chalcopyrite (white) and stannite (light gray) exsolutions in sphalarite (gray).

Fig. 5 - Magnification x 400, in oil.
Bournonite (gray) forms myrmekitic texture with galenite (light gray). Arsenopyrite (idiomorphic and white), sphalarite (dark gray), gangue (black).

Fig. 6 - Magnification x 400, in oil, nicol +.
Bournonite (in the middle) contains parallel twinning laminae developed in different directions. Galenite (light gray) contains fahlerz (gray), sphalarite (dark grey), arsenopyrite (white) and pyrite (white) and bournonite as well. Quartz (black).

Fig. 7 - Magnification x 100.
Electron image of stannite (in the middle). Arsenopyrite in the matrix. Gangue (black to dark gray).

Fig. 8 - Magnification x 100.
Electron image of Cu K_a of Fig. 7.

Fig. 9 - Magnification x 100.
Electron image of Fe K_a of Fig. 7.

Fig. 10 - Magnification x 100.
Electron image of Sn K_a of Fig. 7.

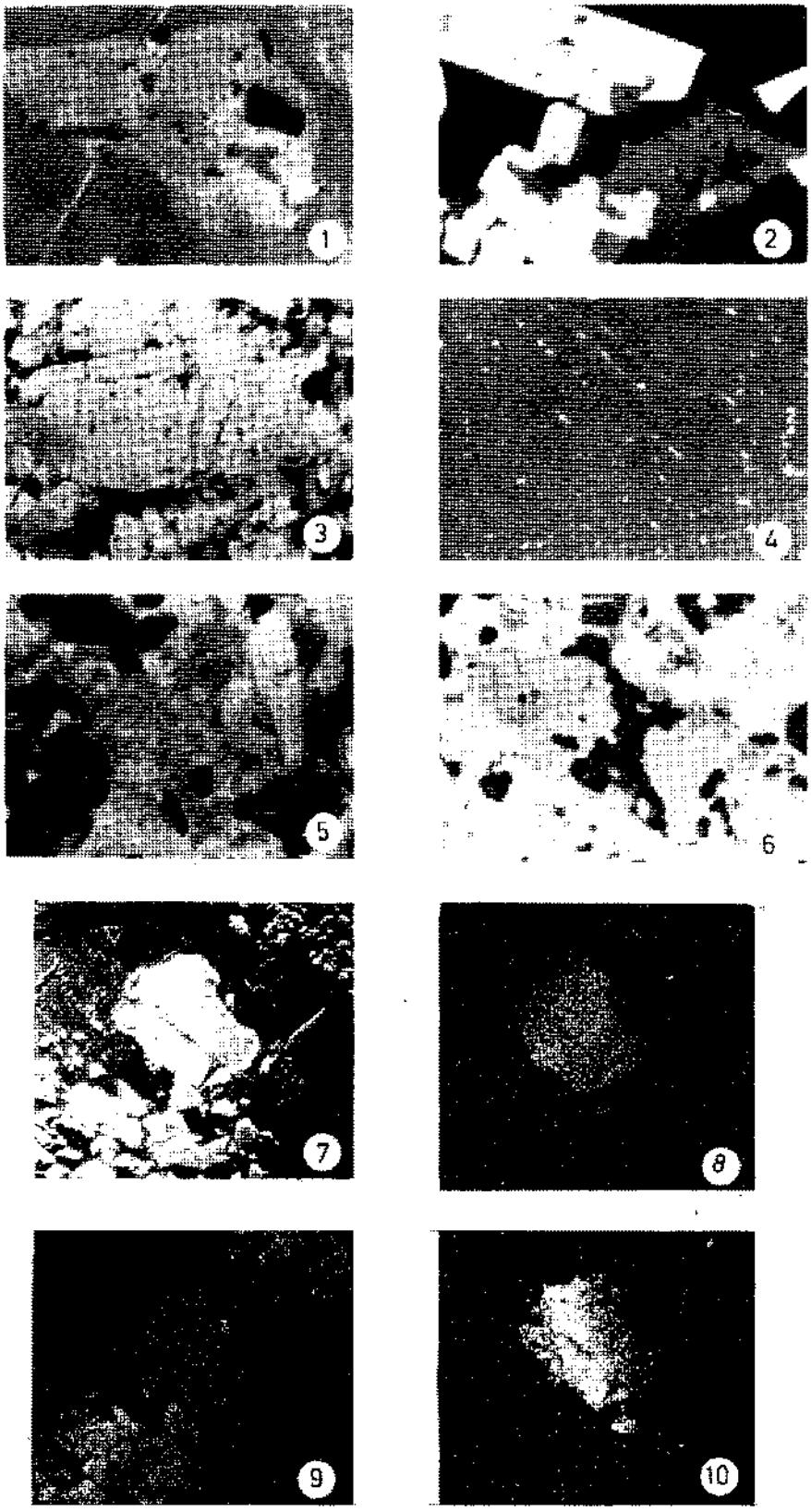
1
2
3
4
5
6
7
8
9
10

SUALTI KÜTLE AKIMI FASİYESLERİ: KAVRAMSAL ELEŞTİRİ VE ORTAMSAL YORUM

Sungu L. GÖKÇEN ve Abdurrahim ŞAHBAZ

Hacettepe Üniversitesi Yerbilimleri Enstitüsü, Ankara

ÖZ. — Denizel ortamlarda büyük çapta Sediment taşıyan unsurlardan birisi de sualtı kütle çekimi akıntılarıdır. Bu kütlesel taşınmalar genellikle kayma, sürüklenme-yuvarlanma ve yoğunluk türü süreçler ile gerçekleşir. Bu mekanizmalarla denizlerin farklı jeomorfolojik ünitelerinde çökeltilmiş resedimente oluşumlardan jeoloji literatüründe en çok incelenmiş olanları türbidit, olistostrom ve melanj fasiyesleridir. Bununla beraber farklı kütle hareketlerinin, dolayısiyle değişik süreçlerin ürünü olan bu kırıntılı fasiyeslerin gerek tanımı, gerekse ilişkileri halen tartışmalıdır, iç ve dış kaynaklı literatürün son 15 yıldaki incelenmesi, bu karmaşıklığın sualtı kütle akımı fasiyeslerinin jeolojik-sedimentolojik karakteristikler, taşınma mekanizmaları, aktüel ortamlardan geliştirilmiş çökelme modelleri ve tüm oluşukların bir türbidit dizisi varsayımı gibi farklı ölçütlere göre ayrı ayrı değerlendirilmesinden kaynaklandığını ortaya koymuştur. Bir diğer tartışmalı konu da, bu fasiyesleri karakterize eden litolojik topluluklar ile bunların ortamsal yorumlandır. Bu çalışmada, sualtı kütle çekimi akıntılarının sınıflandırılması ve ürünlerinin adlandırılmasıyle bu fasiyeslerin belirgin litolojik topluluklarının genellemesi ve ortamsal yorumu, yeni bir düzenleme ile verilmektedir.

GİRİŞ

Bilindiği gibi kara üzerinde veya sualtındaki Sediment taşınması, genellikle sürüklenme (traction), yoğunluk (density) ve süspansiyon (suspension) akıntıları ile gerçekleşir. Birinci tür akıntılar, kara üzerinde ve sığ denizel ortamlarda çapraz tabakalanmalı kırıntıları oluştururken, süspansiyon akıntılariyle denizlerde nefoloid killer, kara üzerinde ise lös oluşumları çökeltilir. Yoğunluk akışları ise Sedimenter jeoloji literatüründe denizel türbidit fasiyesi ile karakteristiktir. Bu akıntılar karalar üzerinde gelişirse, «Nuees ardantes» türü fasiyesleri oluştururlar (örneğin; Avalanjlar, ignimbritler vb.).

Özellikle denizel ortamlarda etkin olan bir dördüncü taşınma şekli ise, gravite kökenli sualtı kütle akıntılarıdır (Subaqueous mass gravity flows). Bu akıntılar, taşınan yük, su-sediment oranı, makaslama kuvvetleri (shear strength), süspansiyon ve türbülâns etmenlerine bağlı olarak, sualtı heyelanlarından distal (ıraksak) türbiditlere kadar çeşitli kırıntılı Sedimenter fasiyesleri çökeltirler. Günümüz hidrokarbon jeolojisinde dokusal özelliklerinin (boylanma, porozite, permeabilite vb.) yanı sıra yanal ve düşey devamlılıkları ile yüzeylendikleri alana göre ekonomik anlamı olan bu fasiyeslerin bazıları plakaların (veya plakacıkların) konum ve hareket yönlerinin saptanması açısından da bölgesel jeolojide büyük önem taşırlar.

Sualtı heyelanları, kütle akmaları ve yoğunluk akış mekanizmaları ile taşınıp çökeltilen bu oluşumların iç ve dış kaynaklı jeoloji literatüründe en çok tartışılan türleri, melanj, olistostrom ve türbidit fasiyesleridir. ilk kez Greenly (1919) tarafından ortaya atılan ve Hsu'nun (1968, 1971, 1974) geliştirdiği melanj terimi ile 1955 yılında Flores'in tanımladığı olistostromlar ve Bell'in 1942 de tanımlayıp, Kuenen ve Migliorini'nin 1950 de ayrıntılarını ortaya koyduğu türbiditler arasındaki jeolojik-sedimentolojik ilişkiler, halen tartışılmaktadır. Ayrıca bunların sınıflandırılmaları ve doğal olarak tanımlanmalarında da çelişkiler vardır.

Bu çalışmada ağırlık adı geçen üç fasiyese verilerek sualtı kütle çekimi akıntıları ve bunların ürünü olan Sedimenter oluşumlar, kavramsal açıdan son 15 yılın literatürü* ışığında, irdelenerek sınıflandırılacak ve ortamsal açıdan yorumlanacaktır.

MELANJ VE OLİSTOSTROM FASİYESLERİ

Melanj

Dış kaynaklı yayınlarda melanj terimi, ilk kez Greenly (1919) tarafından Iskoçya'daki otoklastik breşler için kullanılmıştır. Bailey ve McCallien (1950, 1953) Ankara yöresindeki farklı litolojide bloklar içeren metagrovaklar için aynı terimi kullanmışlardır (Ankara melanjı). Bu fasiyesi Dott(1963), Hsü (1968, 1969, 1971 ve 1974), Wood (1974), Scholl ve Marlow (1974), olistostromlarla karşılaştırmalı olarak, irdelemişlerdir. Dimitrijevic ve Dimitrijevic'in (1973) Yugoslav Dinaridler'indeki «Liguria melanjı» ile Norman'ın (1975a, *b)* «Ankara melanjı» için kullandıkları bu terimi, Friedman ve Sanders'den (1978) sonra Norman ve diğerleri de (1979, 1980) ayrıntılı olarak tartışmışlardır.

Türkçe kaynaklarda melanj kavramını Norman (1972) ilk kullananlardan olup, Ataman ve diğerleri (1974), Norman (1975b), Çapan ve Buket (1975), Gökçen ve Gülen (1977), Çapan (1977), Batman (1978a,b) ve Koçyiğit de (1976, 1979), bu fasiyesin oluşum ve yerleşim mekanizmasını tartışanlar arasındadır.

Bu araştırıcılara göre, Sedimenter melanj, çeşitli kütle akıntısı ürünlerinin (sualtı heyelanı, moloz, tane ve türbit akışlar) devamlı veya aralı olarak bir basende birikmesinden sonra, kırıntı ve matriksin sin-post tektonik bölgesel makaslama kuvvetleri altında deformasyona uğramasından oluşmuş, kısmen metamorfize, karmaşık bir fasiyestir. Doğal olarak bu fasiyesin blok veya tane halindeki bileşenleri magmatik, metamorfik ve Sedimenter kökenlidir.

Bu tanıma uyan Sedimenter melanjın hipotetik oluşumu Şekil 1 de gösterilmiştir. Bölgesel yayılıma sahip melanj fasiyesi plaka veya plakacıkların konum ve hareket yönleri, başka deyişle yitilme (Subduction) ve üzerleme (obduction) zonlarının belirlenmesi açısından da önem taşır.

Olistostromlar

ilk tanımı Flores (1955) tarafından pelitik matriksli kırıntılı ara yığışımlar için yapılan ve Abbate ve diğerlerinde (1970) ayrıntıları verilen olistostrom teriminin 1972 yılına kadarki dış kaynaklı yayın kronolojisi Hoedemaeker'de (1973) bulunabilir. Hendry (1973), Elter ve Travisan (1973), Davies ve Walker (1974), Hsü (1974), Carter (1975), Hampton (1975), Görler (1975), Walker (1975a, *b)* ve Okada ve Kitamura (1978) yayınlarında, bu fasiyesi ayrıntılarıyle işlemişler ve resedimente konglomeralar ile karşılaştırmışlardır.

Olistostromlar bizde Norman (1973, 1975b), Gökçen (1974), Gökçen ve Şenalp (1975), Gökten (1977), Koçyiğit (1976, 1979), Baykal ve Önalan (1979) ile Gökçen (1981) gibi araştırıcılar tarafından Sedimenter jeoloji özellikleri veya oluşum mekanizmaları açılarından incelenmiştir.

Bir kütle akımı ürünü olan olistostromlar sahada çakıllı çamurtaşı, resedimante konglomera ve flaksotürbidit fasiyesleri karmaşığı şeklinde gözlenir. Başka deyişle bu üç fasiyesin Sedimenter özelliklerini kısmen veya toplam olarak içerirler (örneğin, Gökçen ve Şenalp, 1975). Çoğu kez tane

* Dış kaynaklı literatür taramasında Journal of Sedimentary Petrology, Sedimentology ve Sedimentary Geology periyodiklerine ağırlık verilmiştir.

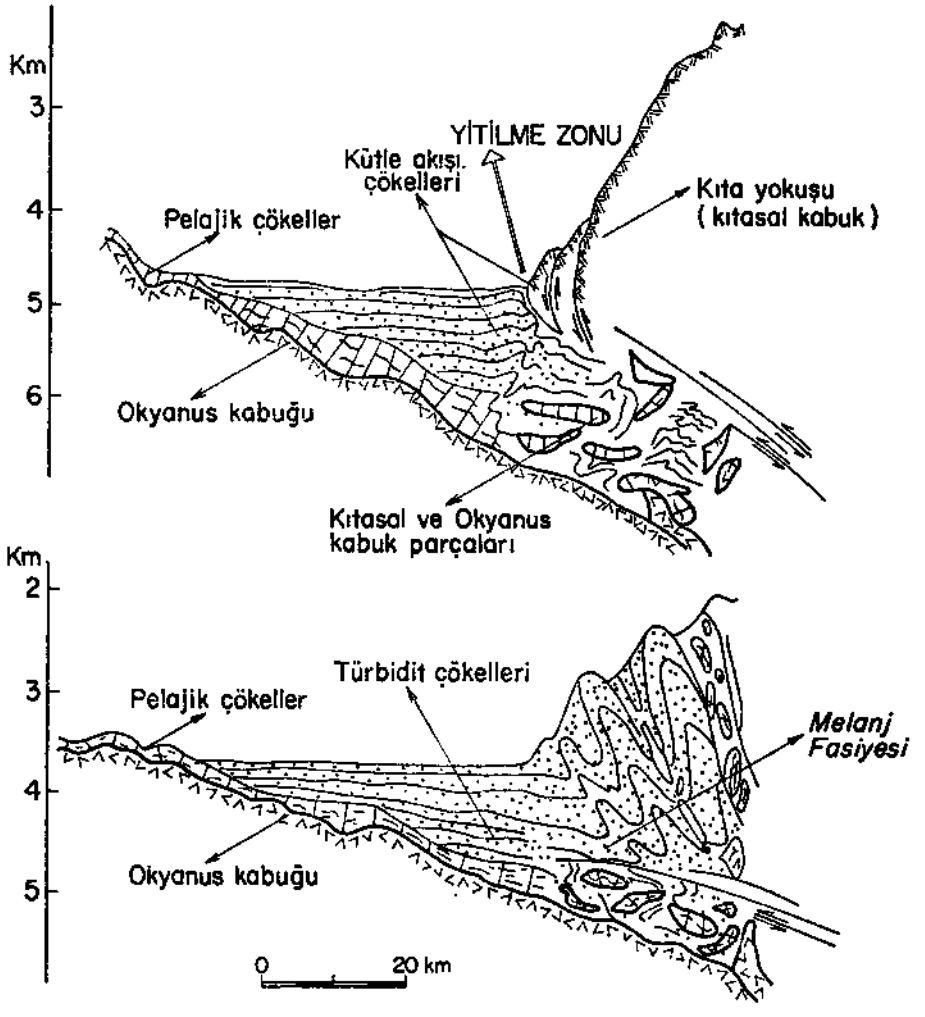

Şek. 1 - Plaka sınırlarında melanj oluşumu (Scholl ve Marlow, 1974 ten).

akıntıları ile taşınıp, çökeltildiği kabul edilen olistostromlar, aslında moloz+tane akışı ürünü çökellerdir (Okada ve Kitamura, 1978). Bu nedenle fasiyes, «olistostromik akıntılarla taşınıp çökeltilmiş ve kendine özgü sınırlı Sedimenter yapılar içeren, değişken kompozisyonlu ve makaslama etkilerinin görülmediği haritalanabilir kırıntılı oluşumlar» şeklinde tanımlanmalıdır (örneğin, Norman 1973; Gökçen, 1974; Koçyiğit, 1979). Olistostromlar ayrıca türbidit fasiyesi katmanları arasında ve haritalanamayacak boyuttaki yerel yığışımlar şeklinde de Sedimenter basenlerde gözlenebilir.

Yakın geçmişte Orta Avrupa literatürünün saha jeologlarının kullandığı, litolojisi içinde bulunduğu fasiyesten farklı ve belirgin doğrultularda dizilmiş blokları da içeren wild fliş (örneğin, Marschalko 1971) fasiyesi de, burada tanımlanmış olistostromlarla genelde eşanlamlıdır, Ayrıca Hsü'de (1974) makaslama kuvvetleriyle deformasyona uğramış Sedimenter melanjları, olistostrom olarak tanımlamakla birlikte, makalenin genel havasında olistostrom ve melanjların ayrılamadığı durumlarda, bunlar için jenetik olmayan genel bir terim niteliğinde «wild fliş» deyiminin kullanılması da önerilmektedir.

Olistostromlara benzer bir diğer denizel fasiyes de, diamiktitlerdir. Oluşum ve Sedimentolojik ayrıntıları Flint ve diğerleri (1960) ile Winn ve Dott'da (1979) verilen bu oluşum, yarı pekişmiş kalın konglomeratik yığışımlar halinde bulunur. Karasal kökenli ve değişik boyutlu bileşenleriyle matriksi ise karbonat içermez. Ayrıca 1.5-2 m büyüklüğünde dev oygu izleri ile yarı belirgin dereceli tabakalanma, fasiyesin belirgin özellikleri arasındadır. Fasiyesin taşınma mekanizması, olistostrom gibi, moloz ve tane akımı karışımıdır.

Üstteki tanımlamalar ışığında Sedimenter melanj ve olistostromlar arasındaki belirgin farklılıklar şöylece özetlenebilir: Olistostromlar yerel veya bölgesel yayılıma sahip ve kütle akışlarıyle taşınıp çökeltilmiş, ayrıca tektonik deformasyona uğramamış resedimente fasiyeslerdir. Buna karşılık Sedimenter melanj heyelandan, düşük enerjili türbid akıntılara kadar çeşitli sualtı kütle çekimi ürünlerinin, etkin makaslama kuvvetleri altında deformasyona uğradığı, bölgesel bir fasiyestir ve bu karmaşık oluşum ayrıca global tektonik açısından da önemlidir.

TÜRBİDİT FASİYESLERİ

Basen analizleri ve paleo taşınma yönlerinin saptanmasında, dolayısiyle petrol araştırmalarında büyük önemi olan bu fasiyesin tanımı, sınıflandırılması ve evrimi Norman (1963), Gökçen (1971), Şenalp ve Fakıoğlu (1977), Kayan ve Gökçen'de (1978) verilmiştir. Bu kaynaklardan da görülebileceği gibi, türbiditler koşullarının uygun olduğu her ortamda meydana gelebilen, birçok tip ve çeşitteki birincil Sedimenter yapılar içeren, geniş yanal devamlılığa sahip, oldukça kalın tabakaların ritmik bir şekilde çamurtaşı-şeyl ile ardalanmasından oluşmuş kırıntılı fasiyeslerdir.

îki sıvı arasındaki yoğunluk farkından kaynaklanmış akıntıların çökelttiği türbiditler makroskobik Sedimenter özelliklerine göre, ultraproksimal, proksimal ve distal gibi alt bölümlere ayrılmaktadır (Walker 1967, 1970, 1976).

1. Bazı yazarlarca flaksotürbidit (Dzulynski ve diğerleri, 1959; Unrug, 1963; Stauffer, 1967; Slaczka ve Thompson, 1975) veya resediment konglomera (Davies ve Walker, 1974, Walker, 1975a,b) deyimi de kullanılan ultraproksimal türbiditler, genellikle köşeli ve iri taneli bileşenlerin oluşturduğu ve proksimal türbiditlere benzer yanal devamlılığa sahip, kalın tabakalardan meydana gelmiş, tabanda bazen büyük ölçekli oygu izleri ile dereceli tabakalanma içeren Sedimenter fasiyeslerdir. Bu alt fasiyes her ne kadar yüksek yoğunluktaki (~ 275-350 gr/lt) türbid akıntılarla taşınıp çökeltiliyor ise de, bazı araştırıcılar oluşumun tane akıntısı ürünü olduğuna da işaret etmektedir (e.g. Slaczka ve Thompson, 1975; Mutti ve Ricci Lucchi, 1972, 1978; Kazancı ve Varol, 1978). Kabul edilmiş türbid akıntı hipotezine göre bu varsayım tartışmalıdır.

2. Proksimal (yakınsak) türbiditler yüksek enerjili ve konsantrasyonlu yoğunluk akışı ürünü olup, kalın, iri taneli, yanal devamlılığı değişebilen, Bouma'nın (1962) Ta ve Tb yapılarını içeren tabakalariyle taban yapısı olarak oygu izleri bulunduran fasiyeslerdir. Bu fasiyesin tabakalar arasındaki şeyl-marn pelajik arakatkısı çok incedir.

3. Düşük enerjili ve az yoğun türbid akıntı ürünü olan distal fasiyes ise, ince, yanal devamlı ve paralel kenarlı, pelajik arakatkısı bol katmanlar ile taban yapısı olarak yiv izleri görülen kırıntılı oluşumlardır. Walker'a (1975) göre, türbiditler, ayrıca ABC indeksi olarak bilinen Sedimenter yapılarının belirginliğine göre de, proksimal ve distal olarak sınıflandırılabilir.

Saha çalışmalarında üstte belirtilen özellikleri dikkate alınarak tanımlanan proksimal ve distal türbiditler, aslında türbid akıntının yüksek veya düşük akış rejimine bağlı olarak sınıflandırılmaktadır (örneğin, Allen, 1970). Bilindiği gibi yüksek enerji spektrumunda ve asılı olarak taşıdığı malzeme miktarı maksimum 275-350 gr/lt olan türbid akıntılar, düzensiz fakat kalın ve ancak Bouma'nın

(1962) Ta-b iç yapılarını oluşturabilen akıntılardır (Friedman ve Sanders, 1978). Bu karakterdeki türbid akıntılar ön kısımları ile pelajik çökeller üzerinde kuvvetli bir aşındırma yaparken (aşınma izleri-scour marks), arka (kuyruk) kısımları ise normal veya karmaşık türdeki dereceli kırıntıları çökeltir. Düşük enerji spektrumundaki (low flow regime) türbid akıntılar, genellikle ince ve paralel kenarlı kırıntılı tabakaları çökeltirler. Bu tür akıntılar güçleri ölçüsünde ancak Bouma'nın Tc-d ve Te bölümlemelerini oluşturabilirler. Sedimenter taban yapısı olarak da, kendi güçleri ile değil, ancak taşıdıkları parçacıklar yardımiyle çizilme izlerini (tool marks) meydana getirirler.

Doğal olarak, enerjisi ne olursa olsun türbid akıntının üzerinde aktığı pelajik çökellerin tıkızlık derecesi de oluşacak türbidit fasiyesinin yakınsak veya ıraksaklığı üzerinde etkendir (Sanders, 1965) (Şek. 2). Türbid akıntıların proksimal veya distal karakterde (yüksek veya düşük enerjide) oluşunu etkileyen en önemli faktörlerden birisi de akışın başlangıcı sırasında durgun suya anî olarak dökülen malzemenin miktarıdır (Lovell, 1969; Gökçen ve Ataman, 1973).

Bazı araştırıcılar günümüzde dahi, türbidit fasiyesin tanımı için çeşitli taban yapılarına ilâve olarak, eksiksiz bir Bouma Ta-e iç yapı dizilimini ön koşul varsayarlar. Türbid akıntıdaki yüksek ve düşük enerji spektrumları hatırlanırsa, böyle bir eksiksiz dizilimin her türbidit fasiyesinde bulunamayacağı kesinlik kazanır. Ancak yüksek akış rejiminden düşük akış rejimine geçiş sırasında çökeltme yapan bir türbid akıntının o anını gösteren fosil kesiminde, Ta-e yapıları eksiksiz gözlenebilir. Ender görülen bu tür geçiş fasiyesi türbiditlerine, medyal-orta yatak türbiditleri denir (Gökçen, 1971; Şenalp ve Fakıoğlu, 1977).

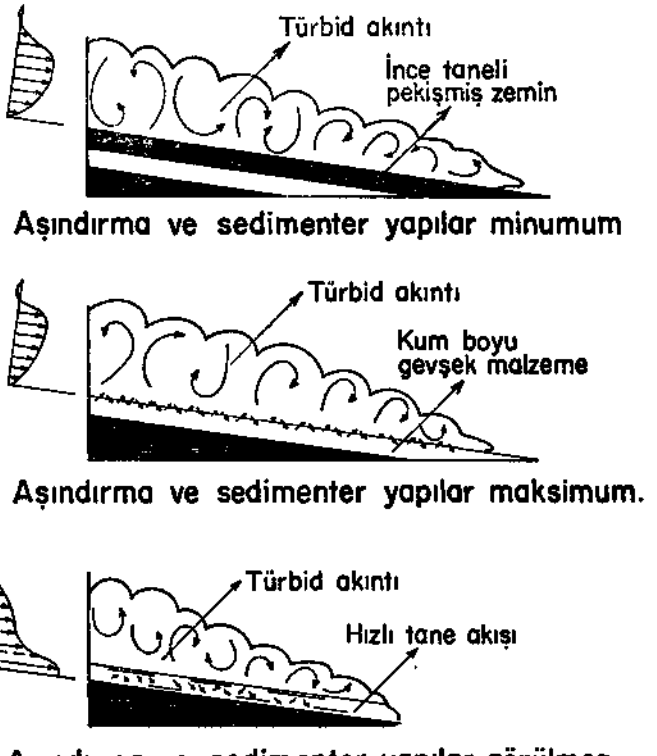

Şek. 2 - Üzerinde aktığı zeminin pekişme özelliğine göre türbid akıntının taban hızı ve aşındırma gücü (Sanders, 1965 ten).

Son 15 yıl içerisinde Sedimenter jeoloji litaratüründe göze çarpan bir diğer konu da, sığ denizel bölgelerde rüzgâr ve fırtına etkisiyle çökelmiş türbiditimsi yapılar içeren kırıntılı fasiyesler ile özellikle okyanus ortamlarındaki dip akıntılardan (contour current) türemiş fasiyeslerdir. İlki özellikle karbonat materyelinin zengin olduğu sahanlık bölgelerinde, bir tür yoğunluk akışı ürünü olan, ikincisi ise aktüel pelajik ortamlarda gözlenmiş bu fasiyeslerin ayrıntıları ve türbiditlerle olan karşılaştırmaları için okuyucuya Kelling ve Mullin (1975) ile Stow ve Lovell (1979) ve Stow (1979) kaynak olarak gösterilebilir.

KAVRAMSAL ELEŞTİRİ VE SINIFLANDIRMA

Sualtı kütle çekimi oluşuklarının adlandırılmalarında, üstte verilmiş melanj, olistostrom ve türbidit tanımlarından da görüleceği gibi, karmaşıklık vardır. Şöyleki aslında belirli akıntıların ürünü olarak değişik ortamlarda oluşan bu fasiyesler, bir grup araştırıcı tarafından sadece Sedimentolojik ortam özelliklerine göre sınıflandırılırken (örneğin Stauffer, 1967; Mutti ve Ricci Lucchi, 1972, 1978; Poole, 1974; Rupke 1977, 1978; Howell ve Link, 1979), bir diğer grup tarafından da ya aktüel sedimentasyon verilerinden kaynaklanmış paleo ortamsal modeller ile (örneğin, Normark, 1970, 1974; Haner, 1971; Kamp ve diğerleri, 1974; Stanley ve Kelling, 1978) veyahut da akış mekanizması açısından ve hipotetik olarak sınıflandırılmakta ve adlandırılmaktadır (örneğin, Fisher, 1971; Hampton, 1972; Middleton ve Hampton, 1976; Seeman, 1978; Hampton, 1979).

Bilindiği gibi kıta kenarındaki sığ denizel bölgede gravite ile başlayan bir sualtı heyelânı, bu kayan kütle içindeki makaslama etkisi-tane konsantrasyonunun azalışı ve su oranı-türbülansın artışına bağlı olarak kütle (moloz, bulamaç ve tane akışları) ve yoğunluk akışlarına geçebilir (Şek. 3 ve 4). Bu nedenle sualtı kütle çekimi akıntılarını, bu fasiyesleri oluşturan mekanizmalar açısından Tablo 1 de verildiği gibi sınıflandırmak daha anlamlı olur.

Bu resedimente fasiyeslerin çökeltildikleri alt ortamlar ile bunları karakterize eden litolojik toplulukların genellemesi de, ayrı bir tartışma konusudur. Son yıllarda kullanılan iki paleocoğrafik model farklı iki görüşe sahiptir. Bunlardan Walker (1975b, 1977), kanal başı ile derin deniz düzlüğü arasındaki konglomera-silı boyu tüm kırıntılı çökelleri, bir türbidit ailesi ve bir türbidit konisi (yelpazesi) kabul etmektedir. Mutti ve Ricci-Lucchi (1972) ise, aynı denizel bölgelerde kaymalardan distal türbiditlere kadar değişen fasiyeslerin oluşturduğu litolojik topluluklardan hareketle, kanal, yelpaze (dış, orta, iç) ve derin deniz düzlüğü ortam modellerini vermektedir. Bu model paleocoğrafik analizlerde daha kolay uygulanabilir görülmekle beraber (örneğin, Ingersol, 1978; Carter, 1979; Howell ve Link, 1979), bölgeden bölgeye gelişebilecek yatay ve düşey yönlü farklılaşmalar ve/veya bazı alt fasiyeslerdeki eksiklikler nedeniyle, Tablo 2 de verildiği düzende genellenmelidir.

SONUÇLAR

Özellikle denizel ortamlarda önemli bir taşınma türü olan sualtı kütle çekimi akıntıları, belirgin özellikleri altta verilmiş, dört kırıntılı fasiyesi çökeltmektedir. Bunlar sırasıyle kaotik çökeller, çakıllı çamurtaşları (olistostrom ve diamiktitler), resedimente konglomeralar (flaksotürbidit) ve türbiditlerdir.

1. Kaotik oluşumlar: Bunlar kanyon başından yelpazeye kadar oldukça geniş bir bölgede kayma ve heyelanlarla oluşan, yapısal (tabakalanma) ve dokusal (fabrik) özelliklerinin bozulduğu çökeltilerdir. Bu fasiyes, kaymalara (slides) oranla küçük ölçeklidir ve hareket yalnızca düşey yönde etkindir. Ayrıca kaya heyelanlarından çok daha düşük eğimler de oluşabilirler.

MOLOZ AKIŞI (Debris Flow)

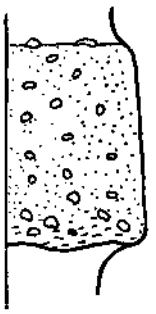

Büyük tanelerin (klastların) oluşturduğu düzensiz üst yüzey

Masif görünümlü ve kötü boylanmış tabaka içinde dağınık klastlar

Az belirgin derecelenme
büyük oygu izleri

BULAMAÇ AKINTISI (Fluidized Flow) (Bazı araştırıcılara göre ara akış türü)

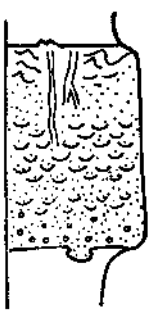

Bazen kumtaşı doykları içeren düzgün üst yüze konvolüt lamina
Üst yüzey ile bağıntılı su sızıntı kanalcıkları

Tabak yapıları

Az belirgin derecelenme

Yiv ve yük–çökme türü taban yapıları

TANE AKIŞI (Grain Flow)

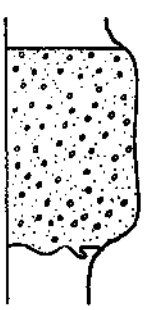

Düzgün üst yüzey

Masif görünümlü tabaka içinde akış yönüne paralel tane yönlenmesi

Ters derecelenme

Taban yapıları ve tabakalar arası enjeksiyon yapıları

TÜRBİD AKINTI (Turbidity Current)

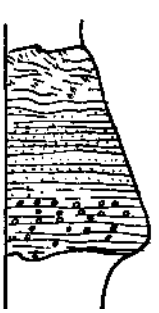

Dalgacıklı veya düzgün üst yüzey Td-Te
Çapraz veya konvolüt lamina -Tc

Paralel laminasyon.Tb

Düzgün veya ender ters derecelenme -Ta

Taban yapıları (Aşınma ve Çizilme İzleri)

Şek. 3 - Middleton ve Hampton'a (1973) göre makaslama kuvvetleri ve tane konsantrasyonunun azalışı ile su içeriği ve türbülansın artışına bağlı olarak bir diğerine geçen sualtı kütle çekimi akış türleri ve çökelttikleri fasiyesler.

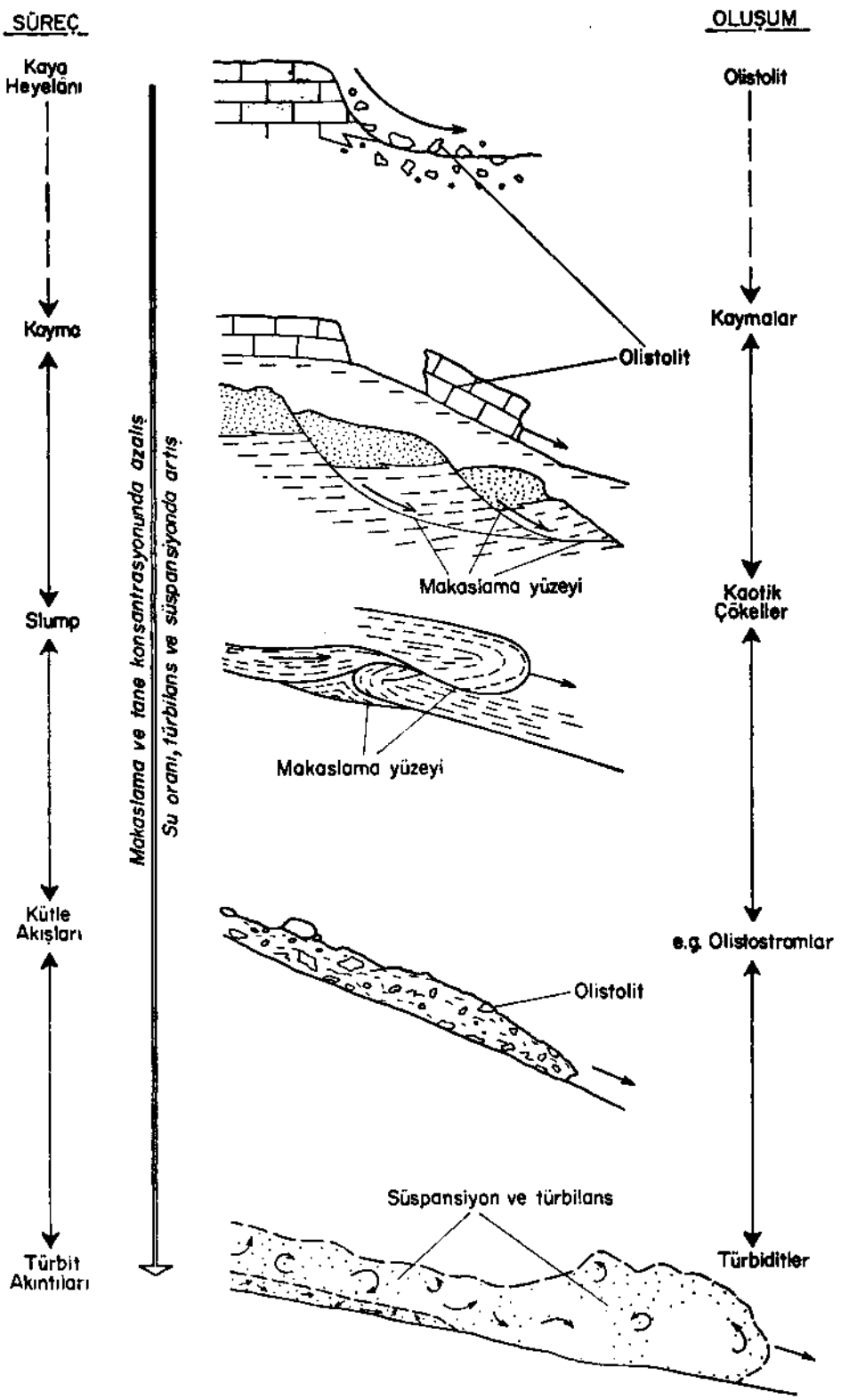

Şek. 4 - Kruit ve diğerlerine (1975) göre, sualtı kaymaları, kütle hareketleri ve türbid akışlar arasındaki süreç-oluşum ilişkileri.

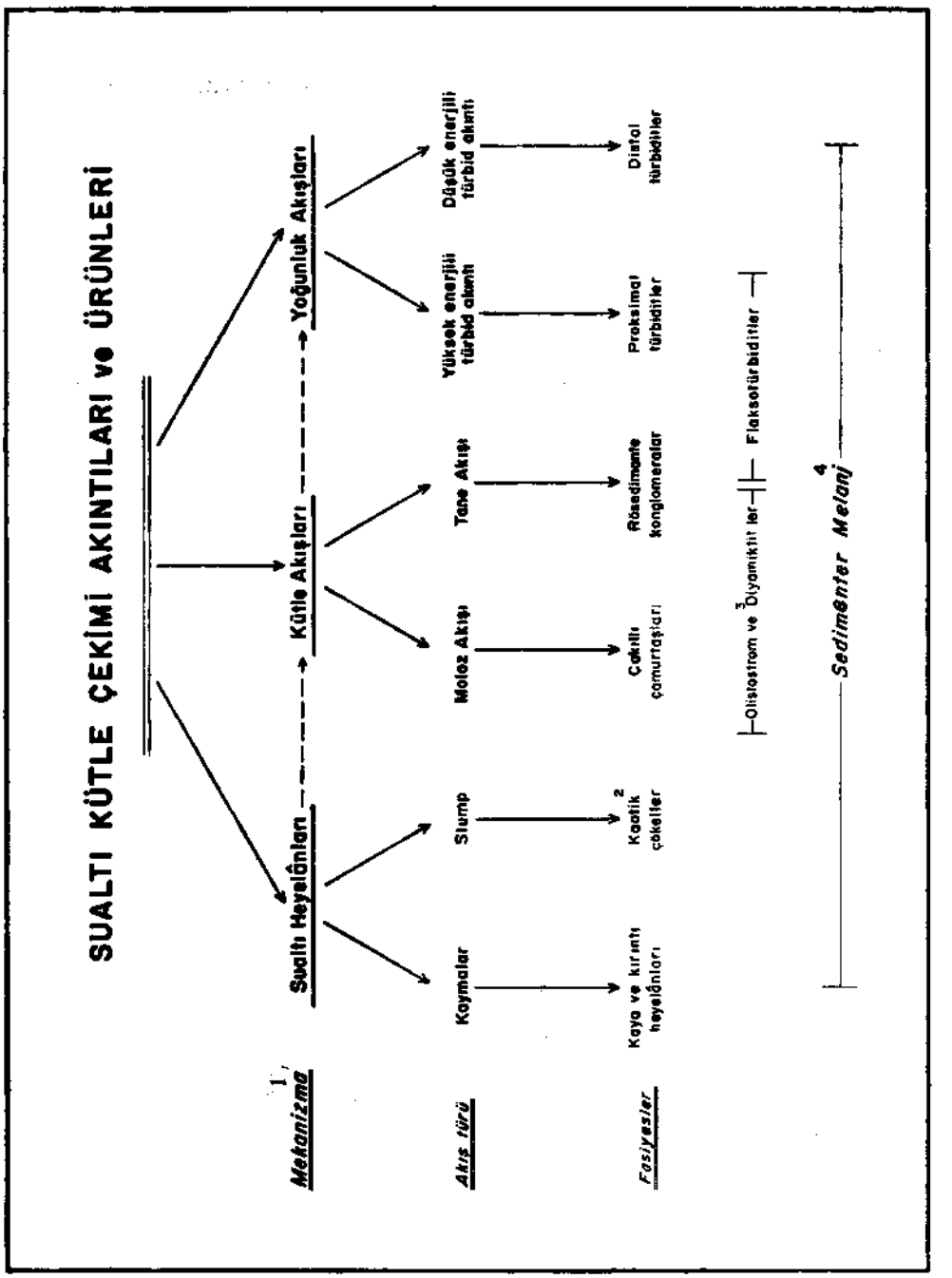

Tablo 1 - Sualtı kütle çekimi akıntıları ve oluşturdukları kırıntılı fasiyeslerin sınıflandırılması.

1 - Gravitasyonal kayma ile başlayan bu akış türlerinin bir diğerine tersinir olmayan geçişi, su içeriğinin ve türbülansın artması, tane konsantrasyonu ile makaslama kuvvetlerinin azalmasına bağlıdır; 2 - Genel anlamda kaotik oluşumlar slump, kıvrımlanmış çökeller ve bu özellikteki yerel Olistostromları veya bunların karmaşığını kapsar; 3 - Diamiktit, ince taneli bir matriks içerisinde boylanmadan (nonsorted) dağılmış kum ve blok boyu karbonatsız malzeme içeren özel bir olistostrom fasiyesidir; 4 - Sedimenter melanj, çeşitli kütle çekimi akıntıları ürünlerinin devamlı veya aralı olarak bir basende birikmesinden sonra, gerek kırıntı ve gerekse matriksin bölgesel makaslama kuvvetleri etkisiyle deformasyonumundan oluşmuş ve kısmen metamorfize karmaşık bir fasiyestir.

ORTAMLAR			JEOMORFOLOJİK ÜNİTELER	BELİRGİN TAŞINMA MEKANİZMASI	GENELLEŞTİRİLMİŞ SEDİMENTER FASİYESLER
Kara			Kıta - Kontinent	Karasal Ortam Sedimentasyonu	
Platform - Sahanlık			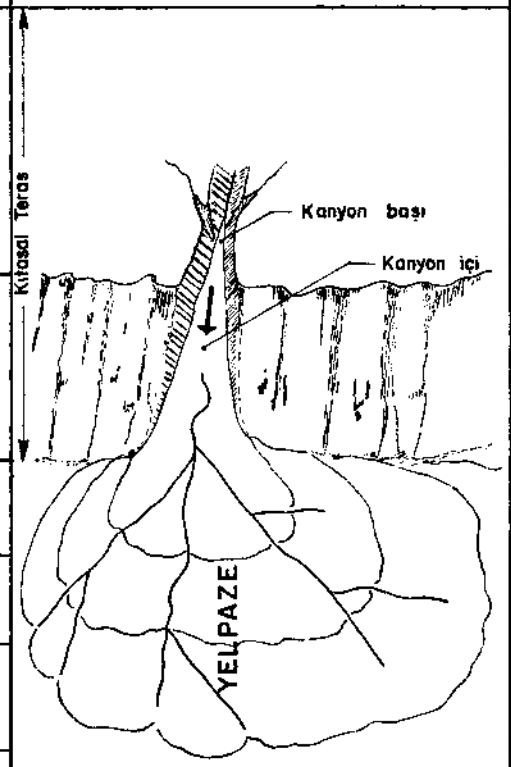	Sürüklenme ve yerel türbid akıntılar	Yuvarlak çakıllı ve çapraz tabakalı konglomera, yerel sığ su türbiditleri (kumtaşları)
Kıta Yokuşu - Yamacı ("Kanal")				Sualtı heyelanı ve kütle akışları (yerel slump'lar)	Kaotik çökeller, bölgesel olistostromlar, çakıllı çamurtaşları ve yerel masif kumtaşları
Derin Deniz Düzlüğü	Kanyon Yelpazesi	İç Yelpaze		Slump, kütle ve yoğunluk akışları (yüksek enerjili türbid akıntılar)	*Çamurlu fasiyes* içinde ender çakıllı çamurtaşı, olistostrom, kaotik çökeller ve kanal dolgusu kumtaşları
		Orta Yelpaze		Tane akışı türü kütle akışı ile yüksek ve düşük enerjili türbid akıntılar	Belirgin pelajik şeyl-marn arakatkılı resedimente konglomera - flaksotürbidit, proksimal ve distal türbiditler ile yerel kaotik çökeller
		Dış Yelpaze			
	Abisal Düzlük			Düşük enerjili türbid akıntılar, dip akıntıları ve pelajik sedimentasyon	Yüksek oranda pelajik marn - şeyl ile dip akıntısı ve distal türbidit çökelleri

Tablo - 2 Sualtı kütle çekimi fasiyeslerinin kanyon ve yelpaze alt ortamlarındaki genelleştirilmiş litolojik toplulukları.

2. Çakıllı çamurtaşları (olistostrom ve diamiktitler): Değişken boylu kırıntıları taşıyan ana unsurun çamur olduğu kütle akışları ile çökeltilmiş fasiyesler, genellikle çakıllı çamurtaşları olarak adlandırılır. Bu oluşumlar da bileşim ve tane boylarına göre iki alt fasiyese bölünebilir.

a. Olistostromlar kıta sahanlığı (kanyon başı), kıta yokuşu ve dış yelpazeye kadar geniş bir bölgede oluşabilen, tane+kütle karmaşığı akıntılarla taşınıp çökeltilmiş, kendine özgü sınırlı Sedimenter yapılar içeren, pelitik bir matriks içinde dağılmış, değişken tane boyu ve bileşimli, makaslama etkilerinin görülmediği, yerel veya bölgesel kırıntılı oluşumlardır.

b. Diamiktitler, yarı belirgin derecelenme ile büyük oygu izlerinin görüldüğü, karbonat içermeyen karasal kökenli ve değişik boyutlu bileşenler ile matrikse sahip, yarı pekişmiş, kalın konglomeratik yığışım halindeki bir olistostrom türüdür.

3. Resedimente konglomeralar (flaksotürbiditler): Bunlar, genellikle kıta yokuşu (yamacı) bölgelerinde, tane+flaksotürbid akıntılarla çökeltilmiş, iri ve köşeli tanelerin oluşturduğu, yanal devamlılığa sahip kalın katmanlardan oluşmuş, dereceli tabakalanma ve bazen büyük ölçekli oygu izleri içeren Sedimenter fasiyeslerdir.

4. Türbiditler, koşulların uygun olduğu her ortamda oluşmakla birlikte, özellikle kıta yamacından itibaren derin denize kadar çok geniş bir bölgede, yoğunluk akıntıları ile taşınıp çökeltilmiş, birçok tip ve çeşitteki birincil Sedimenter yapılar ile çeşitli tipte dereceli bölüm ve laminasyonlar içeren, geniş yanal devamlılığa sahip, oldukça kalın klastik tabakaların ritmik bir şekilde çamurtaşı-şeyl ile ardalanmasından oluşmuş kırıntılı çökellerdir.

Jeoloji, özellikle Sedimentologi literatüründe en çok tartışılan kırıntılı bölgesel fasiyes melanj ise; sualtı heyelanları, slump, moloz, tane ve türbid akışlar gibi çeşitli kütle çekimi akıntısı ürünlerinin devamlı veya aralı olarak bir basende birikmesinden sonra gerek kırıntı ve gerekse matriksin sin ve/veya posttektonik bölgesel makaslama kuvvetleri altında deformasyona uğramasından oluşmuş, kısmen metamorfize, karmaşık bir fasiyestir. Bölgesel yayılıma sahip olan bu oluşum plaka veya plakacıkların konumlarının saptanmasında; başka deyişle yitilme (Subduction) ve üzerleme (obduction) zonlarının belirlenmesinde önemlidir.

Yayma verildiği tarih, 14 şubat 1980

DEĞİNİLEN BELGELER

Abbate, E.; Bartclotti, V. ve Passerini, P., 1970, Olistostromes and olistolitin: Sediment. Geol., 4, 3/4, 521-558.

Allen, J.R.L., 1970, Physical processes of sedimentation: An Introduction. Allan and Unwin, London., 248 s.

Ataman, G.; Çapan, U.Z.; Gökçen, S.L. ve Buket, E., 1974, Plaka tektoniği ilkeleri: Hacettepe. Fen. Müh. Bilim. Derg., 4. 113-178.

Bailey, E.B. ve Callien, C.Mc., 1950, Ankara melanjı ve Anadolu şariyajı: Maden Tetkik ve Arama Enst. Derg., 40,12-22.

———ve———, 1953, Serpantine Lavaş, the Ankara Melange and the Anatolian thrust: Trans. Royal. Soc. Edinburg., 62, 2, 403-442.

Batman, B., 1978a, Haymana kuzeyinin jeolojik evrimi ve yöredeki melanjın incelenmesi 1: Stratigrafik birimler: Yerbilimleri, 4, 1-2, 95-124.

———, 1978b, Haymana kuzeyinin jeolojik evrimi ve yöredeki melanjın incelenmesi 2: Tektonik ve jeolojik evrim: Yerbilimleri, 4, 1-2, 125-134.

Baykal, F. ve Önalan, M., 1979, Şile Sedimenter karışığı (Şile olistostromu): Altınlı Simpozyumu Tebliğleri, Türkiye Jeol. Kur. Yay., 15-26.

Bell, H.S., 1942, Density currents as agents of for transporting sediments: J. Geol., 50, 512-547.

Bouma, A.H., 1962, Sedimentology of some flysch deposites: Elsevier, Amsterdam, 168 s.

Carter, R.M., 1975, A discussion and dassification cf subaqueous mass transport with particular application to grain-flow and flaxoturbidites: Earth.Sci, Rev., 11, 145-177.

———, 1979, Trench-slope channels from the New Zealand Jurassic: the Otekura Formation, Sandy Bay south Otago: Sedimentology., 26, 475-496.

Çapan, U.Z., 1977, Ofiyolit olgusu: T.J.K. Yerbilimleri Konferans Dizisi, Kış Dönemi, 1-3, 16 s.

———ve Buket, E., 1975, Aktepe-Gökdere bölgesinin jeolojisi ve ofiyolitli melanj: Türkiye Jeol. Kur. Bült., 18, l, 11-16.

Davies, LC. ve Walker, R.G., 1974, Transport and deposition of resedimented conglomerates. The Cap Ennage Formation, Cambro-Ordovician, Quebec:J. Sediment. Petrol, 44, 1200-1216.

Dimitrijevic, M.D. ve Dimitrijevic, M.N., 1973, Olistostrome-melange in the Yugoslavian Dinarides and Late Mesozoic plate tectonics: J. Geol., 81, 328-340.

Dott, R.H., 1963, Dynamics of subaqueous gravity depositional process: Amer. Assoc. Pet. Geol. Bull., 47, 104-128.

Dzulynski, S.; Ksiazkiewioz, M. ve Kuenen, Ph. H., 1959, Türbidites in Fliysch of the polish Carpathian Mountains: Bull. Geol. Soc. America., 70, 1089-1118.

Elter, P. ve Trevisan, L., 1973, Olistostromes in the tectonic evalution of the Northern Appennines. Gravity and Tectonics: John Wiley and Sons, New York, 175-178.

Fisher, R. V., 1971, Features of coarse-grained, high-concentration fluids and their deposits: J. Sediment. Petrol., 41, 916-927.

Flint, R. F.; Sanders, J. E. ve Rodgers, J., 1960, Diamictite: a substitute term for symmictite: Bull. Geol. Soc. America, 71, 1809-1810.

Friedman, G. M.; Sanders, J. E., 1978, Principles of Sedimentology: John Wiley Sons, New York., 792 s.

Flores, G., 1955, Discussion, *in* Beneo, E., les resultats des etudes pour la recherche petrolifere en Sicile (Italie). 4 th. World. Petroleum Congress. Rome., Proct. Sect. l, 121-122.

Gökçen, S. L., 1971, Keşan bölgesi türbiditlerinde siklik sedimentasyon, Hacettepe Fen. Müh. Bilim. Derg., l, 1,26-40.

———, 1974, Erzincan-Refahiye bölgesi sedimanter jeolojisi I: Olistolit, türbidit ve olistostrom fasiyesleri: Hacettepe Fen. Müh. Bilim. Derg., 4, 179-205.

———, 1981, Diskriminant analizi ile olistostrom ve türbidit fasiyeslerinin ayırımı. Yerbilimleri, 8 (baskıda).

———ve Ataman, G., 1973, Sedimentologie des rochec detritiques de la formation de Keşan (Paleogene): Un facies a turbidites au sud-Ouest de la Thrace Turquie: Sediment. Geol. 9, 4, 235-260.

———ve Şenalp, M., 1975, Kayma oluşukları, olistostromlar ve türbidit fasiyeslerini ayırıcı ana jeolojik, sedimantolojik ölçütler: T.B.T.A.K. V. Bilim Kongresi Yerbilimleri Tebliğleri, 57-78.

———ve Gülen, L., 1977, Ofiyolit yerleşmesine tektonik bir yaklaşım: Doğa., l, 10-12. 332-334.

Gökten, E., 1977, Yassıpınar (Şarkışla) olistostromu: T.B.T.A.K. VI. Bilim Kongresi Tebliğ Özetleri, 312.

Görler, K., 1975, The determination of former mudflow-directicns in olistostrcmes: Prcc. IX. inter. Cong. Sedimentology. Theme 4, 163-169. Nice.

Greenly, E., 1919, The geology of Anglesey: Great Britain Geol. Surv., Mem., 2, 980.

Hampton, M.A., 1972, The role of subaqueous debris flow generating turbidity current: J. Sediment. Petrol., 42, 775-793.

———, 1975, Competence of fine-grained debris flows: J. Sediment. Petrol., 45, 834-844.

———, 1979, Buoyancy in debris flows: J. Sediment. Petrol., 37. 487-508.

Haner, B.E., 1971, Morphology and sediments of Redondo submarine fan, Southern Califomia: Bull. Geol. Soc. America, 82, 2413-2432.

Hendry, H, H.E., 1973, Sedimentation of deep-water conglomerates in Lower Ordovician rocks of Quebec-composite bedding produced by progressive liguefaction of Sediment: J. Sediment. Petrol., 43, 125-136.

Hoedemaeker, Ph. L, 1973, Olistostromes and other delapsional deposits, and their occurrence in the region of Moratall (Prov. of Murcia, Spain): Seripta. Geol., 19, 1-207.

Howell, D.G., & Link, M.H., 1979, Eocene conglomerate Sedimentology and basin analysis, San Diego and Southern Califomia borderland: J. Sediment. Petrol., 49, 2, 517-540.

Hsü, K.J., 1968, Principles of melanges and their bearing on the Franciscan Konxuille paradox: Bull. Geol. Soc. America, 79, 1063-1074.

———, 1969, Preliminary report and geologie gürde to Franciscan Melanges of the Morro Bay-Jan Simcan Califomia: Califomia D. V. Mines and Geology Special Pub., 35, 45 s.

———, 1971, Franciscan Melanges as a model for eugeosynclinal sedimentation and underthrusting tectonics: J. Geophys. Res., 76, 1162-1170.

———, 1974, Melanges and their distinction from Olistostromes: Soc. Econ. Paleon. Mineral. Special Publ., 19, 321-333.

Ingersol, R.V., 1978, Submarine fan facies of the Upper Cretaceous great Valley sequence, Northern and Central California: Sediment., Geol., 21, 205-230.

Kamp, P.C. Van de.; Harper, J.D.; Coniff, J.J. ve Morris, D.A., 1974, Facies relations in the Eocene-Oligocene in the Santa Ynez Mountains, Califomia: J. Geol. Soc. London., 130, 545-565.

Kayan, T. ve Gökçen, S.L., 1978, Türbid akıntı ve kavramlarının türkçe kaynaklara yerleşimi ve evrimi: Yeryuvarı ve insan., 3, 1. 46-61.

Kazancı, N. ve Varol, B., 1978, Tane akıntısı oluşukları ve çekirdekli kum topları (Seben-Bolu): Doğa., 11, 92-98.

Kelling, G. ve Mulluin, P.R., 1975, Graded limestones and limestone-quartzite couplets: possible storm deposits from the Moroccan Carboniferous: Sediment. Geol., 13, 161-190.

Koçyiğit, A., 1976, Karaman-Ermenek (Konya) bölgesinde ofiyolitli melanj ve diğer oluşuklar: Türkiye Jeol. Kur. Bült., 19, 2, 103-116.

-, 1979, Çorduk Olistostromları: Türkiye Jeol. Kur. Bült., 22, l, 59-68.

Kruit, C.; Brouwer, J.; Knox, G.; Scholenberger, W. ve Vlient, Van A., 1975, Une excursion aux cones d'alluvions en eau profonde d'age Tertiaire pres de San Sebastian (Province de Guipuzcoa, Espagne): 9th. Int. Congress. Sediment., Nice 1975, Excursion 23, 75.

Kuenen, Ph. H. ve Migliorini, CL, 1950, Turbidity currents as a cause of graded bedding: Sediment. Geol., 58, 91-127.

Lovell, J. P.B., 1969, Tyee formation: a study of proximality in turbidites: J. Sediment. Petrol., 39, 935-953.

Marschalko, R., 1971, Termin: Wildflys (term-wildflysch): Geologicke Prace. Spravy., 48, 175-187.

Middleton, G.V. ve Hampton, M.A., 1973, Sediment gravity flows: mechanics of flow and deposition: *in* Turbidites and deep water sedimentation: AGI-Soo. Econ. Paleontologists shart Course Lecture Notes, 1-38.

———ve Hampton, M.A., 1976, Subaqueous Sediment transport and deposition by Sediment gravity flows, p. 197-218: *in* (Stanley, DJ. ve Swift, D.J.P., eds,.) Marine Sediment (sic) transport and enviromental management: New York, John Wiley Sons, 602 p.

Mutti, E. ve Ricci, L.F., 1972, Le türbiditi dell' Appenino settentrionale: introduzione del analizi di facies: Soc. Geol. Italiana, Mem., 11, 161-199.

———ve———, 1978, Turbidites of the Northern Apennines: Introduction to facies Analysis: International. Geology. Review, 20, 2, 125-166.

Norman, T., 1963, ingiltere'nin göller bölgesindeki Ludlovien yaşlı paleo-akıntıların yönleri: Türkiye Jeol. Kur. Bült., 8, 1-2.

Norman, T., 1972, Ankara Yahşihan bölgesinde Üst Kretase-Alt Tersiyer istifinin stratigrafisi: Türkiye Jeol. Kur. Bült., 15,2, 180-276.

———, 1973, Ankara Yahşihan bölgesinde Üst Kretase-Alt Tersiyer sedimantasyonu: Türkiye Jeol. Kur. Bült., 16, l, 41-66.

———, 1975a, Flow features of Ankara Melange: Proc. 9th. Int. Congress. Sediment., Nice 1975, Theme 6, 261-267.

———, 1975b, Çankırı-Çorum-Yozgat bölgesinde Alt Tersiyer yaşlı sedimentlerde paleoakıntılar ve denizaltı heyelanları: Türkiye Jeol. Kur. Bült., 18, 2, 103-110.

; Gökçen, S.L. ve Şenalp, M., 1979, Late Cretaceous-Early Tertiary sedimentation in the Central Anatolian Basin (Turkey): Cretaceous-Tertiary Boundary Events Symp. Proc., 207-213 (Copenhagen).

;————ve————, 1980, Sedimentation pattern in Central Anatolia at the Cretaceous Tertiary Boundary. Cretaceous. Res. l, l, 61-83.

Normark, W.R., 1970, Growth patterns of deep sea fans: Bull. Am. Assoc. Petr. Geol., 54, 2170-2195.

———, 1974, Submarine canyons and fan valleys: factors effecting growth patterns of deep-sea fans: *in* (R.H. Dott. Jr. ve R.H. shaver-editors) Modern and Ancient Geosynclinal sedimentation: Soc. Econ. Paleontol. Mineral. Spec. Publ., 19, 56-68.

Okada, H. ve Kitamura, N., 1978, Significance of Miocene Olistostromes in apparent rear-arc belt in Hokkaido-Japan (abstract): Proc. 10th. Int. Congress. Sediment., Jerusalem 1978, 2, 481-482.

Poole, F.G., 1974, Flysch deposits of Ant Foreland Basin, Western United States: in, Tectonics and Sedimentation (W.R. Dickinson, ed.): Soc. Econ. Paleon. Miner. Special Publ., 22, 58-82.

Rupke, N.A., 1977, Growth of an ancient deep-sea fan: J. Geol., 85, 725-744.

———, 1978, Deep Clastic Seas, m; Sedimentary Environments and Facies (H.G. Reading, ed.): Blackwell Scientific Publ., Oxford-London, 372-415.

Sanders, J.E., 1965, Primary Sedimentary structures formed by turbidity currents and related resedimentation mechanisms: *in* Middleton, G.V. (ed.), Primary Sedimentary structures and Their Hydrodynamic interpretation: Soc. Econ. Paleontol. Spec. Publ, 12, 192-219.

Scholl, D.W. ve Marlow, M.S., 1974, Sedimentary sequence in Modern Pasific Eugeosynclines., p. 193-211 *in* Dott, R.H., Jr. ve Shower, R.H., (eds.) Modern (sic) and ancient geosynclinal sedimentation: Tulsa, Okla., Soc. Econ. Paleontol. Mineral. Spec. Publ., 19, 380.

Seemann, U. 1978, Snow sedimentation-diagenesis and avalanches: A Correlation with Sedimentary rocks: Sediment. Geol., 21, 189-204.

Slaczka, A. ve Thompson, C.V., 1975, Flaksoturbidite Model: Porc. IX inter. Cong. Sedimentology., 6, 175-277, Nice-France.

Stanley, DJ. ve Kelling, G. Edits, 1978, Sedimentation in submarine canyons, fans, and trenches. Dowden, Hutchinson Ross, Inc. Stroudsburg, Pennslvania, 395.

Stauffer, P.H., 1967, Grain-flow deposits and their implication. Jauda Ynez mountains, Califomia: J. Sediment. Petrol., 37, 487-508.

Stow, P.A.V., 1979, Distinguishing between fine-grained turbidites and contourites on the Nova Scotian deep water margin: Sedimentology, 29, 4, 377-388.

———, ve Lowell, J.P.B., 1979, Contourites: Their recognition in modern and ancient sediments: Earth-Science Review, 14, 251-291.

Şenalp, M. ve Fakıoğlu, M., 1977, Bulantı akıntıları ve türbiditler. Yeryuvarı ve İnsan, 2, 2, 25-39.

Unrug, R., 1963, Istebna beds: A fluxo-turbidite formation in the carpation Flysch. Rocz. Pol. Tow. Geol., 33, 49-92.

Walker, R.G., 1967, Turbidite Sedimentary structures and their relation ship to proximal and distal depositional environment: J. Sediment. Petrol., 37, 25-43.

———, 1970, Review of the geometry and facies organization of turbidites and turbidite-bearing basins: *in* lajoie, J. (ed.), Flysch Sedimentology in North America: Geol. Assoc. Can., Spec. Paper, 219-251.

Walker, R.G., 1975a, Upper Cretaceous resedimanted conglomerates wheeler George, Califomia: Description end Field Guide: J. Sediment. Petrol, 45, 105-112.

———, 1975b, Generalized facies models for resedimented conglomerates of turbidite association: Bull. Geol. Soc. America, 86, 373-748.

———, 1976, Facies models 11. Turbidites and associated coarse Clastic deposits: Geosciences. Can., 3, 25-36.

———, 1977, Deposition of Upper Mesozoic resedimented conglomerates and associated turbidites in southwestern Oregon: Bull. Geol. Soc. America, 88, 273-285.

Winn, R.D. ve Dott. R.H., 1979, Deep-water fan-channel conglomerates of late Cretaceous age, Southern chile: Sedimentology, 26, 203-228.

Wood, D.S., 1974, Ophiolites, melanges, blueschists, and ignimbrites: Early Caledonian Subduction in Wales *in* R.H. Dott ve Robert, H.S. (ed.), Modern and Ancient Geosynclinal Sedimentation: Soc. Econ. Paleon. Mineral Special Publ., 19, 334-344.

DESCRIPTION OF TWO NEW SPECIES OF THE GENUS DICTYOPTYCHUS FOUND IN TURKEY

Necdet KARACABEY - ÖZTEMÜR

Mineral Research and Exploration Institute of Turkey

ABSTRACT. — The samples, collected from Upper Cretaceous beds of Hatay and Adıyaman, We studied and two new species of Dictyoptychus are established. In this paper, descriptions of these new species (*D. orontica* n. sp., and *D. euphratica* n. sp.) have been given.

INTRODUCTION

The studied material are collected from Upper Cretaceous beds of Yayladağı-Hatay (Southern Turkey) by Yusuf Tamer; and from Rudistid limestone between Kastel Formation and Terbüzek conglomerate of Kahta-Adıyaman (Southeast Turkey) by Engin Meriç.

After the examination of these collections, we established first occurence of die genus Dictyoptychus in Turkey. Our species differ from known species of Dictyoptychus. In this publication, descriptions of these two new species of Dictyoptychus, are given.

Associated Rudistid fauna and abundant microfossils show that two new species are Maestrichtian in age.

SYSTEMATIC STUDY

Order **: RUDISTIDA** LAMARCK 1819

Family : CAPRINIDAE FISCHER 1887

Genus : Dictyoptychus DOUVILLE 1905

Pictyoptychus orontica n. sp.
(Plate I, fig. 1-3; Plate IV, fig. 1)

Derivatio nominis : After the latin name of Asi River, Orontes.

Holotype : Is deposited at the Museum of Mineral Research and Exploration Institue of Turkey with no. 1039.

Material : One sample, with well preserved two valves.

Diagnosis: Upper valve conical in shape, apex eccentric. Lower valve conical; siphonal region with thin longitudinal ribs and tight festonne growth lamellae. Cross-section triangular. Internal layer contains few, but big polygonal canals, which make a regular row on the outer margin. Cardinal apparatus perpendicular to the anterior margin.B, B' teeth situate between the long arms of the X shaped N tooth. ,

Description: Upper and Lower valve are two cohes with opposite bases. Summits of both valves are situated on a line which cuts the commissure with an angle 60; therefore valves are in shape of cones with their summits slid to reverse sides.

Upper valve is depressed conical and cap-like, 1.5 cm height; apex is inclined strongly towards the antero-dorsal margin. Well preserved places of the valve show fine and tight growth lamellae.-At the eroded parts of the thin external layer, dense and radial canals of the internal layer can be observed (Plate I, fig. 1, 2). As.we have one specimen, we could not obtain a cross-section of Upper valve.

Lower valve is conical in shape with eccentric summit; the height is 5.5 cm. Surface is ornamented with dense and fine growth lamellae. Lamellae of the siphonal region are more marked and transversed by fine costules. At the intersection points, the growth lamellae extend upwardly and therefore they show an «festonne» appearance (Plate IV, fig. 1). This position resembles to the ornamentation of Lower valve of the species *striatus*, but our new species has numerous growth lamellae. Although siphonal region is well marked by this ornamentation, there is not a structure which marks siphonal bands.

Cross-section of the valve is a triangle with rounded corners (Plate I, fig. 3). Maximum thickness of the brown colored external layer is 3.5 cm. Below this layer at the periphery, except of siphonal region, canals of the canal layer (few in number and less complex than the other species) can be seen. These thin walled canals, somewhat rectangular in form, are sitauted along the anterior margin. From «O» accessory cavity, they became much smaller and continue to the ventral margin. Particularly, at the external side of the cardinal teeth, there are two canal groups with four and two canals. At the anterior, inner side of the canals and parallel to it, a band formed by smafly, elongate canals and dense texture, can be seen. There is no canals at the siphonal region.

There is not any trace of ligamental ridge.

Teeth are situated, at equal length to anterior and posterior margin, and on a line normal to the anterior margin. N tooth of the lower valve is well developed, and is in the form of X with two arms extend to anterior and the two other extend to posterior. Between two anterior arms, there is square anterior tooth (B'). The posterior (B) tooth is thin and elongated and is situated between two posterior arms of the N tooth. We cannot differentiate myophore apophyses. The test detritus seen at the end of canals of posterior margin may be mp.

Comparison and remarks: This new species resembles to *persicus* and *paronai*, but differs from it by low conical shape (Kühn, 1929, 1937; Tavani, 1949).

Ornamentation of siphonal region of lower valve resembles mostly to *striattts*. Although new species resembles to *striatus* with its few and big canals on the cross-section of lower valve, accessory cavity (O) extending to the margin, and triangular cross-section; but it is distinguished from *striatus* by following features: anterior and posterior margin of the *striattts* are equal length (at the new species posterior and ventral margin equal), cardinal apparatus somewhat dorso-ventral alignment, regular conical shape of lower valve (Douville, 1910).

It resembles to species *Itesi* with the perpendicular position to anterior margin of the teeth; but l*eesi* differs from our species by the disposition of polygonal canals, thickness of the test, upwardly position of the growth lamellae at the siphonal region and a regular conical shape of lower valve (Kühn, 1929).

Association: The inner part of the lower valve filled with grey sandstone. In thin section of this matrix, there are abundant microfossils:

Orbitoides media (d'Arch.)
Siderolites calcitrapoides Lamarck
Omphalocyclus macroporus Lamarck

At the continuation of this bed, near the village Yaylaçeşmesi, we found *Vautrinia syriaca* (Vautrin).

Type locality: Yeditepe, Yaylaçeşmesi, Hatay.

Stratigraphic level: Maestrichtian.

Dictyoptychus euphratica n. sp.

(Plate II; Plate III; Plate IV, fig. 2,3)

Derivatio nominis: After the old name of the Fırat River.

Holotype: is deposited at the Museum of the Mineral Research and Exploration Institute of Turkey with no. 1042.

Material: One specimen with two valves.

Diagnosis: Upper valve capuloid in shape, eccentric beak in the form of a hook, both sides of the hook deep grooves extend towards siphonal regions, lower valve regular cone, disposition of polygonal canals different compared other species, cardinal apparatus near to anterior margin.

Description: External features: The general appearance of the specimen is similar to a top. Height of the specimen, with two valves, is 11 cm. Dorso-ventral width, at the commissure, are equal to the height: Upper valve is depressed cap-like in shape. Its height, at the beak, is 2 cm. From this point the valve descends regularly to the ventral margin. Summit of the valve approaches 1.5 cm to the antero-dorsal margin.'Summit is in the form of a hook and inclined towards the margin (Plate III, fig. 2). At both sides of the beak, there are deep grooves extending towards siphonal region, and therefore the beak become more distinguishable. The grooves ends nearly 2.5 cm to the siphonal region. The place, between this point and the margin, is a shallow and wide depression (Plate III, fig. 1). This position gives an undulating appearance to the margin of the shell. Surface of the shell is covered with very fine and concentric growth lines. At the margin, there is another shallow depression, behind the posterior groove of the beak's depression, and this corresponds, may be, to S siphonal band.

Lower valve is regular, short and uncurved conical in shape. Its height is 9 cm and width, at commissure, is 10-11 cm. Surface is totally smooth and in some places shows growth lines. At siphonal region, there is not any distinct characteristic marking siphonal bands. The two shallow depressions of Lower valve, corresponding to Upper valve's two shallow depressions, may be mark siphonal bands E and S.

Internal features: At the eroded part of Upper valve, narrow canals can be seen (Plate III, fig. 1). External layer is very thin. Cross-section of lower valve, is rounded oval, at siphonal region (Plate IV, fig. 2,3). Thickness of the external layer is 2.5-4 mm. Internal layer, is thick at the dorsal side and very thin at the ventral side. Canals of this layer are very thinned wall and some places are broken or not preserved. Therefore these canals, at cross-section passing near commissure, cannot be seen. Internal layer composed of thin walled polygonal canals, and these canals have very

different greatness and form. These canals make rows parallel to outer periphery. External row is composed great and quadrangular or hexangular canals. Inntr part of this row, there is another row composed of subquadrangular and big canals. Between these two rows, smaller canals make an interrupted row. At the inner side of the second row, especially at the anterior side, very small canals can be seen on a line parallel to outer periphery. At cardinal region, one of the three big canals, seen at the external side of the teeth, constitutes «O» accessory cavity. At the cross-section passing below this section, cansl layer of the siphonal region is very thin and only one row of elongated oval canals can be seen. Body cavity is somewhat elongated in direction of the beak. There is no trace of L. Cardinal apparatus is near to the, anterior margin. N tooth of the lower valve is irregular and X shape. Anterior tooth situates between anterior arms of N tooth. Posterior tooth cannot be seen distinctly. Myophore apophyses are not preserved.

Comparison and remarks: New species is easily distinguishable, by general form of the upper valve, from the other species of Dictyoptychus.

Canal rows of lower valve are similar to *morgani,* but their disposition are different (Douville, 1904, 1904a).

The species now described, in external appearance and «O» cavity not extending to the periphery, resembles *leesi,* but it goes away by the absence of siphonal pillars.

Association: In the pinkish grey limestone matrix filled shell cavity, we found

Omphalocyclus macroporus Lamarck
Orbitoides media (d'Arch.)
Siderolites calcitrapoides Lamarck
Loftusia sp.
Miliolidae

At the same fossiliferous bed, we found

Pironaea praeslavonica Mil., Sladic, Grubic
Vautrinia syriaca (Vautrin)

Type locality: North of Alidam Köyü, Narince, Kahta-Adıyaman.

Stratigraphic level: Maestrichtian.

ACKNOWLEDGEMENTS

The author would like to express his thanks to Yusuf Tamer and Engin Meriç for the samples, and to Mualla Serdaroğlu for the determination of microfossils.

Manuscript received May 10, 1979

PLATES

PLATE - I

Dictyoptychus orontica n. sp.

Fig. 1 - Lower and Upper valve, external view, X 1

Fig. 2 - Upper valve, from above, X 1

Fig. 3 - Lower valve, cross-section, X 1

N - Tooth of lower valve

O - Accessory cavity

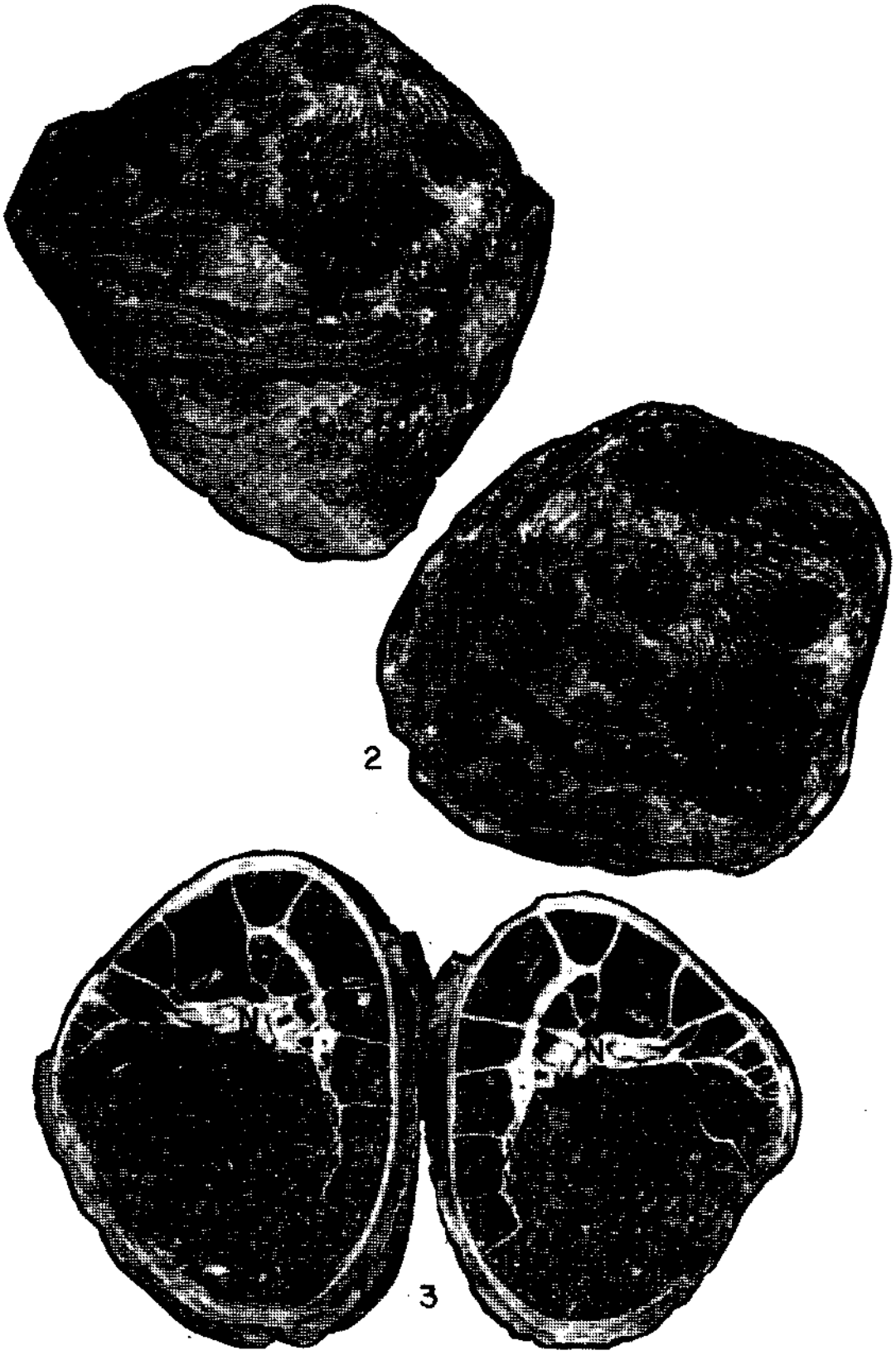
2
3

PLATE - II

Dictyoptychus euphratica n. sp.

Fig. 1 - View of the cardinal region of both valves, X 1

Fig. 2 - View of the siphonal region of both valves, X 1

1

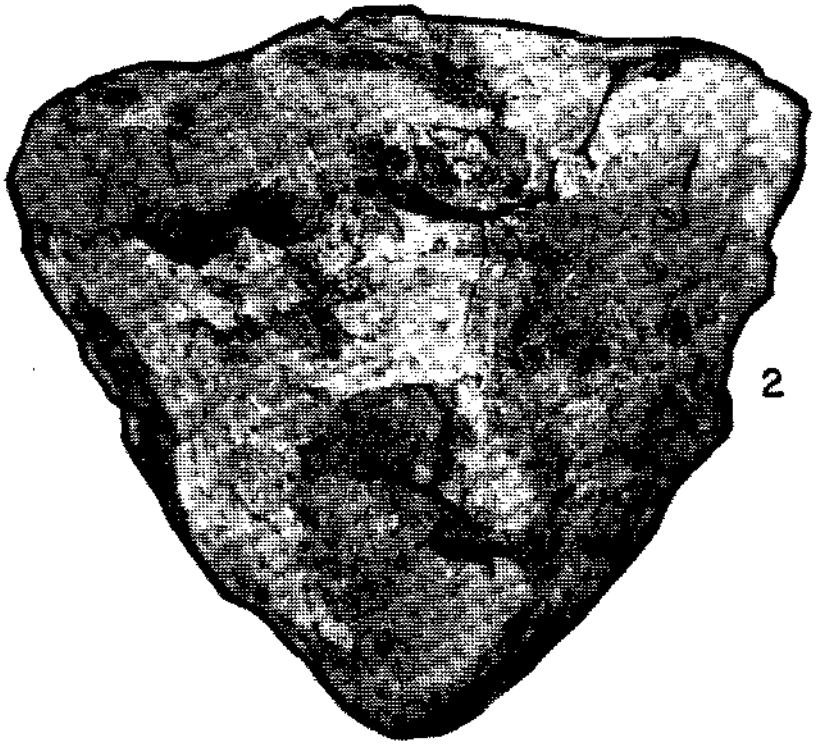

2

PLATE - III

Dictyoptychus euphratica n. sp.

Fig. 1 - Upper valve, from above, x 1

Fig. 2 - Upper and lower valve, vieW of the posterior side, X 1

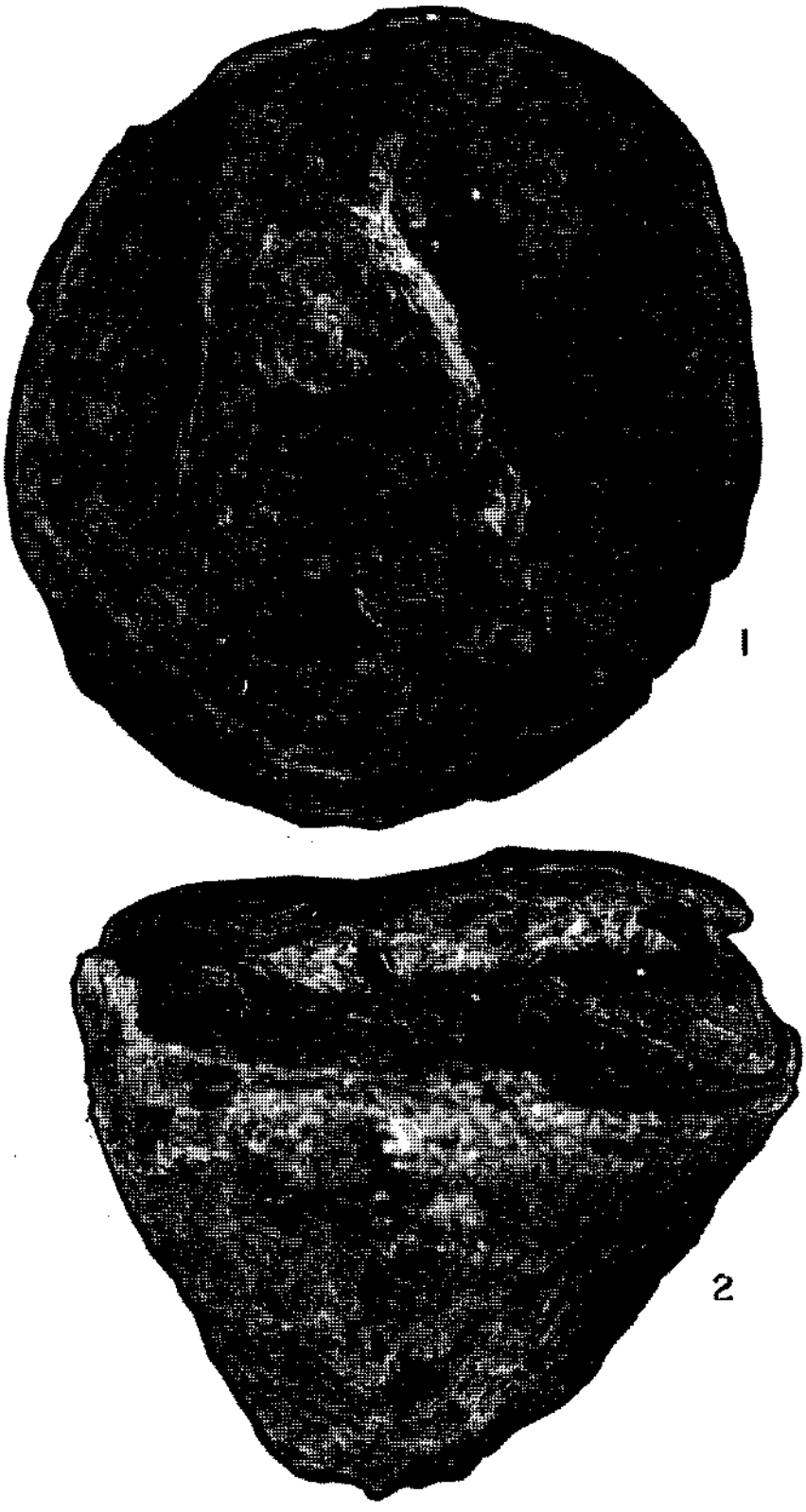
1
2

PLATE - IV

Dictyoptychus orontica n. sp.

Fig. 1 - Upper and lower valve, view of the siphonal region, x 1

Dictyoptychus euphratica n.sp.

Fig. 2, 3 - Lower valve, cross-sections, X 1

N - Tooth of lower valve

O - Accessory cavity


1
2
3

REFERENCES

Douville, H., 1904, Sur quclqucs Rudistes a canaux: Bull. Soc. Geol. France, 5, 5, 519-553.

———, 19040, in J. de Morgan-Mission scicnrifique en Perse. Etudes Geologique, IV, Paleonfolofie. Mollusques fossiles.

———, 1910, Etudes sur les Rudistes. Rudistes de Sicile, d'Algerie, d'Egypte, du Liban et de la Perse: Soc. Geol. France, Paleont., Mem., 41, 1-83, 77 text fig. 1-7 planches.

Kühn, O., 1929, Beitrage zur Palacontologie und Stratigraphie von Oman (Ost-Arabien): Ann. Naturhist. Mus. in Wien, 43, 13-33, 3 pl.

———, 1937, Stratigraphie und Palaeogeographie der Rudisten. II. Rudistenfauna und Oberkreidentwicklung in İran und Arabien: N. Jahrb. Min., 78, Abt. B, 268-284.

Morgan, J., 1905, Note sur la geologie de la Perse: Bull. Soc. Geol. France, 4, 5, 178.

Perkins, B.F., 1969, *in* Moore, CM., Treatise on Invertebrate Paleontology-part N, 2, N 795.

Tavani, G., 1949, Rudiste ed altri Molluschi cretacei della Migiurtinia: Pal. ttalica, XLVI, 11.

THREE NEW SPECIES OF THE GENUS MISEIA AND PROPOSAL OF A NEW SUBFAMILY OF RADIOLITIDAE

Necdet KARACABEY - ÖZTEMÜR

Mineral Research and Exploration Institute of Turkey

ABSTRACT. — The description of the three new species of Maestrichtian age of the genus *Miseia,* which is for the first time found in Turkey, has been given. It is also proposed a new subfamily *(Joufiinae)* of Radiolitidae which has five genera as Colveraia Klinghardt, Joufia Boehm, Miseia Patrulius, Balabania Karacabey-Öztemür, Kurtinia Karacabey-Öztemür, which have some common characteristics encouraging us to gather them under this new subfamily.

INTRODUCTION

The first appearance of the genus Miseia in Turkey has been observed within the samples collected by İzdar, E. from Ballıkaya (Hekimhan-Malatya); by Pisoni, C. from Balaban (Darende-Malatya). Three new species of Miseia have been established from the rudistid limestone of Maestrichtian age. Some common generic characteristics of the genera Colveraia, Joufia, Balabania, Kurtinia belonging to the family Radiolitidae, but nowadays not included in any subfamily and Miseia which is included into the subfamily Sauvagesiinae by Patrulius, give us the opportunity to discuss their position in the systematic.

SYSTEMATIC STUDY

Order: RUDISTIDA LAMARCK, 1819

Family: RADIOLITIDAE GRAY, 1848

Genus: Miseia PATRULIUS, 1974

Miseia regularis n. sp.

(Plate I, fig. 1-4; Fig. 1)

Derivatio nominis: After the very regular ornamentation on both valves.

Material and depository: Holotype, with partly broken upper and lower valves, is deposited at the Museum of Mineral Research and Exploration Institute of Turkey with no. 1130.

Type locality: Rudistid limestone, Ballıkaya, Hekimhan.

Type level: Maestrichtian (middle ?).

Description: *The upper valve* is slightly convex and the apex area is eroded. The postero-ventral region on both valves is broken away. Shell surface is ornamented with 10 or 11 (E and S costae included) radial, rounded costae and fairly deep intervals as grooves which lie from the

periphery up to the apex (Plate I, fig. 1). Costae and intervals are crossed with very thin and tight growth lines. The growth lamellae can be seen in two places. On the siphonal region, especially near the periphery, the two costae corresponding to E and S are larger and more prominent compared to the others (E siphonal costa has been partly observed). On the eroded parts of the subcentral apex and on the broken side of the shell there are one row of rounded holes which arc partly filled with sediments (Plate I, fig. 2). These are the orifices of the radial canals which Patrulius has mentioned in its paper (Patrulius, 1974, p. 176).

We could not correctly define the general shape of the *lower valve* because the end is broken away. It is probably conical. The dorso-ventral diameter is 2.6 cm. Ornamentation consist of 10 or 11 (E and S costae included) longitudinal, subrounded costae and inbetween grooves larger than costae. Costae and intervals are costulated. There are two slightly thick costules on the costae and 4-5 thinner costules on the intervals (Plate I, fig. 3). Costae and intervals are crossed tightly with growth lines. Ligamental ridge is not marked exteriorly, it corresponds one of the intervals which has not any distinct characteristics from the others. As the shell is broken, the E siphonal band has been observed partly on the upper valve. S siphonal band is a larger and less deeper groove than other intervals and has 8-10 costules. This siphonal groove projecting towards the upper valve at the commissure, form the large and elevated S siphonal costa on the upper valve. The cross-section, passing 1 cm below the commissure, shows that the shell wall is thecker at the cardinal region than the siphonal region. The shell wall is prismatic in structure which consists of large, irregular polygonal cells. Among these polygonal cells there are some cells with one or two edges strongly convex or concave, and some of them are radially elongated. Ligamental ridge has 1 cm long and slightly enlarged distally. At the opposite side of the ligamental ridge and on the inner margin of the shell wall there are two pseudopillars. They do not form inward bulges and they are so close that it seems to be contiguous. Each of them is separated from the prismatic structure by a lamella. The external part of the lamella of the S pseudopillar is straight and parallel to the inner border of the prismatic layer (Plate I, fig. 4). The texture of the pseudopilkr is similar to the prismatic layer. The only difference between them is that the external cells of the pseudopillar are slightly elongated in radial direction. The E pseudopillar is partly preserved. The teeth and myophore apophyses has been not observed.

Comparison and remarks: Our new species siffers from species *pajaudi*, *costulata* and *vadensis* of Patrulius by its slightly convex upper valve and strong, large costae on it, and by the ornamentation of the lower valve (Patrulius, 1974). The species now described, in the cross-section through the lower valve, resembles *Miseia costulata* in the texture of the pseudopillars and the largeness of the prismatic cells which form the shell wall. But it goes away from costulata by the form and ornamentation of the upper valve and the very regular ornamentation of the lower valve.

Association: It is found together with *Pironaea praeslavonica* Milov., Slad., Grub., and *Vaccinites loftusi* Wood.

Miseia hekimhanensis n. sp.

(Plate I, fig. 5-8; Fig. 2)

Derivatio riominis: After the type locality name, Hekimhan.

Material and depository: Holotype with upper and lower valve, and two paratypes represented only with their lower valve. Holotype is deposited at the Museum of Mineral Research and Exploration Institute of Turkey with no. 1131,

Fig. 1 - M. regularis n. sp. Transversal section of the lower valve.

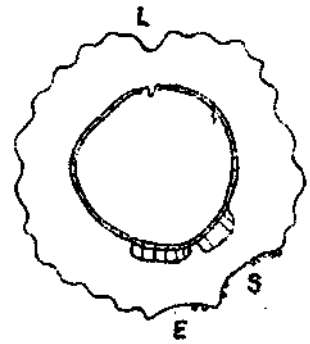

Fig. 2 - M. hekimhanensis n. sp. Transversal section of the lower valve.

Type locality: Rudistid limestone, Ballıkaya, Hekimhan.

Type level: Maestrichtian (middle?).

Description: The *upper valve* is slightly convex. The apex is subcentral. The shell surface is smooth, it has only short costules at the margin of the posterior side. £ and S siphonal bands can be distinguished by two triangular swellings reaching up to apex which are separated by a fairly deep furrow. A deep depression marks the ligament at the dorsal margin (Plate I, fig. 7).

The *lower valve* is low conical. The diameter of the holotype is 2 cm and the height is 1.6 cm. The diameter of the paratype is 1.8 cm. The shell surface is ornamented with subrounded longitudinal costae and grooves narrower than costae. Both are crossed by thin growth lines. The growth lamellae are distinguishable only on the anterior (Plate I, fig. 6). Ligament is represented with a deep groove all along the valve. E and S bands are as large grooves which have 0.5 and 0.6 cm of width at the commissure. The well preserved S siphonal groove is composed of two thin costules at the E side, five at the other side and between them a flat band of 3 mm width bearing only growth lines. The E siphonal band is not well preserved, only two costules have been observed at the S side (Plate I, fig. 5). On the cross-section, the polygonal cells which compose the prismatic layer, are bigger compared to the thickness of the shell wall. In the holotype, at the siphonal region, the number of the cells, in the radial direction, is about three or four (except the cells of the pseudopillar). The inner border cells have thickened wall and are subquadrangular in shape. Pseudopillars, without making the inward bulges, are limited outward with compressed lamella (Plate I, fig. 8). These two lamellae, in holotype, have the same convexity. In paratype the lamella of S is more convex. The inside cells of the pseudopillars are arranged in two rows. The inner row is made of the small subquadrangular and thick walled cells which are similar all over the inner periphery. The outer row is made of slightly elongated in radial direction, large and subrectangular or subsquare cells. The size of the cells of this row is about twice larger than the prismatic layer cells. The number of these cells, in holotype, is 6 in the E pseudopillar and 5 in S pseudopillar. The ligamental ridge is thin and short, no distal enlargement is present. The cardinal teeth are well preserved in the paratype in which the anterior cardinal tooth is bigger than posterior and has subsquare in shape. The myophore apophyses are massive and short, ma is well developed than mp.

Comparison and remarks: Our new species differs from *pajaudi* by the less convexity of its upper valve and by the different texture of pseudopillars. The less convexity of the upper valve and the presence of L differ the new species from vadensis. The largeness of the cells of the pris-

matic layer and shape and texture of the pseudopillars are the common characteristics of costulata with new species. But it differs from *costulata* with its distinct siphonal bands and by the different ornamentation of the lower valve.

Association: Our new species is associated with *Pironaea praeslavonica* Milov., Slad., Grub, and *Vaccinites loftusi* Wood.

Miscia osculata n. sp.

(Plate II, fig. 1-8)

Derivatio nominis: After the presence of the oscules on the upper valve.

Material and depository: Holotype with two well preserved valves and three paratypes. Holotype is deposited at the Museum of Mineral Research and Exploration Institute of Turkey with no. 1134.

Type locality: Rudistid limestone, Balaban, Darende.

Type level: Maestrichtian.

Description *Upper valve,* with 3 cm of diameter, is moderately convex. Apex is subcentral. The upper valve is broken away at the cardinal region where one row of orifices of the canals have been observed under the lamellar layer. Two inward fold at the periphery mark the siphonal grooves of the lower valve. Two deep and triangular depressions with their bases parallel to the siphonal folds, located 3 mm away from the periphery towards the apex, indicate E, S oscules (Plate II, fig. 1 and 5). The deepest parts of the depressions are situated at the bases of triangles. E oscule is isosceles with nearly 90° apex angle. S triangle is also isosceles but with acute angle. S oscule is deeper than E. Two costae, separated with narrow groove, lying from the oscules up to the apex, correspond E and S siphonal bands.

Lower valve is conical with 3.3 cm height and 3 cm of diameter. The surface is much eroded that the costae are not well distinct. But thin and numerous longitudinal costae (10 in one centimeter), separated with narrower intervals, can be seen near the commissure. Siphonal bands are two contiguous grooves and their width are 1 cm at the commissure. They are covered with thin and tight longitudinal costules (Plate II, fig. 3,7). Ligament is marked by a narrow, longitudinal groove at cardinal region (Plate II, fig. 2). The shape of the cross-section, passing through 0.5 cm below the commissure, is circular (Plate II, fig. 4). The maximum width of the prismatic layer is 8 mm at the cardinal region and minimum width 3 mm at the siphonal region. This layer is composed of 4-8 edged polygonal cells. Most of them have 5-6 edges; the cells with 8 edges are bigger than the others and fairly rare. Ligamental ridge is short and thin. The E pseudopillar has no inward bulge and it is limited outward with long lamella which is parallel to the inner border. Thus, narrow and long E pseudopillar has been formed. Inside and outside of the E pseudopillar lamella, parallel to it, very thin lamellae have been observed. The S pseudopillar has a slight inward bulge and is limited outward with a strongly convex lamella. This position makes S pseudopillar narrow and high. From the inside of the S lamella to the inner border there are six very thin, arched lamellae. The inner cell texture of the pseudopillars is not different from the rest of the prismatic layer. Cardinal teeth and myophore apophyses could not been observed in holotype. In paratype, contrary to holotype, the E pseudopillar has a slight inward bulge, and none at S. Less distinct lamellae which limit the pseudopillars, show the same characteristics as holotype. The cells of the pseudopillars are tending to be arranged parallel to the inner border of the pseudopillars. Well preserved cardinal teeth and myophore apophyses are peripheral and well developed at anterior (Plate II, fig. 6)

Comparison and remarks: *Miseia osculata* n. sp. differs from *costulata* by having different convexity of £ and S lamellae and the texture of the pseudopillars; it also differs from v*adensis* with its less convexity of the upper valve, by the similarity of the pseudopillars texture with the prismatic layer and by the presence of L. The new species resembles to *fajaudi,* but *M.osculata* n. sp. differs from it by minute differences and especially by the presence of the oscules on the upper valve. The presence of these oscules is the distinctive feature of the new species among the all Miseia species (Patrulius, 1974).

Association: In the Rudistid limestone, with our species, it is also determined the following genera and species: *Joufia cappadociensis melitenensis* Kar.- Özt., *Coheraia variabilis* Klingh., *Gorjanovicia* sp., *Vaccinites* aff. *sulcatus* Defr., *Orbitoides* sp,

SYSTEMATIC POSITION OF THE GENUS MISEIA AND PROPOSAL OF A NEW SUBFAMILY

Patrulius includes genus Miseia to the subfamily Sauvagesiinac, because the former has «canale» cardinal teeth as genus *Sauvagesia* (Patrulius, 1974). After our study and as Patrulius mentionned in its publication (p. 176), these two genera have many different characteristics. Because of these differences it is not convenient for us to include genus Miseia into the subfamily Sauvagesiinae. Miseia differs from Sauvagesia mainly by having pseudopillars on the lower valve and canals on the upper valve. By the presence of pseudopillars on the lower valve, Miseia can be related to the subfamily Lapeirousiinae, but these pseudopillars are not typical at Miseia.

Miseia can be compared with the genera *Joufia* and *Kurtinia* which nave canals on the upper valve as Miseia, although their number and disposition are different (Boehm, 1898; Snethlage, 1905; Lupu, 1970). Their common characteristics are to have a canal layer after the outer lamellar layer (Karacabey-Öztemür, 1969, 1980).

Kurtinia, in one way, shows similarity with the genera Jouf ia and Miseia by having canal layer, but on the other hand it shows also similarity with *Balabania* and *Coheraia* by having pseudocanals after the canal layer on the upper valve. By having both characteristics of the genera Miseia, Jouf ia and Balabania, Colveraia, genus Kurtinia can be accepted as a transition form between them.

It is certain that these genera belong to the family Radiolitidae, but nowadays they arc not classified into a subfamily (Moore, 1969). Based on the common special shell structure on the upper valve, it seems more convenient to us, to unite these genera, which have canals or pseudocanals or canals and pseudocanals, into a new subfamily of the family Radiolitidae.

The distinctive characteristics of the new proposed subfamily are:

1. Prismatic shell wall of polygonal cells at the lower valve.
2. Fairly well developed L.
3. Pseudopillars in some forms.
4. Canals or pseudocanals or canals and pseudocanals on the upper valve.

We can include the following genera into new subfamily: Joufia Boehm 1897, Miseia Patrulius 1974, Kurtinia Karacabey-Öztemür 1980, Balabania Karacabey-Öztemür 1980, Colveraia Klinghardt 1921.

We put the name *Joufiinae* to the new subfamily, referring to the genus Joufia, the oldest of the genera included in this new subfamily.

Manuscript received ***January 14. 1980***

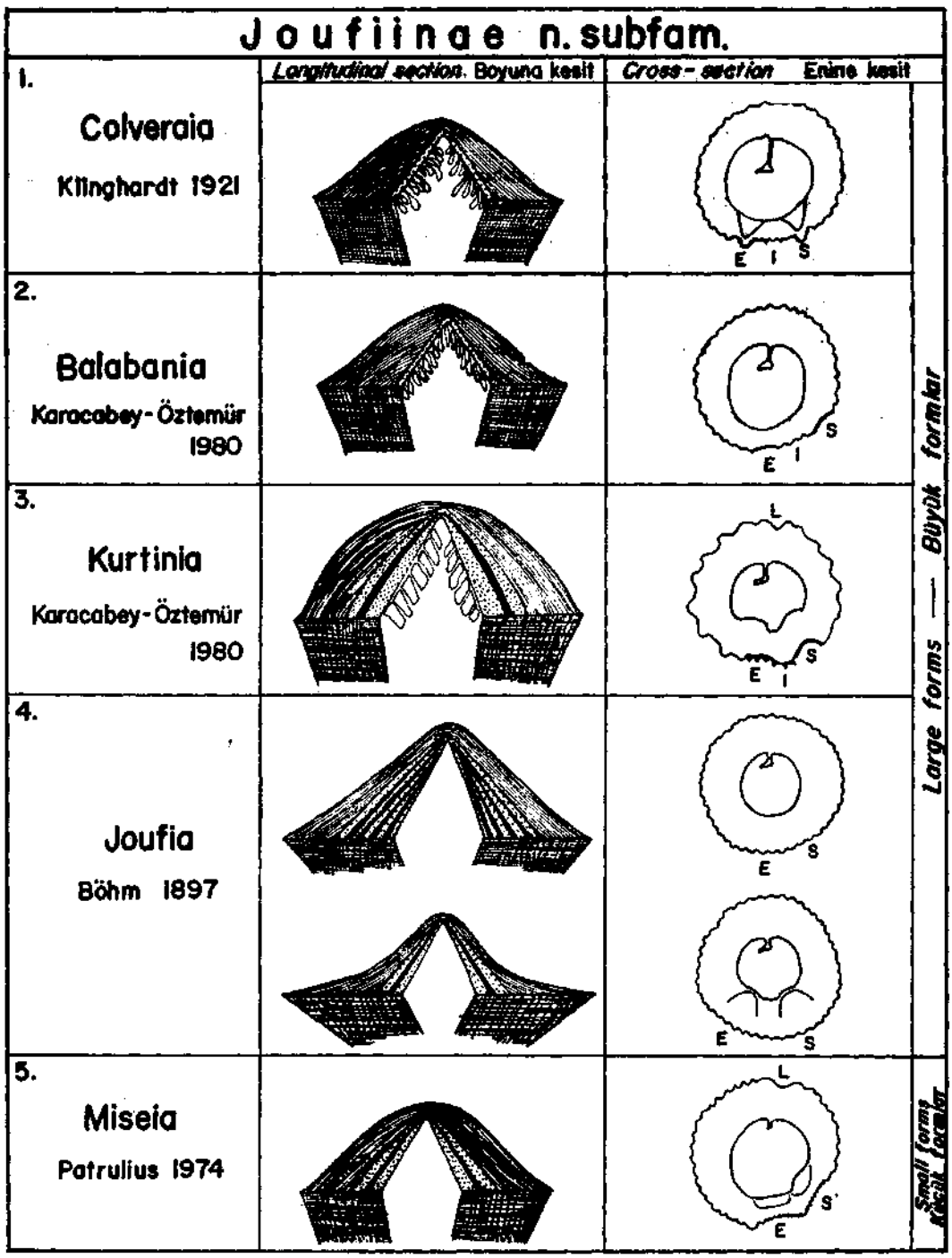

Schematic diagram of the longitudinal and cross-section of the genera which are included in the new subfamily Joufinaer.

BIBLIOGRAPHY

Boehm, G., 1898, Zur Kcnntniss der Gattung Joufia: Zehsch. Deutsch. Geol. Ges., Berlin, 50, 591-592.

Karacabey-Öztemür, N., 1969, Sur une espece de Joufia Boehm prelevee dans la partie orientale de la Turquic: Boll, of the MTA, Ankara, 73, 149-154.

———, 1974, Sur une nouvelle espece de Joufia Boehm en Torque: Bull, of the MTA, Ankara, 82, 77-83.

———, 1980, Two new genera of Radiolitidae (Balabania n. gen., Kurtinia n. gen.) from Turkey: Bull, of the GST, Ankara (in press).

Lupu, D., 1970, La presence du genre Colveraia Klinghardt a ValeaNeagra-Borod(Monts ApusenideNord): Studii si de cercetari de geologie, Bucuresti, 1, 15, 295-300.

Moore, R.C., 1969, Treatise on Invertebrate Paleontology, New York, N, Mollusca 6,2.

Patrulius, D., 1974, Duranddelgaia et Miseia, deux nouveaux genres de Rudistes du Senonien de Padure Craiului (Monts Apuseni): Rep. Soc. Romania Dan Searna Şedintelor, Bucuresti, 60, 3, 169-180.

Saethlage, E., 1905, Über die Gattung Joufia G. Boehm: Berichte der Naturforschenden Ges., Freiburg, 16, 1-8.

P L A T E S

PLATE-I

Miseia regularis n. sp.

Fig. 1 - Upper valve, external view, holotype, X 1

Fig. 2 - Upper valve, lateral view, holotype, x 2

Fig. 3 - Lower valve, holotype, X 1

Fig. 4 - Lower valve, cross-section, holotype, X 3

Miseia hekimhanensis n. sp.

Fig. 5 - Lower valve, external view of the siphonal region, holotype, X 2

Fig. 6 - Lower valve, anterior view, holotype, x 2

Fig. 7 - Upper valve, external view, holotype, X 1,5

Fig. 8 - Lower valve, transversale thin-section, holotype, x 8

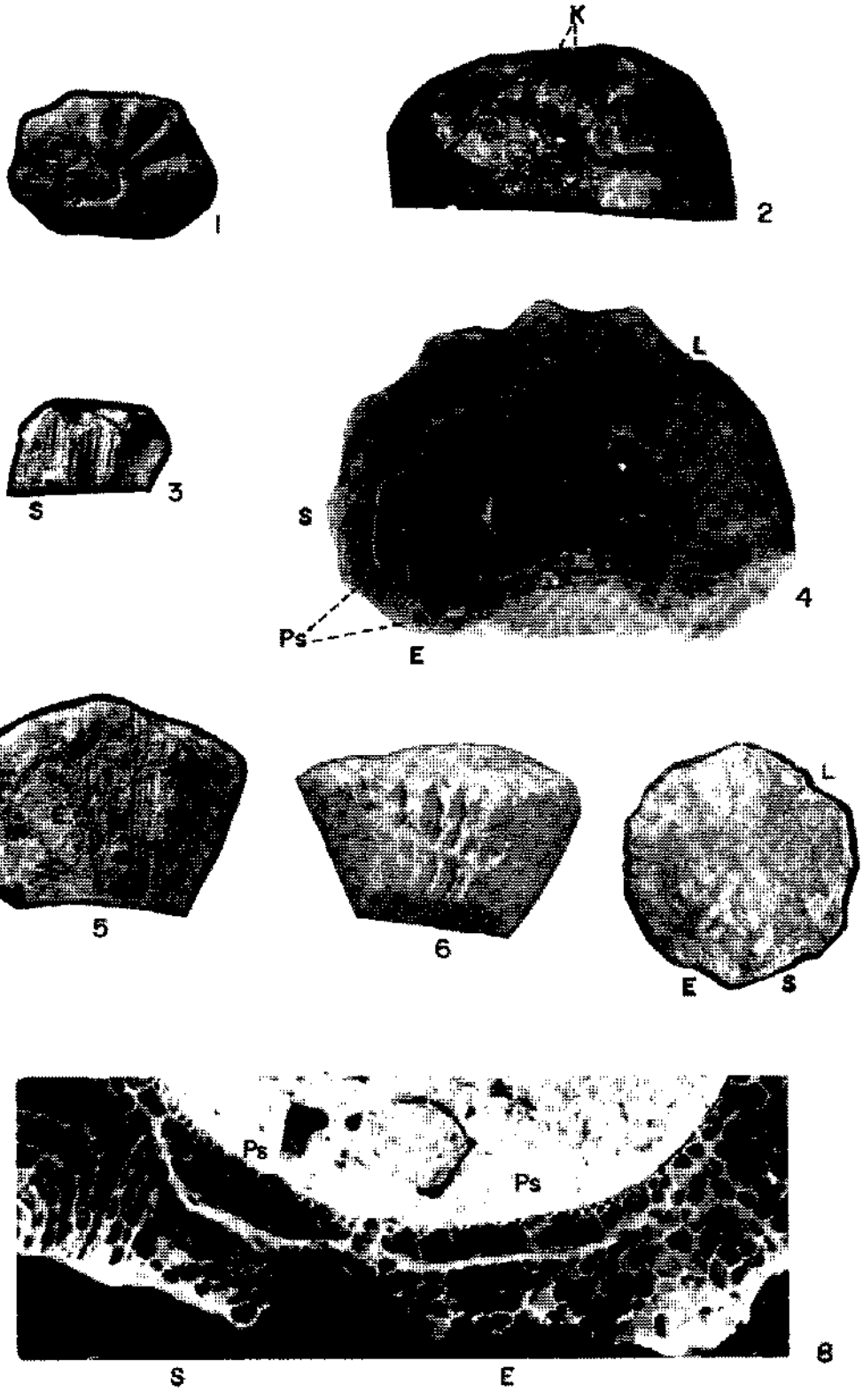
K
1
2
3
S
L
S
4
Ps
E
5
6
L
E
S
Ps
Ps
S
E
8

PLATE - II

Miseia osculata n. sp.

Fig. 1 - Upper valve, external view, holotype, x 1

Fig. 2 - External view of the cardinal region, holotype, x 1

Fig. 3 - External view of the siphonal region, holotype, x 1

Fig. 4 - Lower valve, cross-section, holotype, X 1

Fig. 5 - Upper valve, external, view, paratype, x 1

Fig. 6 - Cross-section, passing near the commissure, paratype, x 1

Fig. 7 - Lower valve, external view of the siphonal region, paratype, x I

Fig. 8 - Lower valve, cross-section, paratype, X 1

Explication of symbols in the plates

K : Orifices of canals
Os: Oscules
O's,Os: Anterior, posterior oscules
E,S: Anterior, posterior siphonal grooves
L: Ligamental groove
B',B: Anterior, posterior cardinal teeth
ma,mp: Anterior, posterior myophore apophyses
Ps: Pseudopillars

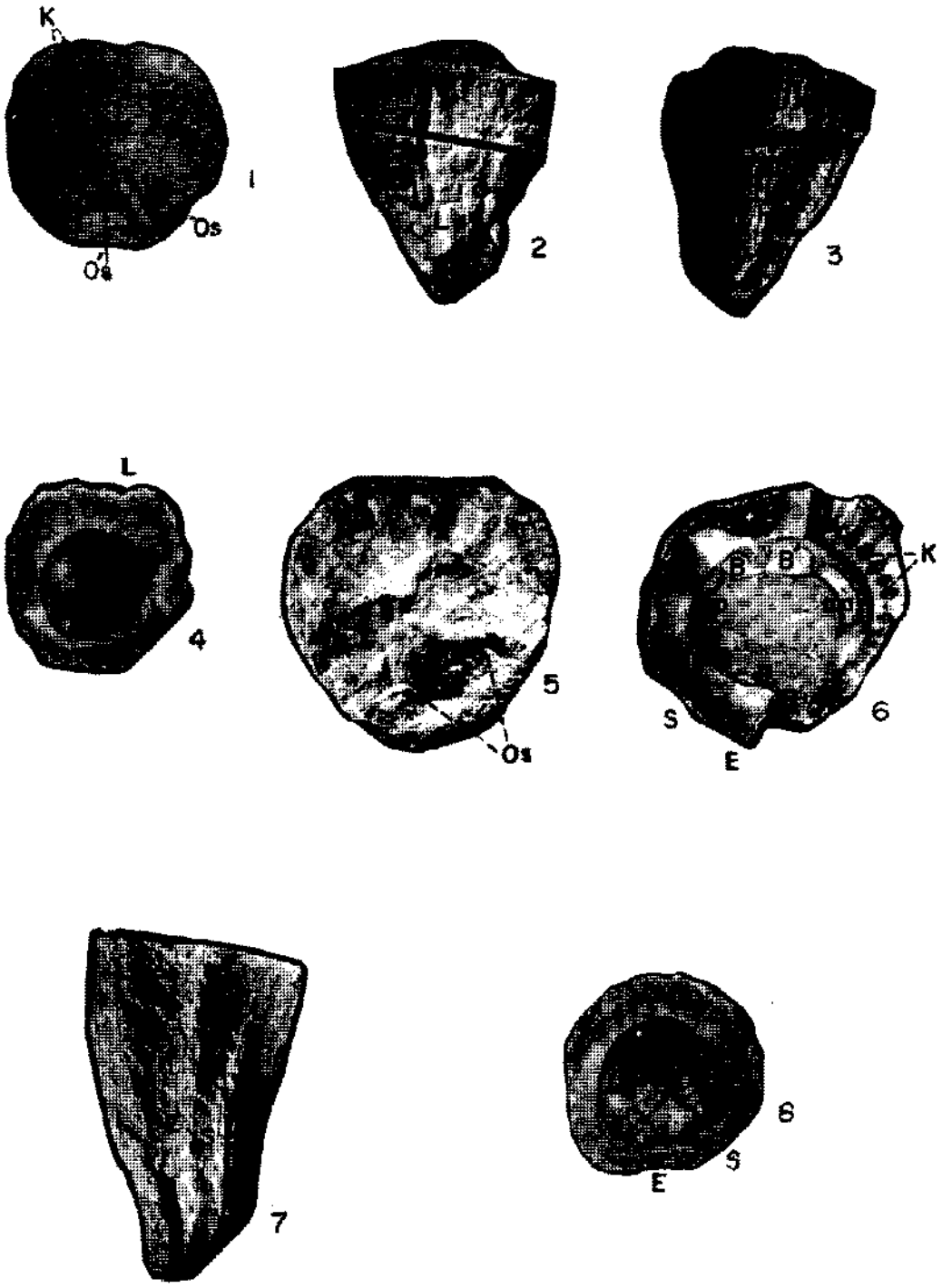
K
Os
1
2
3
L
4
5
Os
B
B
K
S
E
6
7
8
S
E

LOWER JURASSIC RADIOLARIA FROM THE GÜMÜŞLÜ ALLOCHTON OF SOUTHWESTERN TURKEY (TAURIDES OCCIDENTALES)

Emile A.PESSAGNO, Jr.

*Program for Geosciences, University of Texas at Dallas**

and

Andre POISSON

Department de GMogie, Univcrsitt Paris-Sud.

ABSTRACT. — Until recently Mesozoic Radiolaria were ignored in biostratigraphic investigations. This group of planktonic microfossils was neglected because most workers considered them to be too small and difficult to work with and to be universally long ranging.

Investigations now in progress indicate that Radiolaria evolved very rapidly during Mesozoic times. In fact, many genera and species are short ranging, cosmopolitan, and quite distinctive. Because it is now possible to separate matrix-free specimens from radiolarian cherts. Radiolaria are rapidly becoming the most important group of fossils in interpreting the stratigraphy and in turn the structure of many complex orogenic belts (e.g., Semail Ophiolite and Hawasina Complex of Oman) throughout the world.

In the present report eleven new species and three new genera are described from the Lover Jurassic of Turkey and two new species are described from the Jurassic of North America.

INTRODUCTION

Ten years ago with the advent of the Deep Sea Drilling Project (DSDP) the geologic community suddenly became more aware of the importance of planktonic microfossils in stratigraphy. Although the symmetrical arrangement of magnetic anomalies with respect to midocean ridges seemed to confirm the validity of the sea floor spreading hypothesis, the biostratigraphic'data resulting from the actual drilling of the interface between the igneus and sedimentary oceanic crust offered the first direct geotogic evidence for the existence of sea floor spreading. The data resulting from the study of planktonic foraminifera, nannofossils, and other fossil planktonic organisms in fact elevated the sea floor spreading hypothesis to a well founded theory.

Largely as a result of the Deep Sea Drilling Project investigations of all planktonic microfossils have greatly accelerated within the past ten years. Prior to this time practically nothing was known about Mesozoic Radiolaria. However, through the studies of De Wever, *et al.* (1979), Dumitrica (1978), Foreman (1973, 1975), Kozur and Mostler (1972), Pessagno (1976, 1977a, 1977b), Pessagno, Finch, and Abbott (1979), Riedel and Sanfilippo (1974) and others, the geologic history of this group of organisms is gradually unfolding.

In addition to the impetus gained in the study of Radiolaria from the Deep Sea Drilling Project a great deal of impetus has also been gained through advances in technology. For example, the introduction of the scanning electron microscope in the late 1960's allowed the rapid and accurate

illustration of microfossil specimens. The development of hydrofluoric acid technique (Dumitrica, 1970; Pessagno and Newport, 1972) made it possible to extract matrix-free Radiolaria from radiolarian cherts. Previously all Radiolaria occurring in cherts had to be studied in rock thin-section. Now radiolarian cherts of Mesozoic and even Paleozoic age can be accurately dated in most major orogenic belts. As a result the geologic history of many major orogenic belts is more clearly understood (See Irwin, Jones, and Pessagno, 1977; McLaughlin and Pessagno, 1978).

Table - 1

	Occurrence in North America
Hagiastrum infinitum, n. sp.	X
Crucella sp. A	X
Orbiculiforma multifora, n. sp.	
Orbiculiforma sp.aff. *O. mclaughlini* Pessagno	CR
Protopsium ehrenbergi, n. sp.	
Protopsium ispartaense, n. sp.	X
Protopsium sp. A	
Protopsium sp. B	
Protopsium sp. C	
Pseudoheliodiscus yaoi, n. sp.	
Pseudoheliodiscus sp. A	
Pseudoheliodiscus sp. B	
Pantanellium inornatum, n. sp.	CR
Praeconocaryomma parvimamma, n.sp.	CR
Canoptum anulatum, n. sp.	X
Canoptum poissoni, Pessagno	X
Canoptum rugosum, n. sp.	
Katroma neagui, n. sp.	CR
Natoba minuta, n. sp.	

Note: X : occurrence in North America.
CR : occurrence of a closely related form in North America.

A detailed system of radiolarian zonation has been proposed for strata of Late Jurassic (Tithonian) to Late Cretaceous (Maestrichtian) age (Pessagno, 1976, 1977a, 1977b). Studies by Pessagno and Blome in western North America, by Tippit and Pessagno in Oman, by Dumitrica in Romania, and by De Wever in the Mediterranean offer the promise of equally detailed zonal schemes for older (pre-Tithonian) Mesozoic strata.

The purpose of this report is to describe some of the more distinctive elements in a radiolarian assemblage from Lower Jurassic limestones in the Gümüşlü allochton of southwestern Turkey (Taurides Occidentales) (Poisson, 1977). No attempt at this time will be made to describe the entire radiolarian assemblage.

STRATIGRAPHY

The details of the lithostrstigraphy and the tectonic history of the Gümüşlü allochtonous unit are discussed elsewhere in this report (all the detail *in* Poisson 1977).

Pessagno and Blome are in the process of studying well preserved Upper Triassic (Norian) to Upper Jurassic (Caliovian) radiolarian faunas from eastern Oregon and the Queen Charlotte

Islands. Because the radiolarian-bearing strata in these areas also contain megafossils such as ammonites, it has been possible to integrate the radiolarian biostratigraphy to that of the ammonites and in turn to the European stages. Although most of the species level taxa in the Lower Jurassic assemblage remain undescribed, a sufficient number of genera and families have been described to establish broad, easily recognizable biohorizons based on these superspecific taxa.

The more significant of these biohorizons are as follows:

Biohorizon 1: Final appearance of *Paraentactinia* Dumitrica, Upper Hettangian.

Biohorizon 2: First appearance of *Crucella* Pessagno s. s., Lower Sinemurian.

Biohorizon 3: First appearance of *Hsuum* Pessagno, Lower Pliensbachian.

Biohorizon 4: First appearance of *Praeconocaryomma* Pessagno, Lower Pliensbachian.

Biohorizon 5: First occurrence of *Archaeodictyomitridae* Pessagno, Upper Pliensbachian.

Biohorizon 6: Final appearance of *Pseudoheliodiscus* Kozur and Mostler, Post Pliensbachian, pre-Lower-Middle Bajocian.

Biohorizon 7: Final appearance of *Canoptum* Pessagno, Toarcian -? Lower Bajocian.

Biohorizon 8: First appearance of *Parvicingula* Pessagno (= base of Zone 1, Pessagno, *1971 a, b;* revised herein), Lower Bajocian (P)-Lower-Middle Bajocian.

Biohorizon 9: First appearance of *Emiluvia* Foreman, Lower Bajocian (?)-Lower-Middle Bajocian.

Utilizing the biohorizons cited above and the biostratigraphic data presented in Table 1, it can be first surmised that the Turkish assemblage occurs below Biohorizon 5, the first occurrence of the Archaeodictyomitra'dae. In western North America Archaeodictyomitrids have been found in the Upper Pliensbachian Nicely Formation of eastern Oregon. According to Imlay (1968, p. C9) the entire Nicely Formation is assignable to the Upper Pliensbachian and contains an ammonite assemblage that is correlative with the European *Amaltheus margaritatus* and *Pleurococeras spinatum* Zones.

Secondly, it can be established that the Turkish sample occurs at or above Biohorizon 4, the first occurrence of *Praeconocaryomma* Pessagno and the Praeconocaryommidae Pessagno. In North America *Praeconocaryomma* seems to make its first appearance in strata of Early Pliensbachian age. It has been observed, for example, in the uppermost part of the type Maude Formation (QC 537; Queen Charlotte Island, British Columbia; see Locality Descriptions). The Maude Formation according to Frebold ,(1970, pp. 444.445) contains an ammonite assemblage correlative with the European *Tragophylloceras ibex* Zone. *Praeconocaryomma* has not been observed in samples below the top of the Maude Formation or from the underlying Kunga Formation (Rhaetian to Sinemurian).

At the species level *Hagiastrum infinitum,* n. sp., has been observed in the type Maude Formation (QC 532, 534, 537), in late early to early Late Pliensbachian cherts from the Franciscan Complex (NSF 960) of California, and from the Late Pliensbachian Nicely Formation of eastern Oregon (OR 536; see Locality Descriptions). *Protopsium* (?) *ispartaense,* n.sp., and C. *annulatum,* n.sp., have been observed from tfye Franciscan Complex (NSF 960) and *Crucella* sp. A has been observed in the type Maude Formation (QC 532). Other species such as *Katroma neagui,* n.sp., *Praeconocaryomma parvimamma,* n.sp., and *Orbiculiforma* sp. aff. *0. mclaughlini* Pessagno are closely related to forms that occur in North American Pliensbachian samples.

On the basis of the data presented above the.Turkish Lower Jurassic radiolarian assemblage is tentatively assigned to the Lower Pliensbachian. This interpretation largely depends on whether the Maude Island samples record the real first occurrence of *Praeconocaryomma*. At this early stage in our study of Lower Jurassic Radiolaria a Late Sinemurian age can not be ruled out completely. It should also be noted that the radiolaria'n limestone from which our sample (1662-D) was derived occurs below limestone strata (Ammonitico-rosso facies) containing Upper Pliensbachian ammonites.

The Turkish radiolarian assemblage is also of interest in that it is a bona fide Tethyan assemblage dominated by Spumellariina. Given the fact that the fauna is Tethyan and hence a low latitude assemblage, it is surprising that it is not as diversified as those of Pliensbachian age from the Queen Charlotte Island and eastern Oregon (45 species level taxa versus 90+ species level taxa). Jones, *et al*. (1977), on the basis of both convincing paleomagnetic and stratigraphic evidence, demonstrated that Queen Charlotte Islands' structural block is allochthonous and was displaced from low to high latitudes during Mesozoic times. Hence, the diverse Pliensbachian faunas from the Maude Formation are likewise low latitude assemblages. It is conceivable that the Turkish assemblage reflects a more closed system of oceanic circulation which perhaps prevailed during Early Jurassic times.

SYSTEMATIC PALEONTOLOGY

The designation USNM in this section refers to the deposition of type specimens at the U.S. National Museum, Washington, D.C.

Phylum: PROTOZOA

Subphylum: SARCODINA

Class: RETICULARIA

Subclass: RADIOLARIA

Order: POLYCYSTIDA

Suborder: SPUMELLARIINA

Superfamily: SPONGODISCACEA HAECKEL, 1881, emend. PESSAGNO, 1971, 1973

Range: Paleozoic to Recent.

Subsuperfamily: PSEUDOAULOPHACILAE RIEDEL, 1971, emend. PESSAGNO, 1971

Range: Paleozoic to Recent.

Family: HAGIASTRIDAE RIEDEL, 1967, emend. PESSAGNO, 1971

Type genus: Hagiastrum HAECKEL, 1881

Range and occurrence: Mesozoic; world-wide.

Subfamily: HAGIASTRINAE RIEDEL, 1967, emend. PESSAGNO, 1971, 19770

Type genus: Hagiastrum HAECKEL, 1881

Range and occurrence: Mesozoic; world-wide.

Genus: Hagiastrum HAECKEL, 1881, emend. PESSAGNO, 1971, 19770

Type species: *Hagiastrum plenum* RUST, 1885

Range and occurrence: Triassic to Cretaceous, world-wide.

Hagiastrum infinitum PESSAGNO and POISSON, n. sp.
(PL I, fig.1-4, 6, 8)

Description: Test comprised of irregular triangular, tetragonal, and pentagonal pore frames with nodes at vertices. Pore frames somewhat less irregular on ray tips. Pores dominally elliptical. Primary spines spongy at least proximally; distal portions usually broken.

Remarks: *H. infinitum,* n. sp., differs from *H. augustum* Pessagno (1979) by having much slender rays and coarser, more irregular meshwork.

Infinitus-a-um (Latin, adj.): infinite, unbounded.

Measurements: Length of rays exclusive of spines: Holotype: 180 microns, paratypes and hypotypes: maximum 220 microns, minimum 180 microns (7 specimens).

Type locality: Poisson 1662D. See Locality Descriptions.

Deposition of types: Holotype: USNM 263993, paratypes: USNM 263994 and Pessagno Collection.

Range and occurrence: Lower Jurassic (Upper Sinemurian (?)-Lower Pliensbachian) of Turkey. To date this species has only been found in Pliensbachian strata in North America. It has been recovered from Upper Pliensbachian cherts from the Franciscan Complex of California (NSF 960); from the Lower Pliensbachian part of the Maude Formation of the Queen Charlotte Islands (QC 532; QC 534; QC 537);and from the Upper Pliensbachian Nicely Formation of eastern Oregon (OR 536) (See Locality Descriptions). *H. infinitum* is most abundant in the Franciscan sample.

Genus: Crucella PESSAGNO, 1971

Type species: *Crucella messinae* PESSAGNO, 1971

Range and occurrence: Lower Jurassic (Sinemurian) to Upper Cretaceous (Upper Campanian).

Crucella sp. A
(PI. II, fig. 6)

Remarks: This form is characterized by having triangular pore frames except on the distal portion of its four rays.

Range an4 occurrence: *Crucella* sp. A is rare in the Turkish material. It has been observed in the type Maude Formation (Queen Charlotte Island, British Columbia) in strata containing Lower Pliensbachian ammonites (QC 532;.-see Locality Descriptions).

Family: ORBIC&LIFORMIDAE PESSAGNO, 1973

Type genus: *Orbtculiforma* PESSAGNO, 1973

Range: Triassic to Cretaceous so far as known.

Occurrence: World-wide.

Genus: *Orbiculiforma* PESSAGNO, 1973

Type species: *Orbiculiforma quadrat a* PESSAGNO, 1973

Range and occurrence: Same as for family.

Orbiculiforma multifora PESSAGNO and POISSON, n. sp.
(PI. I, fig. 5, 7, 9, 10)

Description: Test with angled periphery having twenty or more peripheral spines; spines circular in axial section lacking alternating grooves and ridges. Central cavity relatively shallow, about half diameter of test; test sloping from edge of central cavity to periphery. Meshwork comprised of pentagonal and tetragonal pore frames; pore frames smaller in central cavity than outside central cavity.

Remarks: *0. multifora,* n. sp.,by virtue of its angled periphery is most similar to *0. maxima* Pessagno (1976) of the Upper Cretaceous. It differs from *0. maxima* (1) by having massive, relatively long peripheral spines which are circular in axial section; (2) by having a mixture of tetragonal and polygonal pore frames; and (3) by having a shallower central cavity. The peripheral spines of *0. maxima* are very short and appear to be predominantly spongy.

Muliforus-a-um (Latin, adj.): pierced with many holes.

Measurements: Holotype: Test diameter 280 microns, diameter of central cavity 140 microns. Measurement of six specimens: Maximum diameter of test 300 micron, minimum diameter of test 120 microns, maximum diameter of central cavity 140 microns, minimum diameter of central cavity 120 microns.

Type locality: Poisson 1662D. See Locality Descriptions.

Deposition of types: Holotype: USNM 263995, paratypes: USNM 263996 and Pessagno Collection.

Range and occurrence: Lower Jurassic (Poisson 1662D; Upper Sinemurian (?)-Lower Pliensbachian) of Turkey.

Orbiculiforma sp. aff. *0. mdaughlini* PESSAGNO, 1977a
(PL II, fig. 7-9)

Remarks: This form differs from *0. mdaughlini* Pessagno (NSF 960 Pliensbachian. See Locality Descriptions) by having a slightly narrower rim around the central cavity and by having tetragonal and pentagonal rather than pentagonal and hexagonal pore frames. It is apparent that the two forms are closely related.

Range and occurrence: Lower Jurassic (Poisson 1662D; Upper Sinemurian (?)-Lower Pliensbachian) of Turkey.

Family: SPONGURIDAE HAECKEL, 1862, emend. PESSAGNO, 1973

Type genus: **Spongurus** HAECKEL, 1862

Range and occurrence: Paleozoic? Mesozoic to Recent.

Subfamily: ARCHAEOSPONGOPRUNINAE PESSAGNO, 1973

Type genus: Archaeospongopnmum PESSAGNO, 1973

Range and occurrence: Jurassic to Recent.

Genus: Protopsium PESSAGNO and POISSON, n. genus.

Type species: *Protopsium ehrenbergi*, n. sp.

Description: Primary test ellipsoidal (sometimes somewhat flattened) with two polar spines, Patagium-like mass of irregularly shaped and distributed pore frames occurring in one plane. Secondary spines of variable size radiating out from primary test into patagium-like mass seemingly offering support for the irregular meshwork. Polar spines with or without alternating grooves and ridges, occasionally bifurcating.

Remarks: *Protopsium*, n. gen., differs from *Archaeospongoprunum* Pessagno (1973): (1) by possessing a patagium-like mass supported by secondary spines; (2) by having polar spines which may or may not have alternating ridges and grooves and which sometimes bifurcate; and (3) by sometimes displaying a somewhat compressed test. *Protopsium* like *Archaeospongoprunum* possesses meshwork arranged in concentric layers. *Protopsium* is a name formed by an arbitrary combination of letters (ICZN, 1964, Appendix D, Pt. IV, Recommendation 40, p. 113).

Range and occurrence: Lower Jurassic (Poisson 1662D; Upper Sinemurian (?)-Lower Pliensbachian) of Turkey. Lower Jurassic (Lower Pliensbachian) cherts from Franciscan Complex. Upper Pliensbachian Nicely Formation of eastern Oregon.

Protopsium ehrenbergi PESSAGNO and POISSON, n. sp.
(PL II, fig. 1-3)

Description: Primary test small, ellipsoidal flattened slightly with tetragonal pore frames with small nodes at vertices. Secondary spines extending from primary test into flattened, rectangular patagium-tilje mass. Polar spines long, triradiate with three narrow grooves alternating with three narrow ridges; ridge tops rounded not sharp. Ridges and grooves of equal width.

Remarks: *P. ehrenbergi*, n. sp., is compared to *P. ispartaense*,n. sp., under the latter species.

This species is named after C.G. Ehrenberg, whose pioneering work in the early to middle 1800's, laid the foundation for micropaleontology.

Measurements: System of measurements after Pessagno (1973). Holotype: dd' = 20 microns, cc' = 20 microns, AA' = 100 microns, BB' = 70 microns. Maximum six specimens: dd' = 20 microns, cc' = 20 microns, AA' = 100 microns, BB' = 70 microns. Minimum for six specimens: dd' = 20 microns, cc' — 20 microns, AA' = 80 microns, BB' = 50 microns.

Type locality: Poisson 1662D. See Locality Descriptions.

Deposition of types: Holotype: USNM 263997, paratypes: USNM 263998 and Pessagno Collectionv

Range and occurrence: Lower Jurassic (Poisson 1662D; Upper Sinemurian (?)-Lower Pliensbachian) of Turkey.

Protopsium ispartaense PESSAGNO and POISSON, n. sp.
(PI. II, fig. 4-5; PI., Ill, fig. 1-9; PI XIII, fig. 4)

Description: Test ellipsoidal with massive tetragonal to pentagonal pore frames and thick, massive polar spines which are circular in axial section. One spine shorter than other, greater in diameter. No patagium-like mass observed.

Remarks: *P.ispartaense,* n. sp., differs from *P.ehrenbergi* by having thick, massive polar spines which are circular in axial section rather than possessing alternating grooves and ridges.

This species is named for the town of Isparta in the type area.

Measurements: System of measurements after Pessagno (1973). Holotype: A'S and AS = 55 microns, cc' = 30 microns, dd' =15 microns, AA' = 80 microns, BB' = 70 microns. Maximum for eight specimens: A'S and AS both = 70 microns, cc' = 30 microns, dd' = 15 microns, AA' = 95 microns, BB' = 75 microns. Minimum for eight specimens: A'S and AS both = 45 microns, cc' = 20 microns, dd' = 15 microns, AA' = 70 microns, BB' = 60 microns.

Protopsium sp. A
(PI. IV, fig. 1, 4)

Range and occurrence: Lower Jurassic (Poisson 1662D; Upper Sinemurian(?)-Lower Pliensbachian) of Turkey. Lower Jurassic (Pliensbachian) cherts from the Franciscan Complex of California (NSF 960). See Locality Descriptions.

Protopsium sp. B
(PI. IV, fig. 2)

Remarks: This form is characterized by a bifurcation of one polar spine.

Range and occurrence: Lower Jurassic (Poisson 1662D; Upper Sinemurian (?), - Lower Pliensbachian) of Turkey. See Locality Descriptions.

Protopsium sp. C
(PI. IV, fig. 3, 5-8)

Remarks: Note flattening displayed by this form.

Range and occurrence: Lower Jurassic (Poisson 1662D; Upper Sinemurian (?) - Lower Pliensbachian) of Turkey. See Locality Descriptions.

Subsuperfamily: SPONGODRUPPILAE HAECKEL, 1887, emend. PESSAGNO, 1973

Range and occurrence: Paleozoic to Recent.

Family: PARASATURNALIDAE KOZUR and MOSTLER, 1972, emend. PESSAGNO, 1979

Type genus: **Parasaturnalis** KOZUR and MOSTLER, 1972

Range and occurrence: Upper Triassic to Upper Cretaceous; world-wide.

Subfamily: HELIOSATURNALINAE KOZUR and MOSTLER, 1972, emend. PESSAGNO, 1979

Type genus: **Heliosaturnalis** KOZUR and MOSTLER, 1972, emend. PESSAGNO, 1979

Range and occurrence: Upper Triassic to Lower Jurassic; world-wide.

Genus: **Pseudoheliodiscus** KOZUR and MOSTLER, 1972 emend. PESSAGNO, 1979

Type species: *Pseudoheliodiscns riedeli* KOZUR and MOSTLER, 1972

Range and occurrence: Karnian (?) - Norian to Toarcian; world-wide.

Pseudoheliodiscus yaoi PESSAGNO, n. sp.
(PI. IV, fig. 9; PI. V, fig. 1, 4, 7-9; PI. XIII, fig. 2)

Description: Test with extremely broad, flat ring having thirteen to fourteen peripheral spines and about twelve auxiliary spines. Central spongy cortical shell occupying most of ring on most specimens; cortical shell comprised of concentric layers of irregular polygonal (triangular, tetragonal, pentagonal) pore frames.

Remarks: *Pseudoheliodiscus yaoi*, n. sp., differs from *P. riedeli* Kozur and Mostler (1972) by having a much broader ring with shorter peripheral spines. It differs from *P.finchi* Pessagno (1979) by having a somewhat wider ring and thirteen to fourteen as opposed to ten or eleven peripheral spines.

This species is named for Dr. Akira Yao (Osaka City University) in honor of his contributions to the study of the Parasaturnalidae.

Measurements: Holotype: Diameter of spongy cortical shell 140 microns; diameter of test including cortical shell and ring, excluding peripheral spines on ring 230 microns; width of ring, exclusive of peripheral spines 30 microns.

Maximum and minimum measurements for eight specimens: Diameter of cortical spongy cortical shell: maximum 150 microns, minimum 135 microns. Diameter of test including cortical shell and ring, excluding peripheral spines on ring: maximum 260 microns, minimum 230 microns. Width of ring, exclusive of peripheral spines: maximum 45 microns, minimum 30 microns.

Type locality: Poisson 1662D. See Locality Descriptions.

Deposition of types: Holotype: USNM 264001, paratypes: USNM 264002 and Pessagno Collection.

Range and occurrence: Lower Jurassic (Upper Sinemurian (?)-Lower Pliensbachian) of Turkey.

Pseudoheliodiscus sp. A
(PL V, fig. 2,3)

Range and occurrence: Lower Jurassic (Poisson 1662D; Upper Sinemurian(?)-Lower Pliensbachian) of Turkey. See Locality Descriptions.

Pseudoheliodiscus sp. B
(PI. V, fig. 5,6)

Range and occurrence: Lower Jurassic (Poisson 1662D; Upper Sinemurian (?)-Lower Pliensbachian) of Turkey. See Locality Descriptions.

Superfijmily: SPHAERALLACEA HAECKEL, 1881, emend. PESSAGNO, 1977a

Range and occurrence: Paleozoic to Recent.

Family: PANTANELilbAE PESSAGNO, *1917 b*

Type genus: *Paritanellium* PESSAGNO, 1977a

Range and occurrence: Triassic to Lower Cretaceous. World-wide.

Subfamily: PANTANEUINAE PESSAGNO, *1977b*

Type genus: Pantanellium PESSAGNO, *1977a*

Range and occurrence: Same as for family.

Genus: Pantanellium PESSAGNO, 1977a

Type species: *Pantanellium riedeli* PESSAGNO, 1977c

Range and occurrence: Upper Triassic (Upper-Middle Norian) to Lower Cretaceous (Upper Valanginian?). World-wide.

Pantanellium inornatum PESSAGNO and POISSON, n. sp.
(PI. VI, fig. 1-9)

Description: Cortical shell, thin, spherical with relatively slender triradiate bipolar spines; triradiate bipolar spines with three rounded, narrow ridges alternating with three narrow grooves. Meshwork of cortical shell comprised of equal number of hexagonal and pentagonal pore frames. Pentagonal pore frames slightly smaller than hexagonal pore frames. Meshwork of first medullary shell thick likewise comprised of hexagonal pentagonal pore frames. Secondary radial beams between cortical shell and first medullary shell circular in axial section.

Remarks: *Pantanellium inornatum* Pessagno, n.sp., differs from *P. riedeli* Pessagno (1977a) (1) by having longer, slender polar spines with narrow ridges separated by narrow grooves; (2) by having smaller, narrower ridges separated by narrow grooves; (2) by having smaller, more numerous pore frames; and (3) by having a thinner walled cortical shell and a thicker walled first medullary shell.

Inornatus-a-um (Latin, adj.): unadorned.

Measurements: System of measurements after Pessagno, (1973). Holotype: A'S = 110 + microns, AS = 85 microns, cc' = 25 microns, dd' = 20 microns, AA' = 85 microns, BB' = 80 microns. Maximum (measurement of specimens): A'S = 110 microns, AS = 85 microns, cc' = 30 microns, dd' = 25 microns, AA' = 90 microns, BB' = 85 microns. Minimum (measurement of nine specimens): A'S = 85 microns, AS = 55 microns, cc' = 25 microns, dd' = 20 microns, AA' = 85 microns, BB' = 75 microns.

Type locality: Poisson 1662D. See Locality Descriptions.

Deposition of types: Holotype: USNM 264003, paratypes: USNM 264004 and Pessagno Collection.

Range and occurrence: Unnamed forms from Upper Sinemurian and Lower Pliensbachian strata in western North America appear closely related to *P.inornatum.* However, this species is presently known only from its type locality in Turkey.

Family: PRAECONOCARYOMMIDAE PESSAGNO, 1976

Type genus: Praeconocaryomma PESSAGNO, 1976

Range and occurrence: Lower Jurassic (Pliensbachian) to Upper Cretaceous (Campanian). World-wide.

Genus: Praeconocaryomma PESSAGNO, 1976

Type species: *Praeconocaryomma unhersa* PESSAGNO, 1976

Range and occurrence: Lower Jurassic (Pliensbachian) to Upper Cretaceous (Campanian). *Praeconocaryomma-likc* forms occur as low as the Upper Paleozoic (Mississippian). However, in all cases where specimens are well enough preserved to permit examination of internal morphology, these forms have proven to be Enactinids.

Pracconocaryomma immodica PESSAGNO and POISSON, n. sp.
(PI. VII, fig. 2-9)

Praeconocaryomma magnimamma (RUST). PESSAGNO, 19770, p. 77, PI. 5, figs. 14-16; PL 6, fig. 1

Description: Cortical shell with prominent mammae which tend to be exceedingly high in relief. Distal surfaces (tops) of mammae imperforate, somewhat flattened, pentagonal in outline; mammae with radially arranged primary spines that are circular in axial section. Each face of pentagonal mammae with large pores; pores separated by stout rays which project into intermammary areas; individual rays bifurcate or trifurcate linking up with rays of adjoining mammae and forming triangular intermammary pore frames. Massive nodes present at point of bifucation or trifucation. Well preserved specimens with thinner rays projecting from bottom side of rays at nodal points forming subsidiary triangular pore frames. Primary radial beams (circular in axial section) continuous with radial beams connecting cortical shell with first medullary shell and first medullary shell with second medullary shell. First medullary shell with triangular meshwork comprised of equilateral triangular pore frames; second medullary shell with polygonal pore frames.

Remarks: *P. immodica,* n. sp., differs from *P. media,* n. sp., (1) by having mammae which are pentagonal rather than hexagonal in outline and which are considerably higher in relief; (2) by having mammae which are more closely spaced; and (3) by having more complex intermammary areas. *P. media* has triangular mammary pore frames closed by a bar at their base; however, the mammary pore frames of *P. immodica* lack the basal bar and are open basally.

This species seems to be the most advanced form in the *P. parvimamma,* n. sp., lineage group. At present it is not possible to link it directly to earlier and simpler forms such as *P. media.* It would, however, appear that the basal bar of the *P. media* mammary pore frames has been lost in the course of the evolution of this lineage.

Immodictis-a-um (Latin, adj.): immoderate, excessive.

Measurements: Holotype: Diameter of cortical shell 206 microns; height of mammae 44 microns. Measurement of ten specimens: Maximum diameter of cortical shell 225 microns, minimum diameter of cortical shell 193 microns, maximum height of mammae 44 microns, minimum height 25 microns.

Type locality: BK 605. Franciscan Complex. See Locality Descriptions.

Deposition of types: Holotype: USNM 264005, paratypes: USNM 264006 and Pessagno Collection.

Range and occurrence: Toarcian to Lower Tithonian-Upper Kimmeridgian in California. Franciscan Complex of California Coast Ranges and North Fork Terraine of Klamath Mountains. Cherts associated with Coast Range Ophiplite at Stanley Mountain, California Coast Ranges.

Praeconocaryomma, media PESSAGNO and POISSON, n. sp.
(PL-VIII, fig. 1-4)

Description: Cortical shell with mammae having radially arranged primary spines which originate in their center. Primary spines circular in axial Section. Distal (top) surfaces of mammae convex, hexagonal in outline. Six sides of each mamma with six very large equilateral pore frames (mammary pore frames) inclined away from faces of mammae. Mammary pore frames with massive bars comprising legs and thinner bars comprising base's; two massive nodes occurring at juncture between legs arid base of each mammary pore frame. Legs of mammary pore frames bowed inwards, aligned with legs of pore frames of opposing mammae forming large equilateral triangular areas. Smaller, less massive equilateral triangular pore frames (intermammary pore frames) inserted in center of large triangular area formed by bases of mammary pore frames (PI. VIII, figs. 1-3). First medullary shell comprised of equilateral triangular pore frames with nodes at vertices,; radial beams circular in axial section and continuous with primary spines in center of each mamma, connecting with first medullary shell at nodal points of triangular pore frames. Second medullary shell with polygonal pore frames.

Remarks: *P. media,* n. sp., has been compared to *P. parvimamma,* n.sp., under the latter species. It differs from *P. immodica,* n. sp., (1) by having mammae which are considerably lower in relief and more widely separated and (2) by having less complex intermammary pore structure.

Medius-a-um (Latin, adj.): middle.

Measurements: Holotype: Diameter of cortical shell 238 microns, height of mammae 25 microns. Measurement of nine specimens: Maximum diameter 244 microns, minimum diameter 213 microns, maximum height of mammae 28 microns, minimum height of mammae 19 microns.

Type locality: NSF 960. Franciscan Complex. See Locality Descriptions.

Deposition of types: Holotype: USNM 264007. paratypes: USNM 264008 and Pessagno Collection.

Range and occurrence: Lower Jurassic (Pliensbachian) so far as known. Franciscan Complex of California (NSF 960).

Praeconocaryomma parvimamma PESSAGNO and POISSON, n. sp.
(PI. VIII, fig. 5-8; PI. IX, fig. 2)

Description: Cortical shell with mammae having radially arranged relatively long primary spines originating from the center of their flat distal (top) surfaces. Primary spines relatively long, circular in axial section. Distal flattened surfaces of mammae hexagonal in outline; six sides of each mamma with massive triangular mammary pore frames at their base; mammary pore frames with massive nodes at their base only; pore frames and sides of mammae sloping gently outward. Six rays originating from position of nodes at base of mammary pore frames, aligned with legs of each mammary pore frame and interconnecting with rays of adjoining mammae. Large subelliptical pores occurring between rays. Cortical shell and two medullary shell connected by radial beams which are circular in axial section. First medullary shell with triangular pore frames having nodes at their vertices; second medullary shell with polygonal (pentagonal?) pore frames.

Remarks: *P. parvimamma,* n. sp., differs from *P. media,* n. sp., (1) by having much smaller, less inclined mammary pore frames and (2) by having mammae which are smaller with flattened distal (top) surfaces.

P. parvimamma appears to be the earliest and simplest form of a lineage group (termed the *P. parvimamma* lineage group herein) which includes at least four morphotypes. The data at hand indicate that the *P. parvimamma* lineage group makes its first appearance in the Lower Pliensbachian (PUpper Sinemurian) and its final appearance in the Lower Tithonian. During the period from Early Pliensbachian to Early Tithonian times this lineage tends to change through an increase in the width and height of mammae and by developing more complex structure in the intermammary areas. All members of this group display a first medullary shell with equilateral triangular pore frames.

It should be noted that the form figured by Pessagno (1977) as *P. magnimamma* (Rust) is assigned to *P. immodica,* n. sp., herein. Rust's (1898, PI. IV, fig. 1) illustration of *A. magnimamma* shows a form with mammae and intermammary areas perforated by numerous small pores. Pessagno originally assumed that the small pores were a figment of Rust's imagination and that the extremely large mammae with long smooth (circular in axial section) primary spines were the distinguishing feature of *P. magnimamma.* Unfortunately, however, a form quite similar to Rust's form occurs in Pliensbachian cherts from the Franciscan Complex. This form is referred to *P.* sp. aff. *P. magnimamma* (Rust) herein.

Parvus-a-um (Latin,adj.): small + *mamma (-ae,* F.) = breast

Measurements: Holotype: Diameter of cortical shell 235 microns, height of mammae 20 microns. Measurement of nine specimens: maximum diameter of cortical shell 260 microns, minimum diameter of cortical shell 200 microns. Maximum height of mammae 20 microns, minimum height 12 microns.

Type locality: Poisson 1662D. See Locality Descriptions.

Deposition of types: Holotype: USNM 264009, paratypes: USNM 264010 and Pessagno Collection.

Range and occurrence: Lower Jurassic (Poisson 1662D; Upper Sinemurian (?)-Lower Pliensbachian) of Turkey. Forms like the Turkish specimens but having broader mammae occur in Lower Jurassic (Pliensbachian) cherts from the Franciscan Complex of California (NSF 960; see Locality Descriptions and PI. IX, fig. 1). Such forms are referred to *P.* sp. aff. *P. parvimamma* herein.

Praeconocaryomma sp. aff. *P. magnimamma* (RUST), 1898
(PI. IX, fig. 3-5)

Remarks: This form may well be the same form figured by Rust (1898, PI. IV, fig. 1) as *Acanthosphaera magnimamma.* Rust illustrates a form (1) with prominent mammae penetrated everywhere by small pores; (2) with long spines which are circular in axial section; and (3) with abundant small pores in the intermammary areas. Unfortunately his illustrations are too schematic to make precise identification possible.

Range and occurrence: Lower Jurassic (NSF 960; Pliensbachian) cherts from the Franciscan Complex. See Locality Descriptions.

Praeconocaryomma sp. aff. *P.parvimamma* PESSAGNO and POISSON, n. Sp.
(PI.-IX, fig. 1)

Remarks: This form appears to be closely related to *P. parvimamma.* Both forms display the same sort of mammary and intermammary pore frames. However, *P.* sp. aff. *P. parvimamma* has considerably broader mammae. In that One of the phylogenetic trends characteristic of the *P. parvimamma* lineage is an increase in the size of the mammae, this form is interpreted as being somewhat more advanced than is *P. parvimamma.*

Range and occurrence: Lower Jurassic (Pliensbachian; NSF 960). See Locality Description.

Suborder: NASSELLARIINA EHRENBERG, 1875

Superfamily: CYRTOIDEA HAECKEL, 1862

Range and occurrence: Paleozoic?; Triassic to Recent.

Subsuperfamily: EUCYRTIDILAE EHRENBERG, 1847

Range and occurrence: Triassic to Recent.

Family: CANOPTIDAE PESSAGNO, 1979

Type genus: Canoptum PESSAGNO, 1979

Range: Upper Triassic (KarnianP-Norian) to Lower Jurassic (Pliensbachian-Toarcian?)

Occurrence: World-wide.

Genus: Canoptum PESSAGNO, 1979

Range and occurrence: Same as for family.

Canoptum anulatum PESSAGNO and POISSON, n. sp.
(PI. IX, fig. 6-9; PI. X, fig. 1-9; PI. XV, fig. 2,4)

Description: Cephalis dome-shaped, lacking a horn. Subsequent chambers trapezoidal in outline, numerous; closely spaced except for final chambers. Post-abdominal chambers eleven to fifteen in number, separated by prominent circumferential ridges; ridges with short, discontinuous costae; approximately fifteen costae visible on a given ridge laterally. Short costae at right angles to circumferential ridges, forming linked-H pattern. Single small, circular pores occurring between two given costae and adjacent to ridge. Pores, ridges, and costae usually buried by microgranular outer layer of shell material except when specimen is excessively etched. Pores in area between ridges usually elliptical in shape, set in linearly arranged, rectangular pore frames; usually buried by outer layer of shell material. Final two post-abdominal chambers (segments) decreasing in width, increasing in height; pentultimate chamber often with tubular extension.

Remarks: *Canoptum anulatum*, n. sp., possesses circumferential ridges that are significantly different from those of the type species of *Canoptum*, *C. poissoni* Pessagno (1979). The linked-H circumferential ridge structure displayed by *C. anulatum* is shared by a number of yet undescribed forms from the Lower Jurassic. Forms with this sort of structure have not been observed below the Hettangian. *C. anulatum* is tentatively included in *Canoptum* in this report. However, it may be desirable in the future to include it under a new genus.

C. *anulatum* also differs from C. *poissoni* by having a slender, more elongate test with more closely spaced post-abdominal chambers (segments).

Anulatus-a-um (Latin, adj.): Beringed, ornamented with rings.

Measurements: Holotype: Length 310 microns, width 95 microns. Measurement of seven specimens: Maximum length 435 microns, minimum length 310 microns, maximum width 100 microns, minimum width 90 microns.

Type locality: Poisson 1662D. See Locality Descriptions.

Deposition of types: Holotype: USNM 264011, paratypes USNM 264012 and Pessagno Collection.

Range and occurrence: Lower Jurassic (Upper Sinemurian (?)-Lower Pliensbachian) of Turkey. Pliensbachian cherts in Franciscan Complex of California (NSF 960; see Locality Descriptions). Forms similar to C. *anulatum,* n. sp., have been observed in the Hettangian Graylock Formation of eastern Oregon. These forms differ from C. *anulatum* by having seventeen to twenty chambers (segments) and somewhat wider tests.

Canoptum poissoni PESSAGNO, 1979
(PI. XI, fig. 1-4)

Canoptum poissoni PESSAGNO, 1979
(PI. X, fig. 2-3)

Range and occurrence: Lower Jurassic (Poisson 1662D; Upper Sinemurian (?)) of Turkey.

Canoptum rugosum PESSAGNO and POISSON, n. sp.
(PI. XI, fig. 5-9; PI. XIII, fig. 3; PL XIV, fig. 1-2)

Description: Test as with genus. Cephalis hemispherical; post-cephalic chambers trapezoidal in outline increasing relatively rapidly in width and height as added. Circumferential ridges absent between cephalis and thorax and between abdomen and thorax; present between abdomen and first post-abdominal chamber and each of subsequent four or five post-abdominal chambers. Circumferential ridge when stripped of outer layer of microgranular shell material displaying linked-H pattern identical to that described for C. *anulatum,* n. sp. Post-abdominal chambers constricted medially, giving rise to lobulate test outline. Inner layer of post-abdominal chambers comprised of two rows of massive tetragonal pore frames between circumferential ridges. Outer microgranular layer on well preserved specimens with rugose surface; rugosities probably a reflection of massive of inner layer.

Remarks: *Canoptum rugosum,* n.sp., differs from C. *anulatum,* n.sp., (1) by having a shorter, broader test with one half to one third the nummer of post-abdominal chambers; (2) by having widely rather than closely spaced circumferential ridges; (3) by having post-abdominal chambers with a rugose surface; and so forth. Both species share the same linked-H circumferential ridge structure.

Rugosus-a-um (Latin, adj.): wrinkled.

Measurements: Holotype: Length 140 microns, width 75 microns. Measurement of eight specimens: Maximum length 165 microns, minimum length 140 microns, maximum width 95 microns, minimum width 65 microns.

Type locality: *Poisson* 1662D. See Locality Descriptions.

Deposition of types: Holotype: USNM 264013, paratypes: USNM 264014 and Pessagno Collection.

Range and occurrence: Lower Jurassic (Upper Sinemurian(?)-Lower Pliensbachian) of Turkey so far as known.

Family: SYRINGOCAPSIDAE FOREMAN, 1973

Type genus: Syringocapsa NEVIANI, 1900

Range and occurrence: Triassic to Cretaceous World-wide.

Genus: Katroma PESSAGNO and POISSON, new genus

Type species: *Katroma neagui* PESSAGNO and POISSON, n.sp.

Description: Test multicyrtid, comprised of cephalis, thorax, abdomen, and with type species one post-abdominal chamber. Post-abdominal chamber terminating in long, cylindrical, open, tubular extension. Cephalis hemispherical with horn; thorax and abdomen trapezoidal in outline. First post-abdominal chamber subspherical, considerably larger than previous chambers and with variable number of medially arranged circumferential spines.

Remarks: *Katroma* differs from *Podobursa* Wisniowski by haying an open tube on its final post-abdominal chamber.

The name *Katroma* is formed by an arbitrary combination of letters (ICZN, 1964, Appendix D, pt. IV, Recommendation 40, p. 113). Its gender is feminine.

Range and occurrence: Lower Jurassic (Upper Sinemurian(?)-Lower Pliensbachian) of Turkey. Lower Jurassic (Lower Pliensbachian) part of Maude Formation of the Queen Charlotte Islands (British Columbia). Lower Jurassic (Upper Pliensbachian), Nicely Formation of eastern Oregon.

Katroma neagui PESSAGNO and POISSON, n. sp.
(PI. XII, fig. 1-5; PI. XV, fig. 3)

Description: Test as with genus. Meshwork consisting of massive tetragonal to pentagonal pore frames (predominantly pentagonal); pores becoming larger on tubular extension of first post-abdominal chamber. Cephalis with crown-like horn with four branches; branching components of horn circular in axial section. Row of short spines (approximately 12 in number) occurring circumferentially around medial portion of post-abdominal chamber; spines circular in axial section. Length of tubular extension on first post-abdominal chamber more than half of total length of test.

Remarks: *Katroma neagui*, n. sp., differs from Late Jurassic and Early Cretaceous species of *Podobursa* (e.g., *P. berggreni* Pessagno) by having twelve rather than three circumferentially arranged spines around the medial portion of the final post-abdominal chamber and by having an open, tubular extension on its final post-abdominal chamber.

This species is named for Dr. Teodor Neagu, University of Bucharest (Romania) in honor of his contributions to Mesozoic stratigraphy and micropaleontology.

Measurements: Holotype: Width abdomen 70 microns, length cephalis-abdomen 110 microns, length first post-abdominal chamber 100 microns, width firts post-abdominal chamber 120 microns, length tube on post-abdominal chamber 310 microns. Measurement of eight specimens: Maximum width of abdomen 70 microns, minimum width of abdomen 50 microns, maximum length cephalis-abdomen 115 microns, minimum length cephalis-abdomen 65 microns, maximum width first post-abdominal chamber 120 microns, minimum length firts post-abdominal chamber 50 microns, maximum length tube on first post -abdominal chamber 310 microns, minimum length tube on first post-abdominal chamber 235 microns.

Type locality: Poisson 1662D. See Locality Descriptions.

Deposition of types: Holotype: USNM 264015, paratypes: USNM 264016 and Pessagno Collection.

Range and occurrence: Forms closely related to *K. neagui* occur in Pliensbachian cherts (NSF 960) from the Franciscan Complex of California; in the Nicely Formation (Upper Pliensbachian; OR 536) of eastern Oregon; and in the Maude Formation (Lower Pliensbachian; QC 534) of British Columbia (See Locality Descriptions). All of these forms share a branched, crown-like horn, but differ in the structure of their meshwork and in the shape of their tests.

CYRTOIDEA *incertae sedis*

The genus listed below cannot be assigned to a family yet.

Genus: Natoba PESSAGNO and POISSON, n. gen.

Type species: *Natoba minuta* PESSAGNO and POISSON, n. sp.

Description: Test tricyrtid comprised of microgranular silica; sparsely perforate. Cephalis with short, rod-like horn; thick-walled, separated from subspherical thorax by pronounced stricture. Abdomen tubular thin-walled; separated from thick-walled thorax by slight stricture. Large subcircular pores in stricture between cephalis and thorax; large slit-like pores in stricture between thorax and abdomen. Abdomen irregularly perforate proximally. Pores on all segments not set in discrete pore frames.

Remarks: *Natoba,* n. gen., is grossly similar to *Ectonocorys* Foreman (1968) from the Upper Cretaceous (Maestrichtian). It differs from this genus by being sparsely perforate, by lacking discrete pore frames, and by having a cylindrical, tubular abdomen. *Natoba* is a name formed by an arbitrary combination of letters (ICZN, 1964, p. 113, Appendix D, pt. 10, Recommendation 40).

Range and occurrence: Lower Jurassic (Upper Sinemurian(?)-Lower Pliensbachian) of Turkey so far as known.

Natoba minuta PESSAGNO and POISSON, n. sp.
(PI. XII, fig. 6-10? PI. XIV, fig. 3-4; PI. XV, fig. 1)

Description: Test as with genus. Abdomen on well preserved specimens comprising half of test length. Pores in stricture between cephalis and thorax, large and circular about eight in number. Pores in stricture between thorax and abdomen, large slit-like, elongate parallel to axis of test growth. Pores on proximal part of abdomen medium sized, irregular in shape and distribution. Weakly developed coste on thorax of well preserved specimens.

Remarks: *Natoba minuta,* n. sp., differs from *Ectonocorys scolia* Foreman (1968, PI. V, figs. 8a-c) by the characteristics cited under the genus and by having a less pronounced stricture between the thorax and abdomen.

Minutus-a-um (Latin, adj.): minute, small.

Measurements: Holotype: Length cephalis 25 microns, width cephalis 30 microns, length thorax 70 microns, width thorax 60 microns, length abdomen 50 microns, width abdomen 60 microns. Measurement of nine specimens: Maximum length cephalis 30 microns, minimum length cephalis 20 microns, maximum width cephalis 30 microns, minimum width cephalis 25 microns, maximum length thorax 70 microns, minimum length cephalis 45 microns, maximum width thorax 70 microns, minimum width thorax 60 microns, maximum length abdomen 80 microns, minimum length abdomen" 50 microns, maximum width'abdomen 70 microns, minimum width abdomen 50 microns.

Type locality: Poisson 1662D. See Locality Descriptions.

Deposition of types: Holotype: USNM 264017, paratypes USNM 264018 and Pessagno Collection.

Range and occurrence: This species is presently known only from the Lower Jurassic (Upper Sinemurian(?)-Lower Pliensbachian) of Turkey.

LOCALITY DESCRIPTIONS

TURKEY

Poisson sample 1662D. — Domuz Dağ Massif, N of Korkuteli, vilayet (Department) of Antalya, Turkey. Gümüşlü unit, Söğütlü dere formation, outcroping in the Söğütlü gorge situated 1 km NW of Gümüşlü village at an altitude of 1400 m (Fig. 1).

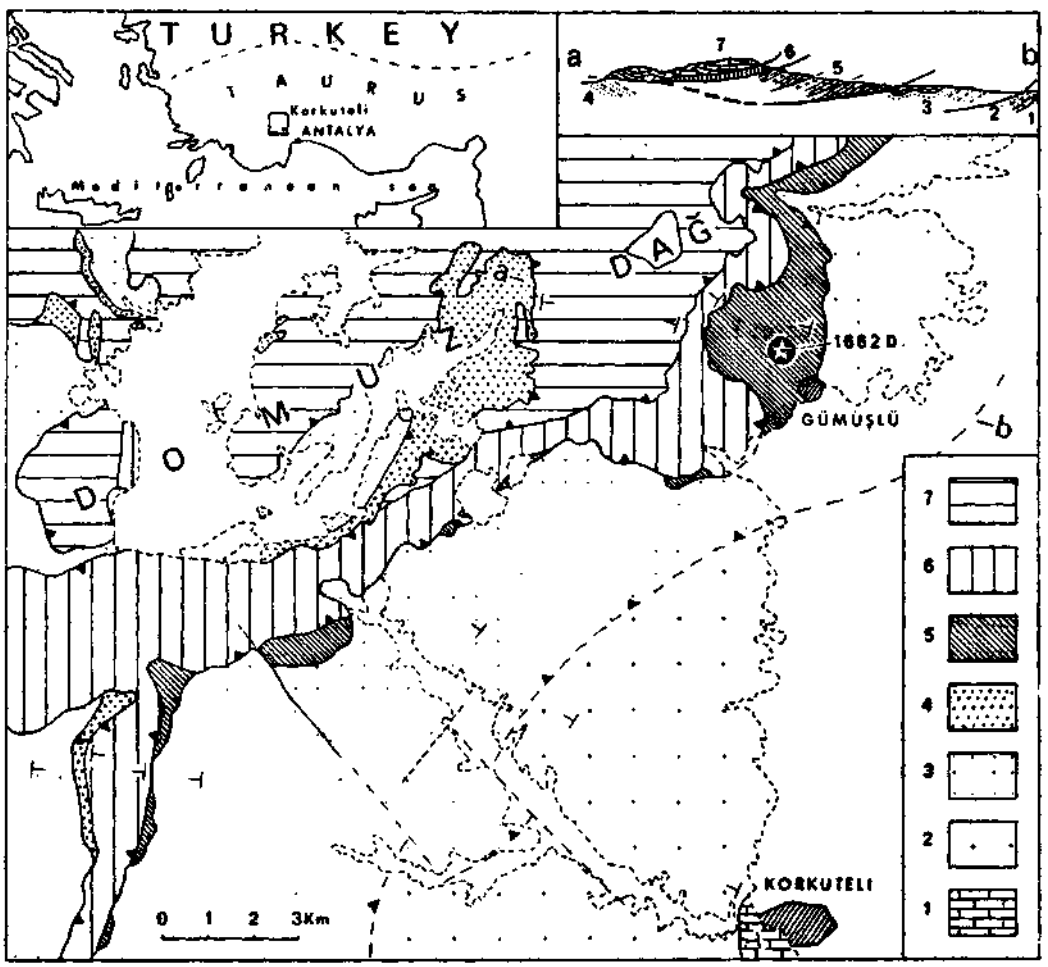

Fig. 1 - Domuz Dağ massif - Location map of the Gümüşlü unit.
Autochtonous (Bey Dağları massif); 1 - Mesozoic neritic limestones; 2 - Miocene flysch.
Allochtonous (Domuz dağ massif); 3 - Yavuz unit (mainly Paleogene flysch); 4 - Yeleme unit (wild flysch and olistostrome of Upper Cretaceous to Paleogene); 5 - Gümüşlü unit; 6 - Gülbahar unit (dolomite and cherty limestones of Upper Triassic age, and pelagic limestones of Upper Jurassic to Senonien, and ophiolitic detritals of Maestrichtian age.

Description of the Söğütlü dereformation

Limits: the base of the formation is limited by a tectonic contact (important thrusting). The formation is overlain by a bioclastic and oolithic member of the Sinekli dere Formation (Dogger-Malm).

Subdivisions and facies: The Söğütlü dere Formation include two members:

Upper member: the Ayıburnu tepe limestones: These are red and yellow «ammonitico rosso» facies rich in ammonites and microscopically rich in «filaments» (thin-valved molluscs) and Protoglobigerina. These limestones represent condensed stratigraphic sequences whose five ammonite zones are reduced to several meters thickness: Margaritatus zone (Middle Domerian), Bifrons, Bayani, and Meneghini zones (Toarcian) and Opalinum (Aalenian) zone. They thin from 20 m in the N to 1 m some 25 km to the S.

Lower member: The Radiolaria limestones: These are an alternance of 10-20 cm thick limestones beds and 1-10 cm thick marls, these latter being dark coloured and containing a quartz and feldspath silt fraction plus carbonaceous plant debris. These limestones are well stratified, regular beds exhibiting light beige weathering colours and grey fresh surfaces. Certain of these beds include a basal layer of vertically graded, neritic calcareous elements (algal tufts and molluscan debris), with turbiditic characteristics. The mudstone texture of these limestones beds includes numerous, well preserved siliceous Radiolaria and fine carbonaceous debris.

The depositional environment of the Söğütlü dere Formation seems to have been that of a basin located near the edge of a carbonate platform.

NORTH AMERICA

California

NSF 960. — San Rafael Mountain area, Santa Barbara County. Red radiolarian cherts overlying pillowed greenstone; normal sedimentary contact. Greenstone with minor recrystallized interpillow limestone. Franciscan Complex. USGS Figueroa Mountain Quadrangle (7.5'): T7N; R29W; section 9; 1.32 miles (2.1 kilometers) west of Cachuma Camp (section 11), adjacent to Happy Canyon Road.

BK 605 — Red radiolarian chert mass in melange. Franciscan Complex. USGS Potter Valley Quadrangle'(7.5'): T16N;R11W; section 8 (Northeast corner) along Potter Valley Road; 0.18 miles (0.3 kilometers) southwest of junction Guntley Ranch Road with Potter Valley Road and California Route 20. Sample from Dr. James Berkland, University of California, Davis.

Eastern Oregon

OR 536— Nicely Formation. Silty, dark gray to reddish brown mudstones and shales containing abundant limestone nodules ranging in size from two inches to three feet. Nodules comprised of dark gray to black calcilutite containing abundant calcified and pyritized Radiolaria. Headwaters of Elkhorn Creek; northeast side of Morgan Mountain. USGS Izee Quadrangle (15'); SW 1/4 of section 12.

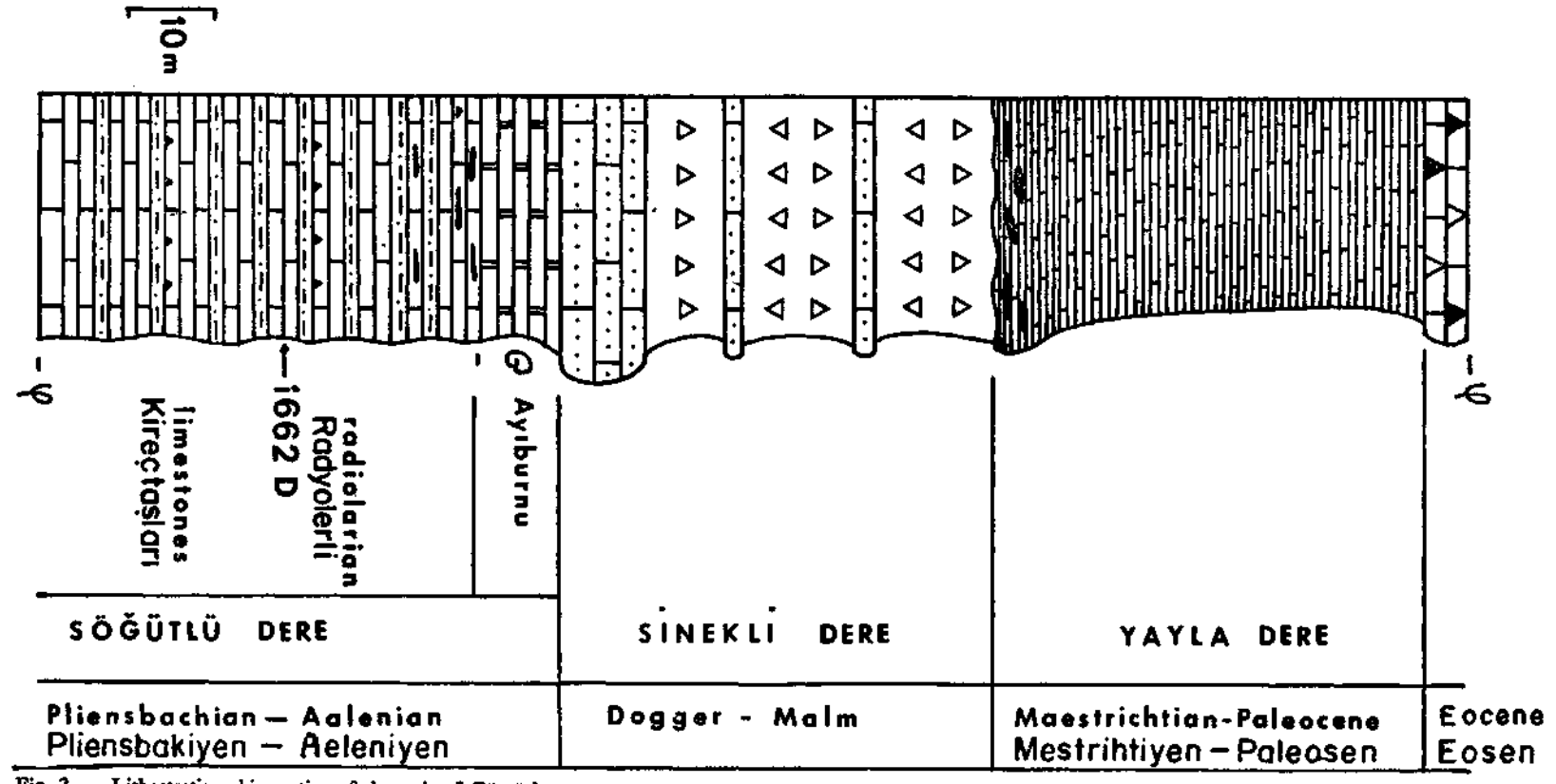

Fig. 2 - Lithostratigraphic section of the unit of Gümüşlü.
Söğütlü dere formation; radiolarian limestones member (Pliensbachian; Ayıburnu member (Pliensbachian; to Aalenian) ammonitico rosso limestones with Ammonites fauna.
Sinekli dere formation; neritic limestones with oolithes (intrabio-oosparites) and *Protopeneroplis striata* Weynschenk (Dogger-Malm); pillow lavas interbeded with oolithic limestones.
Yayla dere formation (Maestrichtian to Paleocene; pelagic limestones with Globotruncaniidae and Heterohelicidae in the lower beds, and Globorotalidae in the upper beds; Brechic limestones (Lower Eocene).

Queen Charlotte Islands, British Columbia

Kunga Island

Type section of the Kunga Formation. See Brown (1968).

QC 550. — Kunga Formation, Black Argillite member (upper part). Flaggy black argillite containing limestone nodules comprised of black calcilutite with abundant silicified Radiolaria. North shore of Kunga Island.

Maude Island

Type section of Maude Formation. See Brown (1968).

QC 509-537. — Maude Formation. Dark gray, medium gray and greenish gray mudstones, shales, siltstones, calcilutites, and sandstones with common limestone nodules (black calcilutite). South shore of Maude Island.

QC 532. — Dark gray calcilutite layer 8 to 10 inches (20 to 25 cm's.) thick containing abundant silicified Radiolaria. About 35 feet (10.6 meters) below contact with overlying Yakoun Formation.

QC 534. — Dark gray calcilutite layer 10 inches (25 cms.) thick containing abundant silicified Radiolaria. About 27 feet (8.2 meters) below contact with Yakoun Formation.

QC 537. — Dark gray calcilutite layer, 6 inches (15 cms) thick containing abundant silicified Radiolaria; 3 feet (0.91 meters) below contact with the Yakoun Formation.

ACKNOWLEDGEMENTS

Pessagno's investigations were supported in part by grants from the National Science Foundation, (DES 72-01528-A01 and EAR 76-22029), the Atlantic-Richfield Company, and from the Exxon Production Research Company. The writers wish to thank Mr. W. T. Rothwell for his care in taking the scanning electron micrographs and in preparing the plates. Mr. Charles Blome and Mrs. Phyllis Tippit are thanked for their help in printing the photographs for the plates.

Field investigations in Turkey (Poisson) were supported in part by the Mineral Research and Exploration Institute of Turkey (M.T.A., Ankara), and by the Centre National de la Recherche Scientifique (C.N.R.S., Paris-Equipe de Recherche Associee Asie alpine occidentale).

Manuscript received May 20, 1980

REFERENCES CITED

Brown, A. S., 1968, Geology of the Queen Charlotte Islands, British Columbia: Department of Mines and Petrol. Resources.

De Wever, P.; Sanfilippo, A.; Riedel, W.R., and Gruber, B., 1979, Triassic radiolarians from Greece, Sicily, and Turkey: Micropaleontology, 24 pis. 1-7 (in press).

Dumitrica, P., 1970, Cryptocephalic and cryptothoracic Nassellaria in some Mesozoic deposits in Romania: Revue Roumaine de Geologie, Geophysique et Geographie, Serie de Geologie, 14, 1, 45-124, pls. 1-21.

———, 1978, Family Eptingiidae, n. fam., extinct Nassellaria (Radiolaria) with sagital ring: Dari de seama ale sedintelor Institului de Geologie si Geofizica (D.S. Inst. Geol. Geofiz.), LXlV, pt. 3 (in press).

Ehrenberg, C. G., 1847, Ubet eine halibiolithische, von Herrn R.Schomburgk entdecke, vorherrschend aus mikroskopischen polycystinen gebildete, Gerbirgemasse von Barbados: Monatber. Kgl. Preuss. Akad. Wiss. Berlin, 382-385.

———, 1875, Fortsetzung der microgelogische Studien als Gesammt-Uebersicht Gebirgsarten der Erde, mit specieller Rucksicht auf den Polycystinen-Mergel von Barbados: Abh. Kgl. Akad. Wiss. Berlin, 1-226, pls. 1-30.

Foreman, H. P., 1968, Upper Maestrichtian Radiolaria of California: Special Papers in Paleontology, 3, i-v, 1-82, pls. 1-98.

———, 1973, Radiolaria from DSDP Leg 20: I*n* Hezeen, *et al*., Initial reports of the Deep Sea Drilling Project, 20, 249-305, pis. 1-16.

———, 1975, Radiolaria from the North Pacific, Deep Sea Drilling Project, Leg. 32. in Larson, R. L., *et al*., Initial reports of the Deep Sea Drilling Project, vol .32 covering Leg 32 of the cruises of the Drilling Vessel Glomar Challenger, 579-676, pls. 1A-F; 2A-2L, 3-9.

Frebold, H., 1970, Pliensbachian Ammonoids from British Columbia and southern Yukon: Canadian Journal of Earth Sciences, 7, 435-456.

Haeckel, E., 1862, Die Radiolarien (Rzhizopoda Radiolaria): Ein Monographie (Reimer, Berlin), 1-572, pls. 1-35.

———1881, Entwwrf eines radiolarien-Systems auf grund von studien der Challenger-Radiolarien: Jena. A. Med. Naturwiss, 15, n. ser. 8 (3), 418-472.

—— 1887, Report on the Radiolaria collected by the H.M.S. Challenger during the years 1873-1876: **Rept** Voyage Challenger, ZooL, 18, p. i-cxxxvii, 1-1893, pls. 1-140, 1 map.

Imlay, R. W., 1968, Lower Jurassic (Pliensbachian and Toarcian) Ammonites from eastern Oregon and California: U.S. Geological Survey Professional Paper 593-C, C1-C51, pls. 1-9.

International Code of Zoological Nomenclature (Adopted by the 15th Internal. Congress of Zoology), 1964,1-176.

Irwin, W. P.; Jones, D. L. and Pessagno, E.A., Jr., 1977, Significance of Mesozoic radiolarians from the pre-Nevadan rocks of the southern Klamath Mountains, California: Geology, 5, 557-562.

Jones, D.L.; Silverling, N. J. and Hillhouse, J., 1977, Wrangellia-A displaced terrane in northwestern North America: Canadian Journal of Earth Sciences, 14, 11, 2565-2577.

Kozur H. and Mostler, H., 1972, Beitrage zur enforaschung der Mesozoischen Radiolarien. Teil I: Revision der Oberfamilie Coccodiscacea Haeckel, 1862, emend, und Beschreibung iher Triassichen Vertreter: Geol. Palaont. Mitt. Insbruck, 2, 1-60, pls. 1-4.

Mclaughlin, R. J. and Pessagno, E. A., Jr., 1978, Significance of age relations above and below Upper Jurassic ophiolite in the Geysers-Clear Lake Region, California. Jour. Research: U.S. Geol. Survey, 6, 6, 715-726.

Neviani, A., 1900, Supplemento alla fauna a Radiolari delle rocce Mesozoiche del Bolognese: Soc. Geol. Ital., Boll., 19, 645-670.

Pessagno, E. A., Jr., 1971, Jurassic and Cretaceous Hagiastridae from the Blake-Bahama Basin (Site 5A, JOIDES Leg. I) and the Great Valley Sequence, California Coast Ranges: Bulls. Amer. Paleon., 60, 264, 1-80, pls. 1-19, text-figs. 1-5.

T.C.
MADEN TETKİK VE ARAMA ENSTİTÜSÜ
GENEL DİREKTÖRLÜĞÜ

Ankara - Turkey

4445

Our Ref. : BDY./9.Neş/20-159/M2/5 135

Your Ref : December 10,14,1981

16 Subat 1982

UNIVERSITY OF HOUSTON LIBRARY
CENTRAL CAMPUS
Central Serials Records
4800 Calhoun Road
Houston,TEXAS 77004

Dear Sirs :

We were pleased to learn from your letter of December 10 and December 14 1981 that you would like to purchase

Bulletin of the Mineral Research and Exploration Institute of Turkey

We enclose herewith our pro-forma invoice covering the cost and postage expenses of the above publication, which we shall send you upon settlement of the invoice.

Very truly yours,

MADEN TETKİK VE ARAMA ENSTİTÜSÜ
Genel Direktörlüğü

Enc : 1 invoice

Özcan YAZLAK
Bilimsel Dökümantasyon ve Yayın
Dairesi Başkanı

FS/fs

V: 106347-2296

T. C.
MADEN TETKİK VE ARAMA ENSTİTÜSU
GENEL DİREKTÖRLÜĞÜ
Ankara - Turkey

15.2.1982

Invoice No. :

INVOICE

UNİVERSİTY OF HOUSTON LIBRARY
CENTRAL CAMPUS,Central Seriels Records
4800 Calhoun Road,Houston,TEXAS 77004.

DESCRIPTION	Qty.	Unit Price TL.	Total TL.
M.T.A.Bulletin Series No:93/94	2	400.--	400.--
Postage and other expenses			250.--
(ONLY SİXHUNDRED AND FİFTHY TURKISH LIRAS)			650.--
Equivalent $ 5.-			
1$ = 130 Turkish liras			

Note: We should like it to be remmited to our current account No:18 with the Ankara Branch of the Central Bank of Turkey,ANKARA

We have been publishing the Bulletins nowadays. After completing the publication the issues will be sent to your address.

P L A T E S

PLATE - I

All figures are scanning electron micrographs of Lower Jurassic Radiolaria. Figures 1,3-10 illustrate Radiolaria from the Lower Jurassic of Turkey (Poisson Sample 1662D; see Locality Descriptions). Figure 2 illustrates a specimen from a Lower Jurassic Franciscan radiolarian chert (NSF 960; see Locality Descriptions).

Fig. 1,4 - *Hagiastrum infinitum* Pessagno and Poisson, n. sp.
Holotype (USNM 263993). Scales: 132 microns and 66 microns respectively.

Fig. 2 - *Hagiastrum infinitum* Pessagno and Poisson, n. sp.
Scale: 100 microns.

Fig. 3,6 - *Hagiastrum infinitum* Pessagno and Poisson, n. sp.

Fig. 8 - Paratype (USNM 263994). Scales: 130, 80, and 40 microns respectively.

Fig. 5,7 - *Orbiculiforma multifora* Pessagno and Poisson, n. sp.

Fig. 9,10 - Holotype (USNM 263995). Scales: 100, 100, 50, and 40 microns respectively.

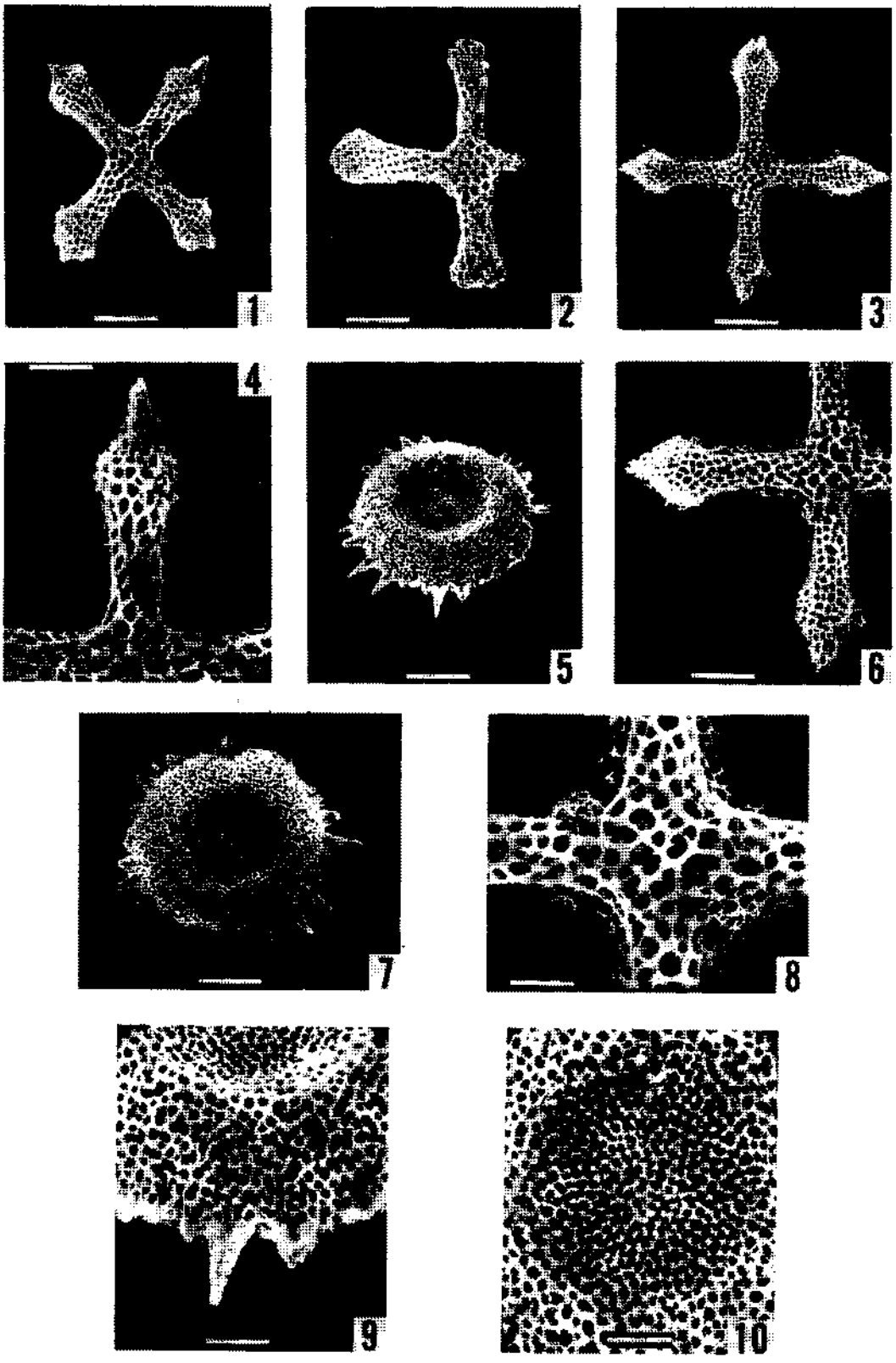
1
2
3
4
5
6
7
8
9
10

PLATE - II

All figures are scanning electron micrographs of Radiolaria from the Lower Jurassic of Turkey (Poisson Sample 1662D; see Locality Descriptions).

Fig. 1,2 - *Protopsium ehrenbergi* Pessagno and Poisson, n. sp.

Paratypes (USNM 263998). Scales: 66 microns each.

Fig. 3 - *Protopsium ehrenbergi* Pessagno and Poisson, n. sp.

Holotype (USNM 263997). Scale: 66 microns.

Fig. 4,5 - *Protopsium ispartaense* Pessagno and Poisson, n. sp.

Holotype (USNM,263999). Scales: 44 and 20 microns respectively.

Fig. 6 - *Crucella* sp. A

Scale: 80 microns.

Fig. 7-9 - *Orbiculiforma* sp. aff. *O. mclaughlini* Pessagno

Scales: 50, 100, and 100 microns respectively.

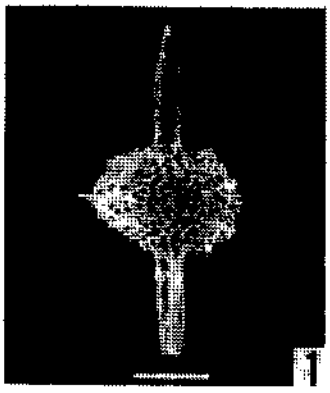
1

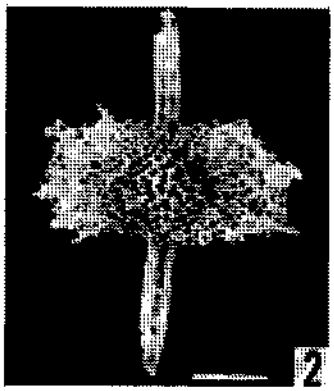
2

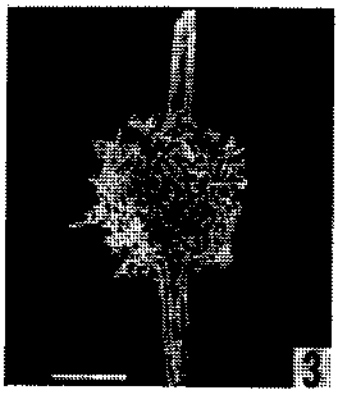
3

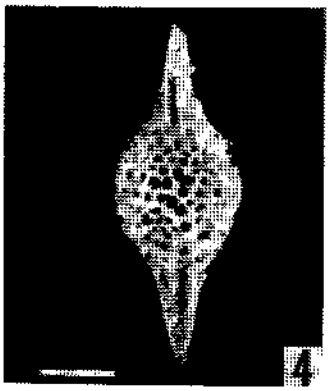
4

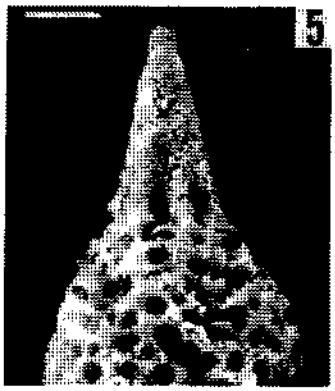
5

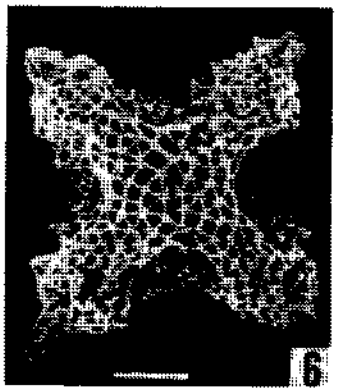
6

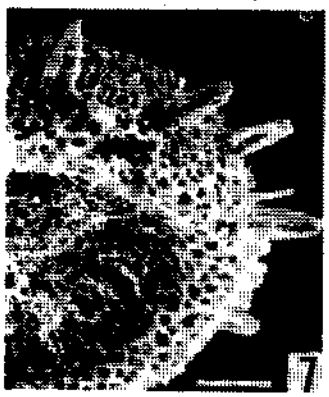
7

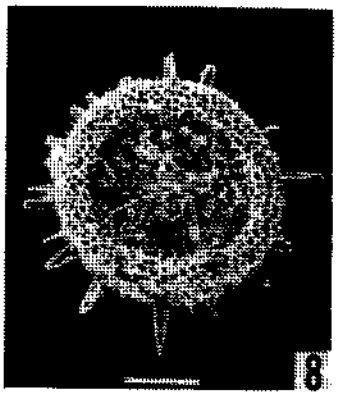
8

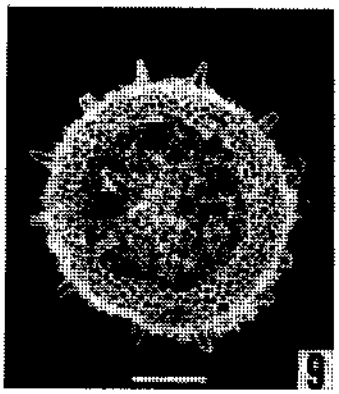
9

PLATE - III

All figures are scanning electron micrographs of the Lower Jurassic Radiolaria from Turkey (Poisson Sample 1662D; see Locality Descriptions).

Fig. 1-6 - *Protopsium ispartaense* Pessagno and Poisson, n. sp.

Fig. 8,9 - Paratypes (USNM 264000). Scales in figures 1-3: 50, 44, and 44 microns respectively. Scales in figures 4-6: 20, 40, and 2,0 microns respectively. Scales in figures 8 and 9: 20 microns each.

Fig. 7 - *Protopsium* (?) *ispartaense* Pessagno and Poisson, n. sp.

Holotype (USNM 263999). Scale: 20 microns. See plate II, fig. 4, 5.

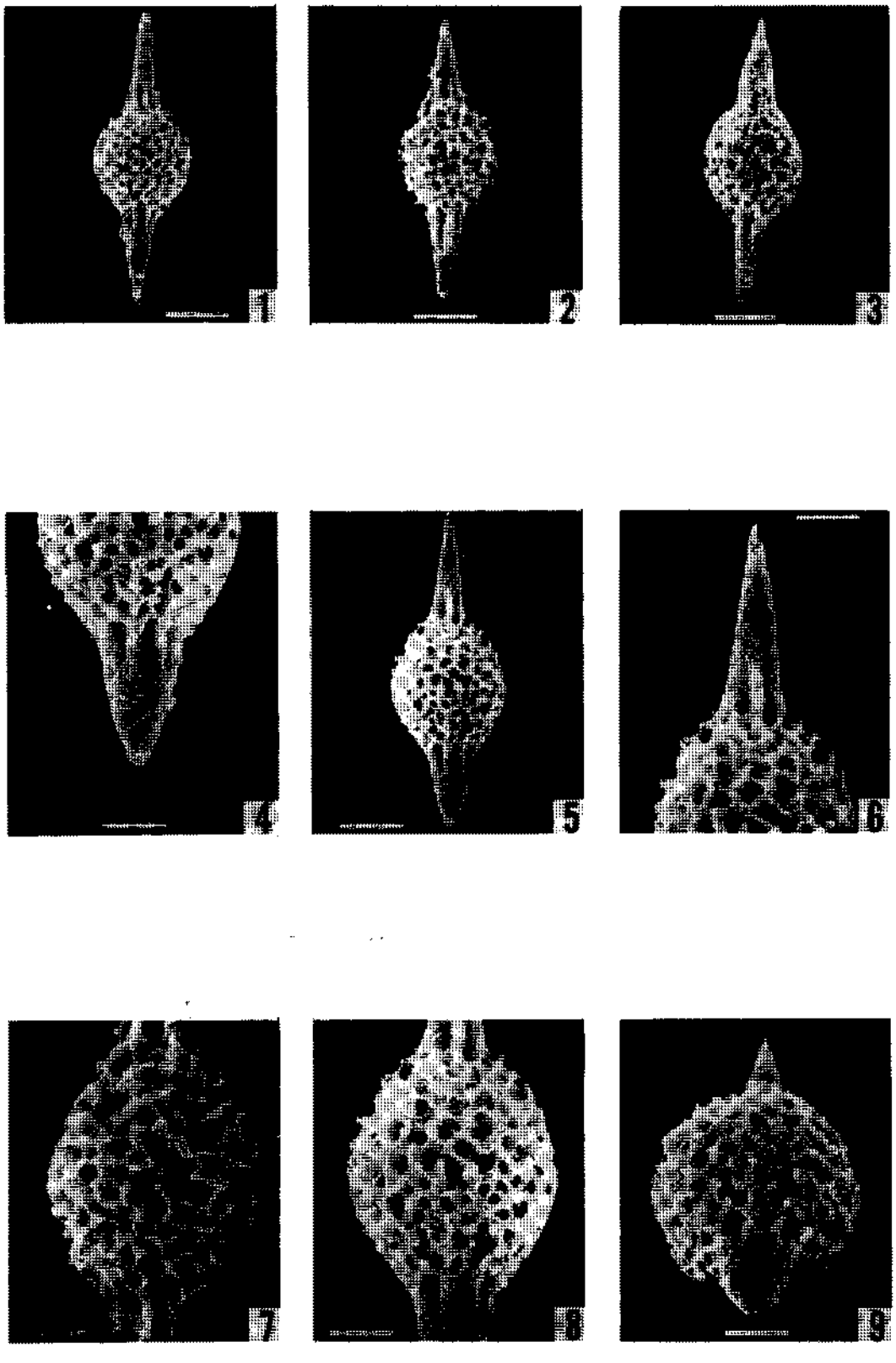

PLATE - IV

All figures are scanning electron micrographs of Radiolaria from the Lower Jurassic of Turkey (Poisson Sample 1662D; see Locality Descriptions).

Fig. 1,4 - *Protopsium* sp. A

Scales: 66 and 32 microns respectively.

Fig. 2 - *Protopsium* sp. B

Scale: 44 microns.

Fig. 3,5-8 - *Protopsium* sp. C

Scale in figure 3: 80 microns. Scales in figures 5-8: 40 microns each.

Fig. 9 - *Pseudoheliodiscus yaoi* Pessagno and Poisson, n. sp.

Holotype (USNM 264001). Scale : 220 microns.

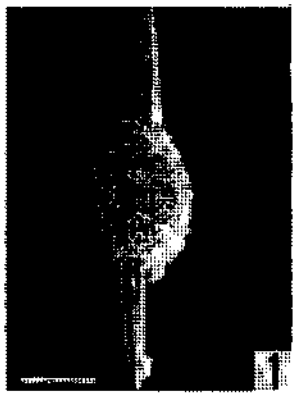
1

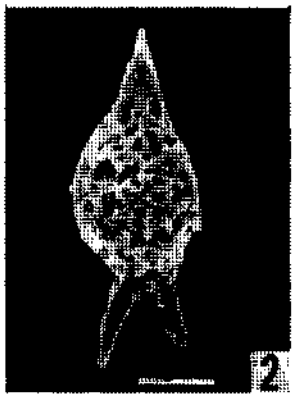
2

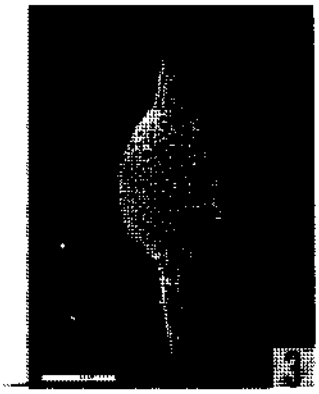
3

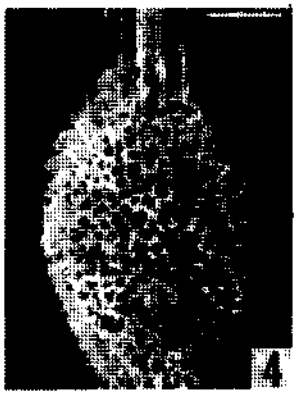
4

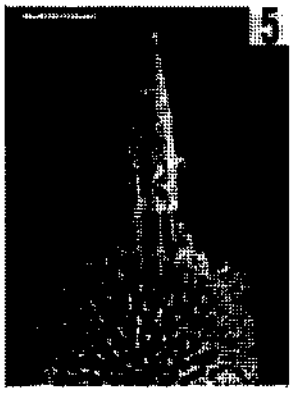
5

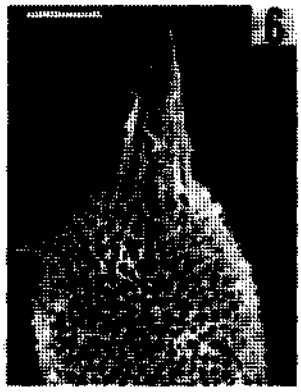
6

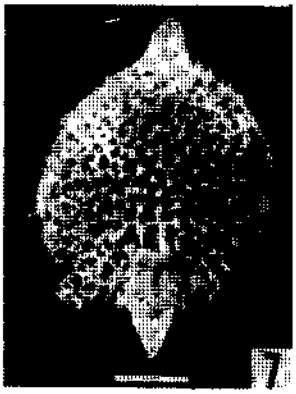
7

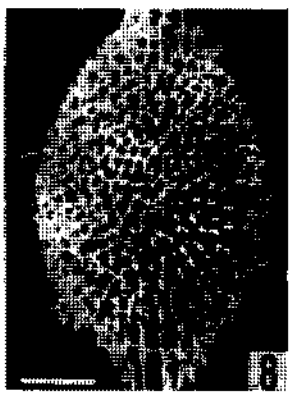
8

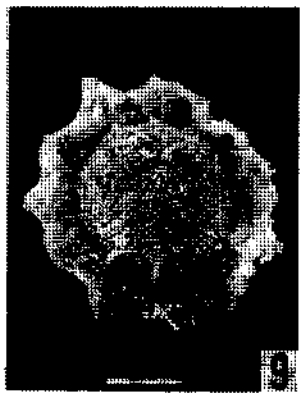
9

PLATE - V

All figures are scanning electron micrographs of Radiolaria from the Lower Jurassic of Turkey (Poisson Sample 1662D; see Locality Descriptions).

Fig. 1,8 - *Pseudoheliodiscus yaoi* Pessagno and Poisson, n. sp.

Fig. 9 - Paratypes (USNM 264002). Figures 1,8: Same specimen; scales: 80 and 32 microns. Scale in figure 9: 32 microns.

Fig. 2,3 - *Pseudoheliodiscus* sp. A

Scales: 80 and 50 microns respectively.

Fig. 4 - *Pseudoheliodiscus yaoi* Pessagno and Poisson, n. sp.

Topotype. Scale: 66 microns.

Fig. 5,6 - *Pseudoheliodiscus* sp. B

Scales: 66 and 36 microns respectively.

Fig. 7 - *Pseudoheliodiscus yaoi* Pessagno and Poisson, n. sp.

Holotype (USNM 264001). Scale: 40 microns. See plate IV, fig. 9.

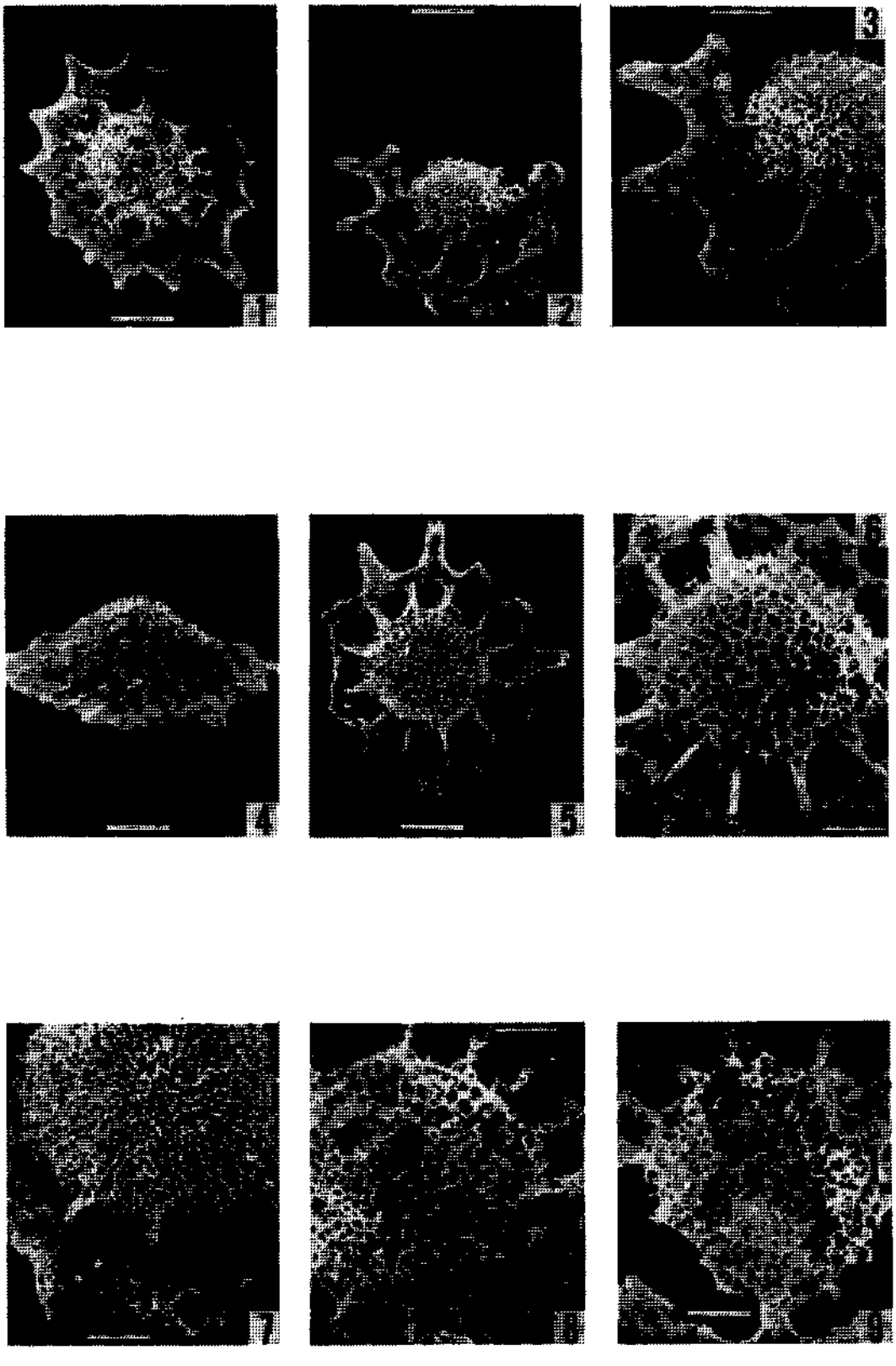

PLATE - VI

AH figures are scanning electron micrographs of Radiolaria from the Lower Jurassic of Turkey (Poisson Sample 1662D; see Locality Descriptions).

Fig. 1-4 - *Pantanellium inornatum* Pessagno and Poisson, n. sp.

Holotype (USNM 264003). Scale in figure 1: 56 microns. Scales in figures 2-4: 28 microns each.

Fig. 5-7 - *Pantanellium inornatum* Pessagno and Poisson, n. sp.

Paratype (USNM 264004). Scales: 56,32 and 32 microns respectively.

Fig. 8-9 - *Pantanellium inornatum* Pessagno and Poisson, n. sp.

Paratype (USNM 264004). Scales: 44 and 20 microns respectively.

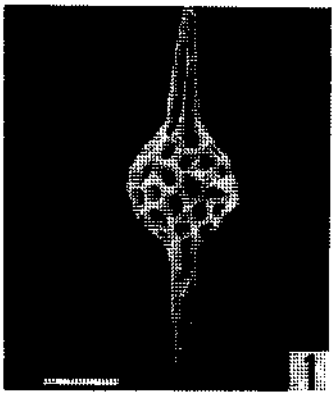
1

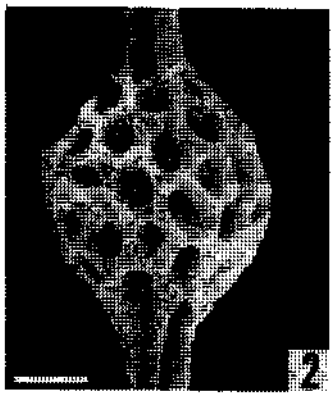
2

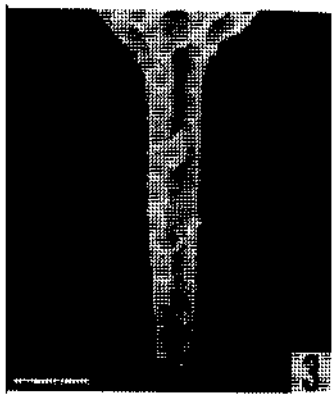
3

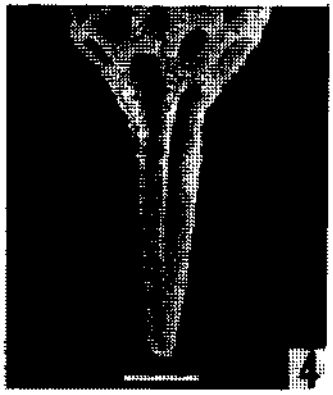
4

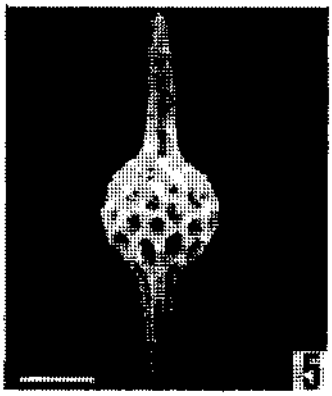
5

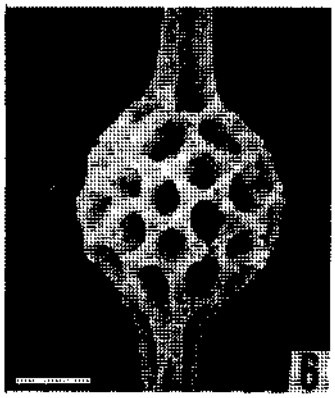
6

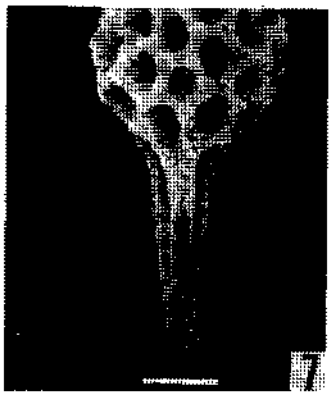
7

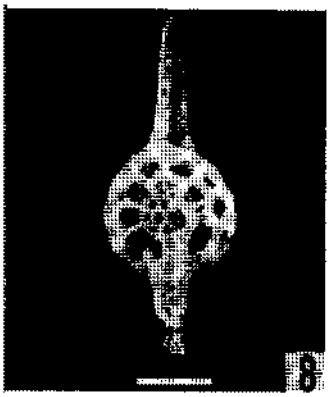
8

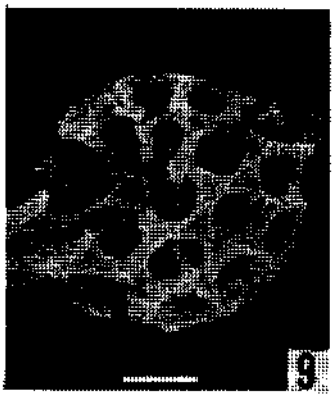
9

PLATE - VII

All figures are scanning electron micrographs of Radiolaria from the Jurassic of North America.

Fig. 1 - *Panlanellium* sp.

QC 550. Black argillite member of the Kunga Formation, Queen Charlotte Islands, British Columbia (Sinemurian). This form appears to be closely related to *P. inornatum*, n. sp.

Scale: 56 microns.

Fig. 2-3 - *Praeconocaryomma immodica* Pessagno and Poisson, n.sp.

Holotype (USNM 264005). BK 605. Franciscan Complex, California Coast Ranges; Upper Jurassic (Zone 1) radiolarian chert.

Scales: 50 and 40 microns respectively.

Fig. 4-6 - *Praeconocaryomma immodica* Pessagno and Poisson, n. sp.

Paratype (USNM 264006). BK 605. Franciscan Complex, California Coast Ranges.

Fig. 7 - *Praeconocaryomma immodica* Pessagno and Poisson, n. sp.

Paratype (USNM 264006). BK 605. Franciscan Complex, California Coast Ranges; Upper Jurassic (Zone 1) radiolarian chert. Scale : 50 microns.

Fig. 8-9 - *Praeconocaryomma immodica* Pessagno and Poisson, n. sp.

NSF 973. Early Tithonian cherts, limestones, siliceous mudstones, and minor tuff breccias overlying Stanley Mountain Ophiolite, California Coast Ranges (See Pessagno, 1977a). Sample from lenticular mass of gray, radiolarian-rich calcilutite. Scales: 26 and 40 microns respectively.

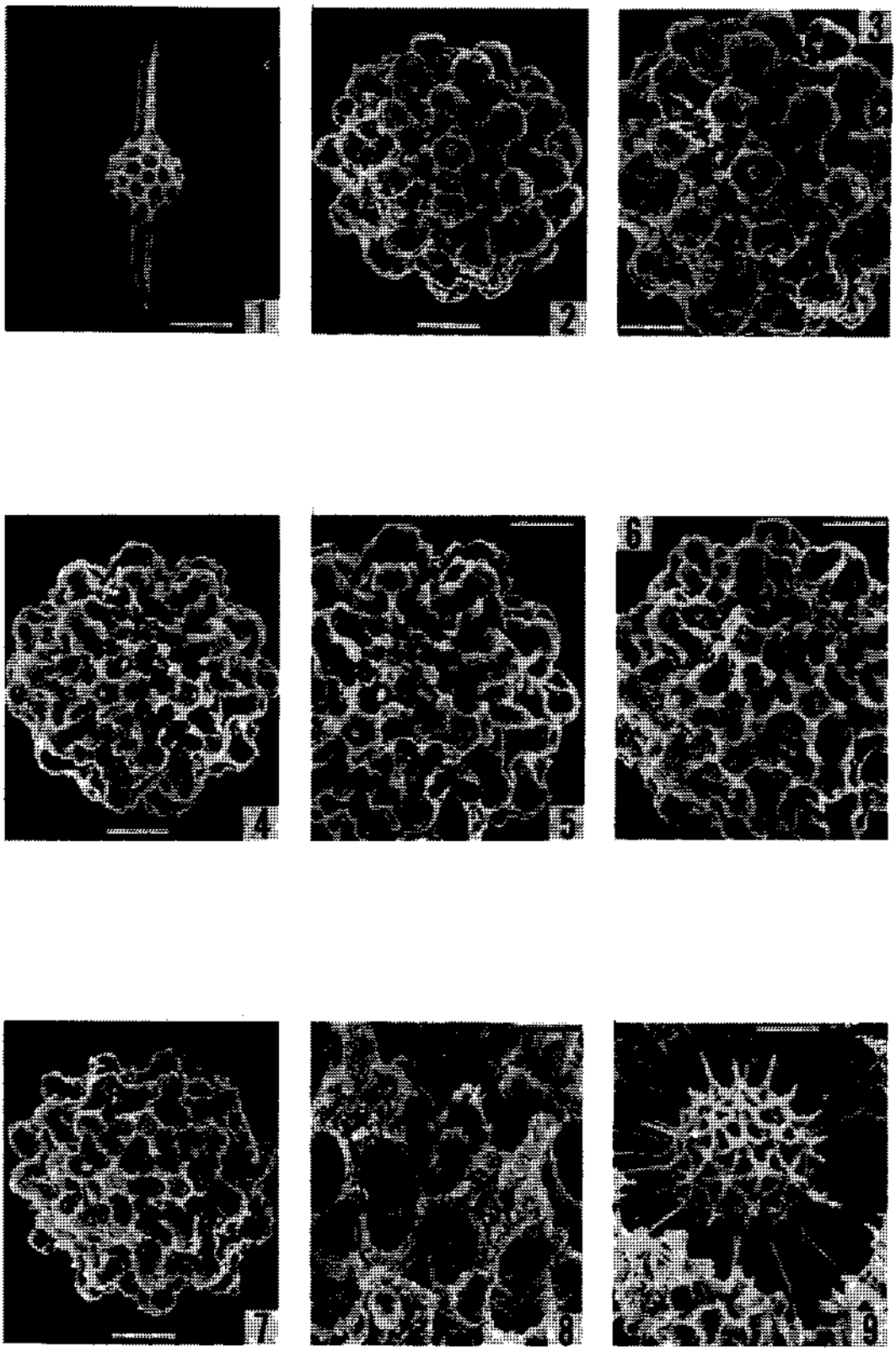
1
2
3
4
5
6
7
8
9

PLATE - VIII

All figures are scanning electron micrographs of Lower Jurassic Radiolaria. Specimens in figures 1-4 are from NSF 960, Franciscan Complex, California Coast Ranges. Specimens in figures 5-9 are from the Lower Jurassic of Turkey (Poisson Sample 1662D). See Locality Descriptions.

Fig. 1-3 - *Praeconocaryomma media* Pessagno and Poisson, n. sp.

Holotype (USNM 264007). Scales: 56, 40, and 32 microns respectively.

Fig. 4 - *Praeconocaryomma media* Pessagno and Poisson, n. sp.

Paratype (USNM 26/W08). Scale: 56 microns.

Fig. 5-7 - *Praeconocaryomma parvimamma* Pessagno and Poisson, n. sp.

Holotype (USNM 264009). Scales: 66, 66, and 32 microns respectively.

Fig. 8-9 - *Praeconocaryomma parvimamma* Pessagno and Poisson, n. sp.

Paratypes (USNM 264010). Figure 9 showing internal structure; triangular pore frames of first medullary shell barely visible. Scales: 66 and 56 microns recpectively.

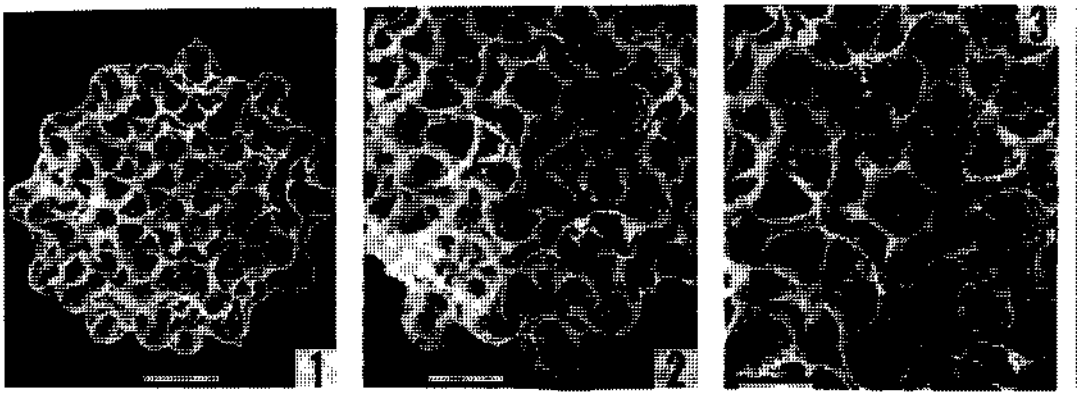
1
2
3

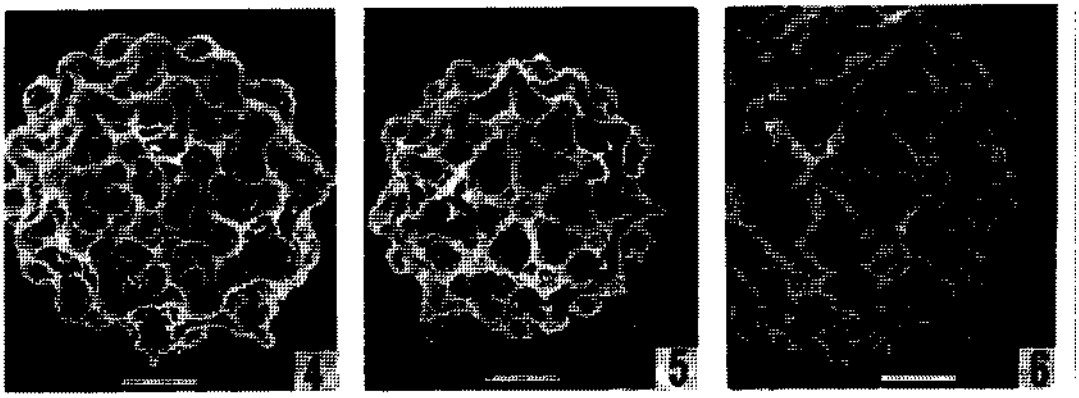
4
5
6

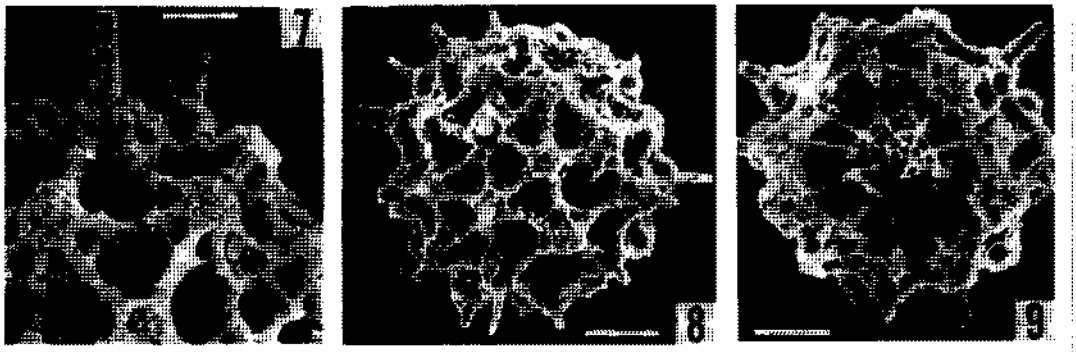
7
8
9

PLATE - IX

All figures are scanning electron micrographs of Lower Jurassic Radiolaria. Specimens in figures 1, 3-5 are from Franciscan cherts (NSF 960), California Coast Ranges. Specimens in figures 2,6-9 are from the Lower Jurassic of Turkey (Poisson Sample 1662D). See Locality Descriptions.

Fig. 1 - *Praeconocaryomma* sp. aff. *P. parvimamma* Pessagno and Poisson, n. sp. This form differs from *P. parvimamma,* n. sp., by having broader, flatter mammae. Scale: 66 microns.

Fig. 2 - *Praeconocaryomma parvimamma* Pessagno and Poisson, n. sp.

Paratype (USNM 264010). Internal structure. Same specimen as figured in plate VIII, fig. 9, but at higher magnification. Scale: 40 microns.

Fig. 3-5 - *Praeconocaryomma* s,p. aff. *P. magnimma* (Rüst)

This may well be the same form figured by Rüst (1898). However, Rust's illustrations are far too generalized to permit certain correlation. Scales: 66, 40, and 40 microns respectively.

Fig. 6-9 - *Canoptum anulatum* Pessagno and Poisson, n. sp.

Holotype (USNM 264011). Scale in figure 6: 100 microns; scales in figures 7-9: 40 microns each.

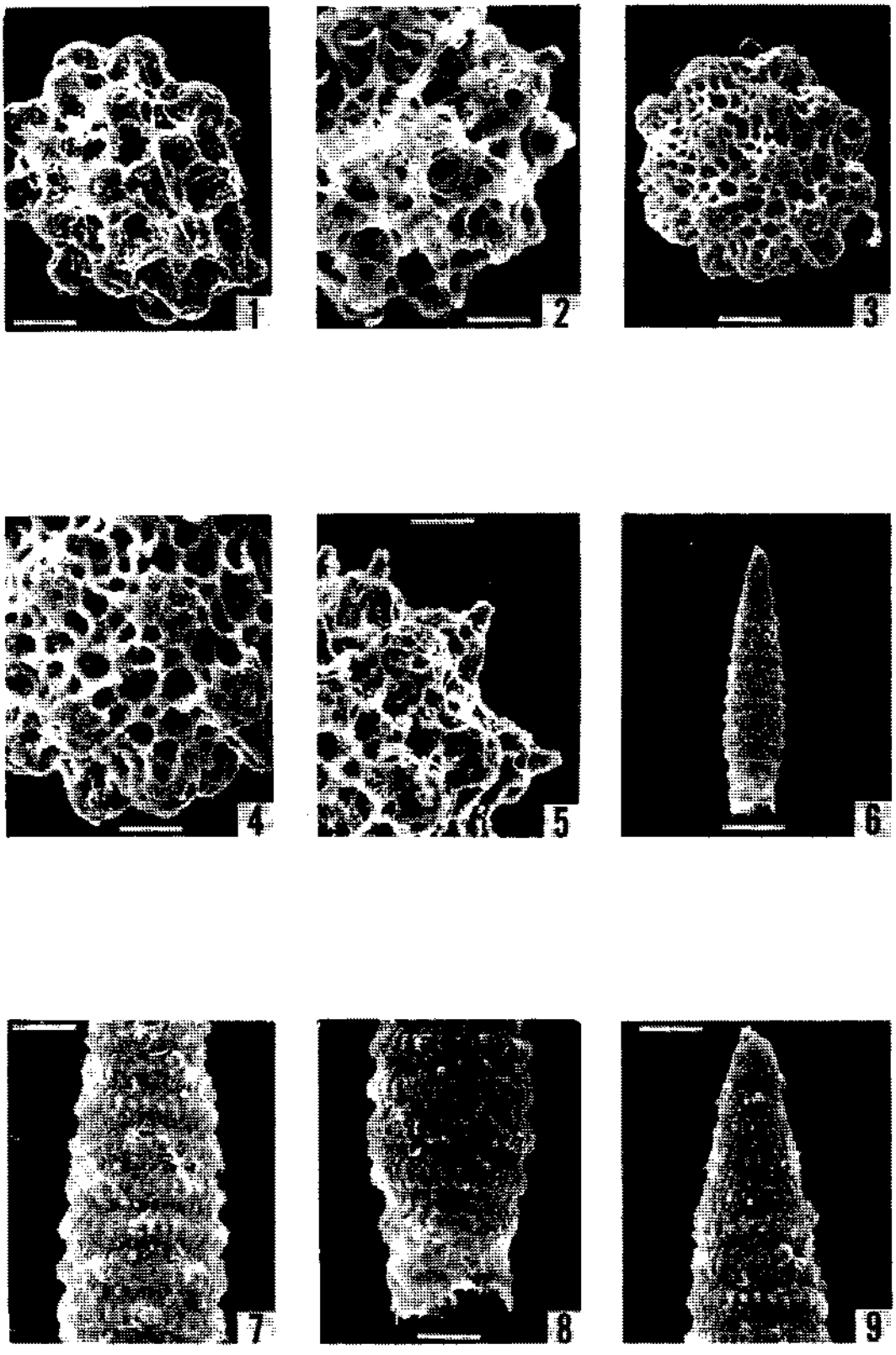
1
2
3
4
5
6
7
8
9

PLATE - X

All figures are scanning electron micrographs of Lower Jurassic Radiolaria from Turkey (Poisson Sample 1662D; see Locality Descriptions).

Fig. 1-4 - *Canoptum anulatum* Pessagno and Poisson, n. sp.

Paratype (USNM 264012). Scales in figures 1-3: 100, 28, and 28 microns. Figure 4 shows interior of test. Note coarse polygonal pore frames comprising inner layer of two layered test; scale: 20 microns.

Fig. 5-6 - *Canoptum anulatum* Pessagno and Poisson, n. sp.

Paratype (USNM 264012). Scales: 100 and 32 microns.

Fig. 7-9 - *Canoptum anulatum* Pessagno and Poisson, n. sp.

Paratype (USNM 264012). Figure 7: natural section of test; scale: 28 microns. Figures 8-9: Note linked-H pattern of circumferential ridges. Normally this pattern is obscured by outer layer of microgranular silica with specimens that are better preserved. Scales: 80 and 40 microns respectively.

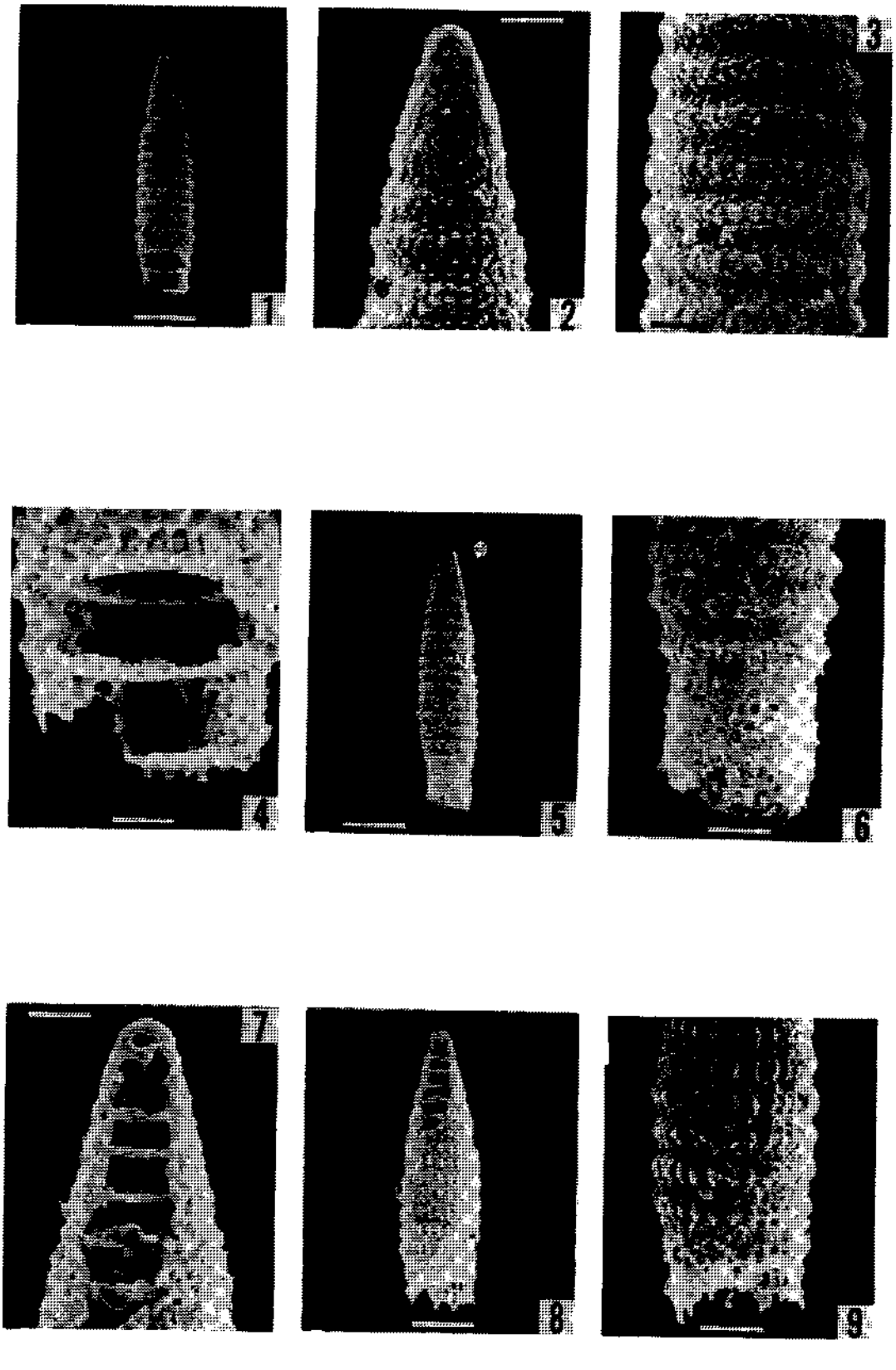
1
2
3
4
5
6
7
8
9

PLATE - XI

All figures are scanning electron micrographs of Lower Jurassic Radiolaria from Turkey (Poisson Sample 1662D; see Locality Descriptions).

Fig. 1-3 - *Canoptum poissoni* Pessagno

Holotype (USNM 251862). Figure 3 shows interior of test with inner layer comprised of coarse polygonal pore frames. Scales: 66, 32, and 13.2 microns respectively.

Fig. 4 - *Canoptum poissoni* Pessagno

Paratype (USNM, 251862). Scale: 80 microns.

Fig. 5,6 - *Canoptum rugosum* Pessagno and Poisson, n. sp.

Holotype (USNM 264013). Scales: 40 and 24 microns respectively.

Fig. 7-9 - *Canoptum rugosum* Pessagno and Poisson, n. sp.

Topotype. Specimen destroyed during electron microscopy. Microgranular layer mostly eroded away from ridges. Note linked - H pattern of circumferential ridges.

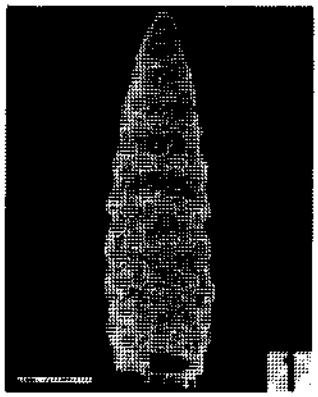
1

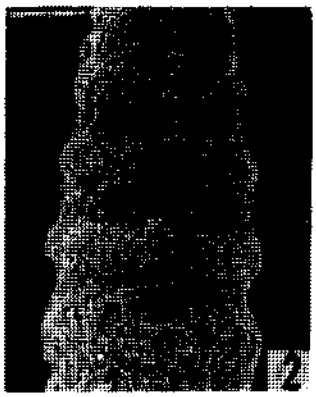
2

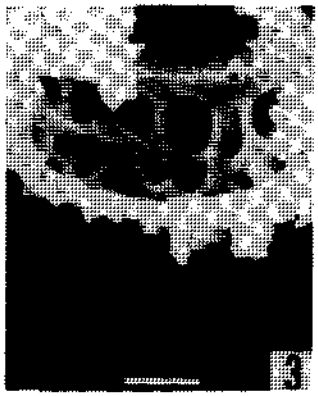
3

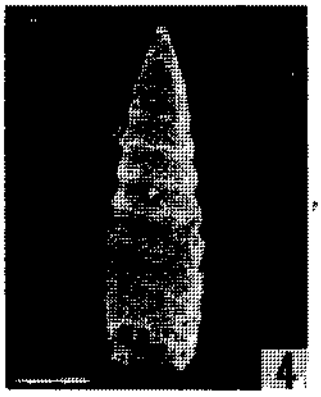
4

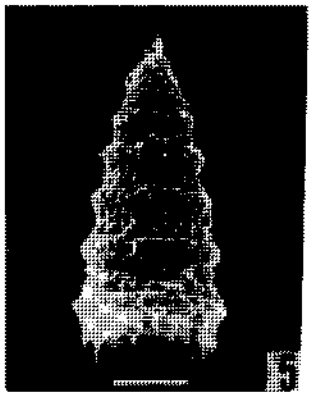
5

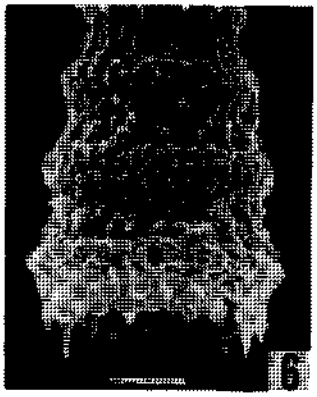
6

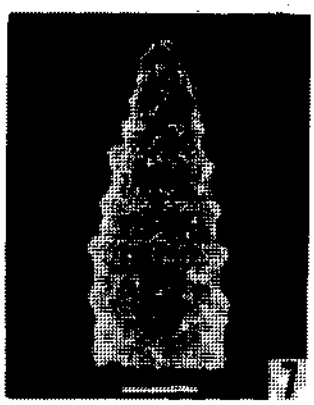
7

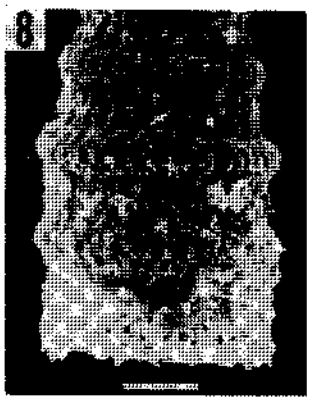
8

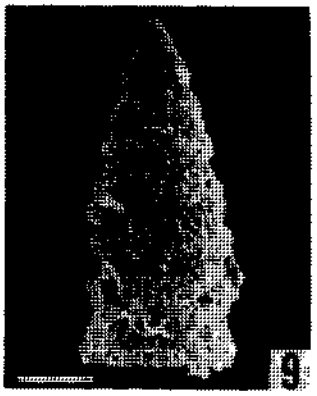
9

PLATE - XII

All figures are scanning electron micrographs of Radiolaria from the Lower Jurassic of Turkey (Poisson Sample 1662D; see Locality Descriptions).

Fig. 1-4 - *Katroma neagui* Pessagno and Poisson, n. sp.

Holotype (USNM 264015). Scale in figure 1 : 132 microns. Scales in figures 2-4: 50 microns each.

Fig. 5 - *Katroma neagui* Pessagno and Poisson, n. sp.

Paratype (USNM 264016). Scale: 100 microns.

Fig. 6,7 - *Natoba minuta* Pessagno and Poisson, n. sp.

Holotype (USNM 264017). Scales: 36 and 20 microns respectively.

Fig. 8 - *Natoba minuta* Pessagno and Poisson, n. sp.

Paratype (USNM 264018). Scale: 36 microns.

Fig. 9,10- *Natoba minuta* Pessagno and Poisson, n. sp.

Paratype (USNM 264018). Note large pore (cephalopyle ?) at base fo cephalis and slightly costate nature of abdomen. Scales: 36 and 20 microns respectively.

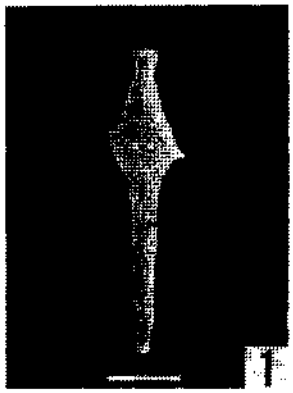
1

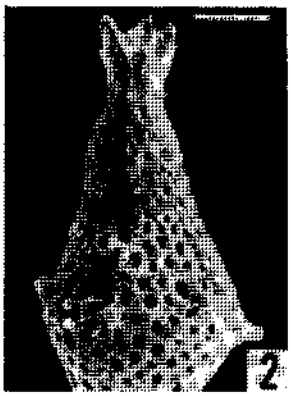
2

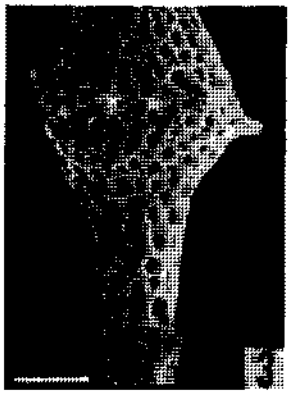
3

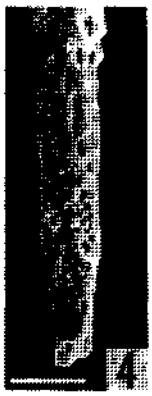
4

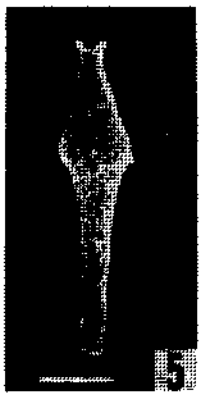
5

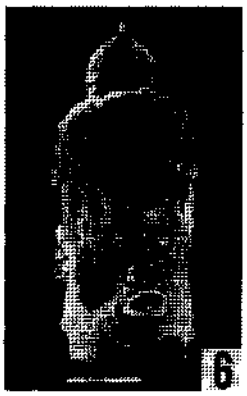
6


7

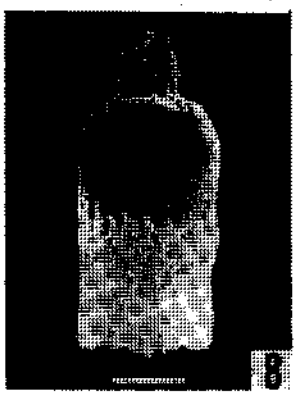
8

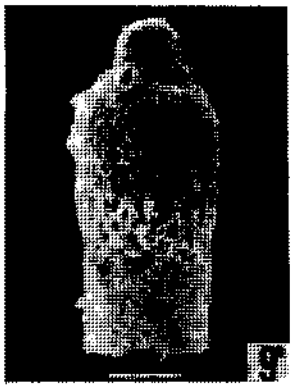
9


10

PLATE - XIII

Transmitted light photomicrographs of Lower Jurassic Radiolaria from Turkey (Poisson Sample 1662D; see Locality Descriptions).

Fig. 1 - *Protopsium ehrenbergi* Pessagno and Poisson, n. sp.

Paratype (USNM 263998). Scale: 32 microns.

Fig. 2 - *Pseudoheliodiscus yaoi* Pessagno and Poisson, n. sp.

Paratype (Pessagno Collection). Note concentric nature of spongy meshwork comprising the cortical shell. Scale: 76 microns.

Fig. 3 - *Canoptum rugosum* Pessagno and Poisson, n. sp.

Paratype (USNM 264014). Scale: 72 microns.

Fig. 4 - *Protopsium ispartaensf* Pessagno and Poisson, n. sp.

Paratype (USNM 264000). Note concentric nature of spongy meshwork. Scale : 68.5 microns.

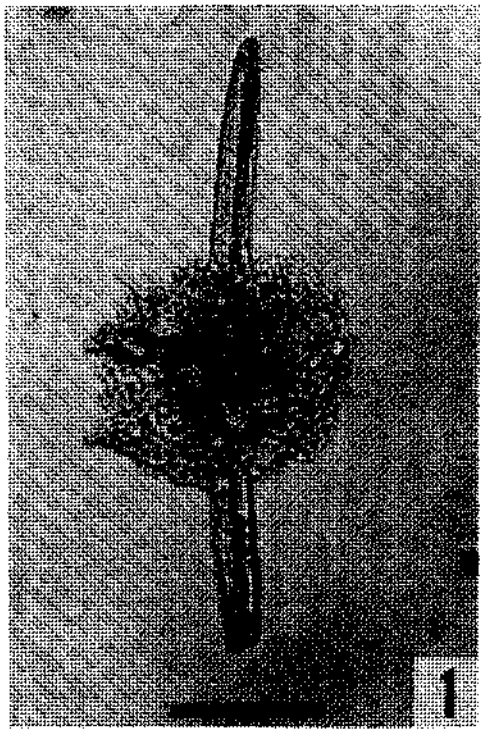
1

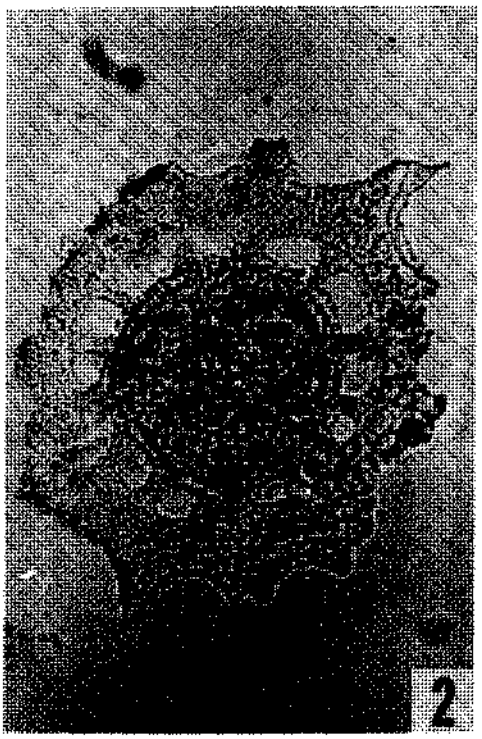
2

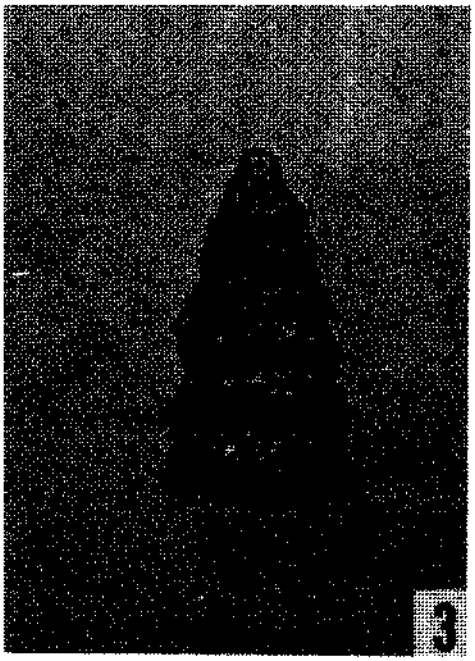
3

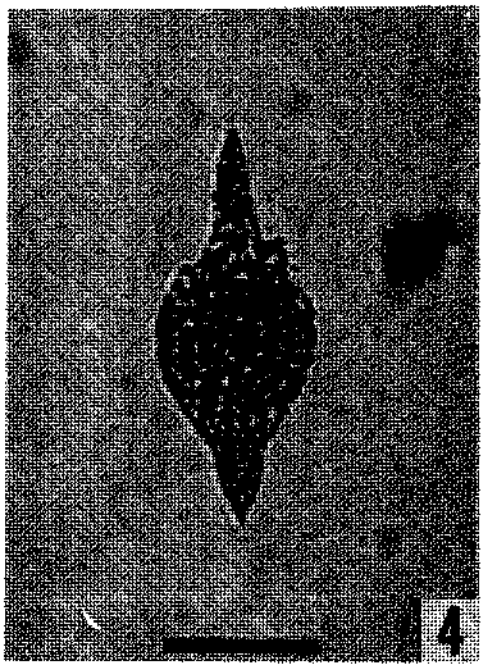
4

PLATE - XIV

Transmitted light photomicrographs of Lower Jurassic Radiolaria from Turkey (Poisson Sample 1662D; see Locality Descriptions).

Fig. 1,2 - *Canoptum rugosum* Pessagno and Poisson, n. sp.

Paratype (Pessagno Collection). Scales: 66 and 33 microns respectively.

Fig. 3,4 - *Natoba minuta* Pessagno and Poisson, n. sp.

Paratype (Pessagno Collection). Scales: 72 and 36 microns respectively.

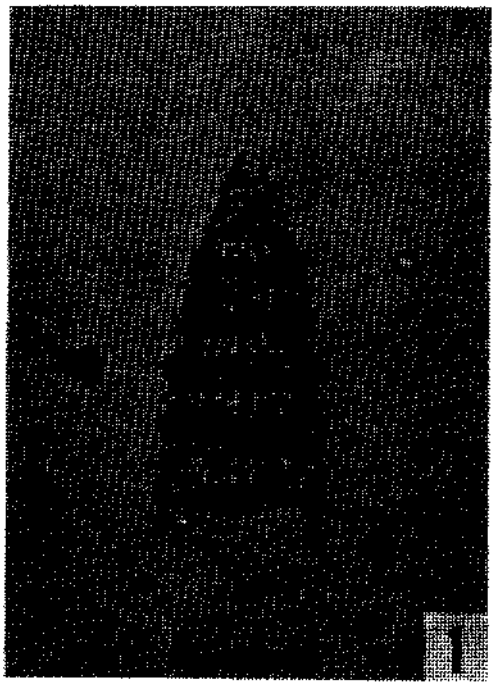
1

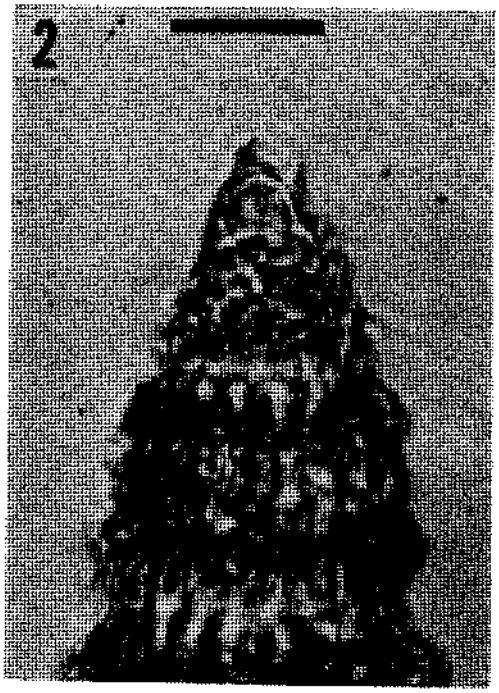
2

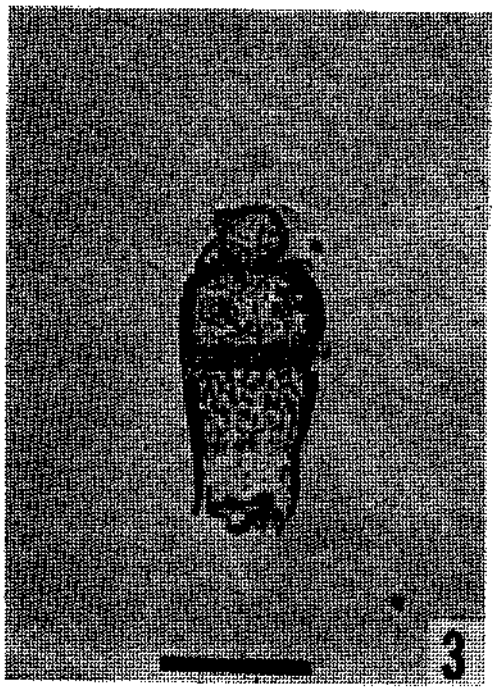
3

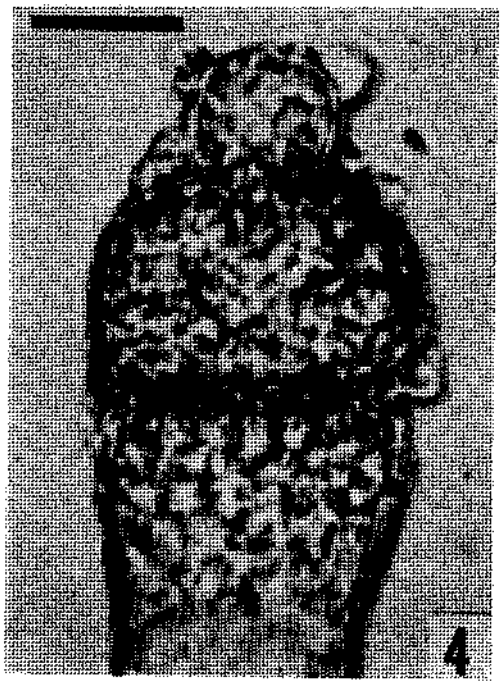
4

PLATE - XV

Transmitted light photomicrographs of Lower Jurassic Radiolaria from Turkey (Poisson Sample 1662D; see Locality Descriptions).

Fig. 1 - *Natoba minuta* Pessagno and Poisson, n. sp.

Paratype (USNM 264018). Part of cephalis appears to be enclosed by thorax. Scale: 71 microns.

Fig. 2,4 - *Canoptum anulatum* Pessagno and Poisson, n. sp.

Paratype (USNM 264012). Scales: 35 and 70 microns respectively.

Fig. 3 - *Katrotna neagui* Pessagno and Poisson, n. sp.

Paratype (Pessagno Collection). Scale: 71 microns.

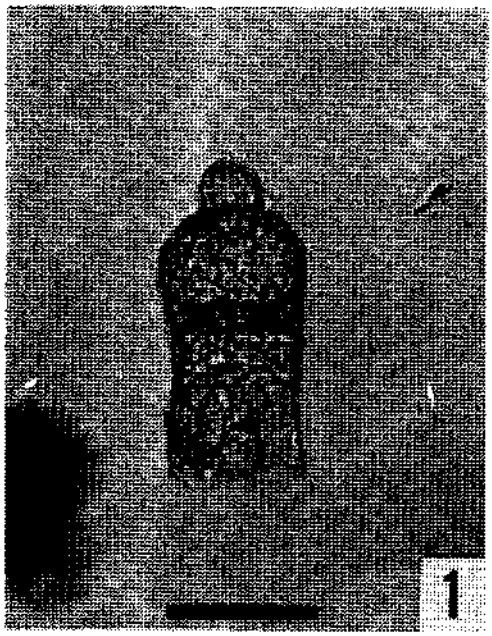
1

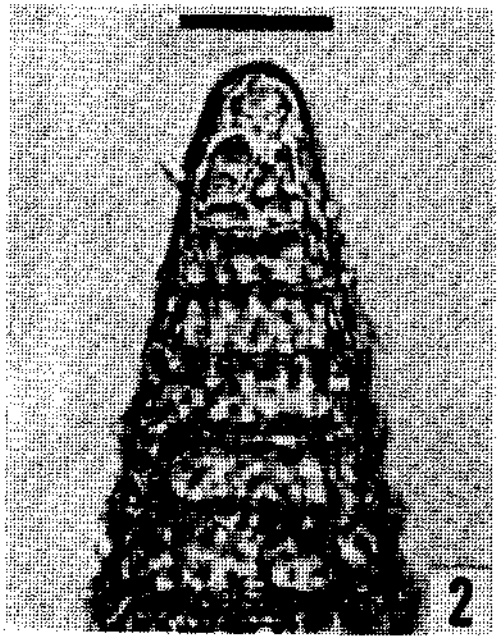
2

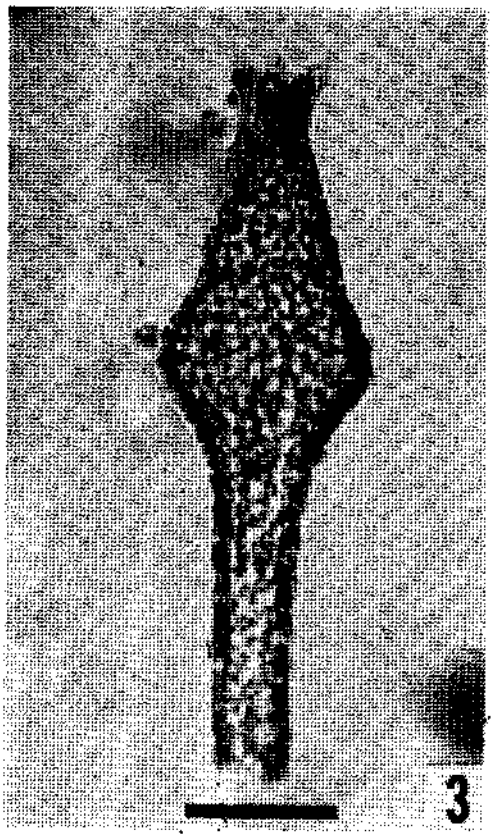
3

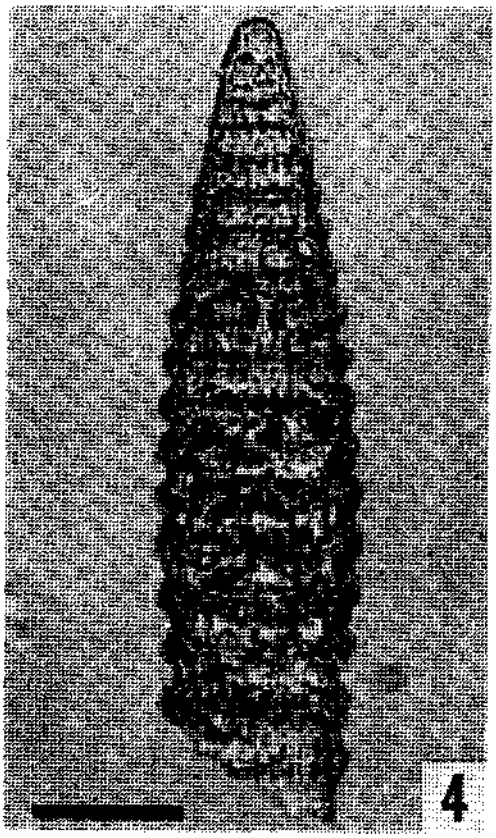
4

Pessagno, E. A., Jr., 1973, Upper Cretaceous Spumellariina from the Great Valley sequence, California Coast Ranges: Bulls. Amer. Pal., 63, 276, 49-102, pls. 9-21.

———, 1976, Radiolarian zonation and stratigraphy of the Upper Cretaceous portion of the Great Valley sequence, California Coast Ranges: Micropalecntology Special Paper, 2, 1-95, 14 pls. 10 text-figs.

———, 1977a,Upper Jurassic Radiolaria and radiolarian biostratigraphy of the California Coast Ranges: Micropaleontology, 23, 56-113, pls. 1-12, text-figs. 1-4.

———, 1977b, Lower Cretaceous radiolarian biostratigraphy of the Great Valley Sequence and Franciscan Complex, California Coast Ranges: Cushman Foundation for Foraminiferal Research, Special Publication, 15, 1-86, pls. 1-12.

———, 1979, *in* Pessagno, Finch, and Abbott (1979), Systematic Paleontology.

———; Finch, J. W. and Abbott, Patrick L., 1979, Upper Triassic Radiolaria from the San Hipolito Formation, Baja California: Micropaleontology, 76 p. (ms.), 9 pls. 6 text-figs., (in press).

———and Newport, R. L., 1972, A technique for extracting Radiclaria from radiolarian cherts: Micropaleontology, 18, 2, 231-234, pl. 1.

Poisson, A., 1977, Recherches geologiques dans les Taurides occidentalcs (Turquie): Thesis Universite Paris Sud Orsay France, 796.

Riedel, W. R., 1967, *in* The Fossil Record: A symposium with documentation: Chapter 8 (Protozoa), 291-298.

———and Sanfilippo, A., 1974, Radiolaria from the southern Indian Ocean. DSDP Leg. 26. *in* Davies, T.A. *et al*., Initial reports of the Deep Sea Drilling Project, 26, 771-813, pls. 1-15.

Rüst, E., 1885, Beitrage zur Kenntniss der fossilen Radiolarian aus Gesteinen des Jura: Paleontographica, 31 (ser. 3, v. 7) 269-321, pls. 26-45.

———, 1898, Beitrage zur Kenntniss der fossilen Radiolarien aus Gesteinen des Jura und der Kreide: Palaeontographica, 45, 1-67, pls. 1-19.

KARADENİZ'İN GÜNCEL ÇÖKELLERİ VE URANYUM İÇERİKLERİ

Abdullah GEDİK, Taner SALTOĞLU ve Hüseyin KAPLAN

Maden Tetkik ve Arama Enstitüsü, Ankara

ÖZ. — Karadeniz'in güney yarısından, belirli özelliklere göre seçilen 53 durak noktasından alman karot örneklerinden, ön Sedimentolojik gözlemlere göre bölünerek elde edilen 546 örnekte; ağırlık kayıpları, uranyum, organik karbon, altın, gümüş, molibden, kalsiyum oksit ve diğer majör elementlerin tayinleri yapılmış ve her örnek yaklaşık 40 element açısından optik yayım spektroskopisi ile rutin olarak taranmıştır.

Karadeniz'in durgun havzalarında yer alan güncel çökeller kendine özgü bir uranyum konsantrasyonuna sahiptirler. Bu çökellerdeki uranyum içeriği 105°C de kurutulmuş örneklerde maks. 28 ppm e kadar çıkabilmesine karşın, ortalama 6 ppm dir. Çökellerin uranyum içeriği ile kokolitler arasında bir ilişki izlenmektedir. Benzeri tarzda diğer bir ilişki uranyum ile organik karbon arasında da bulunmaktadır.

Söz konusu uranyum içeriği; günümüz uranyum fiyatları ve piyasa koşullarında, orta ve uzun vadede ekonomik bir değer taşımamaktadır.

GİRİŞ

Karadeniz çeşitli yıllarda, çoğunluğu Sovyetler Birliği olmak üzere Türk, Bulgar, Amerikan, Alman, İngiliz ve diğer bazı ülkelerin araştırmacıları tarafından oluşum, Struktur, biyoloji ve jeokimya yönlerinden incelenmiş ve bu konularda 5000 in üzerinde bilimsel yayın yapılmıştır. Bunlardan Woods Hole Oşinografi Enstitüsünün (WHOI) R/V Atlantis II gemisi ile 1969 yılında, Degens ve Ross yönetiminde çeşitli ülkelerden araştırmacıların da katılmış oldukları bir Karadeniz araştırma gezisi sonuçları bir araya getirilmiş ve yayınlanmıştır (Ross ve diğerleri 1974). Bunlardan Rona ve Joensu (1974) tarafından yazılan «Karadeniz'de Uranyum Jeokimyası» konulu bir makalede, Karadeniz deniz dibi çökellerinden alınan bazı örneklerin 60 cm kalınlığa kadar 50-20 ppm uranyum içerdikleri (105°C de kurutulmuş olarak) belirtilmiştir. O gün için uranyum açısından üzerinde fazla durulmayan bu çalışmadan sonra Degens ve diğerleri (1977) tarafından; Karadeniz'in dip çukurunun 296 000 km^2 lik bir alanında 1 m derinliğe kadar olan çökellerin küllerinin ortalama 100 ppm U_3O_8 içerdiği ve toplam rezervin $6.7x10^6$ ton U_3O_8 olduğu öne sürülmüştür. Karadeniz'in 6-7 noktasından alındığı anlaşılan örneklerle yapılan bu araştırma, Türk ve dünya kamuoyunda büyük bir ilgi uyandırmıştır. Bunun üzerine bazı üniversitelerimiz ve ilgili kamu kuruluşlarımız, Karadeniz deniz gibi çökellerini ayrıntılı olarak incelemek için harekete geçmişlerdir. Bu arada MTA Enstitüsünde de bu çökellerin ayrıntılı bir ön etüdünün yapılması gereksinimi duyulmuş ve 1978 yılının ilk aylarında MTA Enstitüsü Genel Direktörlüğü ile Deniz Kuvvetleri Komutanlığı arasında dip çökellerinden örnek alınması konusunda işbirliği kararı alınmıştır. Konu ile ilgili kuruluşların oluşturduğu «Karadeniz Doğal Kaynakları Araştırma Projesi» yönetim kurulunun 28 ağustos 1978 tarihinde yaptığı toplantıda, proje yönetim ve yürütme kurulu başkanlığı MTA Enstitüsü Genel Direktörlüğüne verilmiştir.

Belirlenen durak noktalarından örnekler alınması işlemi, Deniz Kuvvetleri Komutanlığı Seyir, Hidrografi ve Oşinografi Dairesinin 1978 yaz programma alınmış ve A 594 Çarşamba gemisi 53 durak noktasından karot alıcı ağırlıklı boru (gravity core) ile 12 eylül 1978-12 ekim 1978 tarihleri arasında toplam 53 adet karot örneği almıştır (Şek. 1). Bu durak noktalarının tümü Sovyet-

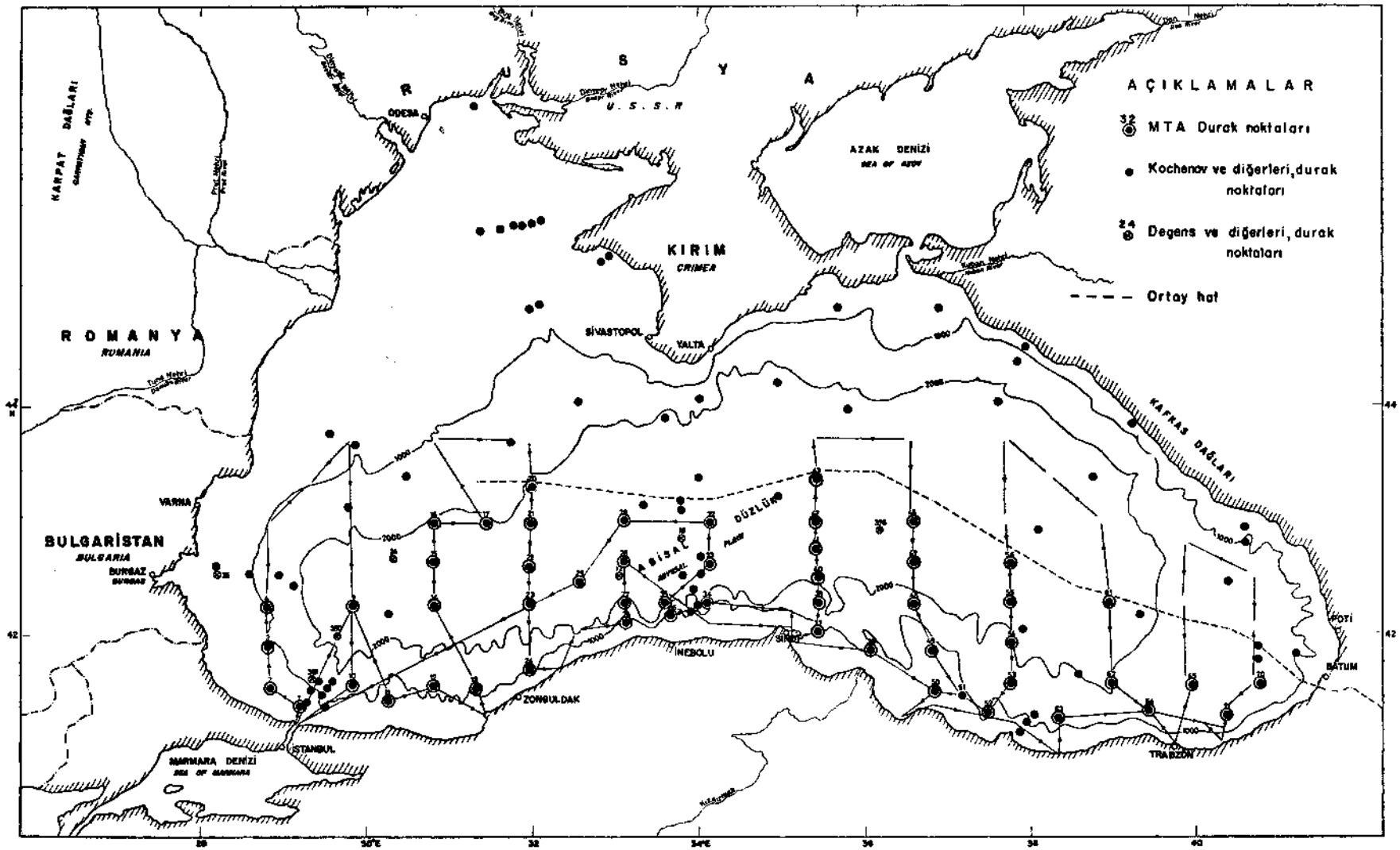

Şek. 1 - Karadeniz'in derinlik ve çeşitli çalışmalarda alınan örneklerin durak noktalarını gösterir harita.

ler Birliği ile ülkemiz arasında saptanmış «Ortay hattın» güneyinde kalmaktadır. Alınan karot boyları ise 68.5 cm-145.5 cm arasında değişmektedir. Alınan bu örnekler üzerinde yapılacak çalışmalar için MTA Enstitüsünce oluşturulan «Karadeniz Deniz Dibi Çökellerinin incelenmesi Projesinin birincil amacı, söz konusu çökellerin rasyonel bir şekilde incelenerek, ekonomik açıdan daha gerçekçi verilerin ortaya konması olmuştur.

YAPILAN TEST, ANALiZ VE DETERMİNASYONLAR, UYGULANAN YÖNTEMLER

Karadeniz tabanından alınmış 53 karot örneği üzerinde ilk gözlemler yapıldıktan sonra, çökelsel durumları da göz önüne alınarak enlemesine kesilip laboratuvar çalışmaları için 546 örnek oluşturulmuş ve çeşitli incelemeler bu örnekler üzerinde yapılmıştır.

Su ve uçucu madde tayinleri

Orijinal örnekler önce 40°C ye ayarlı etüvlerde sabit tartıma gelinceye kadar bekletilmiş ve daha sonra öğütülmüş haldeki örneklerde 105°C deki ağırlık kayıpları tayin edilmiştir. Orijinal örneğe göre 105°C deki ağırlık kaybı hesapla bulunmuştur (Tablo 1).

Uranyum tayini

546 örneğin uranyum tayinleri MTA Enstitüsü laboratuvarlarında yapılmıştır. Tayinlerde flüorimetrik yöntem uygulanmış olup, flüorimetrik ölçümlere kadar şu işlemler yapılmıştır. 105°C de kurutma, tartım alındıktan sonra organik maddelerin uzaklaştırılması için kızdırma, HF-HNO_3 karışımı ile çözünürleştirme, Al $(NO_3)_3$ çözeltisi-etilasetat fazlarındaki ekstraksiyon ve NaF-LİF karışımı ile eritme yapılmıştır. Uranyum tayinleri 105°C de kurutulmuş bu örneklerde yapılmıştır. Daha sonra hesap yolu ile orijinal örneklerin uranyum içerikleri de saptanmıştır. [Üç örnek bir başka yöntemle uranyum analizi için Geol. Surv. of Canada lâboratuvarlarına gönderilmiştir.] Nötron aktivasyon yöntemi ile tayinleri yapılan bu örneklerin analiz sonuçları MTA Enstitüsü laboratuvarlarının sonuçları ile büyük bir uyum içindedir (Tablo 2). MTA Enstitüsü laboratuvarlarından elde edilen U_3O_8 değerleri ile her karotta 0-60 cm, 60-120 cm ve 0-120 cm aralıklarında U_3O_8 tenörü ağırlıklı ortalamaları hesaplanmış (Şek. 2) ve Calcomp GPCP II programı ile Karadeniz'in güney yarısındaki çökeller, için uranyum izotenör haritaları çizilmiştir (Şek. 3,4,5).

Organik karbon tayini

Çökelsel ön gözlemlere de dayanılarak seçilen 130 tek ve kompozit örnekte, organik maddelere bağlı olan karbonun tayini yapılmıştır. 40°C de kurutulmuş örneklerden tartımlar alındıktan sonra, bünyelerindeki karbonatlara bağlı olankarbon, HCI çözeltisi ile uzaklaştırılmış ve organik karbon K. Burger'e göre yarı mikroelementer analiz cihazı ile tayin edilmiştir. Yine Calcomp GPCP programı ile çizilen organik karbon izotenör haritası, Şekil 6 dadır.

Su, kül ve yanma ısısı tayinleri

Karadeniz'in orta bölümlerindeki çökeller için karakteristik dört karotun sekiz adet tek ve kompozit örneklerinde su, kül ve yanma ısısı değerleri tayin edilmiştir. Bu tayinlerde, su için T.S. -690, kül için T.S. -1042 ve ısı değeri için de DIN -S 1900 daki yöntemler uygulanmıştır. % 4-35 CaO içeren bu örneklerin yanma ısıları ve organik karbon arasındaki ilişkiyi gösterir grafik, Şekil 7 de gösterilmiştir.

Tablo 1 - 40°C ve 105°C lerde ağırlık kayıplarının karotlara göre ağırlık ortalamaları

Durak no.	*Ağırlık kaybı (40°C)*	*Ağırlık kaybı (105°C)*
1	43.05	44.53
2	—	—
3	—	—
4	46.36	47.30
9	50.48	51.67
10	—	—
11	46.84	47.71
12	52.96	54.20
13	—	—
14	41.26	42.12
15	50.96	52.06
16	57.13	57.78
17	60.74	61.64
20	55.54	56.31
21	63.29	64.84
22	58.78	59.78
23	50.48	51.42
24	39.81	40.87
25	50.46	51.79
26	40.07	41.24
27	56.96	58.41
28	58.04	59.82
29	63.93	64.95
32	53.61	55.46
33	52.26	53.47
34	56.53	57.66
35	45.27	46.37
36	45.22	46.30
37	54.11	55.47
38	43.51	44.92
39	45.81	46.70
40	45.06	46.72
41	42.54	44.04
42	49.35	50.46
43	57.84	59.29
46	66.26	67.69
47	51.63	52.97
48	39.36	40.37
49	55.28	56.54
50	41.18	42.72
51	55.27	56.27
52	53.14	54.64
53	54.26	55.83
54	55.19	56.53
55	57.59	58.97
56	49.13	50.36
61	41.88	42.96
62	48.50	49.85
63	40.65	42.62
64	55.05	56.93
65	48.51	49.93
70	50.29	51.76
71	59.56	61.00

DURAK NO:	105 °C'de kurutulmuş numunelerde		DURAK NO:	105 °C'de kurutulmuş numunelerde	
	0-60 Cm. aralığında	60-120 Cm. aralığında		0-60 Cm aralığında	60-120 Cm aralığında
1	3	2	36	2	2
2	3	3	37	3	4
3	4	6	38	3	3
4	3	3	39	4	2
9	3	3	40	2	3
10	3	2	41	4	2
11	2	2	42	4	4
12	3	3	43	4	9
13	3	3	46	10	16
14	2	3	47	6	3
15	6	3	48	4	3
16	12	2	49	7	2
17	15	3	50	3	3
20	13	2	51	3	4
21	13	4	52	3	3
22	12	3	53	6	5
23	2	2	54	10	3
24	3	2	55	13	3
25	5	3	56	7	2
26	3	3	61	4	2
27	8	10	62	4	3
28	6	8	63	4	2
29	13	4	64	4	3
32	5	7	65	3	3
33	7	5	70	2	2
34	4	3	71	5	6
35	3	3			

Şek. 2 - Karadeniz'de 53 durak noktasından alman karotların metrajlarına göre ağırlık ortalamaları (U_3O_8 ppm olarak).

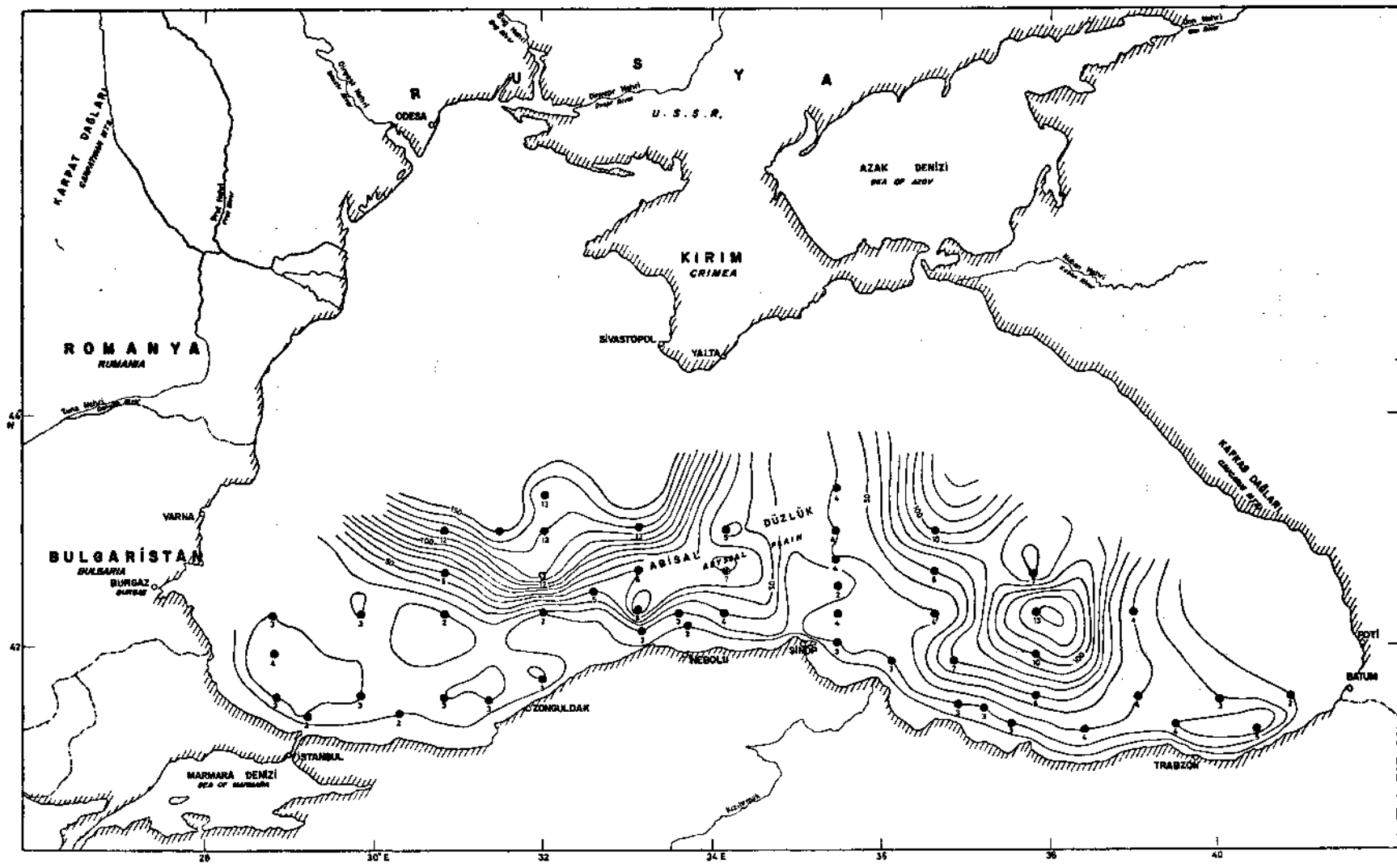

Şek. 3 - Karadeniz'in güney yarısındaki çökellerin 0-60 cm aralığındaki U_3O_8 izotenör haritası (105°C de kurutulmuş örneklerde ppm olarak).

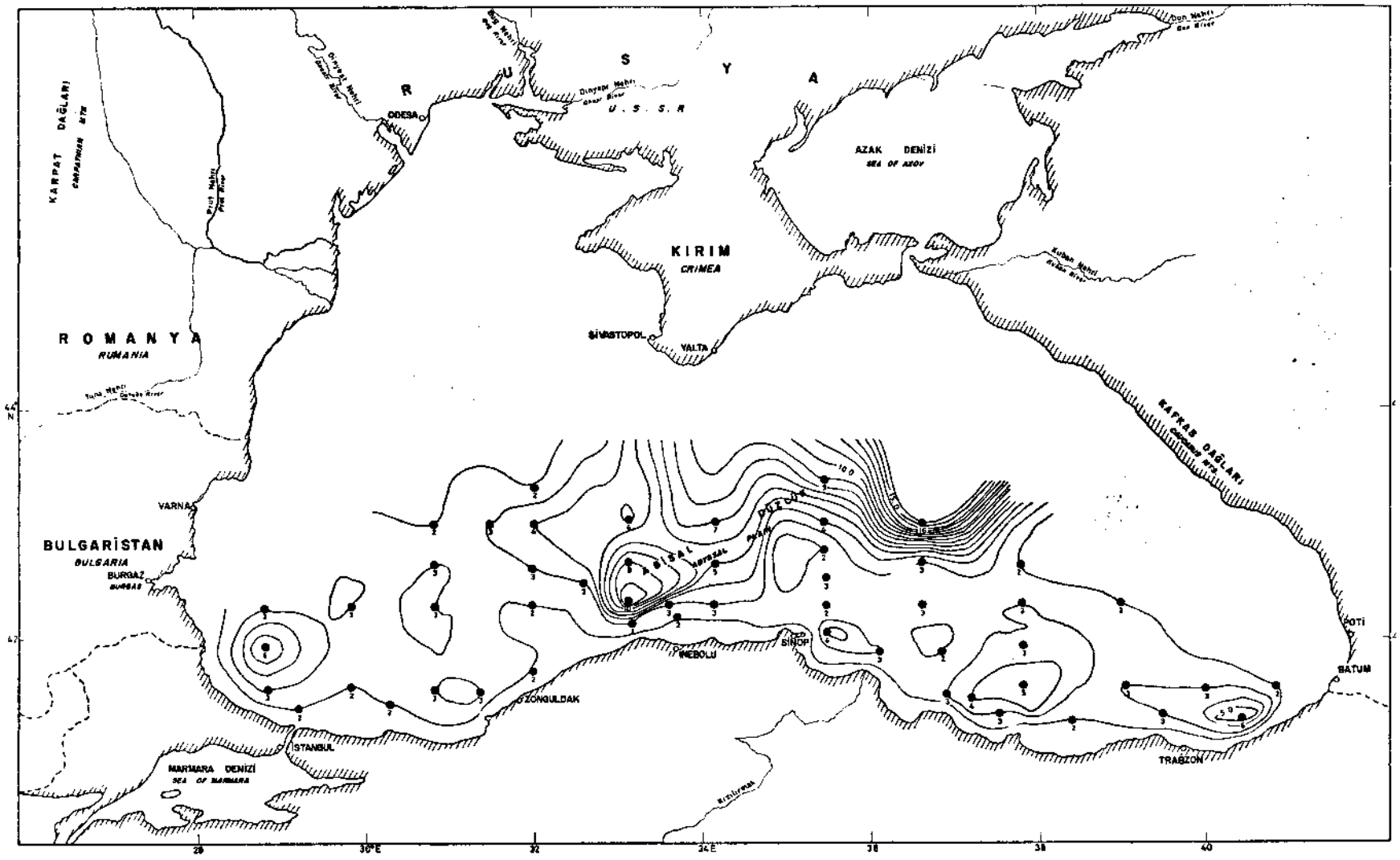

Şek. 4 - Karadeniz'in güney yarısındaki çökellerin 60-120 cm aralığındaki U_3O_8 izotenör haritası (105°C de kurutulmuş örneklerde ppm olarak).

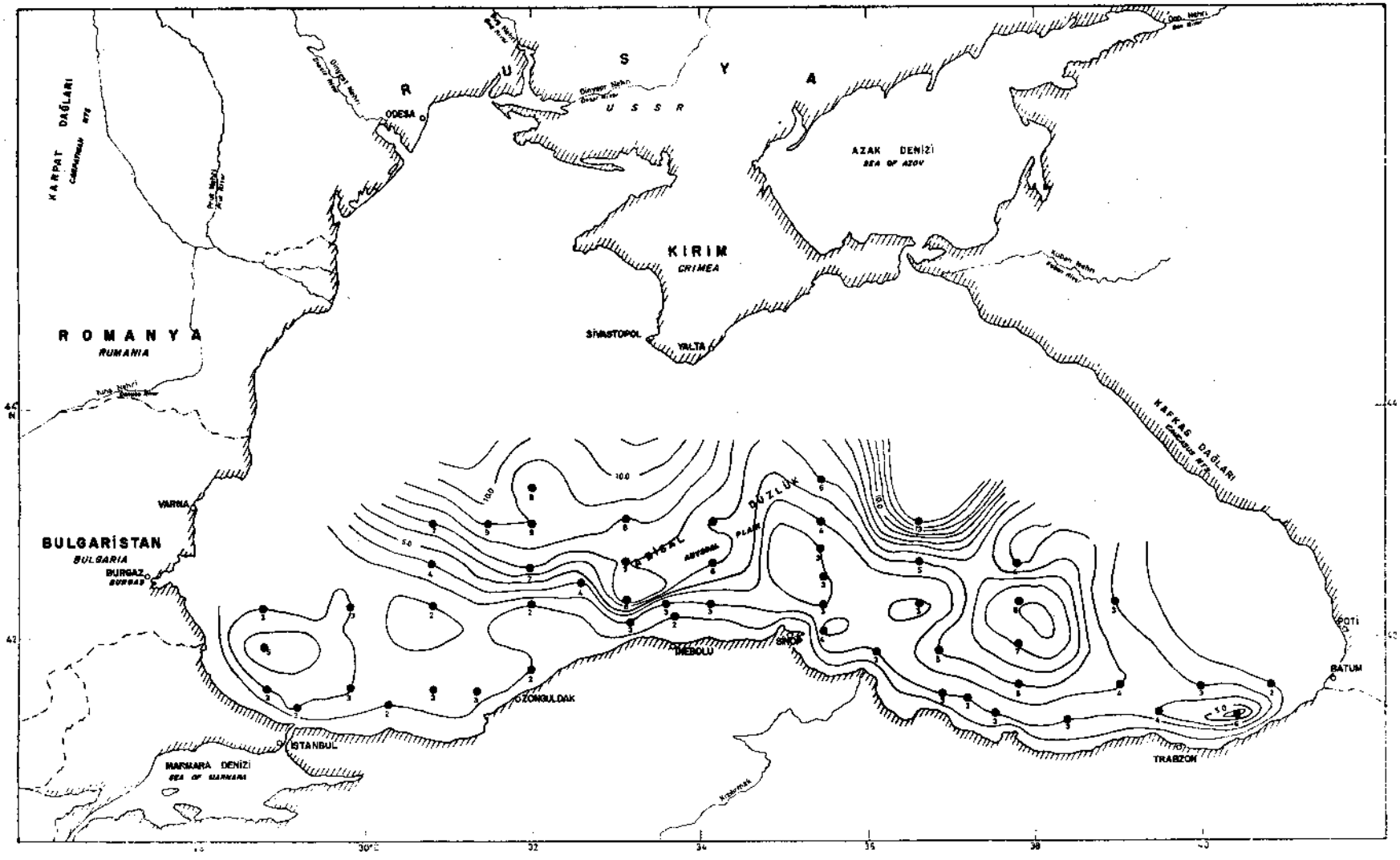

Şek. 5 - Karadeniz'in güney yarısındaki çökellerin 0-120 cm aralığındaki U_3O_8 izotenör haritası (105°C de kurutulmuş örneklerde ppm olarak).

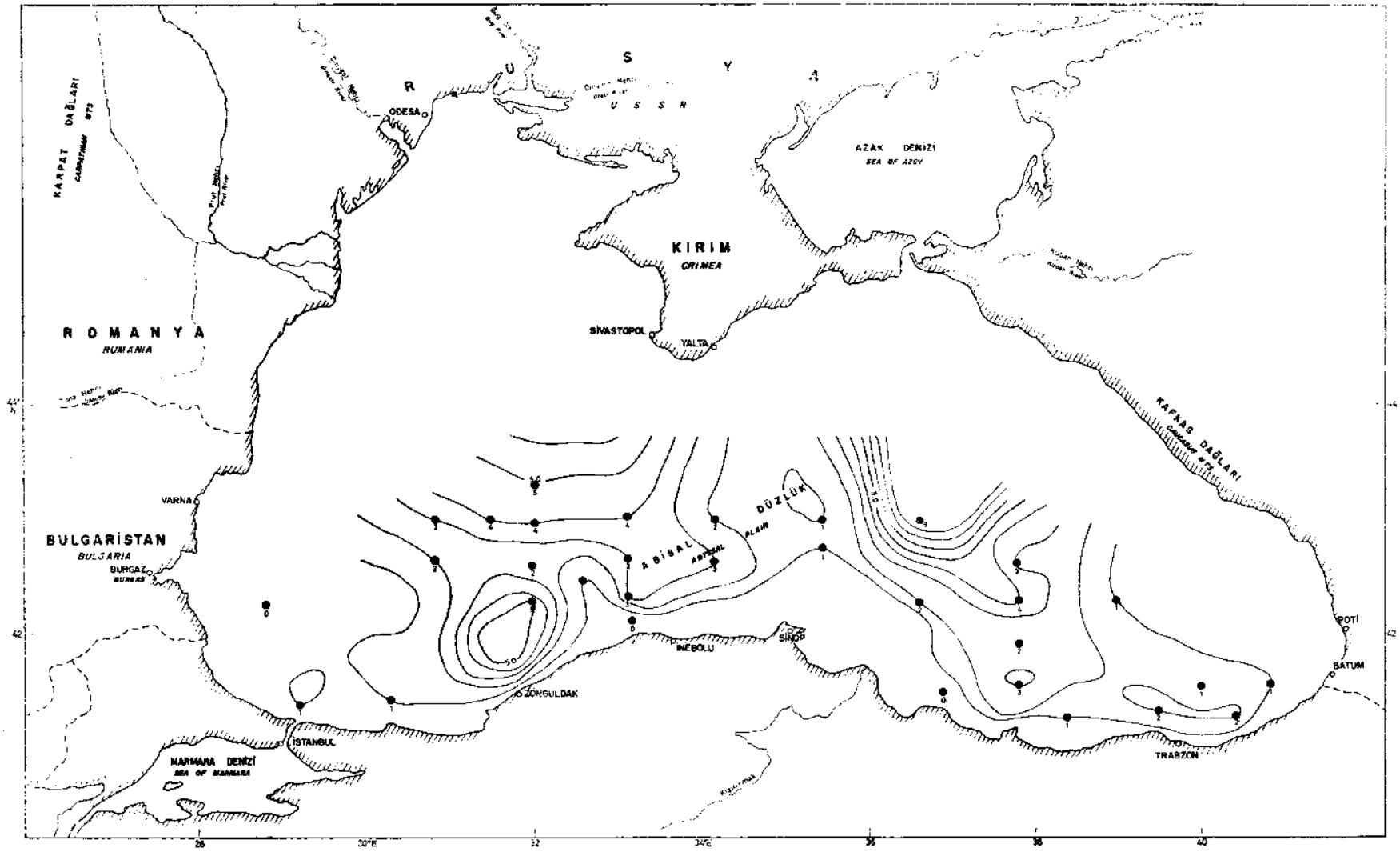

Şek. 6 - Organik karbon izotenör haritası (40°C de kurutulmuş örneklerde % olarak).

Tablo 2 - Ayrı yöntemlerle yapılan uranyum analizi sonuçlarının karşılaştırılması

Durak no.	*Metraj (cm)*	*Flüometrik yöntem ile MTA Enstitüsü lab. analiz sonuçları (U_3O_8 ppm)*	*Nötron aktivasyon yöntemi ile Geol. Surv. of Canada lab. analiz sonuçları (U_3O_8 ppm)*
32	76-86	6	5.7
46	51-60	20	21.3
46	95-105	17	17.2

Durak No.	Metraj (cm)	Nem (%)	Kül (%)	Hidrojen (%)	Alt ısı (kCal /Kg)	Üst ısı (kCal / Kg)	Organik karbon (%)
16	0 - 18	2.46	58.40	1.18	472	551	4.02
16	18 - 38	6.0	57.53	2.21	1576	1731	11.28
21	21 - 51	5.5	63.89	2.49	1301	1469	10.10
29	0 - 18	3.0	62.83	1.40	374	468	2.98
29	27 - 62	6.0	68.0	2.18	1054	1207	7.94
46	0 - 142	3.46	66.82	2.15	1157	1294	8.96
46	94 - 108	3.04	66.80	1.25	684	770	5.38
46	108 - 142	4.75	57.69	3.19	1933	2134	14.25

Şek. 7 - Değişik örneklerde yapılan, kül, hidrojen, yanma ısısı ve organik karbon analizleri.

Optik spektrografik tayinler

546 örnekte optik yayım spektrografi yöntemiyle doğru akım arkı kullanılarak, yaklaşık 40 elementin tayinleri yapılmıştır. Rutin çalışma şartlarına göre tayinleri yapılan elementlerin dedeksiyon limitleri Tablo 3 ile verilen değerlerin kesinlik dereceleri Tablo 4 de gösterilmiştir. Sr,Co,Cr,Cu,Mn,Pb,V,Ti,Mo,Zr,Y,B,Ni ve Ba elementlerinin örneklerdeki tayin değerlerinin karotlara göre ağırlıklı ortalamaları Tablo 5 te verilmiştir. Ca,Mg,Na,Al,Si ve Fe elementleri hariç, Tablo 3 te verilen ve Tablo 5 te yer almayan diğer elementler dedeksiyon limitleri dışındadır.

Altın ve gümüş tayinleri

İnebolu açıklarındaki lokasyonları da kapsayan 1, 11, 26, 27, 28 no.lı durak noktalarından alınan beş karota ait, 105°C de kurutulmuş 102 örnekte, atomik apsorpsiyon spektrometresi ile Au ve Ag tayinleri yapılmıştır. Bu tayinler için «U.S. Geological Survey Bulletin 1289»da verilen yöntemler uygulanmıştır. Çalışma şartlarına göre altın ve gümüş için bu yöntemle dedeksiyon limiti, 0.2 ppm olarak belirlenmiş ve bu örneklerin hiç birinde altın ve gümüş bulunamamıştır. Ayrıca kupelasyon yöntemiyle yapılan tayinlerde de aynı sonuca varılmıştır.

Tablo 3 - Optik yayım spektrografi laboratuvarında analizleri yapılan elementler ve dedeksiyon limitleri

Element	*% DL*	*Element*	*% DL*
Co	0.002	Tl	0.004
Cr	0.002	Ta	0.2
Cu	0.0004	W	0.1
Ga	0.004	Sb	0.01
Ge	0.002	Zn	0.04
Mn	0.0002	As	0.1
Nb	0.004	Ba	0.02
Pb	0.002	Ca	0.01
Sn	0.002	Mg	0.001
Ti	0.01	Sr	0.04
V	0.01	Na	0.4
Ag	0.0002	Li	0.1
Bi	0.001	Al	0.02
In	0.004	Si	0.01
Mo	0.004	Fe	0.01
Sc	0.004	Th	0.2
Y	0.002	U	0.2
Zr	0.004	Pd	0.0004
Au	0.002	Te	0.2
B	0.01	Be	0.0002
Cd	0.01	P	0.4
Ce	0.2	Yb	0.001
La	0.01	Eu	0.01
Ni	0.002	Tm	0.002
Nd	0.1	Sm	0.04
		Ho	0.004

Not: Verilen dedeksiyon limitleri optimal şartlar için geçerlidir. İnterferenz ve farklı matriks dedeksiyon limitlerini yükseltebilir.

Tablo 4 - Yarı kantitatif optik spektrografik analizde rapor edilen değerler ve kesinlik dereceleri

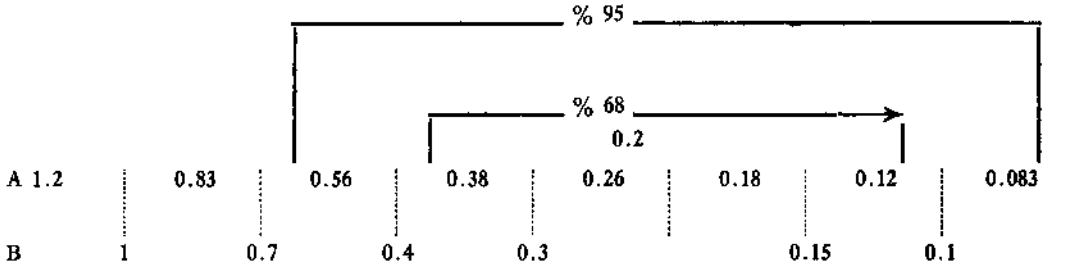

A — Geometrik aralıklar.

B — Rapor edilen değerler.

Not: % 0.2 olarak verilen analiz değerinin 0.38–0.12 arasında olma olasılığı % 68, 0.56–0.083 arasında olma olasılığı % 95 tir.

Molibden tayini

Molibden-uranyum ve molibden-organik karbon ilişkilerini araştırmak için belirli karotlara ait 105°C de kurutulmuş 109 örnekte kolorimetrik yöntemle Mo tayinleri yapılmıştır.

Majör elementlerin tayinleri

Değişik karotlara ait 105°C de kurutulmuş 73 örnekte, x ışınları floresans spektrometresi ile 636 majör element tayini yapılmış ve çökelsel gözlemlere göre belirlenen bu karakteristik örneklerde elementlerin gösterdikleri konsantrasyon değişiklikleri izlenmiştir.

KARADENİZ HAKKINDA GENEL BiLGiLER

Karadeniz fizyografik bakımdan dört bölüme ayrılabilmektedir. Bunlar kıta sahanlığı, kıta yamacı, havza önlüğü ve derin düzlükler bölümleridir. Kıta sahanlığının sınırı Karadeniz'de genellikle 100 m derinliğe inmektedir. Bu derinlik Azak denizi güneyinde ve Kırım yarımadası çevresinde 130 metreye kadar varmaktadır. Güney ve doğuda birkaç kilometre daralırken, Kırım yarımadasının batısında 200 kilometreye kadar genişlemektedir. Rize kuzeyinde 2-3 km, Orta Karadeniz Bölgesinde 35 km lik bir şelfve dar bir yamaçta kıtasal yokuş ve abisal düzlüğe geçilmektedir. Basen yamacında büyük kayma kütleleri vardır. Kuzey Anadolu'da Karadeniz'e dökülen Çoruh, Kızılırmak, Yeşilırmak ve Sakarya nehirleri yöresinde, şelfin dar oluşu ve çökelleri kapanlayacak önemli deltaların yokluğu nedeniyle gelen çökeller mevcut kanyonlar yoluyle havzanın derin kısımlarına kadar ulaşmaktadır (Aksaray, 1978).

Kıta yamacı özellikle Türkiye kıyılarında, Kafkas dağları çevresinde ve Kırım yarımadası önlerinde çok parçalanmıştır. Eğim 1: 40 dolayındadır. Kıta yamacı genellikle 1800-2000 m derinliklerine kadar ulaşmaktadır. Eğimi 1:1000 den daha düşük olan derin düzlükler bazı yerlerde 2000 m, bazı yerlerde ise 2160 m derinlikten başlamaktadır.

Bu düzlükler ile yamaçların alt sınırı arasında yer alan önlük kuşağı (Basin Apron) Karadeniz'de çok geniş alanlar kaplamaktadır. Karadeniz'de topografik olarak iki değişik türde kıta yamacı seçilebilir. Bunlardan biri, denizaltı kanyonları tarafından derin olarak yarılmış oldukça dik eğimli yamaçlar durumunda iken, diğeri çok tatlı eğimli düzlemsel yamaçlar şeklindedir. Ereğli açıklarındaki Ereğli kanyonunun gen işliği 4km, yüksekliği 350 m, Sakarya kanyonunun genişliği ise 11 km olup, yüksekliği 550 m kadardır. Kanyonlar kıyıya dik veya eğik olarak şelften kıta yokuşuna doğru uzanırlar. Kıyıya paralel olanları da vardır. Ancak, bunlar kayma kökenlidirler (Aksaray, 1978).

Tuna nehrinin deltası derin düzlüklere kadar uzanmaktadır. Ancak bu delta günümüz koşullarında gelişmesini sürdürmemektedir. Deniz kuzeyinde buzul sonrası yükselme sonucu, Tuna'nın taşıdığı malzeme günümüzde haliçlerde çökelmekte ve su dolaşımı engellenmiş derin düzlüklere taşmamamaktadır. Karadeniz havzasının orta kuşağı, su dolaşımı engellenmiş derin deniz düzlüğü olup, eğimi 1:1000 den azdır. Bu düzlük Yalta'nın güneyindeki 2206 m derinliğine doğru eğimlidir. Bu derin düzlük havzanın doğu kısmında daha iyi gelişmiştir.

KARADENİZ'İN GÜNCEL ÇÖKELLERİ

Karadeniz'in derin düzlüklerindeki çökellerin yaklaşık 20-30 cm lik en üst kısmı ortalama % 40 dolayında kalsiyum karbonat taşımaktadır. Bu birim son 3000 yılda çökelmiştir. Kalsiyum

Tablo 5 - Optik yayım spektroskopisi ile yapılan tayinlerin karotlara göre ağırlıklı ortalamaları

					E L E M E N T L E R									
Durak no.	*Sr*	*Co*	*Cr*	*Cu*	*Mn*	*Pb*	*V*	*Ti*	*Mo*	*Zr*	*Y*	*B*	*Ni*	*Ba*
1	G	G	0.007	0.005	0.025	G	0.015	0.3	G	0.008	G	G	0.002	0.02
2	G	0.003	0.01	0.003	0.07	0.002	0.01	0.3	G	0.015	G	0.0055	0.004	0.04
3	G	0.002	0.008	0.004	0.05	0.0015	0.01	0.25	G	0.007	G	0.0085	0.005	0.055
4	G	G	0.007	0.0015	0.036	G	0.003	0.15	G	0.003	G	0.0035	0.0015	0.025
9	G	G	0.006	0.002	0.064	G	0.002	0.019	G	0.004	G	0.0040	0.0014	0.011
10	G	0.0015	0.006	0.002	0.05	0.002	G	0.2	G	0.01	G	0.005	0.0035	0.03
11	0.07	G	0.004	0.0015	0.065	G	0.007	0.2	G	0.006	0.002	0.002	0.0025	0.01
12	G	G	0.0075	0.0030	0.004	G	0.007	0.14	G	0.002	G	0.006	0.003	0.025
13	G	0.0025	0.007	0.003	0.05	0.002	0.01	0.2	G	0.0065	G	0.0055	0.004	0.035
14	0.001	0.0008	0.009	0.002	0.042	G	0.0005	0.13	G	0.0065	G	0.0025	0.003	0.01
15	0.002	0.0002	0.001	0.002	0.0039	G	0.006	0.17	G	0.004	G	0.025	0.003	0.023
16	0.02	0.002	0.0065	0.004	0.08	G	0.01	0.2	0.0025	0.008	0.0015	0.0055	0.004	0.05
17	0.015	0.002	0.0075	0.004	0.06	G	0.01	0.15	0.0015	0.0055	0.001	0.004	0.004	0.04
20	0.015	0.002	0.006	0.003	0.0045	G	0.009	0.15	0.003	0.007	G	0.07	0.005	0.045
21	0.025	0.002	0.0075	0.007	0.07	G	0.01	0.15	0.0025	0.007	0.0015	0.0065	0.005	0.25
22	0.001	0.0001	0.006	0.003	0.08	G	0.009	0.13	0.002	0.001	G	0.006	0.004	0.036
23	0.008	G	0.007	0.003	0.04	G	0.005	0.14	G	0.004	G	0.005	0.003	0.02
24	G	0.01	0.004	0.002	0.034	G	0.005	0.01	G	0.0015	G	0.003	0.005	0.005
25	0.017	0.002	0.01	0.003	0.05	G	0.008	0.16	G	0.004	G	0.005	0.004	0.02
26	G	0.002	0.01	0.003	0.08	G	0.009	0.3	G	0.01	0.002	0.008	0.004	0.03
27	0.03	0.0025	0.01	0.006	0.2	G	0.012	0.3	0.0035	0.0075	0.002	0.015	0.005	0.02
28	0.015	0.0025	0.01	0.004	0.06	G	0.009	0.25	0.0015	0.0075	0.002	0.015	0.006	0.025
29	0.02	0.002	0.006	0.0035	0.15	G	0.009	0.15	0.002	0.006	0.002	0.0045	0.004	0.02
32	G	0.001	0.01	0.0045	0.04	0.001	0.005	0.15	0.001	0.0025	G	0.003	0.006	0.02
33	0.024	0.0009	0.009	0.0035	0.09	G	0.004	0.1	G	0.003	G	0.003	0.0035	0.03
34	G	G	0.007	0.002	0.035	G	0.006	0.1	0.0005	0.002	G	0.004	0.003	0.02
35	G	G	0.007	0.002	0.04	G	0.007	0.2	G	0.005	G	0.0045	0.003	0.03
36	0.02	G	0.004	0.01	0.05	G	0.006	0.2	G	0.01	G	0.004	0.003	0.02
37	G	0.0002	0.007	0.002	0.05	G	0.005	0.2	G	0.005	G	0.005	0.0035	0.025
38	G	0.0001	0.006	0.002	0.03	G	0.002	0.1	G	0.003	G	0.0008	0.003	0.006
39	G	0.0001	0.008	0.003	0.07	G	0.003	0.1	G	0.001	G	0.0008	0.003	0.001
40	0.01	0.0008	0.02	0.003	0.07	G	0.006	0.2	G	0.005	G	0.004	0.008	0.004
41	G	0.002	0.02	0.003	0.08	G	0.005	0.2	G	0.006	G	0.005	0.009	0.02
42	0.005	0.0015	0.015	0.0035	0.05	G	0.01	0.2	G	0.0045	G	0.003	0.006	0.02
43	0.03	0.002	0.01	0.005	0.07	G	0.005	0.2	G	0.006	G	0.005	0.007	0.05
46	0.01	0.003	0.01	0.008	0.035	G	0.015	0.15	0.006	0.005	0.002	0.001	0.01	0.03
47	0.015	0.003	0.01	0.0035	0.45	G	0.005	0.15	G	0.004	G	0.005	0.007	0.03
48	0.055	0.002	0.01	0.003	0.06	G	0.005	0.15	G	0.004	G	0.004	0.01	0.02
49	0.02	0.0006	0.01	0.004	0.045	G	0.005	0.15	G	0.002	G	0.0015	0.0075	0.015
50	G	0.0007	0.015	0.003	0.05	G	0.0035	0.15	G	0.002	G	0.003	0.009	0.02
51	G	0.0015	0.02	0.02	0.1	G	0.006	0.095	G	0.007	G	0.003	0.009	0.01
52	G	0.001	0.01	0.003	0.09	G	0.006	0.15	G	0.003	G	0.004	0.08	0.02
53	0.03	0.002	0.01	0.003	0.08	G	0.004	0.2	G	0.005	G	0.005	0.008	0.03
54	0.05	0.025	0.01	0.006	0.09	G	0.05	0.2	0.001	0.005	G	0.003	0.009	0.03
55	G	0.002	0.01	0.004	0.08	G	0.009	0.2	0.001	0.005	G	0.004	0.01	0.03
56	0.01	0.002	0.0065	0.003	0.05	0.002	0.007	0.2	G	0.007	0.001	0.0025	0.003	0.02
61	G	0.001	0.005	0.005	0.04	G	0.007	0.2	G	0.0055	0.001	0.0015	0.0025	0.015
62	G	0.002	0.006	0.003	0.008	G	0.01	0.1	G	0.01	G	0.001	0.003	0.035
63	G	0.0006	0.01	0.003	0.08	G	0.0045	0.15	G	0.0025	G	0.0035	0.0075	0.025
64	G	0.004	0.009	0.004	0.07	G	0.006	0.2	G	0.005	G	0.004	0.008	0.025
65	G	0.002	0.006	0.003	0.04	G	0.0045	0.2	G	0.004	G	G	0.002	G
70	G	0.002	0.004	0.004	0.04	G	0.003	0.2	G	0.004	G	G	0.002	G
71	G	0.002	0.003	0.003	0.04	G	0.002	0.15	G	0.003	G	G	0.002	0.015

karbonatın çok büyük bir bölümü organik kökenli olup, kokolitlerden meydana gelmiştir. Kokolitli seviyeler beyaz ince laminalar halindedir. Bu seviyenin kalınlığı Ross ve diğerleri (1974) tarafından 30 cm olarak belirtilmektedir. Doğu-batı yönünde yaptığımız deneştirme kesitinde de görüldüğü gibi, söz konusu kokolitli seviyenin kalınlığı 20 cm dolayındadır (Şek. 8).

En üstteki kokolitli birimin altında pelte kıvamında koyu siyah renkli ve organik karbonca zengin ikinci bir birim bulunmaktadır. Bu birim su dolaşımı engellenmiş abisal düzlüklerde görülmektedir. Deneştirme kesitinde de izlendiği gibi, 16 no.lı karotta 18-38 cm, 17 no.lı karotta 16-37 cm, 21 no.lı karotta 16-47.5 cm, 29 no.lı karotta 18-51 cm, 32 no.lı karotta 41-47 cm, 42 no.lı karotta 21-31 cm ve 46 no.lı karotta 46-51 cm arası organik karbonca zengindir. Bu birim C_{14} yaş tayinleri saptamalarına göre, günümüzden yaklaşık 3000 ile 7000 yıl öncesini kapsayan sürede çökelmiştir (Ross ve diğerleri, 1974). 17 no.lı karotta 24-33 cm arasının organik karbon içeriği % 13.85 tir. Bu değer 46 no.lı karotta 108-142 cm arasında ise % 14.25 tir (Tablo 2). Organik karbonca zengin pelte kıvamındaki bu çökellerin kendi başlarına enerji kaynağı olabilecekleri, yürütülmekte olan araştırmalardan anlaşılmaktadır (Çete, 1976). Örneklerin organik karbon içerikleri ve yanma ısıları arasındaki ilişki Şekil 9 da gösterilmiştir. Organik karbon yüzdesi çökelme hızıyle ters orantılı durumdadır. Zira çökelme hızının düşük olduğu bölgelerin özellikle organik karbonca zengin olduğu izlenmektedir.

Organik karbonca zengin birimin altında ise, karadan türemiş kırıntı oranı yüksek çökeller yer almaktadır. Bu üçüncü birim Karadeniz'in çok büyük bir bölümünde devamlılık göstermekte olup, kalınlığı çökme hızının yüksek olduğu yerlerde artmaktadır. Kuzeybatı Anadolu kıta sahanlığından alınan 1 ve 11 no.lı durak noktalarındaki örnekler, karadan türemiş ince kırıntıların yanı sıra bol miktarda lamellibranchiata, gastropoda foraminifera ve Ostracoda içermektedir. Karadeniz'in doğu kısımlarında ise bu çökeller arasına bulantı akıntıları çökelleri sokulmaktadır (karot no. 71, 70, 65, 62, 61, 56, 50 48).

Organik kökenli kalsiyum karbonat çökelmesi doğu ve batıda iki ayrı derin düzlükte en yüksek değerlere ulaşmaktadır. Kırıntılı çökeller, organik karbonat içeriğinin yüksek olduğu bu bölgelerde çok azdır veyahut da hiç yoktur. Kıta sahanlığında görülen yüksek kalsiyum karbonat içeriği ise, lamellibranchiata kavkılarından ileri gelmektedir.

KARADENİZ'İN GÜNCEL ÇÖKELLERİNDEKİ URANYUM İÇERİĞİ VE DAĞILIMI

Karadeniz çökellerindeki nispî olarak yüksek uranyum konsantrasyonları, havzanın durgun orta kısımlarındadır ve kıyıya doğru gidildiğinde uranyum içeriğinde sürekli bir azalma izlenmektedir (Şek. 2,3,4,5). Bir başka deyişle çökelme hızının en düşük olduğu bölgelerdeki çökellerde uranyum konsantrasyonu artmakta, kıyılardan kısıntılı malzeme gelişinin fazla olduğu, dolayısiyle çökelme hızının arttığı kısımlara doğru gidildikçe de uranyum içeriği azalmaktadır. Bu nedenledir ki, yaptığımız uranyum izotenör haritaları ile Ross ve diğerleri (1974)tarafından hazırlanan çökelme hızı bölgelerini gösterir harita arasında bir uyum söz konusudur.

Diğer taraftan Karadeniz dip çökellerinin en üst kısmını oluşturan kokolitli birim ve bunun hemen altındaki organik karbonca zengin birim de havzanın durgun orta kısımlarında yer almaktadır. Bu durum, kokolitlere bağlı organik kökenli kalsiyum karbonat-organik karbon benzerliğinin nedenlerini bir bakıma açıklar niteliktedir. Nitekim en üst kokolitli birimin bulunduğu yerlerde uranyum içeriğinin de artmakta olduğu çalışmalarımızla da kanıtlanmıştır. Bu birimdeki kokolit dağılımı ile uranyum içeriği arasında doğrudan bir ilişki söz konusudur. Benzeri durum, organik karbonca zengin

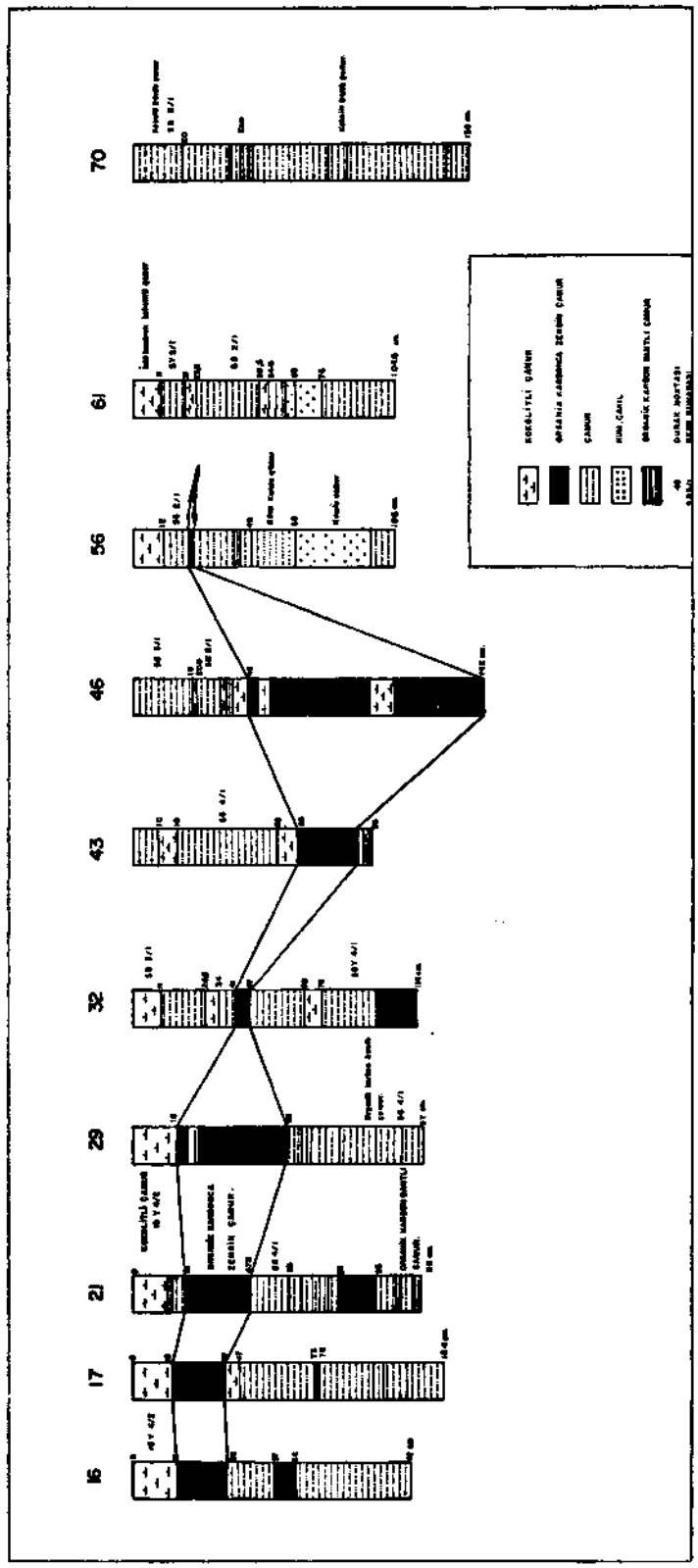

Şek. 8 - Karadeniz'in su dolaşımı engellenmiş derin düzlüklerinden alınan karot örneklerinin deneştirilmesi.

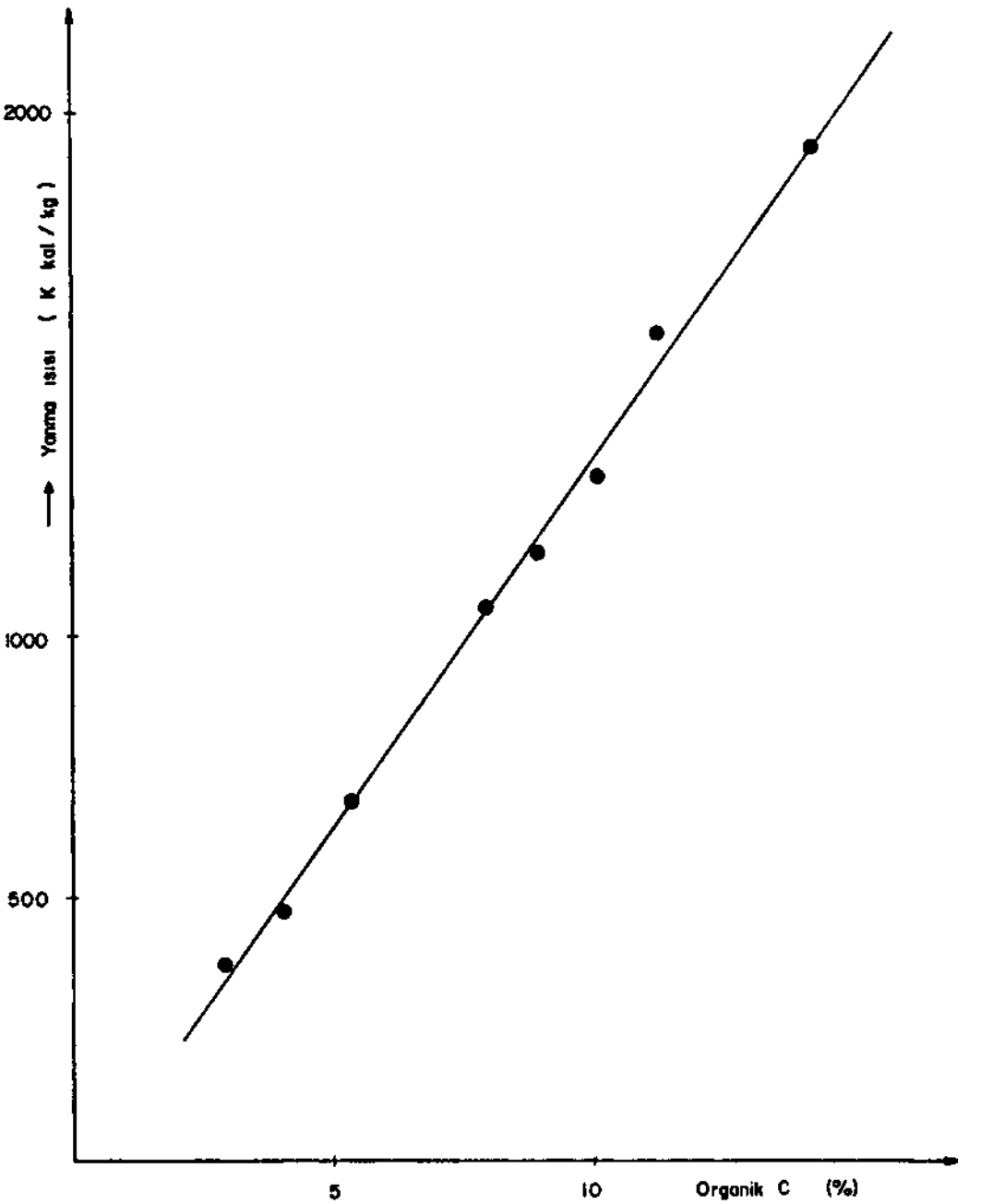

Şek. 9 - örneklerin organik karbon içerikleri ve yanma ısıları arasındaki ilişkiyi gösterir grafik.

birimin organik karbon içeriği ile uranyum içeriği için de geçerlidir ve organik karbonla uranyum arasında da doğrudan bir ilişki görülmektedir (Şek. 10). Bu nedenledir ki organik karbon ve uranyumun derin dip çökellerindeki yanal dağılımları büyük bir uyumluluk içindedir (Şek. 6 ve 3, 4, 5). Benzeri bir ilişki organik karbonla molibden arasında da gözlenmektedir (Şek. 11). 109 değişik örnekte yapılan uranyum, molibden ve organik karbon analizlerinin sonuçları, metrajlara göre Şekil 12 de verilmiştir.

Organik karbon-uranyum ilişkisi yönünden ayrıcalıklı tek durum Zonguldak açıklarında görülmektedir. Burada çökellerdeki karbon içeriğinin fazla olmasına karşın, uranyum içeriği azdır. Bu aykırı görünüm, buralardaki çökellere karalardan çok fazla miktarda kırıntılı karbon gelişi ile açıklanabilir. Nitekim Shimkus ve Trimonis (1974) Karadeniz'deki organik karbon çökelmesinin büyük bir bölümünü aneorobik bakterilerin kimyasal ve mikrobiyolojik faaliyetlerine, 1:3 lük bir bölümünü de nehirler tarafından taşınan karbona bağlamaktadırlar. Buna benzer ayrıcalıklı diğer bir durum, $CaCo_3$ - U_3O_8 ilişkisi yönünden de söz konusudur. Daha sığ kısımlarda rastlanan kalsiyum karbonat zenginleşmesi ister organik kökenli olsun, isterse karalardan kırıntı halinde taşınan malzeme ile ilişkili olsun, bu bölümlerde $CaCO_3$ artışı veya azalışı ile çökellerin uranyum içeriğinde artma veya azalma olmamaktadır ve bir ilişki söz konusu değildir.

Bu durum 11 no.lı karotta açık bir şekilde görülmektedir. Diğer taraftan kıyılardan taşınan değişik bileşimdeki kırıntılı malzeme, dip çökellerindeki kokolitlerin miktarlarını da olumsuz yönde etkilemektedir. Uranyum içeriğinin yüksekçe olduğu kısımlar için, bazı istisnalar dışında çok kaba anlamda 2000 m eşderinlik eğrisini yanal sınır olarak kabul etmek mümkündür (Şek. 1).

Karadeniz çökellerinde rastlanan diğer denizlerdekinden daha yüksek uranyum içeriği, havzanın durgun orta kısımlarındaki çökellerin yüzeyden itibaren yaklaşık 40-60 cm kalınlığındaki kısmında yer almaktadır. Geneldeki bu durumdan farklılıklar, 32 ve 46 no.lı durak noktalarından alınmış karotlarda görülmektedir. Bunlarda, uranyum içeriği yüksek olan çeşitli seviyeler halindeki kısımların karot tabanında (114 ve 142 cm) bile halen devam etmekte oldukları izlenmektedir. Daha altta yer alan bu kısımlardaki uranyum içeriği de yine bazı kokolit seviyeleri veyahut da organik karbonca zengin kısımlar ile ilişkilidir.

Karadeniz'in güncel çökellerindeki uranyumun kokolitlerle ve organik karbonla olan ilişkisine Rona ve Joensu (1974) tarafından da değinilmiştir. Bunun yanı sıra Degens ve diğerleri (1977), özellikle uranyum-kokolit ilişkisine değinirlerken, Kochenov ve diğerleri (1965) ise yüksek uranyum içeriğini, doğrudan, söz konusu çökellerdeki organik madde miktarına bağlamışlardır.

Yaptığımız çalışmalarda en yüksek uranyum içeriği 17 no.lı durak noktasından alınan karotun 24-33 cm aralığında, 9 cm kalınlıktaki, 105°C de kurutulmuş örnekte U_3O_8 tenörü 28 ppm dir. Su dolaşımı engellenmiş abisal düzlüklerdeki çökellerin 0-100 cm kalınlığındaki uranyumca zengin üst kısmın ortalama U_3O_8 tenörü, 105°C de kurutulmuş örneklerde 6 ppm dir. Bu değer 9, 14, 15, 16, 17, 20, 21, 22, 23, 25, 27, 28, 29, 32, 33, 40, 41, 42, 43, 46, 47, 54, 55, 56, 61, no.lı durak noktalarından alınmış karotlardan 283 örneğin ağırlıklı ortalamalarından hesaplanmıştır.

Su dolaşımı engellenmiş abisal düzlüklerin dışında 28 durak noktasından alınan çökellerin yine 0-100 cm aralığında, 204 örneğin analiz sonuçlarına göre ortalama U_3O_8 tenörü 3 ppm dir. Bu değerlerle Agamirov (1963) ve Kochenov'un (1965) yaptıkları değişik türdeki araştırmaların sonuçları arasında bir uyum olduğu söylenebilir. Ayrıca Baturin (1973) tarafından yapılan uranyum dağılım haritası ile çalışmalarımız sonucu ortaya çıkan haritalar arasında bir benzerlik olduğu görülmektedir (Şek. 13, 14). Diğer yandan Degens ve diğerleri (1977) ise, Karadeniz abisal çökellerindeki U_3O_8 konsantrasyonunun 110°C de kurutulmuş örneklerde nadiren 50 ppm i aştığı ve ortalama değer olarak 25 ppm in alınabileceğini ifade etmektedirler.

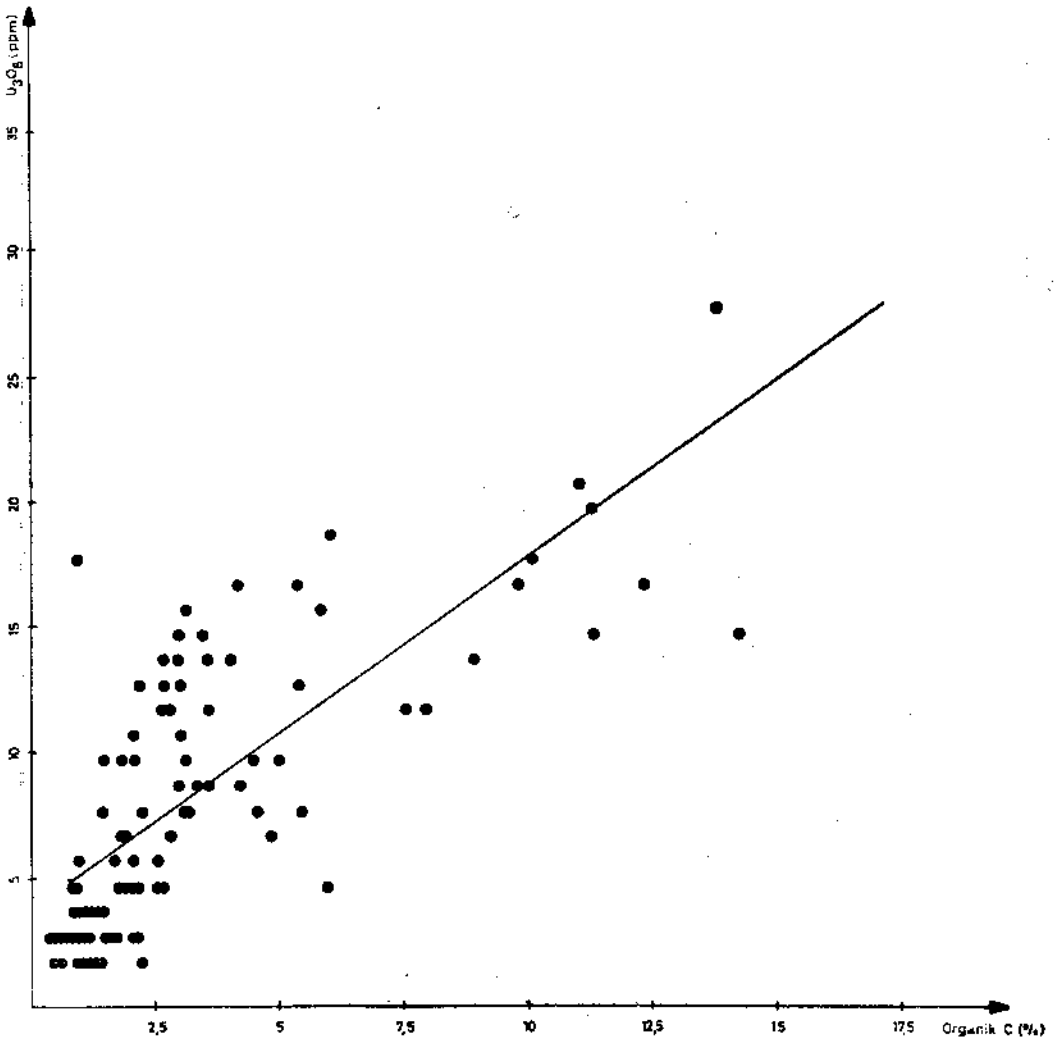

Şek. 10 - U_3O_8-organik karbon arasındaki ilişkiyi gösterir grafik.

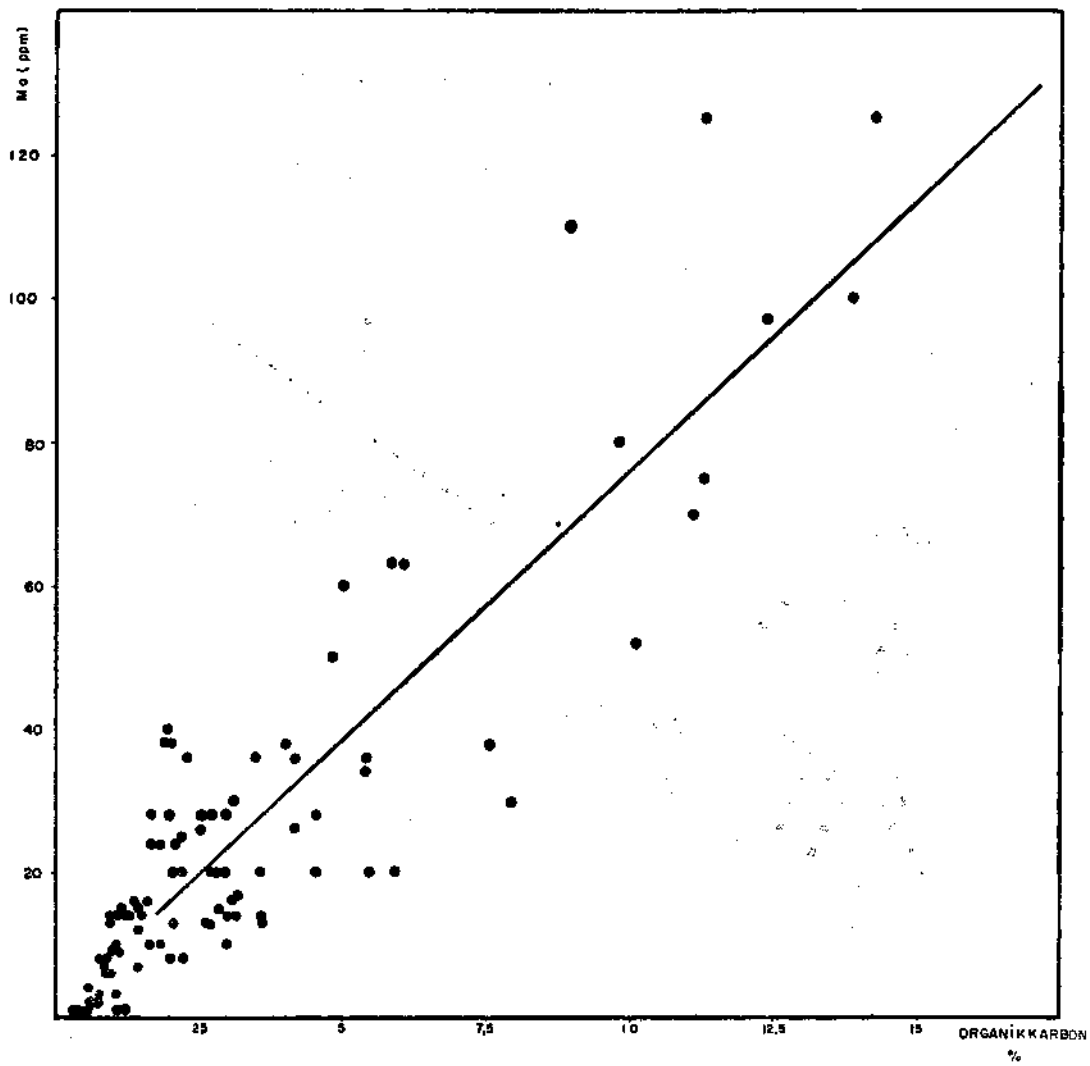

Şek. 11 - Organik karbon-molibden arasındaki ilişkiyi gösterir grafik.

Durak No.	Metraj (cm)	U_3O_8 (ppm)	Mo (ppm)	Organik karbon (%)	Durak No.	Metraj (cm)	U_3O_8 (ppm)	Mo (ppm)	Organik karbon (%)
1	0 - 55	3	< 1	0.99	40	40 - 55	2	8	0.85
1	55 - 115	2	< 1	0.94	40	81 - 84.5	5	20	5.91
11	0 - 107	2	< 1	0.85	40	95.5 - 106	4	16	1.61
16	0 - 18	14	38	4.02	41	38 - 48.5	8	20	5.42
16	18 - 38	20	75	11.28	42	0 - 31	3	6	0.89
16	38 - 57	4	3	0.83	42	31 - 37	8	15	1.45
16	57 - 77	2	< 1	0.46	42	37 - 100.5	4	10	1.06
16	77 - 112	2	< 1	0.44	42	100.5 - 120	5	8	0.83
17	0 - 24	16	63	5.84	46	0 - 19	4	7	0.86
17	24 - 33	28	75	13.85	46	19 - 20.5	16	14	3.15
17	33 - 50	12	58	7.56	46	295 - 35	5	10	0.87
17	50 - 80	3	2	0.74	46	35 - 37.5	12	14	3.57
17	80 - 102	2	2	0.62	46	37.5 - 40	4	14	1.18
17	102 - 124	3	< 1	0.35	46	40 - 94	17	95	12.37
20	0 - 10	13	20	5.41	46	94 - 108	17	34	5.38
20	11 - 30	21	70	11.09	46	108 - 142	15	125	14.25
20	30 - 40	15	125	11.30	47	6 - 9	12	20	2.82
21	0 - 14	9	15	3.34	47	13 - 19	13	14	3.02
21	14 - 21	15	36	3.47	47	31.5 - 35	10	24	1.82
21	21 - 51	18	52	10.10	47	52 - 56	13	36	5.40
21	51 - 116	3	4	0.57	48	15 - 24	7	10	1.84
22	0 - 14.5	14	20	2.96	49	0 - 31	7	40	1.94
22	14.5 - 17	19	63	6.06	49	31 - 60.5	8	20	4.52
22	17 - 17.5	18	13	0.97	50	9 - 24	3	10	1.64
22	17.5 - 46	14	110	8.94	51	102 - 119	5	28	1.99
23	32.5 - 37	5	13	2.70	52	0 - 20	3	24	2.04
25	0 - 13	11	16	3.06	53	0 - 25	8	20	2.21
25	33 - 39.5	8	24	3.08	53	75 106.5	5	20	2.08
26	0 - 60	3	< 1	0.50	54	0 - 15.5	10	24	2.09
26	60 - 114	3	< 1	0.40	54	17 - 54	12	24	2.61
27	0 - 40	7	15	2.83	55	0 - 7	14	20	2.69
27	40 - 86.5	8	17	3.19	55	13 - 24.5	17	26	4.18
28	0 - 20	12	13	2.65	55	24.5 - 50	17	80	9.81
28	20 - 67	3	3	0.81	56	0 - 12	14	13	3.61
28	67 - 125	9	36	4.19	56	12 - 22	3	8	2.01
29	0 - 18	15	10	2.98	56	22 - 24	10	28	4.51
29	18 - 23	9	40	3.56	56	24 - 106	2	8	2.23
29	23 - 27	4	9	1.01	61	0 - 11	4	9	1.13
29	27 - 62	12	32	7.94	61	11 - 21	3	9	0.93
29	62 - 117	4	7	1.44	61	21 - 25.5	6	14	0.96
32	0 - 11	11	13	2.06	61	25.5 - 50.5	3	9	1.11
32	11 - 28.5	3	9	0.96	61	50.5 - 54.5	13	35	2.19
32	28.5 - 34	13	14	3.04	61	54.5 - 104.5	2	8	0.92
32	34 - 69	3	3	0.77	62	35 - 36	6	28	1.66
32	69 - 76	9	28	2.96	63	0 - 28.5	5	36	2.29
32	76 - 97.5	10	12	1.46	64	46 - 48	3	28	1.67
32	97.5 - 114	10	60	5.02	64	56 - 59	6	38	2.02
33	0 - 13	13	28	2.72	65	0 - 44	2	14	1.31
33	20.5 - 29.5	10	30	3.12	65	44 - 68.5	3	14	1.51
33	65 - 93	7	50	4.82	70	0 - 44	2	14	1.20
34	90 - 107	3	16	1.37	70	44 - 136	2	15	1.15
35	32 - 52.5	3	< 1	0.41	71	0 - 58	5	38	1.91
39	0 - 6	4	14	1.18	71	58 - 105	6	26	3.53
39	6 - 12	5	24	1.75	71	105 - 145.5	5	28	2.56
39	12 - 32	5	6	0.98					

Şek. 12 - 109 değişik örnekte yapılan uranyum, molibden ve organik karbon analizlerinin sonuçları.

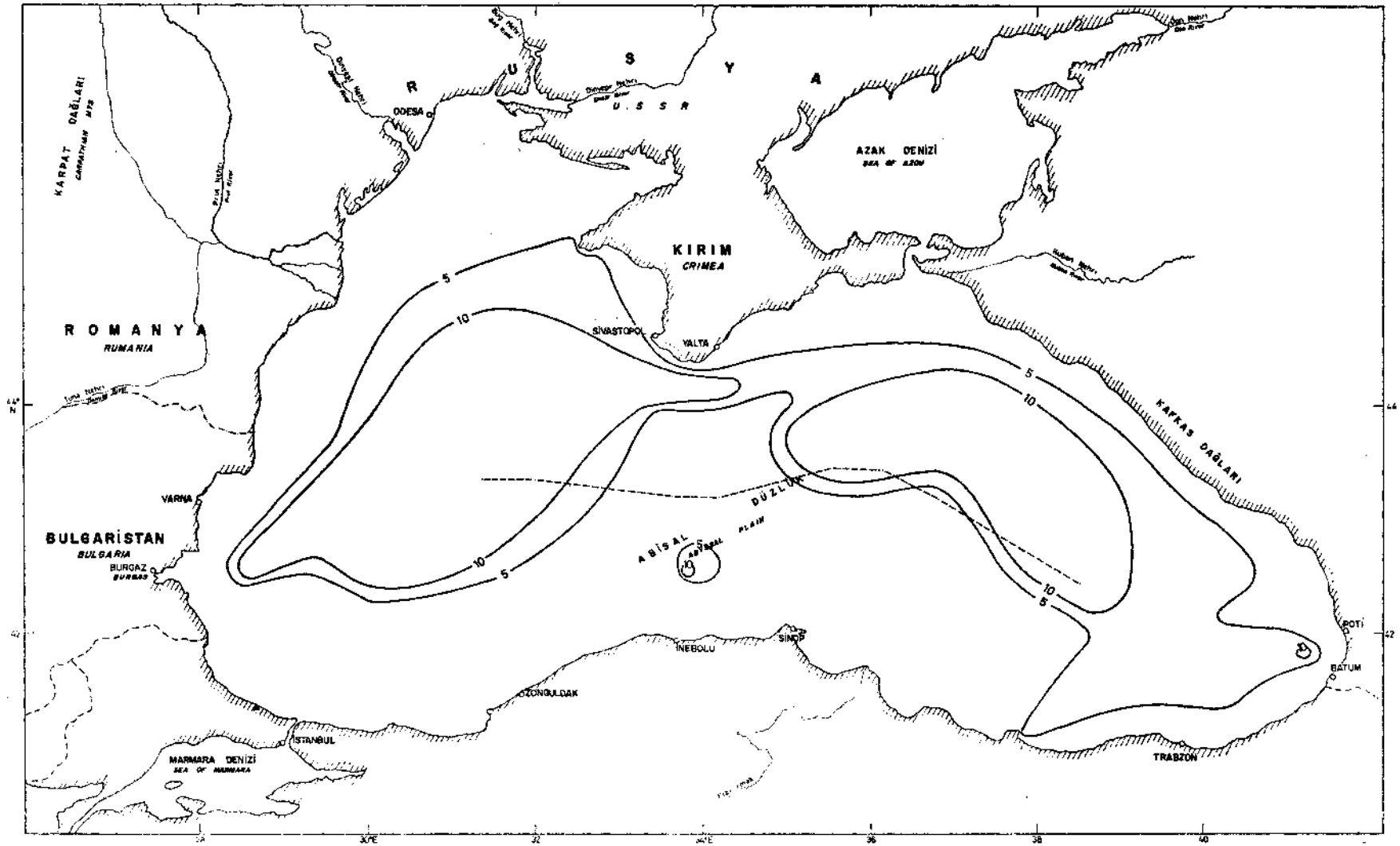

Şek. 13 - Kochenov ve diğerleri (1965) tarafından yapılan, Karadeniz dip çökellerinde uranyum dağılımı haritası.

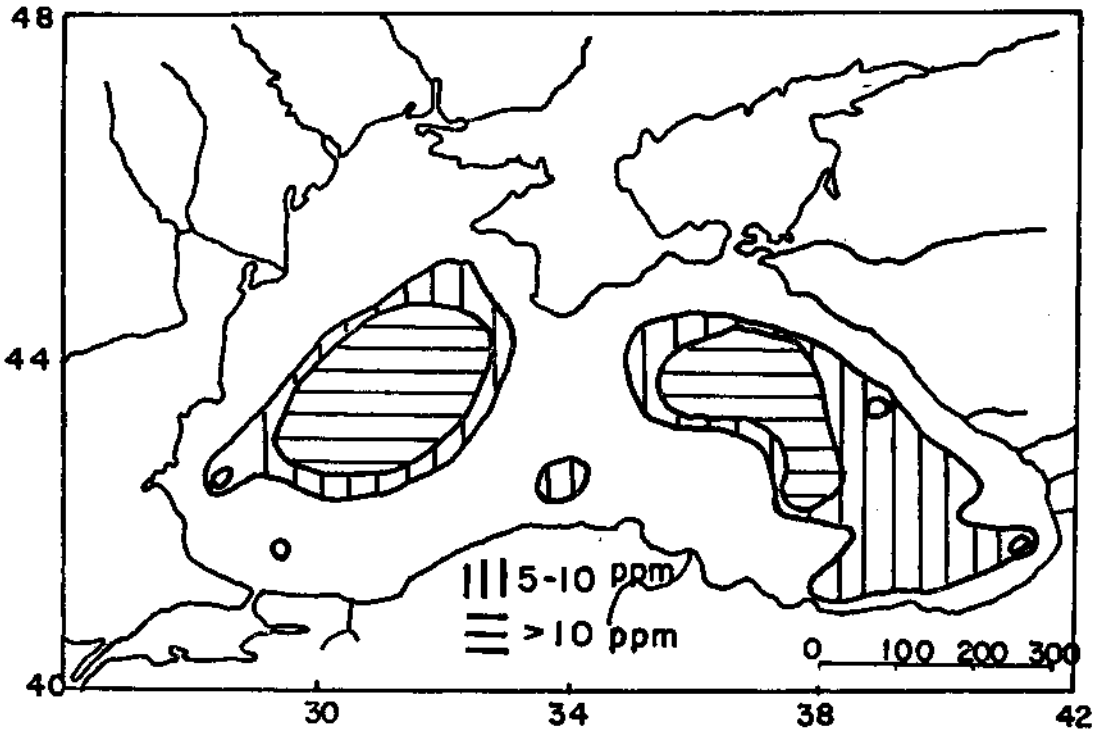

Şek. 14 - Baturin (1973) tarafından yapılan Karadeniz dip çökellerinde uranyum dağılımı haritası.

SONUÇLAR

— Karadeniz'in su dolaşımı engellenmiş düzlüklerde yer alan güncel çökeller kendine özgü bir uranyum konsantrasyonuna sahiptirler.

— Bu çökellerdeki uranyum içeriği ile kokolitler arasında bir ilişkinin bulunduğu gözlenmektedir.

— Aynı şekilde doğrudan bir ilişki uranyum ile organik karbon arasında da söz konusudur.

— Organik karbon ile molibden arasında da benzeri bir ilişki izlenmektedir.

— Organik karbonca zengin birimin organik karbon içeriği 40°C de kurutulmuş örneklerde % 14-15 e kadar çıkabilmektedir. Organik karbon içeriği % 14-15 olan örneğin yanma ısısı ise 1930 KCal/kg dır.

— Çökeller ortalama % 50-55 oranında bağlı olmayan su içermektedirler. Kokolit ve organik karbon oranları yüksek örneklerin 105°C de kurutulmalarındaki ağırlık kayıpları ise, % 85 e kadar ulaşabilmektedir.

— Yaptığımız çalışmanın sonuçları, Karadeniz dip çökellerinin Degens ve diğerleri (1977) tarafından öne sürülenden daha az bir uranyum içeriğine sahip olduğunu göstermiştir. Diğer taraftan bulduğumuz uranyum içerikleri ile Agamirov (1963) ve Kochenov'un (1965) yaptıkları değişik türlerdeki araştırmaların sonuçları arasında bir uyum olduğu söylenebilir. Ayrıca Baturin (1973) tarafın-

dan yapılan uranyum dağılım haritası ile bu çalışma sonucu ortaya çıkan haritalar arasında bir çelişki görülmemiştir.

— Söz konusu uranyum içeriği; günümüz uranyum fiyatları, piyasa koşulları ve teknolojik imkânların maliyeti dikkate alındığında orta ve uzun vadede ekonomik bir değer taşımamaktadır.

KATKI BELİRTME

Karadeniz deniz dibi çökellerinin incelenmesi projesi çalışanları ve katkıları:

Laboratuvarlar Dairesi

Taner Saltoğlu: Proje koordinatörü; Ramiz Arbak, Ergül Ayaz: Ağırlık kaybı, su kül, kalori ve organik karbon analizleri; Şahin Taş, Muammer Güler, Durmuş Ağaçdelen: Optik spektrografik analizler; Ercan Alpaslan, Tanıl Akyüz, Macide Türkalp: XRF analizleri; Tülin Kavlakoğulları, Zühal Gencer, Gülhan Özden: Uranyum analizleri; Ali Balaban: Molibden analizleri; Hulusi Sancar, Cengiz Tuncer: Altın ve gümüş analizleri; Nurgün Güngör: XRD analizleri; Eşref Aydın, Mehmet Öztuğ: Mikroprob incelemeleri.

Radyoaktif Mineraller ve Kömür Dairesi

Hüseyin Kaplan, Yusuf Tahir: Sedimentolojik gözlemler, ekonomik jeoloji yorumları ve redaksiyon çalışmaları; Kayhan Baysal, İsmet Cemal, Savaş Uçakçıoğlu: Deniz Kuvvetleri A 594 gemisinde örneklerin alınması; Nevin iyigün, Mükremin Onmaç, Yusuf Cakol, Koksal Bayraktar, Ali Tülümen: Gravity core yapımı ve bunların açılması için aygıt geliştirme; Ruhşen Arslan, Nesrin Tulu: Palinolojik etütler.

Petrol ve Jeotermal Enerji Dairesi

Abdullah Gedik: Sedimentolojik gözlemler, bilimsel yorumlar ve redaksiyon çalışmaları.

Proje çalışanları dışında çalışmalarımıza katkıda bulunan Sedat Uz, Esen Arpat, Aykut Yıldırım, Muhittin Şenalp, İbrahim Çetintürk, Nahit Kırağlı, Namık Çağatay, Erdinç Sivritepe, Demet Mergen, Nevin Sorguç, Füsun Ceyhan ve Deniz Kuvvetleri Komutanlığı ile A 594 Çarşamba gemisi personeline teşekkür ederiz.

Yayına verildiği tarih, 6 kasım 1980

DEĞİNİLEN BELGELER

Agamirov, S. Sh., 1963, Precipitation of Uranium in the Bottom of the Black Sea. Geokhimiya 1: 92-93. Engl. tr., Geochemistry, 1: 104-106.

———, 1963, Geochemical Balance of the Radioactive Elements in the Black Sea Basin, Geokhimiya 6:612-614. Engl. tr., Geochemistry, 6: 630-633.

Aksaray, F., 1978, Karadeniz şelfinin yapısı: Türkiye Dördüncü Petrol Kongresi.

Baturin, G.N., 1973, Uranium and Sedimantation in Black and Azov Seas: Litologiya i Poleznye Iskopaemye, 5, 21-32,

Çete, M., 1976, Doğu Karadeniz'de organik karbon aramaları: Yeryuvarı ve insan, şubat 1976, 42-45.

Degens, E.T. ve Ross, D.A. (Edi), 1974, The Black Sea-Geology, Chemistry, and Biology: Memoir 20 AAPG.

———; Khoo, F. ve Michaleis, W., 1977, Uranium anomaly in Black Sea: Nature, 269, 566-569.

Deuser, W.G., 1971, Organic-carbon budget of the Black Sea: Deep Sea Res., 18, 995-1004.

Gedik, A., 1976, Karadeniz'de Chain Oseanografi gemisi ile yapılan bilimsel araştırmalar: Yeryuvarı ve insan, şubat 1976, 39-43.

Kochenov, A.V.; Baturin, G. N.; Kovaleva, S. A.; Emel'yanov, E. M. ve Shimkus, K. M., 1965, Uranium and Organic Matter in the Sediments of the Black and Mediterranean Seas: Geokhimiya 3, 302-313.

Rona, E. ve Joensu, O., 1974, Uranium Geochemistry, in Black Sea. The Black Sea, Geology, Chemistry and Biology. Memoir 20 AAPG.

Shimkus, K. M. ve Trimonis, E. S., 1974, The Black-Sea Geology, Chemistry and Biology Memoir 20: Am. Assoc. Petr. Geol., 249-278.

DESCRIPTION OF NEW *BORELIS* SPECIES FROM THE HATAY (S OF TURKEY) AND ELAZIĞ REGION (E OF TURKEY)

Ercüment SİREL and Hatice GÜNDÜZ

Mineral Research and Exploration Institute of Turkey, Ankara

ABSTRACT. — Two new species of Foraminiferida; *Borelis arpati* n. sp. and *Borelis merifi* n. sp. are described; the former occurring in the Middle-Upper Miocene of the Babatorun region (SE of Hatay) and the latter occurring in the Lower-Middle Oligocene of the Sanbuğday village (E of Elazığ).

INTRODUCTION

A project on the Tertiary biostratigraphy of the southern and southeastern Anatolia has been carrying out by the present authors since 1977 in the region of Muş (E of Turkey), Elazığ (E of Turkey), Kahramanmaraş (SE of Turkey) and Hatay (S of Turkey). The description of two new *Borelis* species and biostratigraphy of the Hatay and Elazığ regions (Fig. 1) was investigated as a part of this 'project. The biostratigraphy of these regions can only be demonstrated on a generalized stratigraphic column representing the whole regions (Fig. 2 A,B).

The holotypes and paratypes are deposited in the personal collection of the authors.

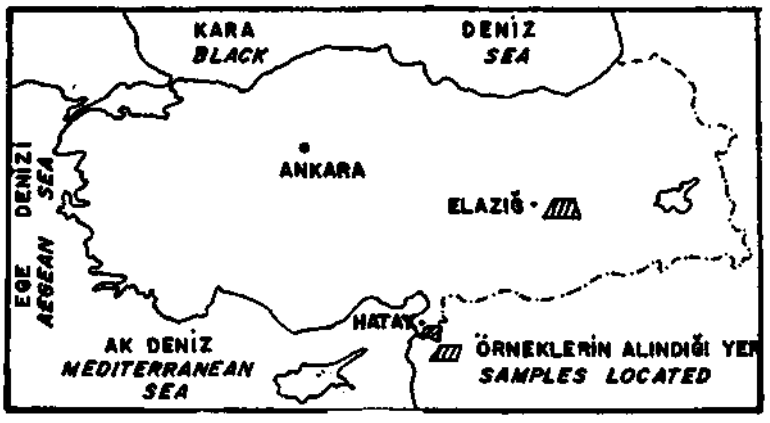

Fig. 1 - Location map.

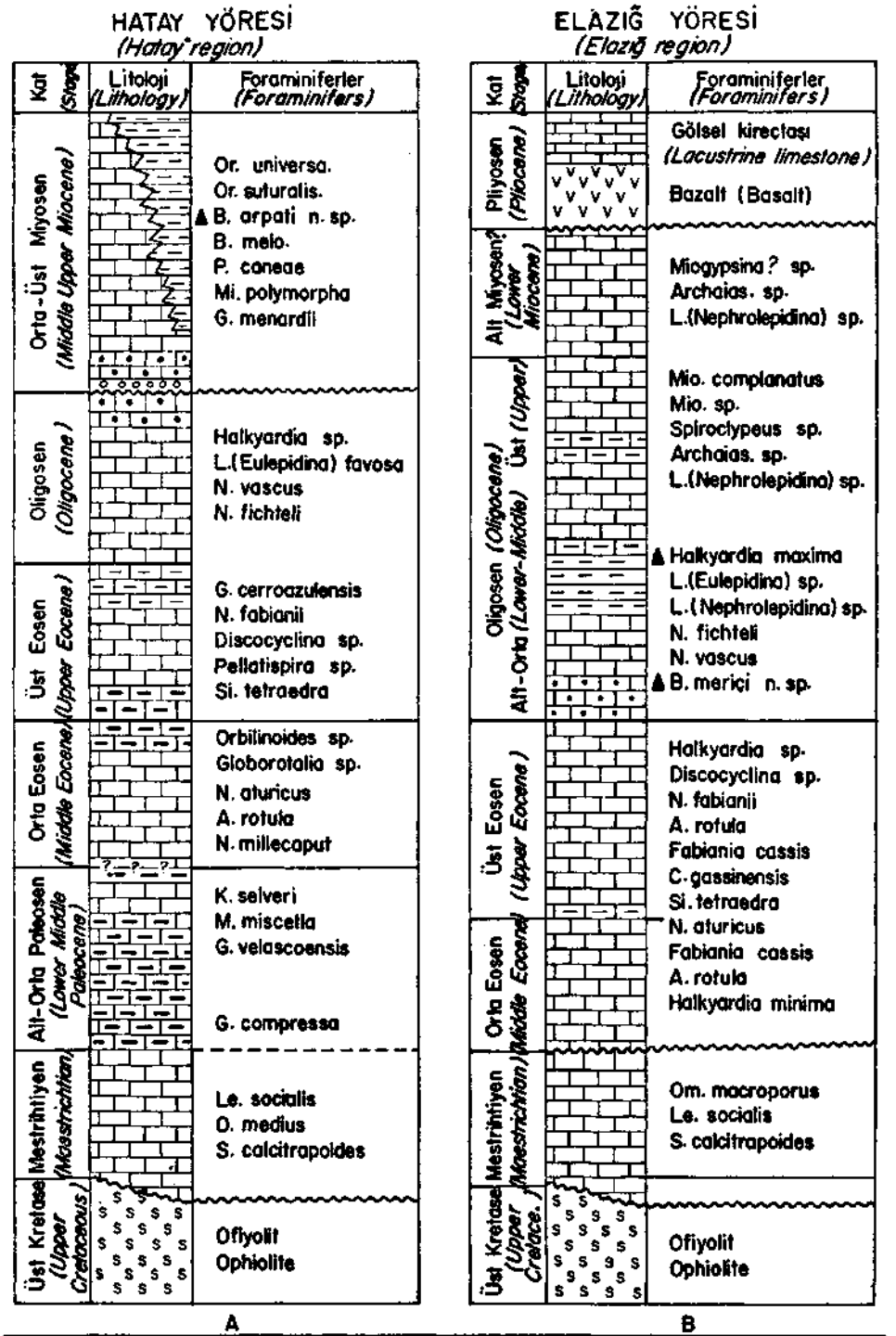

Fig. 2 - Generalized columnar section of Hatay and Elâzığ regions.

SYSTEMATIC STUDY

Family: ALVEOLINIDAE EHRENBERG, 1839

Genus: Borelis de MONTFORT, 1808

Borelis arpati n. sp.
(PL I, fig. 1-8)

Derivation of name: This name is dedicated to geologist Esen Arpat who has made valuable works on the geology of Turkey.

Holotype: It is an axial section from the free specimen, collection no (Hat-1); illustrated by (PL I, fig. 1).

Material: Examined material consist 5 free specimens in the sandy marl from the type locality, about 15 measurable specimens in random thin section of sandy limestone from the Ayışığı village (S of Hatay).

Type locality: Büyüktepe, in Babatorun town (SE of Hatay).

Type level: Middle-Upper Miocene (Langhian-Tortonian).

Diagnosis: Small, elongated nautiloid in shape, index of elongation 0.52-0.67, the width of the proloculus 50-62 m; spherical proloculus followed by 2-3 streptospirally coiled whorls with 8-11 undivided nepionic chambers and adult chambers in regular whorls; Y-shaped septula very rare.

Description: Test is small and elongated nautiloid in shape. The axial diameter varies between 0.35 and 0.55 mm, the equatorial diameter reaches 1.15 mm. The index of elongation 0.52-0.67, but the mean values are around 0.6. There are 30 chambers within the 6 whorls in an equatorial diameter of 0.91 mm (PL I, fig. 2).

Undifferentiated nepionts have a very small spherical proloculus followed by streptospirally coiled 2-3 whorls with 8-11 undivided chambers. The diameter of proloculus ranges from 50 to 62 m.

Very thin growth spiral of the test is subdivided by thin septa into more broad chambers. There are 6 chambers within the last whorls of paratype (PL I, fig. 2). The preseptal passage are occupying 1/5 of the chamber. The mtercanieral foramina are well developed.

The adult chambers are subdivided by the parallel thin septula into parallel chamberlets; the septula are arranged in an alignment pattern from one chamber to the next (PL I, fig. 8) and showing rarely Y-shaped structure. The cross-section of the chamberlets are generally teeth-like and rarely subrectangular in shape; but around the polar region they become circular; their width increase from the polar region to the equatorial part. The basal layer is very thin and its thickness is always smaller than the height of the chamberlets.

Comparisons and remarks: *Borelis arpati* n. sp. differs from *Borelis curdica* (Reichel, 1936-1937) by the absence of well developed Y-shaped septula, elongated nautiloid instead of spherical and slightly nautiloid in shape and by having fewer chambers in the whorls.

New species differs from *Borelis melo* (FichteFand Moll, 1803) in being more nautiloid (index of elongation: 0.52-0.67, instead of 0.9-1.1) and by having 4-6 chambers per whorl instead of 7 in the *B. melo*.

Associated Foraminifers: *Orbulina universa* d'Orbigny, *0. bilobata* (d'Orb.), *0. suturalis* Bronnimann, *Globoquadrina altispira* (Cushman and Jarvis), *Borelis melo, Planorbitlinel'a caneae* Frudenthal.

Borelis meriçi n. sp.
(PI. I, fig. 9-13)

Derivation of name: This name is dedicated to Assoc. Prof. Dr. Engin Meriç.

Holotype: It is an axial section from the free specimen, collection no: (El. 1); illustrated by (PI. I, fig. 10).

Material: Examined material consist 53 free specimens in the silty and sandy argilleous limestone from the type locality.

Type locality: Bağtepe, NE of Sarıbuğday village, NE Palu (E of Elazığ).

Type level: Lower-Middle Oligocene, *Nummiitites fichteli* range zone.

Diagnosis: Small, oval *Borelis* with thickened basal layer in the columellar region, axial length varies between 1.4 and 1.8 mm; equatorial diameter ranges from 0.7 to 0.84 mm; index of elongation varies 1.5-1.8, the diameter of proloculus 39-62 m, spherical proloculus followed by 1-2 streptospirally? coiled whorls with 10 small nepionic chambers and regular 8-9 whorls with divided adult chambers; Y-shaped septula absent.

Description: Test is small and oval in shape. The axial diameter ranging from 1.4 to 1.8 mm; the equatorial length varies between 0.7 and 0.84 mm. Index of elongation is 1.5-1.8, but the mean values are around 1.6. There are 10 nepionic chambers and 61 divided adult chambers within the 10 whorls in an equatorial diameter of 0.82 mm (PI. I, fig. 11).

The spherical juvenile stage has a small spherical proloculus followed by streptospirally? coiled whorls with 10 small spheric undivided chambers (in paratype; PI. I, fig. 11). The diameter of proloculus is 39-62 m.

Very thin growth spiral of the test is subdivided by thin septa into more chambers. There are 9-10 chambers within the last whorl of the paratype (PL I, fig. 11). The prescptal passage is almost occupying 1/4 of the chamber.

The adult chambers are subdivided by the parallel thin septula into parallel small chamberlets; the septula are arranged in an alignment pattern from one chamber to the next (PI. I, fig. 9) and not showing Y-shaped structure. The chamberlets are very small and arranged very closely; the cross-section of the chafnberlcts are generally subcircular and ovoid in shape. The basal layer of all whorls is very thin exceptionally in the columellar region; its thickness are smaller than the height of the chamberlets.

Comparisons and remarks: *Borelis meriçi* n. sp. is distinguished from *Borelis inflata* (Adams, 1965) by having columellar thickening, higher index of elongation (1.5-1.8 instead of 1-1.3)and by having coarser internal texture. The holotype of *B. meriçi* has 9-10 whorls in an axial section of 1.56 mm; whereas the holotype of *B. inflata* has 10-11 whorls in an axial section of 1.29 mm.

Borelis pygmaea (Hanzawa, 1930) differs from new species in being fusiform (index of elongation; 2.2-3.2 may be more); also *B. pygmaca has* a very coarser internal texture comparing to *B. meriçi.*

Borelis philippinensis Hanzawa (1949), is an inadequately described *Borelis,* differs from *B. meriçi* by external shape (index of elongation; 1.35-1.56 instead of 1.5-1.8) and by having delicate internal structure; it has 10 whorls in an axial section of 0.95 mm (Hanzawa, 1949, PI. IX, fig. 4) whereas *B. meriçi* has 9-10 whorls in an axial section of 1.56 mm (in holotype).

Borelis parvulus Hanzawa (1957), is an inadequately described *Borelis,* differs from *B. meriçi* by its delicate internal structure; the holotype of *B. parvulus* has 8 whorls in oblique random section of 0.64 mm; whereas *B. meriçi* has 9-10 whorls in an axial section of 1.56 mm (in holotype).

Associated Foraminifers: *Nummulites fichteli* Michelotti, *N. vascus* Joly and Leymerie, *Halkyardia maxima* Cimerman, *Lepidocyclina (Nephrolepidina)* sp., *L. (Eukpidma)* sp., *Austrotrillina* sp., and *Spiroclypeus* sp..

Manuscript received April 22, 1981

REFERENCES

Adams,C.G., 1965, The Foraminifera and stratigraphy of the Melinau limestone, Sarawak and its importance in Tertiary correlation: The Quart. Jour, of the Geol. Soc. of London; 121, 283-338.

Fichtel, L. and Moll, J.P.C., 1803, Testacea microscopies aliaque minuta ex generibus Argonauta et Nautilus ad naturam delineata et descripta, Wien.

Hanzawa, S., 1930, Note on Foraminifera found in the Lepidocyclina Limestone from Pabeasan, Java: Tohoku Univ. Sci. Rep. (2), 14/1, 94-95.

———, 1949, *Borelis philippinensis* n.sp. from Luzon. P.I: Japanese Jour. Geol Geogr., Tokyo, 21, 1/4, 155-157.

———, 1957, Cenozoic Foraminifera of Micronesia: The Geol. Soc. of Amer., mem. 66, 1-163.

Reichel,M., 1936-1937, Etude sur les alveolines: Soc. Paleont., Suisse. mem., 17, 59, 1-146.

P L A T E

PLATE - I

Borelis arpati n. sp.

Fig. 1 - Axial section, holotype (Hat-1), x 76

Fig. 2 - Equatorial section, paratype (Hat-2), x 63

Fig. 3 - Axial section, paratype (Hat-3),X 70

Fig. 4 - Axial section, young specimen (Hat-4), x 59

Fig. 5 - Tangential section (Hat-5), x 39

Fig. 6 - Axial section, more elongated nautiloid form, paratype (Hat-6), x 64

Fig. 7 - Axial section (Hat-7), x 68

Fig. 8 - Tangential section (Hat-8), x 79

Specimens from: fig 1-3 Middle-Upper Miocene (Langhian-Tortonian) type locality.

Specimens from: fig 4-8 Middle-Upper Miocene (Langhian-Tortonian) Ayışığı village (S Hatay).

Borelis meriçi n. sp.

Fig. 9 - Tangential section, paratype (El-2), x 40

Fig. 10 - Axial section, holotype (El-1),x62

Fig. 11 - Equatorial section, paratype (El-3), X 66

Fig. 12 - Axial section, paratype (El-4), X 51

Fig. 13 - Axial section, paratype (El-5), x 56

All specimens from Lower-Middle Oligocene of the type locality.

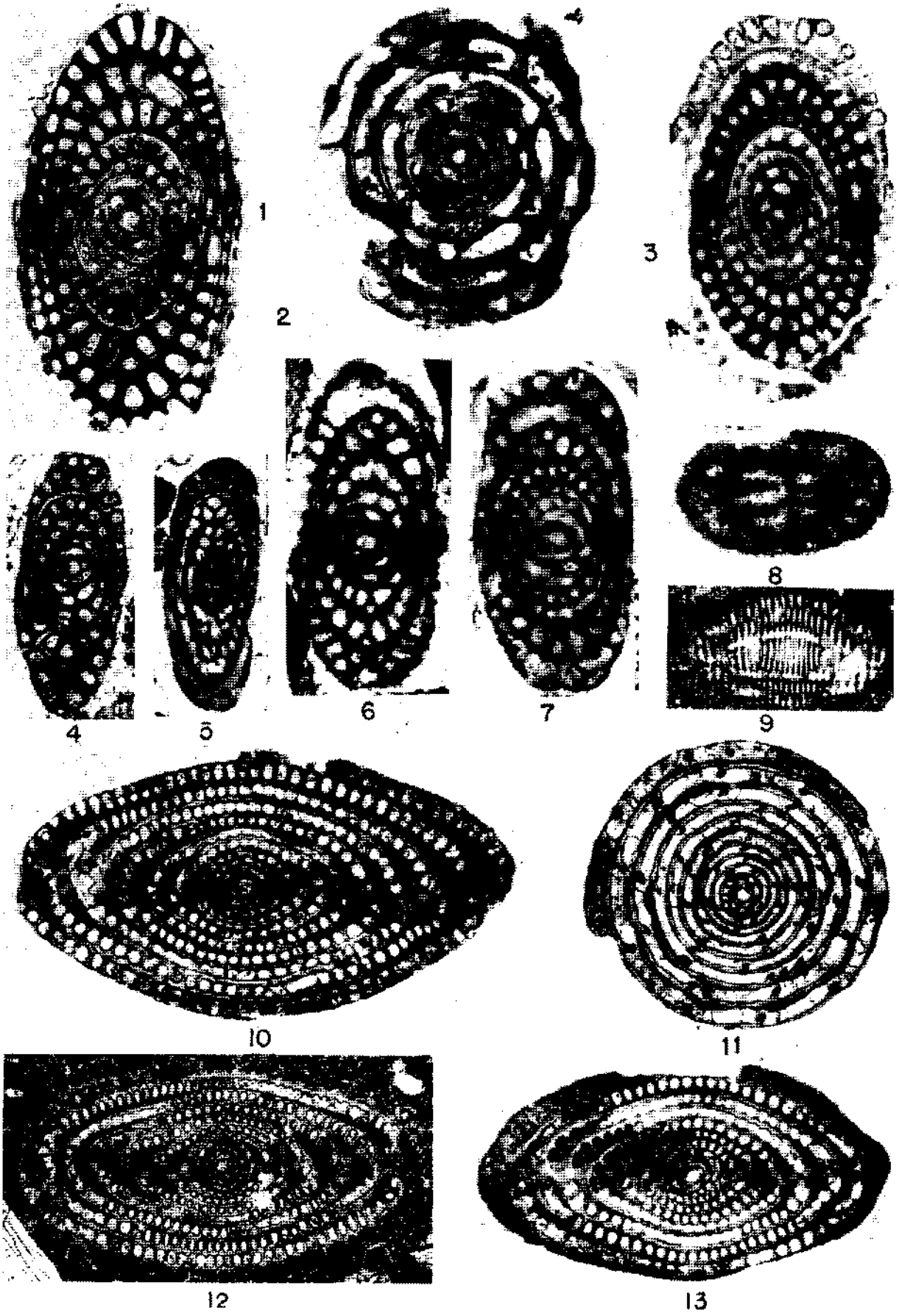
1
2
3
4
5
6
7
8
9
10
11
12
13

A NOTE ON CHROME SPINELS AND ORE MINERALS FROM THE KÜRE AREA, NORTHERN TURKEY

Musa **GÜNER**

Department of Geology, University of Lund, Sweden

The Küre area is situated 20 km from the Black Sea coast in the western part of the Pontides. Its geology, the massive sulfide deposits and the paleomagnetism are treated in special publications (Güner, in press). The present paper reports work done on chrome spinels and ore minerals from the Küre rocks. Spinels, in which chromium is a major component, occur in peridotite, serpentinite, and metasomatites. Geologically, they play an important part as a connecting link between the Küre basaltoids and their alteration products (Güner, in press). In the course of study, microprobe analyses, reflectivity measurements and determinations of the Vickers hardnesses of the chrome spinels were made. Reflectivities and Vickers hardnesses were also determined for the different sulfide minerals of the massive ores and the oxide phases of the disseminated ores and basaltoids.

The microprobe chemical analyses of chrome spinels were made by a Cambridge Scientific Instruments «Geoscan Mk II». For the measurements of reflectivity the writer used a Leitz Microscope Photometer MPW mounted on an Ortholux-Pol polarizing microscope connected to a light-measuring device (type BN 5002 T) with a high-stability current supply (type NSHM). A solid filter of 546 nanometres wavelength, was also employed. The reflectivity standard was a SiC (R=20 %) crystal,, polished and calibrated by Carl Zeiss Company. The Vickers microindentation hardness was determined using a Leitz DURIMET Small-Hardness Tester. Loads of 25, 50, 100, and 200 grams at indenting periods of 15 to 20 seconds were employed.

Chrome spinels

To describe briefly the occurrence of the chrome spinels in different rock types the following code is used for the sake of simplicity: Spinel A = peridotite spinel, spinel B = serpentinite spinel, and spinel C = metasomatite spinel.

The sizes of the individual spinel grains commonly vary between ca 0.5 and 2.5 mm. Their macrocolors are dusky red, the colors under the microscope being as follows:

	In thin-section	*In reflected light*
Spinel A	black	light gray to pinkish gray
Spinel B	black to brown	light bluish to light gray
Spinel C	black to brown	light bluish to light gray

The grains of spinel A are euhedral to subhedral and exhibit some zoning. They are often rimmed by magnetite. Ilmenite forms exsolulion intergrowths. Inclusions of silicate minerals are rare and mostly comprise olivine and hornblende. Spinel B is more or less altered to and intergrown with serpentine, the intermineral borders being rather irregular. Serpentinization commonly results

in marked corrosion. In spinel B, magnetite occurs as crack fillings and rims around the larger anhedral grains. Spinel C is characterized by numero Wintergrown, small patches of silicate minerals, chiefly chlorite or uralite. Its grains are rounded, euhedral or subhedral. This spinel is often rimmed by magnetite and hematite. In essence, spinel B is similar to spinel C„ the differences being a function of the type and degree of alteration of the ultrabasic rock that is the parent of the metasomatites..

The results of the microprobe analyses are shown in Table 1. This table demonstrates substantial compositional variation between the different grains of spinel A. The compositional specifics of this spinel type include relatively high contents of Ti and total Fe. In contrast, the contents of Cr are substantially lower than those in spinels B and C.

Table 1 - Chemical microprobe analyses (weight percent) of Küre chrome spinels

Element	*Element (%)*	*Oxide (%)*	*Element (%)*	*Oxide (%)*	*Element (%)*	*Oxide (%)*	*Element (%)*	*Oxide (%)*
	Spinel A1		**Spinel A2**		**Spinel A3**		**Spinel A4**	
Mg	4.22	7.00	4.64	7.69	4.38	7.27	5.19	8.60
Al	6.35	11.99	6.13	11.58	6.00	11.33	9.29	17.57
Si	0.11	0.23	—	—	0.10	0.22	0.10	0.21
Ti	2.29	3.82	2.47	4.12	2.59	4.33	0.83	1.38
Cr	24.69	36.08	25.19	36.82	24.65	36.03	23.80	34.78
Mn	0.47	0.60	0.35	0.46	0.40	0.52	0.34	0.44
Fe	29.79	38.33	28.75	36.98	29.06	37.38	26.76	34.43
Total	67.91	98.06	67.52	97.63	67.18	97.07	66.31	97.40
Mg/(Mg+Fe)	24.55		27.03		25.73		30.80	
	Spinel A5		**Spinel A6**		**Spinel A7**		**Spinel A8**	
Mg	5.43	8.99	3.69	6.13	3.76	6.23	3.84	6.36
Al	9.68	18.29	6.64	12.54	5.71	10.79	6.49	12.26
Si	0.08	0.17	0.10	0.21	0.08	0.17	0.79	1.69
Ti	0.76	1.27	1.57	2.63	2.44	4.07	1.81	3.02
Cr	24.62	35.98	21.51	31.44	20.76	30.34	20.36	29.75
Mn	0.37	0.47	0.44	0.57	0.31	0.40	0.31	0.40
Fe	25.19	32.41	33.49	43.08	35.39	45.53	31.21	40.15
Total	66.21	97.70	67.45	96.00	68.45	97.54	64.79	93.62
Mg/(Mg+Fe)	33.09		20.21		19.61		22.01	
	Spinel A9		**Spinel A10**		**Spinel B1**		**Spinel B2**	
Mg	6.10	10.11	6.02	9.98	8.61	14.27	8.78	14.55
Al	8.70	16.44	8.72	16.48	12.13	22.93	12.20	23.06
Si	0.20	0.42	1.37	2.93	0.09	0.18	—	—
Ti	0.28	0.47	0.35	0.58	—	—	—	—
Cr	32.13	46.96	31.12	45.48	32.27	47.31	32.67	47.74
Mn	0.39	0.50	0.47	0.61	0.42	0.54	0.38	0.49
Fe	18.65	23.99	17.60	22.64	12.30	15.82	12.10	15.57
Total	66.44	98.89	65.71	98.79	65.92	101.06	66.12	101.40
Mg/(Mg+Fe)	42.88		43.99		61.64		62.48	
	Spinel B3		**Spinel C1**		**Spinel C2**		**Spinel C3**	
Mg	7.75	12.85	9.14	15.15	9.33	15.47	9.26	15.35
Al	12.03	22.73	7.06	13.34	7.86	14.85	7.83	14.79
Si	0.08	0.17	0.17	0.36	0.09	0.18	0.08	0.17
Ti	—	—	—	—	0.07	0.12	0.07	0.12
Cr	31.82	46.56	38.94	56.92	38.02	55.57	38.20	55.83
Mn	0.43	0.56	0.76	0.99	0.60	0.77	0.49	0.63
Fe	14.03	18.05	11.23	14.45	10.90	14.03	10.79	13.88
Total	66.17	100.91	67.30	101.19	66.87	100.99	66.71	100.77
Mg/(Mg+Fe)	55.92		65.13		66.28		66.33	

Note: All iron as FeO.

Figure 1 shows that Mg and Cr show a markedly antithetic behaviour versus Fe, whilst no such relationship exists between $A1_2O_3$ and Cr_2O_3.

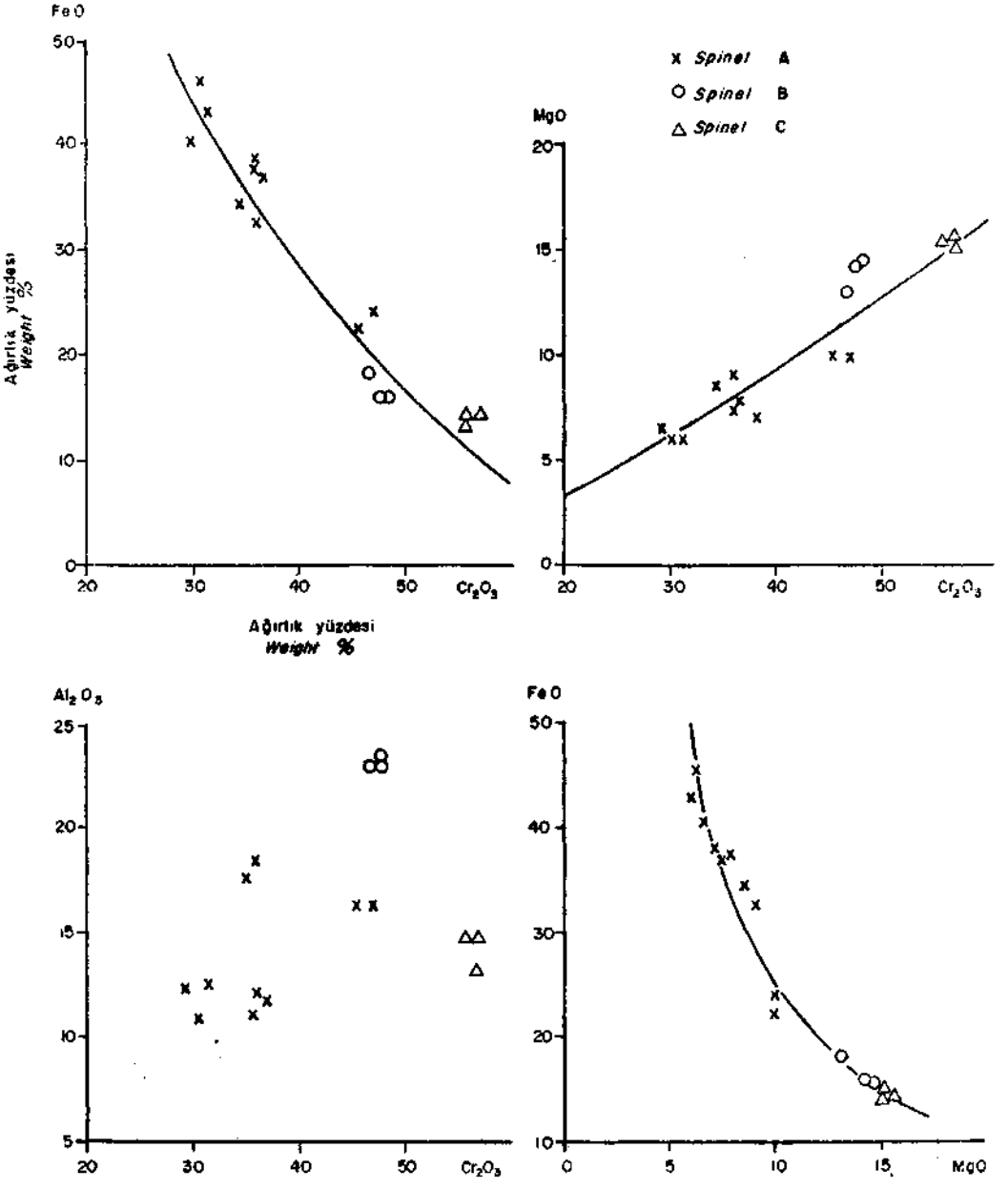

Fig. 1 – Variations of FeO, MgO and Al_2O_3 versus Cr_2O_3 and FeO versus MgO in chrome spinels from Küre. All iron as FeO.

The noticeable variations of reflectivity and Vickers hardness of the chrome spinels (Table 2) are probably due to differences in chemical composition between the individual grains, which is substantiated by the fact that the greatest variations are found in spinel A which is also chemically the most variable. In contrast, the variations in hardness are not very much larger in spinels of type A than in types B and C (1050-1480, versus 1250-1530 and 1190-1560, respectively). In general, reflectivity increases and hardness decreases with increasing contents of Fe and Ti and simultaneously decreasing Cr and Mg.

Table 2 - Reflectivities and Vickers micro-indentation hardnesses of Küre chrome spinels

	Reflectance in % (wavelength of 546 nanometres)			*Vickers micro-indentation hardness (in kg/mm²)*		
Mineral	*Number of measurements*	*Range*	*Average*	*Number of indentations*	*Range*	*Average*
Spinel A	72	12.85-15.12	13.89	62	1048-1478	1227
Spinel B	26	10.78-11.28	11.06	27	1254-1533	1388
Spinel C	36	11.80-13.86	12.57	53	1187-1561	1381

Table 3 - X ray powder diffraction data of the chrome spinels

hkl	*Spinel A*[1] *dA°*	*I*	*Spinel B*[2] *dA°*	*I*	*Spinel C*[3] *dA°*	*I*
111	4.80	15	4.78	25	4.79	20
022	2.94	35	2.92	25	2.93	25
133	2.51	100	2.49	100	2.50	100
004	2.08	25	2.07	45	2.07	35
224	1.70	5	1.69	5	1.69	10
115,333	1.60	30	1.59	40	1.60	30
044	1.47	40	1.46	40	1.47	40

[1] Spinel A from peridotite.
[2] Spinel B from serpentinite.
[3] Spinel C from low-temperature metasomatite.

Ore minerals

The determinations of reflectivity and Vickers micro-indentation hardness for the sulfide minerals and the oxides are summarized in Table 4. The obtained values are compared with values given by Uytenbogaardt and Burke (1973).

Table 4 - Reflectivity and Vickers micro-indentation hardness for sulfide minerals and oxides from Küre

Mineral	Reflectance in % (wavelength of 546 nanometres)			Vickers micro-indentation hardness (in kg/mm²)		
	Number of measurements	Range	Average	Number of indentations	Range	Average
Pyrite	82	50.37-51.82	51.13	—	—	—
Chalcopyrite	84	44.89-47.79	46.38	26	187-216	204
Bornite	14	19.50-21.45	20.42	28	80.5-111	96.5
Covellite	10	7.00-23.00	—	20	70.5-123	98.0
Sphalerite	20	16.36-16.74	16.50	28	168-247	216
Digenite	24	19.69-20.13	19.95	44	97.6-160	122
Tennantite	18	28.57-29.68	29.00	32	351-480	385
Carrollite	14	40.00-41.19	40.68	48	370-642	518
Galena	14	41.10-41.74	41.44	26	65.5-94.0	74.7
Idaite	38	20.46-25.00	22.12	6	258-315	286
Magnetite[1]	12	20.36-20.50	20.44	30	459-560	494
Ilmenite[2]	18	15.38-18.79	17.43	—	—	—
Titanite[3]	22	9.65-12.00	10.67	30	810-1049	914
Limonite, colloform	30	11.51-13.36	12.37	14	391-464	420
ibid semicolloform	10	18.70-20.50	19.44	12	275-493	318

[1] From disseminated ores.

[2] From peridotite and basaltic rock.

[3] From basaltic rock and amphibolitized diabase.

Indentation trials on polished pyrite grains were not successful due to the cracking of the grains even at light loads. The reflectance of .pyrite, ranging from about 50.4 to 51.8 % is generally lower than the average stated in the literature. This may be due to the presence of impurities (Co?). The reflectance for sphalerite ranges from ca 16.4 to 16.7 % and is thus strikingly lower than usual, which is due to Fe-substitution (Uytenbogaardt and Burke, 1973). The hardness of carrollite varies strongly. Anhedral carrollite masses filling interstices in brecciated pyrites are much softer than euhedral grains. Neither the Vickers hardness nor the reflectance of digenite is quite in accordance with literature data. Compared with the value tabulated by Uytenbogaardt and Burke (1973), the Vickers hardness is much higher, the reflectance being distinctly lower. Impurities or compositional differences may be an explanation, but as* far as reflectivity is concerned there is a marked dependence on the length of time passing between final polishing and measurement. This aspect is illustrated particularly well by bornite, where reflectivity varies from about 19.5 to 21.5 % as a function of time (Fig. 2). The time effect is due to the gradual oxidation of the polished mineral surface, a relative stabilization of the reflectance occurring after approximately 3 days in the case of bornite. In these determinations of reflectivity, an average of four measurements were made

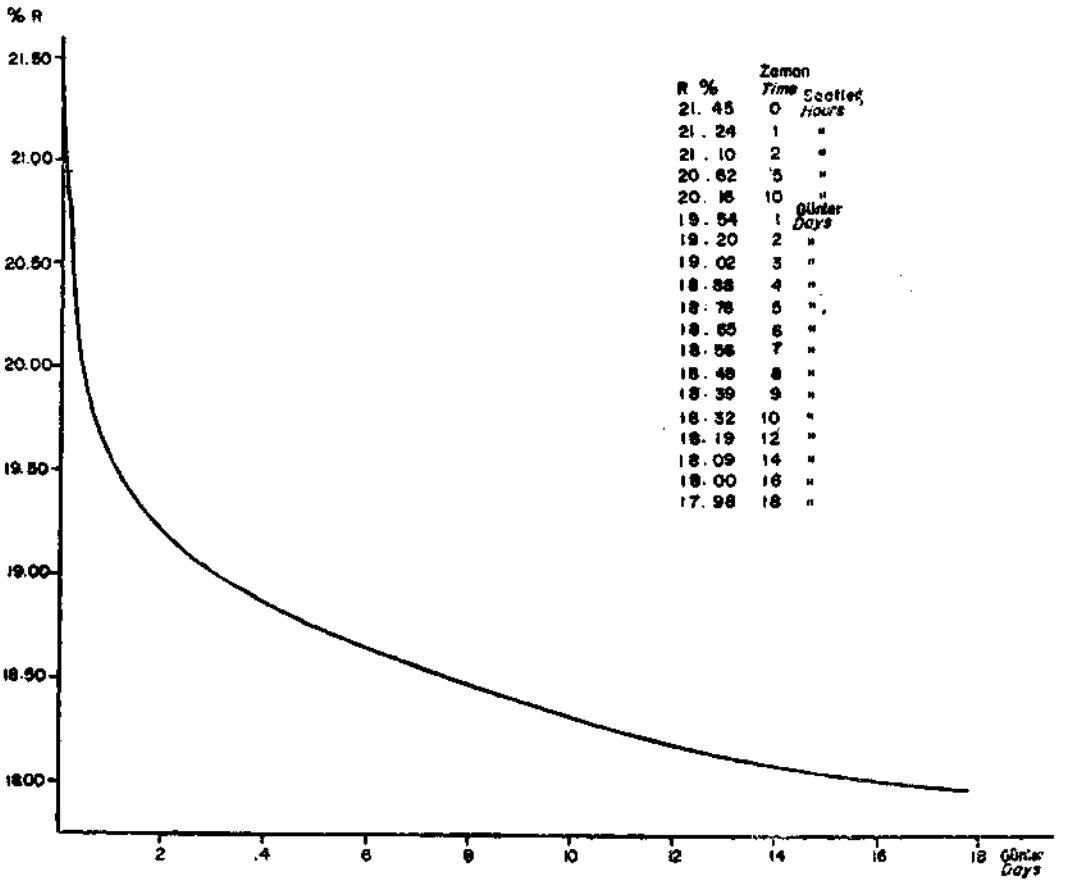

Fig. 2 - The decrease of the reflectance of bornite as a function of the time lapse between final polishing and measurement.

per mineral grain. Care was taken to measure the same parts of the grain. The determinations of Vickers hardness and reflectivity for magnetite yielded fairly stable values ranging from about 460 to 560 and from about 20.4 to 20.5 % respectively.

Manuscript received April 28, 1980

REFERENCES

Fregerslev, S. and Carstens, H., 1976, Chromian spinels in impact melt rocks of Lake Mien, Sweden: Geol. Foren. Forhandl., 98, Stockholm.

Güner, M., in press, Geology and massive sulfide ores of the Küre area, northern Turkey.

———, in press, A paleomagnetic study of some basaltoids and ores from the Pontic Ranges, northern Turkey.

Ketin, 1., 1962, Explanatory Text of the Geological Map of Turkey (Sinop): M.T.A. Publ.

Odsner, O., 1961, Atlas der wichligsten Mineralparagenesen im mikroskopischen Bild. Bergakademie Freiberg.

Stanton, R.L., 1972, Ore petrology: McGraw-Hill, New York.

Uytenbogaardt, W. and Burke, E. A. J., 1973, Tables for microscopic identification of ore minerals :Elsevier, Amsterdam.

OBSERVATIONS SUR IMAGES LANDSAT D'ALIGNEMENTS DANS LES TRAVERTINS D'ANTALYA: DISCUSSION DES RELATIONS PROBABLES ENTRE NEOTECTONIQUE ET HYDROGEOLOGIE

Can AYDAR et Jean - François DUMONT

Mineral Research and Exploration Institute of Turkey

INTRODUCTION

Un vaste entablement de travertins Kuaternaires (De Planhol, 1956) couvre la partie occidentale de la plaine cotiere d'Antalya. Avec une faible couverture vegetale, une morphologic en larges paliers peu erodes, et une bonne reflection optique, ces travertins se pretent a une etude, a partir des images Landsat, de la fracturation. Les observations ont ete realisees sur un appareil «Additive Color Viewer) sur les images n° E 2235-07565 du 14 septembre 1975. Une precedente etude (Masson *et al.* 1975) n'avait pas permis de deceler d'alignement dans les travertins d'Antalya. Une meilleure qualite d'image ou un facteur saisonnier plus favorable parait etre a 1'origine de ces nouvelles observations.

DIRECTIONS D'ALIGNEMENT DANS LES TRAVERTINS

Trois directions majeures d'alignements ont ete reconnues (Fig. 1):

a. Des alignements NE-SW discontinus et soulignes par des variations probables de vegetations apparaissent dans la portion nord des travertins. Vers le NE ils traversent la vallee de l'Aksu (Miocene superieur et Pliocene) et continuent dans les unites du front de 1'accident de 1'Aksu (Poisson, 1977) chevauchantes sur le Miocene.

b. Des alignements NW-SE sont soulignes par des bandes ou des lignes sombres dans la partie Nord des travertins. Mais cette direction est aussi exprimee morphologiquement par une ligne prolongeant la portion de cote NW-SE imme'diatement a 1'Est de la ville d'Antalya. Vers le NW ces alignements se prolongent dans des calcaires du Katran Dağ.

c. Les alignements N-S sont moins frequents mais tres continus. L'un d'eux traverse les travertins du Nord au Sud jusqu'a la cote, la ligne de cote a 1'Ouest d'Antalya montrant en deux endroits un inflechissement a 1'intersection avec des alignements N-S. Cette direction est bien connue dans la partie Nord du golfe d'Antalya (graben de Kovada, accident de Kırkkavak).

DISCUSSION

Les alignements observes montrent une liaison probable avec des accidents tectoniques, en 1'occurence des failles que l'on peut suivre dans les unite's tauriques environnantes du golfe d'Antalya. Cette partie des Taurides a ete tres tectonisee jusqu'a la fin du Miocene (chevauchement de l'Aksu sur les marines du Tortonien). Or, on saperçois que les alignements NE-SW recoupent 1'accident de 1'Aksu, etlui sont done posterieurs. II en est de meme pour les alignements NW-SE qui traversent la bordure orientale tectonisee au Miocene superieur des Bey-Dağları. Quand a la

direction N-S, son activite recente est connue au moins par le fosse Plio-Quaternaire de Kovada situe dans le prolongement septentrional des alignements observes. II s'ensuit que les directions observees peuvent etre rapportees en priorite a la tectonique post-Miocerie terminal, a la neotectonique.

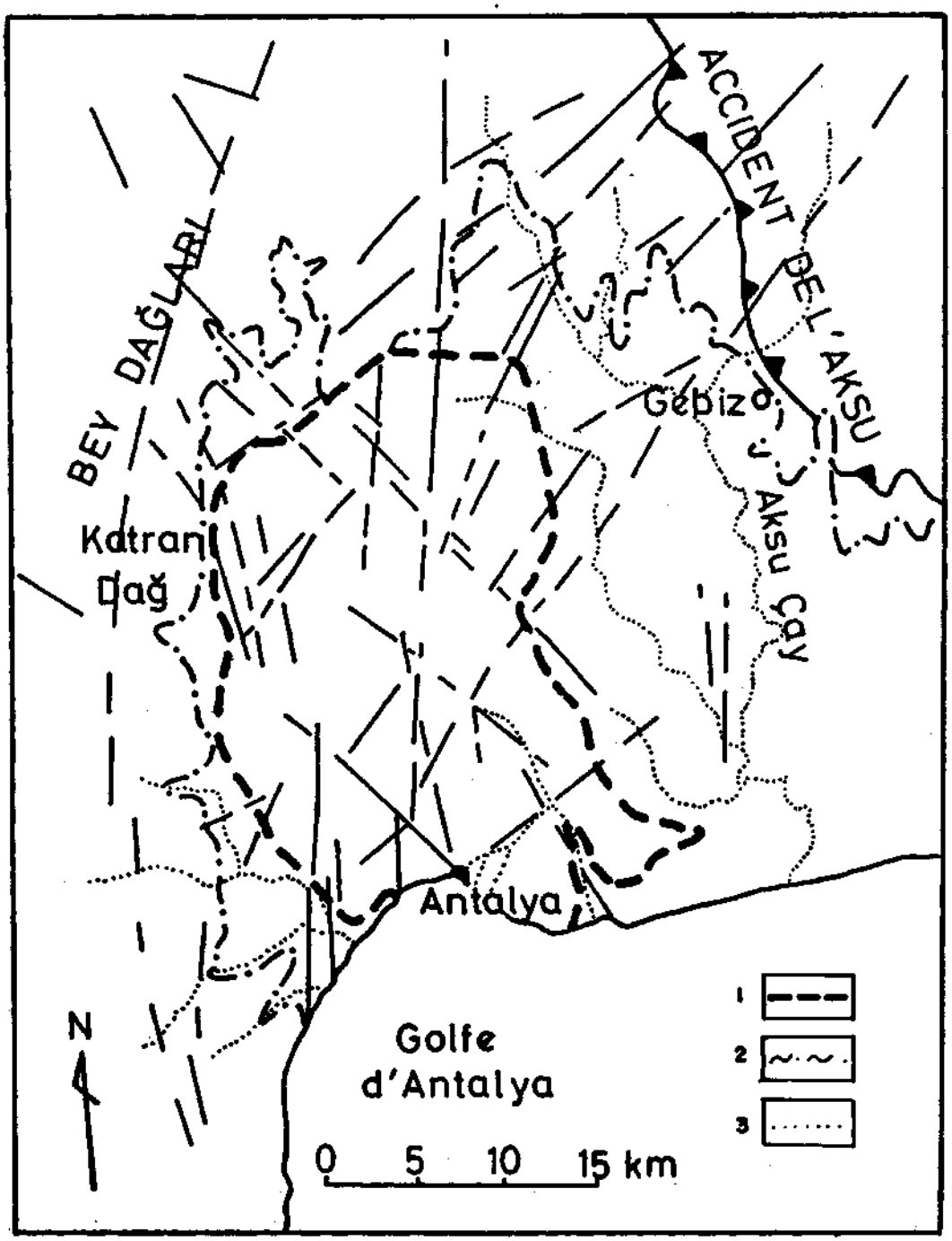

Fig. 1. Schéma des alignements repérés dans les travertins d'Antalya et aux alentours. 1 - limite des affleurements de travertins. 2 - limite des affleurements de quaternaire (vers l'Ouest) et de Plio-Quaternaire (vers l'Est). 3 - réseau hydrographique.

Les alignements observes dans les travertins sont-ils tectoniques? Rien ne permet de le dire pour 1'instant, et jusqu'a present aucune faille n'y a ete observee et decrite.

II nous parait plus juste de penser au depart que ces alignements ne traduisent, dans les travertins, que des zones de circulation karstique suffisamment importantes pour influencer la vegetation en surface. Ces lignes de circulation karstique peuvent suivre le trace de failles reelles, affectant donc les travertins, ce qui resterait a prouver. Mais il serait aussi possible que ces lignes d'ecoulement karstique ne soient pas tectoniques dans les travertins, et qu'elles suivent le trace de failles cicatrisees par ces travertins. Ces ecoulement karstiques relativement lineaires peuvent creer des lignes de faiblesses capables de former des escarpements si un front d'erosion vient a les degager. Reste a savoir pourquoi la circulation d'eau dans les travertins suivrait preferenciellement le trace des failles Plio-Quaternaires recouvertes par ces travertins.

Une reponse peut etre avancee en fonction des observations faites dans le SW de l'Anatolie sur les relations entre la neotectonique et la circulation des fluides geothermiques: II apparait en effet que les failles recentes, que l'on peut rapporter a la neotectonique Plio-Quaternaire sont tres favorables a la circulation souterraine des eaux, surtout du fait de Pimportance des tectoniques distensives depuis la fin du Miocene. Sous cette table poreuse que constituent les travertins d'Antalya, il est probable que la circulation de 1'eau suivant les failles les plus recentes sous-jacentes aux travertins se repercute dans ceux-ci en longues trainees d'ecoulement karstique.

Nous sommes bien conscient du caractere hypothetique des explications avancees; une etude plus poussee incluant conjointement une investigation photo-aerienne detaillee, un bilan des fracturations Plio-Quaternaires des terrains aux environs des travertins et 1'etude hydrogeologique des alentours constituerait une approche methodologique prometteuse pour mieux comprendre le cheminement de 1'eau dans les travertins d'Antalya.

REMERCIEMENTS

Nous sommes redevables a Messieurs E. Arpat et J. Angelier pour leurs commentaires critiques, et leurs suggestions; nous leurs exprimons ici nos remerciements.

Manuscript July 3, 1980

BIBLIOGRAPHIE

Angelier, J. et LePichon X., 1978, Les mouvements egeens ve l'evolution cinematique de la Mediterranee orientale: XXVI Congres Assemblee Pleiniere C.I.E.S.M, Antalya.

Biju-Duval, B.; Lampercin, C; Rivereau, J.C. et Lopez, N., 1976, Commentaire de l'esquisse photogeologique du domaine Mediterranean. Grands traits structuraux a partir des images du satellite Landsat 1. Revue I.F.P., XXXI, 3, 365-400.

Dumont, J.F. et Kerey, E., 1975, L'accident de Kırkkavak, un decrochement majeur dans le Taurus occidental (Turquie): Bull. Soc. Geol. France, (7), 6, 1071-1073.

Erinç, S.Bener, M.; Sungur, K. et Göçmen, K., 1971, 12 Mayıs 1971 Burdur Depremi: Public. Fac. LettresUniv. Istanbul, no 1707.

Kocaefe, S. et Ataman, G., 1976, Seismo-tectonic events at the Anatolia, 1: investigation of the region in the Antalya-Fethiye-Denizli triangle: Public. Earth Sc. Hacettepe Univ., 2, 1,55-70, Ankara.

Masson, P.; Mercier, J. L. etBrunn, J. H., 1975, Essai d'interpretation structurale de la «courbure d'lsparta* (Turquie) d'apres 1'examen des images MSS prises par le satellite ERTS-1: Bull. Soc. Geol. France, (7), 6, 1074-1081.

Planhol, X. de, 1956, Position stratigraphique et signification morphologique des travertins subtauriques de 1'Anatolie sud-occidentale: Actes 4° Congres INQUA Rome-Pise, 1, 467-471.

Poisson, A., 1974, Chronologie de evenements tectoniques depuis le Cretace superieur sur la bordure nord-occidentale du golfe d'Antalya (Turquie): XXIV Congres Assemblee Pleiniere C.I.E.S.M., Monaco.

MENDERES MASÎFÎNDE PARAGONİT MİNERALİNİN VARLIĞI, ALAŞEHİR-MANİSA

Remzi AKKÖK

İ. *T. Ü. Maden Fakültesi, İstanbul*

Alaşehir'in 20 km güneyinde yer alan Derbent bucağı civarındaki granat-mikaşistlerden alı nan numunelerin içerdiği mineraller mikroprob yöntemleriyle analiz edilmiş ve tek bir numuned almandin granat + biyotit + muskovit + plajiyoklaz+kuvars parajenezi ile birlikte paragonit minera linin varlığı saptanmıştır (Çizelge 1).

Çizelge 1 - Granat-mikaşistlerde saptanan paragonit mineralinin analiz sonuçları

	Oksitlerin ağırlığı (%)				
	1	*2*	*3*	*4*	*5*
SiO_2	44.98	44.78	44.89	44.57	44.42
Al_2O_3	38.40	39.20	38.68	37.94	37.47
TiO_2	0.17	0.09	0.07	0.08	0.14
FeO	0.31	0.23	0.29	0.27	0.44
MnO	0.00	0.00	0.00	0.01	0.01
MgO	0.10	0.06	0.10	0.09	0.27
CaO	0.13	0.28	0.16	0.13	0.19
Na_2O	5.60	5.19	5.43	6.54	6.12
K_2O	2.06	1.01	1.09	0.93	1.22
Toplam	91.75	90.84	90.71	90.56	90.28
Formül hesaplamada 22 oksijen kullanılmıştır					
	İyon oranları				
Si	5.982	5.961	5.992	5.986	5.995
Al^{IV}	2.018	2.039	2.008	2.014	2.005
Al^{VI}	4.004	4.113	4.080	3.994	3.957
Ti	0.017	0.009	0.007	0.008	0.014
Fe^2	0.034	0.026	0.032	0.030	0.050
Mn	0.000	0.000	0.000	0.001	0.001
Mg	0.020	0.012	0.020	0.018	0.054
Ca	0.019	0.040	0.023	0.019	0.027
Na	1.444	1.340	1.405	1.703	1.602
K	0.350	0.172	0.186	0.159	0.210

Paragonit mineraline özellikle orta dereceli metamorfik kayaçlarda yaygın olarak rastlanmasına karşın, düşük dereceli metamorfik kayaçlarda ender olarak rastlanılmaktadır (Zen, 1960; Miyashiro, 1973). Petrolojik çalışmalar paragonit mineralinin Sedimenter, magmatik ve yüksek dereceli meta-morfik kayaçlarda bulunmadığını göstermiştir.

Eugster ve Yoder (1954), paragonitin bozunum koşullarının 1 kb PH2O da 625°C ve 2 kb $P_{H2}o$ da 660°C olduğunu saptamışlardır. Daha sonra, Sand ve diğerleri (1957), paragonitin bozunum sıcaklığının 1 kb P_{H2o} da 625°C olduğunu göstermişlerdir. Chatterjee (1970, 1972) deneysel olarak paragonit+kuvarsın üst duraylılık sınırını araştırmıştır. Bu iki mineralin 4 kb P_{H2O} da 560°C nin üzerinde ve 5 kb $P_{H2}o$ da 590°C nin üzerinde duraylı olmadığını saptamıştır.

Deneysel bulgular göz önüne alındığında, granat-mikaşistlerde sadece bir yerde paragonitin bulunması, bölgedeki etken sıcaklık ve basınç çiftinin paragonit+kuvarsın üst duraylılık sınırını aştığını, paragonit mineralinin bulunduğu kesimde ise, yerel olarak daha düşük sıcaklık ve basınç koşullarının egemen olduğunu belirtebilir.

Yayma verildiği tarih, 1 nisan 1980

DEĞİNİLEN BELGELER

Chatterjee, N. D., 1970, Synthesis and upper stability of paragonite: Contr. Mineral. Petrol., 27, 244-257.

———, 1972, The Upper Stability Limit of the Assemblage Paragonite+Quartz and Its Natural Occurrences: Contr. Mineral. Petrol., 34, 288-303.

Eugster, H. P. ve Yoder, H. S., 1954, Paragonite: Geophys. Lab. *A.* Rep. Director for 1953-1954, 111-114.

Miyashiro, A,, 1973, Metamorphism and metamorphic belts: London: George Allen ve Unwin.

Sand, L. B.; Roy, R. ve Osborn, E. F., 1957, Stability relations of some minerals in the Na_2O-Al2O3-SiO2-H_2O system: Econ. Geol, 52, 169-179.

Zen, E-an., 1960, Metamorphism of Lower Paleozoic rocks in the Vicinity of the Taconic Range in west-central Vermont: Am. Mineral., 45, 129-175.

PELİTİK ŞİSTLERDE SAPTANAN KARIŞMAMIŞ PLAJİYOKLAZLAR, ALAŞEHİR-MANİSA

Remzi AKKÖK

İ. T. Ü. Maden Fakültesi, İstanbul

Alaşehir'in 20 km güneyinde yer alan Derbent bucağının 3 km doğusunda kahverengi, orta-kaba taneli ve iyi yapraklanmalı pelitik şistler izlenmektedir. Bu şistlerde almandin granat+biyotit + muskovit+plajiyoklaz+kuvars+opak mineral parajenezi egemendir.

Plajiyoklazların mikroprob yöntemleriyle analizleri sonucunda bileşim bakımından birbirlerinden .oldukça farklı iki plajiyoklaz türünün (An 0.7.0.9 ve An 26.6-27.5) bir porfiroblastta karışmamış olarak bulunduğu saptanmıştır (Çizelge 1). Bu tür karışmamış plajiyoklazlara, «peristerit» denilmektedir (Crawford, 1966). Plajiyoklaz porfiroblastının içerdiği albit miktarının oligoklaz miktarına oranı, bir numunede dahi taneden taneye farklılık göstermektedir. Albit ve oligoklazın tanedeki dağılımı ise düzensizdir (Şek. 1).

Çizelge 1 - Pelitik şistlerde plajiyoklaz analizleri

	Oksitlerin ağırlığı (%)			
	Tane 1		*Tane 2*	
SiO_2	67.89	62.50	67.77	62.71
Al_2O_3	19.90	23.74	19.64	22.78
TiO_2	0.00	0.01	0.00	0.10
FeO	0.02	0.02	0.07	0.05
MnO	0.00	0.00	0.00	0.01
MgO	0.00	0.00	0.01	0.01
CaO	0.13	5.06	0.19	5.54
Na_2O	11.02	7.68	11.39	7.99
K_2O	0.05	0.05	0.05	0.12
Toplam	99.01	99.06	99.12	99.31
	Formül hesaplamada 32 oksijen kullanılmıştır.			
	İyon oranları			
Si	11.947	11.117	11.940	11.168
Al	4.129	4.978	4.080	4.783
Ti	0.000	0.001	0.000	0.013
Fe^2	0.003	0.003	0.010	0.007
Mn	0.000	0.000	0.000	0.003
Mg	0.000	0.000	0.003	0.003
Ca	0.025	0.964	0.036	1.057
Na	3.760	2.649	3.891	2.759
K	0.011	0.011	0.011	0.027
Anortit	0.7	26.6	0.9	27.5
Albit	99.0	73.1	98.8	71.8
Ortoz	0.3	0.3	0.3	0.7

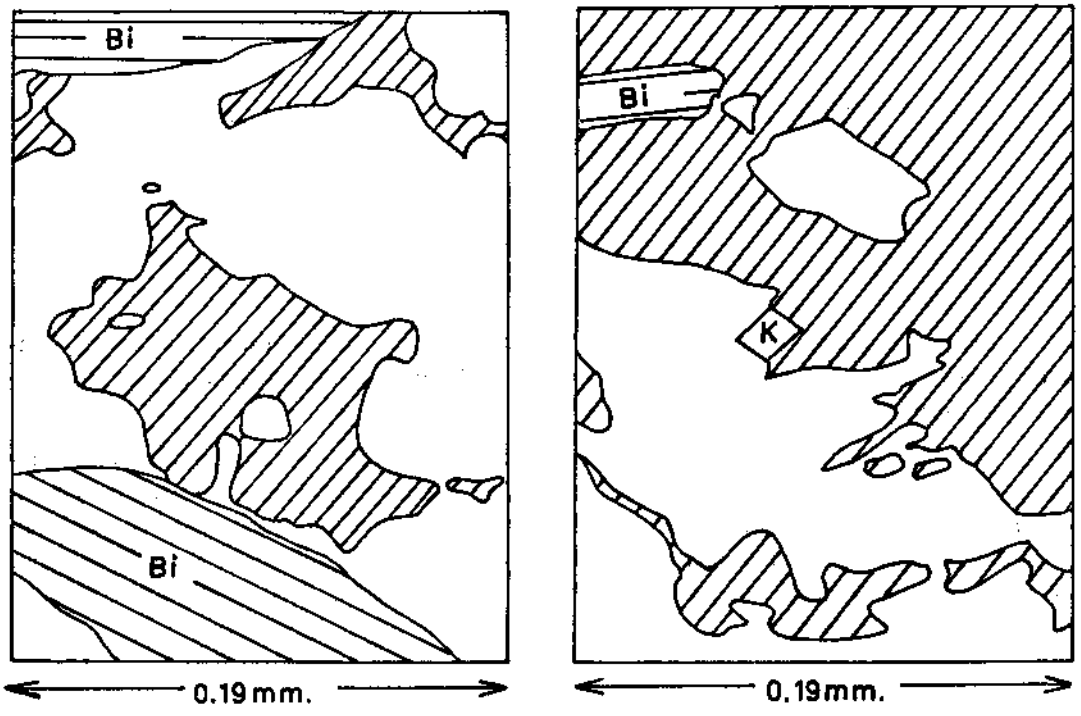

Şek. 1 - Aynı numuneden iki plajiyoklaz porfiroblastının CaK_α X ışını taraması.
Boş alan - Albit; Çizgili alan - Oligoklaz; Bi - Biyotit; K - Kuvars.

Karışmamış Plajiyoklazların kristal yapıları, X ışınları teknikleri kullanılarak araştırılmıştır (Laves, 1954; Gay ve Smith, 1955; Brown, 1960). Bu araştırmacıların hepsinin ortak görüşü, An_2 ile An_{18} arasında bileşimi olan düzenli Plajiyoklazların, birbirlerine karışmamış An_{0-1} ile An_{25}-28 bileşimli iki faz oluşturabileceğidir. Ancak karışmamış Plajiyoklazların oluşum koşullarını açıklayacak ayrıntılı bir araştırma henüz yapılmamıştır. Fakat Crawford (1966), bunun genel anlamda bir eks-solüsyon sonucu oluştuğunu belirtmektedir. Araştırmacıya göre, düşük albit yapısı çok az miktarda anortit katı eriyiğine yer verirken, diğer plajiyoklaz çok miktarda anortiti yapısına alabilmekte ve ancak An_{25} e ulaştığında duraylı olabilmektedir.

Brown (1962), peristeritik eriyiğin üst duraylılık sıcaklığının 550°C civarında olabileceğini ve bunun basınçla biraz daha yüksek değere çıkabileceğini belirtmiştir. Bu nedenle, pelitik şistlerde peristeritin varlığı, bize bu yörede metamorfizma sıcaklığının 550°C civarında olabileceğini göstermektedir.

Yayma verildiği tarih, l nisan 1980

DEĞİNİLEN BELGELER

Brown, W. L., 1960, The crystallographic and Petrografic significance of peristerite unmixing in the acid plagioclase: Z. Kristallog., 113, 330-344.

———1962, Peristerite unmixing in the plagioclases and metamorphic facies series: Norsk Geol. Tidsskr., 42, 2. Halvbind (feldspar vol.), 354-382.

Crawford, M. L., 1966, Composition of plagioclase and associated minerals in some schists from Vermont, U.S.A. and South Westland, New Zealand, with inferences about the peristerite solvus: Contr. Mineral. Petrol., 13, 269-294.

Gay, P. ve Smith, J. V., 1955, Phase relations in the plagioclase feldspar: Composition range Ano to An_{70}: Acta Cryst., 8, 64-65.

Laves, F., 1954, The coexistence of two plagioclases in the oligoclase Composition range: J. Geol., 62, 409-411.

DR.CAHİT ERENTÖZ'Ü KAYBETTİK

Ülkemizin ilk jeologlarından değerli yerbilimci Dr.Cahit Erentöz'ü 29 mayıs 1981 tarihinde kaybettik.

Türkiye jeolojisine ve Maden Tetkik ve Arama Enstitüsüne önemli hizmetler veren Dr. Cahit Erentöz, 1910 yılında İstanbul'da doğmuştur. 1932 yılında Harp Okulundan İstihkâm Subayı olarak mezun olduktan sonra subaylık yılları döneminde istanbul Üniversitesi Fen Fakültesine de devam ederek, 1939 yılında Jeoloji Bölümünü bitirmiş ve 1943 yılında aynı fakültede Jeoloji Doktorası yapmıştır. 1949 yılında İstihkâm Binbaşısı rütbesinde iken ordudan ayrılarak MTA Enstitüsünde jeolog olarak göreve başlamıştır.

Enstitünün çeşitli kademelerinde hizmet veren Dr. Cahit Erentöz 1957-1961 yılları arasında Jeoloji Şubesi Müdür Vekili, 1961-1967 yıllarında Jeoloji Şubesi Müdürü, 1967-1973 yılları arasında Petrol ve Jeotermal Enerji Şubesi Müdürü ve 1973-1975 yıllarında da Genel Direktörlük Teknik Başmüşavirliği görevlerinde mümtaz hizmetlerde bulunmuştur. 1975 yılında emekliye ayrılmıştır.

Ayrıca meslektaşlarının sevgi ve saygınlığını kazanan Dr. Erentöz, 1963 ve 1966 yıllarında Türkiye Jeoloji Kurumunun Başkanlığını yapmıştır.

Yaşamının büyük bir kısmını Enstitümüzde geçiren, mesleğinin aşığı olarak disiplinli ve takipçi bir karakteriyle Enstitümüze ve Türkiye jeolojisine değerli hizmetlerde bulunmuştur. Ülkemizdeki yerbilimleri ile ilgili kuruluşların ilk rehberi olan ve yerbilimcilerin odalarında simgelenen birçok gelişmiş ülkelerin henüz tamamlayamadıkları ve onların takdirlerini kazanmış olan 1:500 000 ölçekli Türkiye Jeoloji Haritası, onun disiplinli ve yılmayan azmi ile hazırlanmıştır.

Ülkemizde ilk jeotermal enerji çalışmalarını o başlatmış ve 1968 yılında Sarayköy-Kızıldere'de ilk defa sıcak buhar Enstitümüz tarafından keşfedilmiştir. Ne mutlu ki başlattığı çalışmanın meyvesi olan jeotermal enerjiye dayalı ilk elektrik santralının kuruluşunu görmenin erdemine kavuşmuştur.

Bunların yanında Türkiye jeolojisine büyük katkısı olan birçok rapor ve yayınları kapsayan eserler bırakmıştır.

Disiplinli, azimli usta bir yerbilimci olduğu kadar, tatlı sert, fakat kalbi insancıl hislerle dolu, yardımsever, müşfik bir karaktere sahipti. Bir taraftan amir, aynı zamanda bir baba şefkatiyle herkesin yanındaydı. Bu özelliklerinden dolayı da onunla her kademede birlikte çalışanların kalbinde taht kuran silinmez hatıralar bırakmıştır.

Yaşam kuralı olarak insan maddeten ölümsüz olamayacağına göre, meslektaşlarının ve dostlarının kalbinde bıraktığı unutulmaz hatıralarla daima anımsanacaktır.

Merhuma Tanrıdan rahmet, geride bıraktığı saygıdeğer kederli ailesine, dostlarına ve tüm meslektaşlarına başsağlığı dileriz.

Dr. Mehmet F. AKKUŞ